The Role of Regulatory T cells in Immunity to Malaria

Richard Adam Morter

St Edmund Hall

University of Oxford

A thesis submitted for the degree of

Doctor of Philosophy

Trinity term 2019

50,000 words (excluding references)

The Role of Regulatory T cells in Immunity to Malaria

Richard Adam Morter, St Edmund Hall, University of Oxford

Thesis submitted for the degree of Doctor of Philosophy, Trinity term 2019

Abstract

Immunity to malaria caused by *Plasmodium falciparum* is complex and poorly understood. Because of this, there remains no highly efficacious vaccine against disease. For the candidate malaria vaccines in the pipeline, immunogenicity has been observed to decline when tested in target populations in malaria-endemic countries, compared to malaria naïve volunteers in the UK. One potential explanation for this observation would be increased levels of immunoregulation caused by repeated malaria infections in endemic populations. Importantly, regulatory T cells (Tregs) are thought to expand during malaria infection, but the role they play in shaping the immune response and in determining disease outcomes remains unclear. It is also unknown whether malaria-expanded Tregs contribute to the suppression of responses to heterologous antigens such as vaccines. This thesis explores the role Tregs play in immunity to malaria using a controlled human malaria infection model in semi-immune Kenyan adults. It also investigates whether Treg activity is associated with the immunogenicity of an experimental pre-erythrocytic vaccine against malaria, ChAd63 / MVA ME-TRAP, in malaria-naïve adult populations and a malaria-exposed infant cohort in Burkina Faso. Cellular and cytokine responses are probed by ELISA, flow cytometry, antigen-specific *in vitro* assays and multiplex qPCR transcriptomics. The data presented identifies potential roles for Tregs in both natural and vaccine-induced immunity to malaria. Improving the immunogenicity and efficacy of malaria vaccines will require identifying reasons why current vaccines work sub-optimally in target populations, as well as greater knowledge of naturally protective immune responses to malaria, to inform the design of new vaccines. This thesis contributes data to both aspects of vaccine design.

Acknowledgments

I would like to thank my supervisors for allowing me the opportunity to undertake this project. Being embedded in exciting clinical trials has allowed me to explore research questions I am greatly interested in. I am very grateful for the guidance and support I've received over the past few years to conduct this work. Thank you to Professor Adrian Hill and Associate Professor Katie Ewer for making my time at the Jenner Institute a pleasure. Thank you to Professor Philip Bejon and Doctor Francis Ndungu at the KEMRI-Wellcome Trust Research programme – I have learnt a lot about tropical medicine, malaria and applied research under your guidance. I would also like to thank my advisor, Professor Helen McShane for project and careers advice.

None of this work would have been possible without the large clinical trials teams working in Oxford and Kenya. Thank you to Georgie Bowyer, Duncan Bellamy, Amy Flaxman, Jonathan Powlson and Carly Bliss for help in the Jenner labs, Mehreen Datoo, Navin Venkatraman and all the nurses in the clinic, as well as all the RAs and clinicans who came before them who processed samples used in this thesis. Thank you to Oliver Hague, an FHS student I supervised and whose work contributed to the Burkina Faso data set presented in this thesis. In Kilifi, I thank Jedidah Mwacharo, Domtila Kimani and Diana Nyabundi for help integrating into the lab and thanks to the large CHMI study team who conducted the trial. There are many other colleagues I cannot name individually but have helped along the way, to whom I am also grateful. I would also like to thank all the members of the IITM programme for advice along the way. It is great to have such a supportive group!

Finally, thank you to all my family and friends. I hope I can do you proud.

Table of contents

List of figures

List of tables

List of abbreviations

3D7	*Plasmodium falciparum* strain '3D7'
4NPP	4-nitrophenylphosphate disodium salt hexahydrate
ACT	Artemisinin-based combination therapy
AF	Alexa Fluor
AMA-1	apical membrane antigen 1
APC	antigen presenting cell
APC	allophycocyanin
BCG	Bacillus Calmette–Guérin
BCR	B cell receptor
BSA	bovine serum albumin
BV	Brilliant Violet™
C-1	one day prior to CHMI
C+14	14 days following CHMI
CCL	CC chemokine ligand
CCR	CC chemokine receptor
CCVTM	Centre for Clinical Vaccinology and Tropical Medicine
CD	cluster of differentiation
cDNA	complementary DNA
CFSE	carboxyfluorescein succinimidyl ester
CGMR-C	Center for Geographic Medicine - Coast
ChAd(63)	chimpanzee adenovirus (serotype 63)
CHMI	controlled human malaria infection
CHMI-SIKA	controlled human malaria infection in semi-immune Kenyan adults
CHUD	Centre Hospitalier Universitaire le Dantec
CI	confidence interval
CNFRP	Centre National de Recherche et de Formation sur le Paludisme
CSP	circumsporozoite protein
C_T	cycle threshold
CTLA	cytotoxic T lymphocyte-associated protein
CV	coefficient of variation
Cvac	PfSPZ vaccination with chloroquine chemoprophylaxis
CXCL	CXC chemokine ligand
CXCR	CXC chemokine receptor
Cy	cyanine
DC	dendritic cell
DGEA	differential gene expression analysis
DMSO	dimethyl sulphoxide
DNA	deoxyribonucleic acid
DNase	Deoxyribonuclease

DoD	Day of diagnosis
DVI	direct venous inoculation
EBO-Z	Ebola Zaire strain
EDTA	ethylenediaminetetraacetic acid
ELISA	Enzyme-linked immunosorbent assay
ELISpot	Enzyme-linked immunospot assay
ExoI	exonuclease 1
FACS	fluorescence-activated cell sorting
FC	fold change
FCS	foetal calf serum
FDR	false discovery rate
FoxP3	forkhead box P3
FSC	forward scatter
g	gram
g	gravity
GAP	genetically attenuated parasite
GCP	Good Clinical Practice
GMC	Geometric mean concentration
GMP	Good Manufacturing Practice
GMT	Geometric mean titre
GP	glycoprotein
H_2SO_4	sulphuric acid
HBsAg	hepatitis B surface antigen
HIV	human immunodeficiency virus
ICS	intracellular cytokine staining
IDO-1	indoleamine 2,3 dioxygenase-1
IFC	integrated fluidics chip
IFN	interferon
Ig	immunoglobulin
IL	Interleukin
ILC	Innate lymphoid cell
IM	intramuscular
IPTp	intermittent preventative treatment in pregnancy
IQR	interquartile range
IRS	indoor residual spraying
ITN	insecticide-treated net
IV	intravenous
KEMRI	Kenya Medical Research Institute
l	litre
L-Glut	L-glutamine
Limma	Linear Models for Microarray Data
LLoD	lower limit of detection

LPS	lipopolysaccharide
LSA-1	liver stage antigen 1
M	mole
mAb	monoclonal antibody
MACS	magnetic-activated cell sorting
ME	multi epitope string
ME-TRAP	multi epitope string and thrombospondin-related adhesion protein
mg	milligram
MHC	major histocompatability complex
min(s)	minutes
ml	mililitre
mM	milimole
MSP-1	merozoite surface protein 1
MVA	modified vaccinia ankara
NAI	naturally-acquired immunity
NaN_3	sodium azide
NEAA	non-essential amino acids
NIHR	National Institutes for Health Research
NK cell	natural Killer cell
nM	nanomole
NRES	National Research Ethics Service
NTM	non-tuberculous mycobacteria
OD	optical density
OxTREC	Oxford tropical research ethics committee
PAMP	pathogen-associated molecular pattern
PBMC	peripheral blood mononucleocyte
PBS	phosphate buffered saline
PCA	principal component analysis
PCR	polymerase chain reaction
PE	R-phycoerythrin
Pen/Strep	penicillin/streptomycin
Pf	*Plasmodium falciparum*
PFA	paraformaldehyde
PfRH5	*Plasmodium falciparum* reticulocyte-binding homologue 5
PfSE	*Plasmodium falciparum* schizont extract
PfSPZ	*Plasmodium falciparum* sporozoite (vaccine)
pfu	plaque forming units
pg	picogram
PI	principal investigator
pM	picomole
PRR	pattern recognition receptor

QC	quality control
qPCR	quantitative polymerase chain reaction
RDT	rapid diagnostic test
RNA	ribonucleic acid
RNase	ribonuclease
ROS	reactive oxygen species
RPMI	Roswell Park Memorial Institute
rRNA	ribosomal RNA
SEB	Staphylococcal enterotoxin B
sec(s)	seconds
SERU	Scientific and Ethics Review Board
SFC	spot forming colonies
SIKA	semi-immune Kenyan adults
SMC	seasonal malaria chemoprevention
SPSS	Statistical Package for the Social Sciences
SPZ	sporozoite
SSC	side scatter
T9/96	*Plasmodium falciparum* strain 'T9/96'
TB	tuberculosis
TCR	T cell receptor
TE	Tris/EDTA buffer
Teff	effector T cell
TGF	transforming growth factor
Th	T helper cell
Th1	T helper 1
Th17	T helper 17
Th2	T helper 2
TMB	tetramethylbenzidine
TNF	tumor necrosis factor
TNFRII	tumor necrosis factor receptor 2
TRAP	thrombospondin-related adhesion protein
Treg	regulatory T cell
UCAD	Université Cheikh Anta Diop
UK	United Kingdom
UNG	uracil-N-glycosylase
UNICEF	United Nations Children's Fund
uRBC	uninfected red blood cell
URC-B	Unité de Recherche Clinique de Banfora
USA	United States of America
VAC	malaria vaccine trial identifier code prefix
VLP	virus-like particle

vp	viral particles
WHO	World Health Organisation
µg	microgram
µl	microlitre
µM	micromole

Statement of authorship

This thesis has been written by Richard Morter and all work contained within is that of Richard Morter. All analysis and laboratory work has been completed by Richard Morter, unless otherwise stated.

For the CHMI study, design and conduct of clinical procedures and primary laboratory assays (including only: malaria qPCR and anti-schizont ELISA) was coordinated at the KEMRI-Wellcome Trust Research Programme, Kilifi, Kenya by Prof. Philip Bejon (PI), Dr. Patricia Njuguna (lead clinician; 2015-2017), Dr. Mainga Hamaluba (lead clinician; 2017-date) and Dr. Melissa Kapulu (study co-ordinator). Laboratory assays were performed by KWTRP malaria immunology lab group members under the supervision of Dr. Melissa Kapulu. Richard Morter contributed to the team of laboratory members performing the qPCR assay and processing PBMC and plasma samples for storage during the CHMI study conducted in 2018. Cell sorting presented in Chapter 4 was performed by Richard Morter under the supervision of Oscar Kai (KWTRP FACS facility manager). Statistical advice for the transcriptomics data was provided by Dr. Nelson Kibinge (KWTRP post-doctoral bioinformatician) and analysis was performed primarily by Richard Morter. All other assays relating to CHMI as well as data analysis was completed by Richard Morter. Direct supervision was provided by Dr. Francis Ndungu (PI in cellular immunology) and Prof. Philip Bejon.

For the vaccine studies, all clinical trials were designed and conceived at the Jenner Institute, University of Oxford by Prof. Adrian VS Hill (PI) and the study clinicians. Conduct of the VAC50 trial in Burkina Faso was co-ordinated at the Centre National

de Recherche et de Formation sur le Paludisme by Prof. Sodiomon Sirima (PI), Dr. Alfred Tiono (clinician) and Dr. Issa Nébié (immunologist). ELISpot, ELISA and intracellular cytokine staining assays to measure vaccine immunogenicity as well as freezing and storage of plasma and PBMC was performed by the clinical trial laboratory teams at each site under the supervision of Assoc. Prof. Katie Ewer (Senior Immunologist), prior to the commencement of the DPhil project. However, Richard Morter was trained and involved in performing all of these assays during subsequent clinical trials. Cell sorting presented in Chapter 6 was performed by Richard Morter under the supervision of Dr. Helen Ferry (NDM Experimental Medicine division, FACS facility manager). All other assays as well as all data analysis was performed by Richard Morter. Direct supervision was provided by Prof. Katie Ewer and Prof. Adrian Hill.

Chapter 1

1. Introduction

1.1. Malaria – parasitology

1.1.1. Epidemiology

Malaria is caused by different species of the apicomplexan parasite *Plasmodium sp* and is spread via the bite of an infected Anopheles mosquito. Worldwide, an estimated 219 million cases of malaria occur per year resulting in around 435 000 deaths, according to the most recent World Health Organisation (WHO) estimates[1]. The burden of disease is carried predominantly by children under the age of 5, who account for 61% of all malaria-related deaths worldwide. Pregnant women and their offspring are also an at-risk population due to the complications associated with placental malaria infection. The deadliest of all *Plasmodia* is *Plasmodium falciparum* which causes the greatest rate of death per case. The vast majority of cases of *P. falciparum* malaria occur in Africa (92%). Other species of importance to humans include *P. vivax, P. malariae, P. ovale and P. knowlsei*[2]. Malaria is a significant global health problem being the 6th most common cause of death in low-income countries[3]. In children below the age of 5 living in sub-Saharan Africa, 9.3% of all deaths are caused directly by malaria[4], with a significant number of additional deaths likely indirectly caused as well[5].

Currently-available control measures for malaria mostly target the mosquito vector, to limit transmission of infectious parasites. The deployment of insecticide treated bed nets (ITNs) and indoor residual spraying (IRS) of insecticides has been prolific[6] across sub-Saharan Africa since major initiatives began in the year 2000. Between 2015 to 2017 alone, 624 million ITNs were distributed worldwide[1]. These interventions are cost effective and 97% are delivered to users free of charge, funded by national governments or international agencies like UNICEF, limiting barriers to access for vulnerable communities. Other less-commonly used methods include seasonal malaria chemoprevention (SMC)[7] and intermittent preventive treatment in pregnancy (IPTp)[8]. Combined, these measures are thought to have contributed to a sustained global fall in the incidence of malaria between 2000 and 2015. An estimated 663 million clinical cases were averted during that time and ITNs were the largest contributing factor behind this (63% of averted cases), according to modelling studies[9]. However since 2015, progress in further reducing the incidence of malaria has stalled[1]. Mathematical models suggest the implementation of an efficacious vaccine alongside current control measures would help to reduce the prevalence of malaria further[10]. Developing a highly efficacious vaccine will require improving our understanding of the mechanisms of naturally-acquired immunity (NAI) to malaria and the design and evaluation of efficacious vaccines against disease.

This thesis will focus solely on immunity against *P. falciparum* as a causative species of malaria and the production and evaluation of a *P. falciparum*-specific vaccine.

1.1.2. Life cycle and pathogenesis

A schematic illustration of the *P. falciparum* life cycle is presented in Figure 1.1. Infection begins with the bite of a human by a parasite-infected mosquito (usually *Anopheles gambiae* in sub-Saharan Africa[11]). Whilst taking a blood meal, the mosquito injects infectious sporozoite-stage parasites into the skin which quickly migrate via the vasculature to the liver[12]. Here, sporozoites invade hepatocytes and over a period of approximately 7 days divide and mature into merozoites. The merozoites erupt from hepatocytes and are then capable of infecting red blood cells. The vast majority of merozoites infecting red blood cells enter into an asexual reproductive cycle where they mature into schizonts which divide and release further merozoites. An asexual reproductive cycle lasts approximately 48 hours and involves multiple mitotic divisions leading to exponential parasite growth in the blood. Increasing parasite densities in blood leads to the clinical manifestations of malaria infection. A small proportion of invading merozoites commit to becoming sexual gametocytes. These are taken up by another mosquito in a subsequent blood meal where they reproduce sexually and the offspring develop into sporozoites which can in turn, be transmitted to another person.

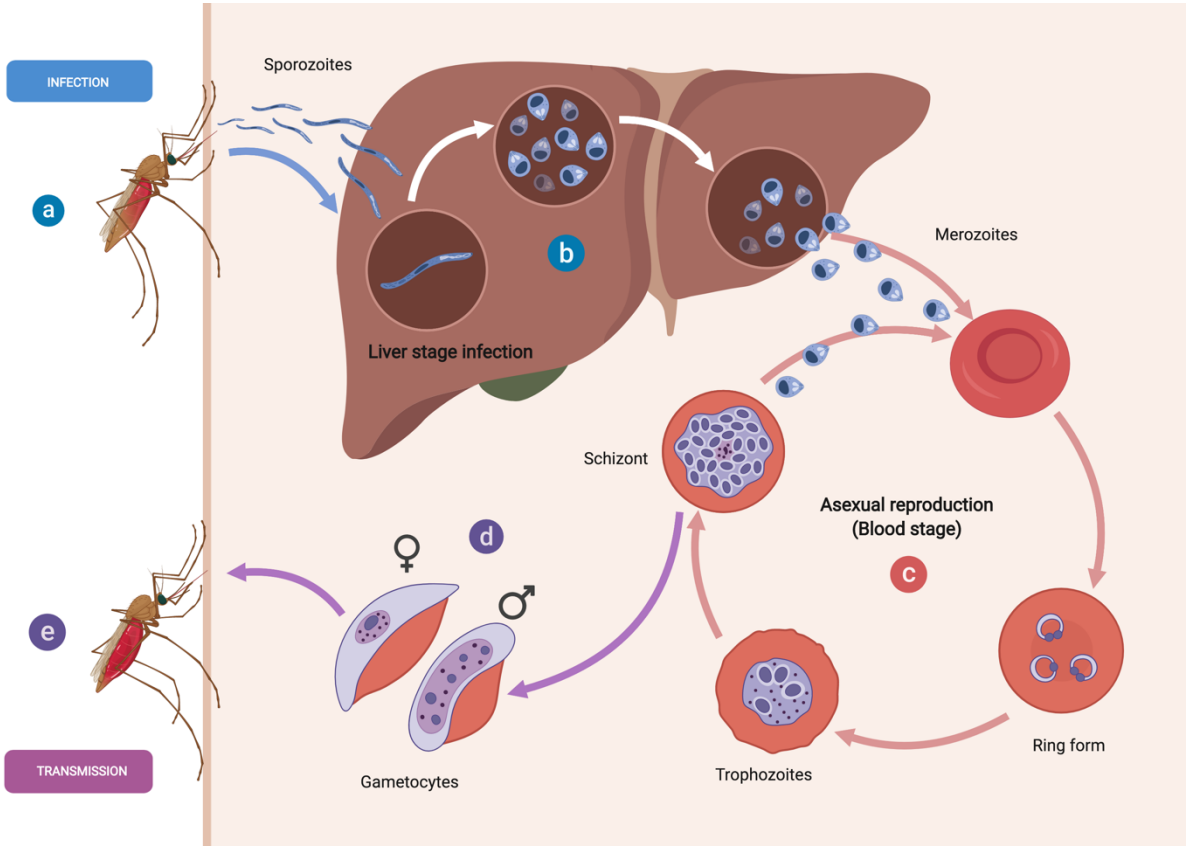

Figure 1.1: P. falciparum malaria life cycle (a) *Infected mosquito injects sporozoites into the skin which migrate to the liver.* ***(b)*** *Sporozoites invade hepatocytes, mature and emerge as merozoites.* ***(c)*** *Merozoites infect red blood cells and reproduce asexually to produce more merozoites.* ***(d)*** *Some blood stage parasites mature into gametocytes instead of following the asexual cycle.* ***(e)*** *Gametocytes are taken up in a blood meal by another mosquito, reproduce and mature into sporozoites which can be transmitted to another person. (Figure by R. Morter, designed in BioRender.com).*

1.1.3. Pathology and clinical disease

Growth of asexual parasites in the blood is the primary cause of the clinical syndrome associated with malaria[13]. Symptoms generally correlate with blood-stage parasite density[14], whilst liver stage infection is quiescent, even in malaria-naïve individuals. Semi-immune individuals can tolerate blood-stage parasitaemia without symptoms[15].

Malaria infection can be classified as either severe or uncomplicated based on clinical criteria[16], or it can be completely asymptomatic. Uncomplicated infection results in a relatively non-specific acute febrile illness. Severe infection is life threatening and its pathology is complex.

There are numerous different mechanisms by which malaria can cause severe disease. Malarial anaemia is a common complication of infection, especially amongst children and can cause both morbidity and mortality[17]. Parasitised and unparasitised red blood cells can lyse during infection, either because of asexual reproduction or through immune-mediated mechanisms. Infection also promotes dyserythropoesis. Both mechanisms contribute to anaemia. Cerebral malaria is also a severe, late-stage complication of infection with a high risk of mortality[18]. Infected red blood cells can sequestrate the brain microvasculature causing obstruction. This causes multiple neurological complications including seizures and/or coma. Other complications of severe infection include hypoglycaemia due to competition for resources with subsequent metabolic acidosis, shock/cardiovascular collapse, acute kidney injury and acute respiratory distress syndrome[19].

However, it is apparent that the host inflammatory response to infection may drive, or at least exacerbate the pathology of infection, in addition to the pathology caused by the parasite itself[20]. Increased inflammation has been associated with worsened pathology and outcomes from severe disease forms including cerebral malaria[21] and malarial anaemia[17]. Figure 1.2 shows that the risk of severe malaria decreases through childhood and is almost negligible after the age of 5 in a high transmission area. The risk of uncomplicated clinical illness also wanes such that most adult

infections are asymptomatic. Despite this, it is usual to continue to get repeated infectious episodes of malaria throughout adult life[22], suggesting that complete protective immunity is uncommon, but immunity which prevents morbidity and subsequent mortality occurs frequently. It is thought that an aspect of adaptive immunity to malaria includes preventing the excessive inflammatory responses primarily responsible for the pathology of disease (so-called 'anti-disease immunity'), rather than preventing parasitaemia entirely[23].

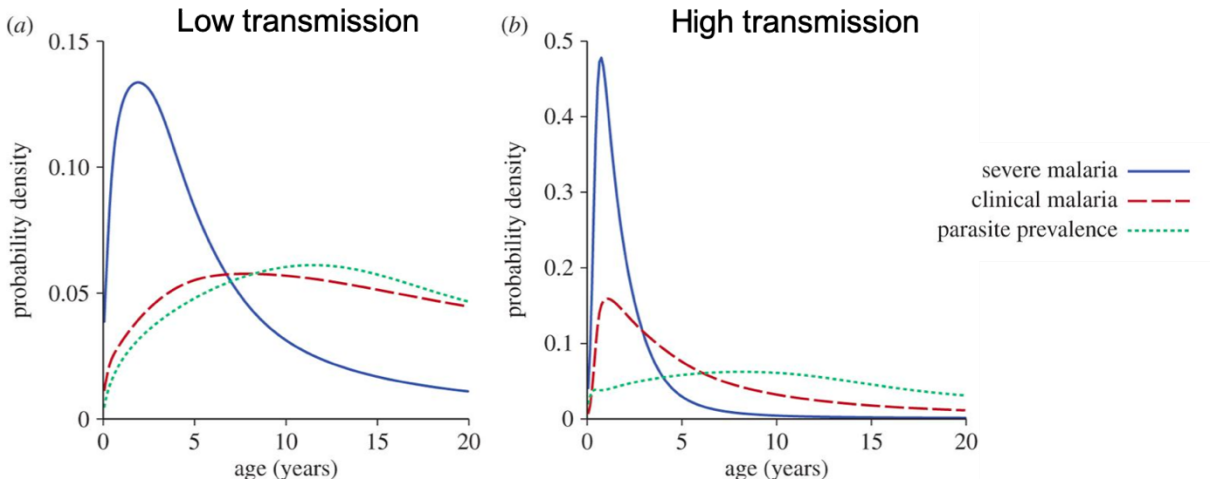

Figure 1.2: Modeling the prevalence of parasites and symptoms from malaria through age *Adapted from Griffin et al (2015)[22].*

1.1.4. Treatment and diagnosis

Diagnosing malaria generally involves methods to detect parasites in blood. Malaria has traditionally been diagnosed by microscopy on blood films usually stained by Giemsa stain[24]. Microscopy remains the gold standard and most popular tool used in the clinic[25]. It is relatively cheap to perform and accessible even in rural and remote settings. Examination of slides allows quantification of parasite density and speciation

of the infecting *Plasmodia*. However, reading slides requires skilled microscopists and inherent in this is variability in interpretation between individuals and laboratories. Microscopy is also relatively insensitive with an estimated detection threshold of 50 parasites / μl of blood[25].

Another more recent development has been rapid diagnostic tests (RDTs) which are increasingly being used in general clinical settings[25]. RDTs are immunochromatography-based tools which use monoclonal antibodies (mAb) against parasite antigens embedded in a test strip. A positive result is indicated by a coloured line appearing on the strip where antigen binds the mAb. RDTs are cheap and much simpler to use than microscopy resulting in better standardisation. Speciating malaria infections is not possible by RDT, although some tests now allow *P. falciparum* infections to be distinguished from infections caused by other species.

Other methods based on nucleic acid amplification have been developed[26]. The most established is qPCR – a quantitative extension to the polymerase chain reaction (PCR). Here, primers specific to 18S rRNA genes are used to amplify *Plasmodia*-specific DNA[27]. Quantification is facilitated by a fluorescent probe which binds to amplified DNA. The method is highly sensitive, able to detect down to approximately 10 parasites / ml, with even more sensitive adaptations still being developed. It also facilitates standardisable absolute quantitation of parasite densities. qPCR is more expensive per test than RDT or microscopy and requires more upfront capital investment, making it currently a less-feasible option for routine clinical use. However nucleic acid-based methods are commonly used in clinical research settings.

Treatment guidelines for malaria have been set by the WHO[28]. The first line treatment for uncomplicated malaria caused by *P. falciparum* in non-special-risk groups is artemisinin-based combination therapy (ACT), e.g. artemether-lumefantrine or artesunate-amodiaquine. Severe infection is treated with intravenous or intramuscular artesunate followed by ACT. Chemoprophylaxis is also available for travellers or special-risk groups and ACT is not generally used for this purpose. In most cases ACT or IV artemisinin has sterile efficacy against *P. falciparum* and resolves infection completely but there is growing concern about the spread of antimalarial drug resistance[29]. Artemisinin is used in combination with other compounds to minimise the risk of resistance developing. However, a recent report suggests that a genetic mutation which confers resistance against an ACT using dihydroartemisinin and piperaquine has spread rapidly amongst parasites across southeast Asia[30]. Concerns exist about these resistant strains spreading to other continents with high disease burdens, such as Africa. Resistance to older first-line treatments such as chloroquine have spread almost universally across regions where *P. falciparum* is present[28] and the same might happen for ACT as well without intervention. This underlines the need for an efficacious malaria vaccine to complement ongoing control strategies.

1.2. Malaria – immunology

1.2.1. The immune system

The human immune system is broadly composed of two arms; the innate and adaptive. Both arms play key roles in the control of infectious diseases and there is much cross-over between the two. The innate immune response is fast-acting but does not

improve with prior exposure to a particular pathogen and is not pathogen-specific. It is generally insufficient for the complete control and clearance of a pathogen alone. The adaptive immune response requires parts of the innate system for initiation and learns to tackle specific pathogens in a targeted and specific manner. Through the development of 'immune memory', the adaptive response improves in terms of speed and effectiveness with prior exposure to the pathogen. The adaptive immune response is the most effective system to combat infectious agents. The development of the immune response to malaria through naturally acquired immunity and the design of malaria vaccines primarily functions through the training of the adaptive immune response.

1.2.2. The innate immune response

If an infectious pathogen breaches the primary defences, such as the mucosal barriers and the skin, it initially comes into contact with the innate immune system. This system is comprised of both cellular and soluble protein components.

Cells of the innate immune system are primarily phagocytic cells, of which the two most abundant are macrophages and neutrophils[31]. These cells are responsible for ingesting pathogens and pathogen-infected cells and targeting them for destruction. Neutrophils are highly abundant and circulate in blood[32]. They are very responsive to extracellular signalling and tend to be the first cell type to reach the site of an infection. Macrophages are less abundant and are normally tissue resident[33]. They have additional functions over neutrophils in communicating between the innate and

adaptive immune systems. Both macrophages and neutrophils recognise pathogen-associated molecular patterns (PAMPs)[34] which are common and conserved molecular structures foreign to the host, such as lipopolysaccharide (LPS), found on bacterial cell surfaces. Upon recognition of these ligands by surface-bound pattern recognition receptors (PRRs), the cells engulf the pathogen by a process of phagocytosis. Inside the cell, they are destroyed by the activation of the respiratory burst which releases toxic reactive oxygen species (ROS) such as hydrogen peroxide[35].

In malaria, phagocytic cells are important in clearing infected erythrocytes[36]. In particular, macrophages in the blood (called monocytes) have been found to play an essential role in parasite clearance in mouse models[37]. The role of neutrophils on the other hand is less certain. Their levels significantly increase during malaria infection[38], however this is seen to correlate with inflammation and disease severity rather than parasite clearance[39,40]. Their activity was also associated with vascular pathology in cerebral malaria in one study[41]. Inappropriate neutrophil activity is therefore potentially linked to the immune-mediated pathology seen during malaria infection.

Other cells of the innate immune response which might play a role in immunity to malaria include dendritic cells (DCs), Natural Killer cells (NK cells) and $\gamma\delta$ T cells. DCs are another type of phagocytic cell and along with macrophages, they play an essential role in presenting antigen to cells of the adaptive immune system[42,43]. Antigens are small molecular signatures, usually peptides, which are specific to different pathogens and illicit immune responses. Cells of the adaptive immune system recognise them to mount antigen-specific immune responses. NK cells recognise a restricted set of

antigenic signatures associated with infected host cells and target them for killing. These cells play a role in clearing infected hepatocytes in liver stage infection[44] and potentially erythrocytic infection as well[45]. γδ T cells are a small population of lymphoid cells which can also recognise a limited selection of antigens. They have been seen to increase in number during malaria infection[46,47] and are potentially able to release cytotoxic granules which target merozoites[48]. Although NK cells and γδ T cells share some similarities to adaptive immune cells, they are capable of recognising only a limited set of antigens and are therefore considered to be innate-like immune cells.

Another important feature of the innate immune response to malaria is the cytokine response. Cytokines are small signalling molecules secreted by different immune cell types[49]. When an innate immune cell recognises a pathogen, it triggers the release of pro-inflammatory cytokines and these drive the process of inflammation. The role of inflammation is to recruit further immune cells, complement and acute-phase proteins to the site of the infection. Although there are measurable cytokine responses to pre-erythrocytic stages of the malaria parasite, it is the blood stage that triggers the inflammation associated with clinical malaria[20].

Specific pro-inflammatory cytokines that have been shown to play an important protective role in the control of parasitaemia in malaria include Tumour necrosis factor alpha (TNFα)[50,51], Interferon gamma (IFNγ)[52,53], Interleukin 12 (IL-12)[54] and Interleukin 18 (IL-18)[55]. However all these cytokines have also been implicated in the immunopathology of malaria as well[56]. In one study, TNFα concentrations were significantly higher in children with cerebral malaria than those without[57] whilst IL-12

and IFNγ have been associated with liver injury in mouse malaria models[58] as well as progression to cerebral malaria[59] and malarial anaemia[60].

Overall these data suggest that a certain level of an innate inflammatory response to malaria is necessary to control infection. However, over-exuberant responses lead to immunopathology and ultimately death. Through repeated exposures, the innate immune system must be trained to respond proportionately to malaria infection.

The innate immune response to malaria is summarised in Figure 1.3.

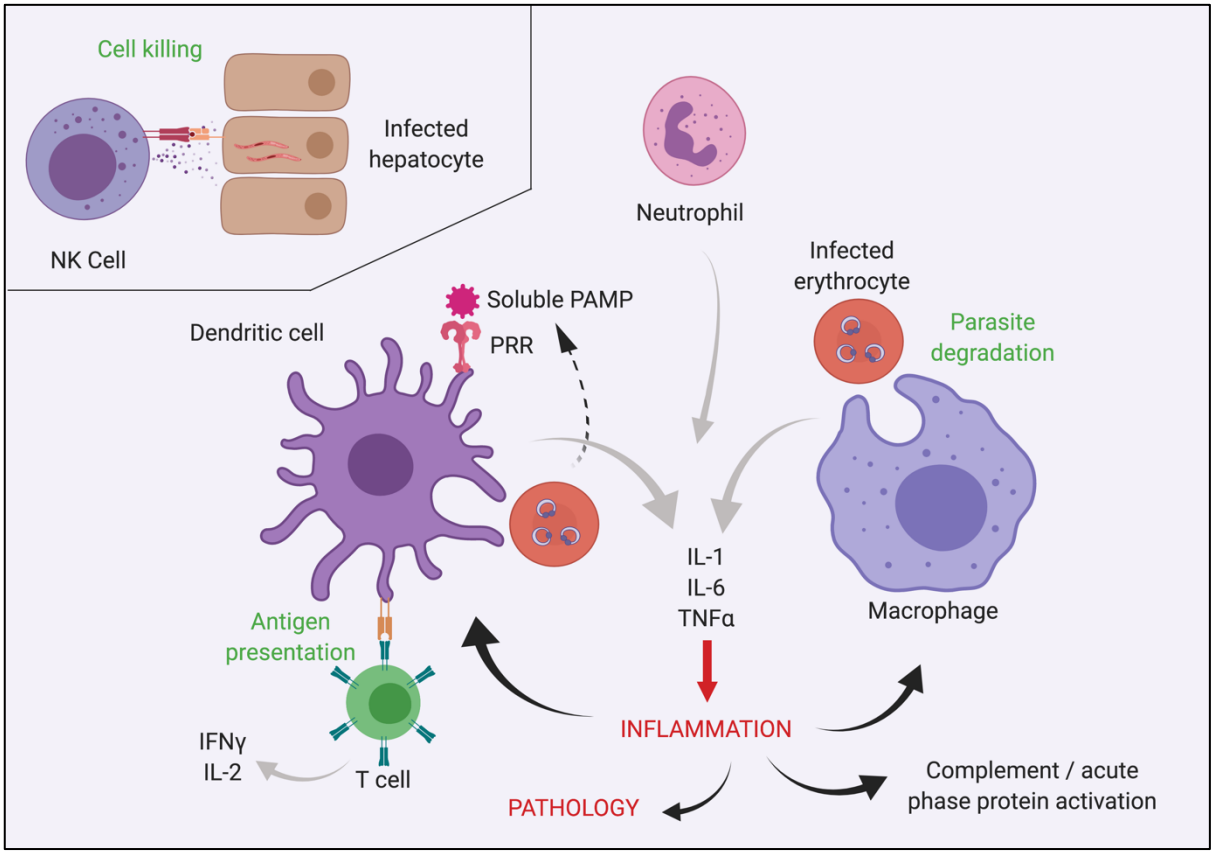

Figure 1.3: The innate immune response to malaria *(Figure by R. Morter, designed in BioRender.com).*

1.2.3. The adaptive immune response

1.2.3.1. Biology of adaptive immunity

The second arm of the immune system is adaptive immunity. Lymphocytes are the cells involved in this arm of the response, of which T and B cells are the primary subsets[61]. T and B cells have diverse receptors (TCR and BCR) which are able to recognise different antigens. Lymphocytes are clonal for only one receptor and are thus specific for only one antigenic epitope. Lymphocyte responses are described as 'antigen-specific'. Before these cells encounter antigen for the first time they are said to be naïve and do not have their effector functions activated.

T cells recognise cognate antigens presented on major histocompatibility complexes (MHC) via the TCR. Cognate TCR-MHC interactions cause intracellular signalling pathways which initiate cellular activation processes. The T cell population is composed of CD4+ and CD8+ T cells. CD4+ T cells respond to antigen presented on MHC class II molecules which are exclusively expressed by professional antigen presenting cells (APCs) such as DCs and macrophages. CD4+ T cells respond to exogenous and endogenous antigens from the pathogens and infected host cells that APCs phagocytose. CD8+ T cells bind antigen presented on MHC class I which is expressed on all nucleated cells. CD8+ T cells therefore primarily respond to endogenous antigens from intracellular pathogens.

CD4+ T cells are called T 'helper' cells and help to orchestrate immune responses[62]. There are different subsets of CD4+ T cells, of which Th1 and Th2 are the best-characterised. The subset a CD4+ T cell becomes is dependent on the context in

which it experiences antigen (e.g. the anatomical location or the cytokine milieu). Th1 CD4+ T cell responses are dominated by the production of IFNγ which helps activate CD8+ T cells to tackle intracellular infections as well as production of complement-fixing antibodies. Th2 responses are initiated in response to extracellular pathogens, are dominated by the production of IL-4 and IL-5 to promote the function of B cells. There are other subsets with more niche functions such as Th17 and Regulatory T cells which will be discussed separately.

CD8+ T cells are also called cytotoxic T cells[63]. In recognising antigen expressed on MHC I, these cells identify infected host cells. Upon recognition of an infected host cell, they then degranulate and release cytotoxic molecules such as perforin, granulysin and granzyme B which cause cell lysis and apoptosis via activation of caspases.

B cells[64] express BCRs which are effectively surface-bound antibody molecules. When a BCR binds to its cognate antigen, the cell engulfs the whole receptor-ligand complex and antigenic peptide is presented on MHC II. The B cell then has to interact with a CD4+ T cell which recognises the MHC-bound antigen in order to become fully activated. The B cell receives further signalling from the T cell to initiate activation and differentiation into an effector cell known as a plasma cell. These cells are capable of producing large amounts of soluble antibody.

Antibodies are small soluble proteins which bind to their cognate antigens with high affinity. They have various functions to protect the host from infectious pathogens[65]. Firstly, antibodies can cause infectious particles to agglutinate by cross-linking, which

makes them easier to detect and phagocytose. They can also neutralise pathogens by binding to their ligands, preventing interactions with host receptors. Antibodies also activate complement-mediated attack, enhance the phagocytic activity of phagocytes by opsonisation and cause antibody-dependent cellular cytotoxicity by binding to infectious particles, which assists their recognition by other components of the immune response.

There are different isotypes of antibodies, each of which is adapted to perform specific functions[66]. The prevailing isotype varies depending on the type and location of pathogen they are intended to target. Naïve B cells express immunoglobulin M (IgM) and IgD. When an activated B cell receives co-stimulation from a CD4+ T cell, the additional signalling it receives from the T cell can dictate what isotype the B cell begins to express. This process is called class switching[67]. There are three further isotypes that B cells can express, IgG, IgA and IgE. IgG is the most abundant isotype expressed in humans. Another process B cells go through following activation is called somatic hypermutation[68]. This is where the BCR sequence mutates to generate diversity and the cells possessing receptors with greatest affinity for the antigen are selected for survival and further differentiate into memory B and plasma cells.

When naïve lymphocytes experience antigen for the first time, the response is slow since co-stimulation from other cells is required for activation to ensure the response is necessary. The response is also not optimised since B cell class switching and somatic hypermutation as well as CD4+ T cell subsetting needs to occur. Most activated lymphocytes will apoptose after infection, however a subset will remain and are described as ‘memory’ cells since they have previously experienced antigen[69].

Upon re-experiencing their cognate antigen, the response from memory cells will be much more rapid[70]. Memory cells require less co-stimulation to become active and they have an increased propensity to proliferate and differentiate into effector cells targeting the invading pathogen. Class switching and somatic hypermutation has already occurred in the case of B cells and CD4+ T cells will belong to the most effective subset. This is the reason why for many pathogens, subsequent infections are either less severe or do not occur at all because the adaptive immune response, through antigen experience, is already trained and primed to deal with it effectively.

1.2.3.2. Adaptive pre-erythrocytic immunity to malaria

The adaptive immune response to malaria differs between parasite life cycle stages. Infectious sporozoites are extracellular pathogens before they invade hepatocytes. An antibody response with robust B cell and Th2-type T cell induction is functionally the most suitable response to neutralise the parasite at this stage by preventing binding of the sporozoite to hepatocyte receptors. However, the speed at which the parasites migrate to and enter hepatocytes during natural infection makes it difficult for them to be detected by the immune system. Sero-epidemiological studies have shown antibodies against the most abundant protein on the sporozoite surface, circumsporozoite protein[71] (CSP) are difficult to detect in all but the most highly exposed individuals living in hyperendemic settings[72,73]. These studies also showed a significant age-related effect where anti-CSP antibodies were only frequently detected in older adults[74]. This is evidence that natural anti-sporozoite immunity is difficult to develop and is a cumulative effect of frequent and sustained infection over a long period of time. There is also a lack of evidence that naturally-acquired anti-CSP antibodies correlate with protection. One study in an endemic area in Kenya revealed

no difference in anti-CSP antibody titre between people who became re-infected over a 96-day follow-up period and those that did not[75]. Nevertheless, various vaccines against malaria based on the CSP antigen have been developed with demonstrable efficacy by inducing higher antibody titres than naturally occur[76,77].

The hepatocytic stage of infection is intracellular and the lack of clinical illness induced at this stage again suggests it is mostly immunologically quiescent. Because it is intracellular, an effective immune response would be CD8+ T cell and Th1-type CD4+ T cell dominated. CD8+ T cells might control hepatocyte infection in two ways, either by lysing infected cells which express MHC-bound parasite-specific antigen on their cell surfaces or preventing intrahepatic spread of parasites via localised secretion of IFNγ and other pro-inflammatory cytokines[78]. Significant work has been done to identify protective pre-erythrocytic T cell epitopes which are processed and presented on MHC molecules by infected hepatocytes. Numerous studies have found naturally-occurring CD8+ T cell responses against CSP[79–81] and one even showed that these were associated with absence of blood-stage parasitaemia[82,83]. Other immunogenic antigens which have been identified in different studies include Liver-stage antigen 1 (LSA-1)[84,85] and thrombospondin-related adhesion protein (TRAP)[86–88]. Data on the protective efficacy of naturally-acquired responses to LSA-1 is mixed but generally suggests a protective function. One study reported that IFNγ production to LSA-1 peptide was associated with reduced parasite prevalence[89] and a delay in time to reinfection[85]. Another suggested that CD8+ T cell proliferation to LSA-1 rather than IFNγ production correlated with protection from clinical malaria[90]. Other studies report instead that concentrations of an anti-inflammatory cytokine IL-10 in response to LSA-1, rather than IFNγ, is correlated with protection[91–93]. For TRAP, again the picture is

mixed with some studies suggesting natural responses are very low and do not correlate with protection[88], whilst measuring TRAP responses with different assays did show an effect[94,95].

Overall, naturally-occuring responses to liver-stage antigens such as TRAP and LSA-1 are found to be low and this may underlie some of the heterogeneity between different studies. However, in studies where robust responses were seen, there did seem to be a correlation with protection. These findings have encouraged the development of these antigens as vaccine candidates.

1.2.3.3. Acquired immunity to blood-stage malaria

The blood stage of *P. falciparum* infection is the most immunogenic, inducing broad and high-magnitude responses. However, because of the complexity of parasite-host interactions at this stage, our knowledge of the mechanistic processes is still incomplete. It is known that antibody responses to blood stage antigens can play an important role in protection. Early experiments showed that transferring IgG from immune adults to infected children resulted in reduced parasitaemia and resolution of febrile illness[96]. The most immunogenic antigens are merozoite surface ligands, and anti-merozoite antibodies mediate protection by neutralising merozoite interactions with red blood cells to prevent invasion. However there is much heterogeneity in the profiles of antibodies raised against different antigens between individuals and they appear to be difficult to acquire, requiring years of repeated infections[97]. It is still not clear which particular antigens are most important for antibody responses, which has hindered vaccine design[98]. One of the major problems is that there are many different *P. falciparum* parasite strains which have genetically diverse surface antigens[99] and

parasites can switch on and off the expression of different antigens during the course of a blood stage infection as a mechanism for immune evasion[100]. This means exposure to many different parasites through multiple infections is required to generate a repertoire of antibodies which facilitate measurable protection.

The adaptive cellular response to blood-stage infection is also complex and even less-well understood than antibody responses. CD4+ and CD8+ T cells do appear to be induced by blood-stage infection and the response appears to be Th1-skewed with the production of IFNγ[101]. Pro-inflammatory cytokines produced by T cells may be important for controlling the growth of parasites in erythrocytes[102]. However the same pro-inflammatory cytokines are implicated in the pathology of severe malaria[103]. This may indicate that there is a balance to be found between generating enough inflammation to illicit a protective response and limiting inflammation to prevent pathology.

There is some evidence that the adaptive immune response to malaria can develop a regulatory element, including the expansion of anti-inflammatory regulatory T cells (Tregs) which suppress the function of other immune cells. In very young children who have not yet experienced enough malaria episodes to acquire a fully protective antibody repertoire against malaria, rapidly developing regulatory responses may be the only way to protect themselves against pathology and ultimately death[104]. Tregs responses are seen during malaria infection[105] and anti-inflammatory cytokines also begin to be upregulated[106,107]. Higher ratios of anti- to pro-inflammatory cytokines appear to be protective of severe malaria[108]. However, there is also debate as to whether these responses are helpful or whether the malaria parasite is hijacking this

mechanism as a means to escape immune pressure[109,110]. There is some evidence that *P. falciparum* itself drives expansion of Tregs populations[111,112] and that higher Treg and anti-inflammatory responses promote parasite growth[113,114]. Consistent with this, it appears *P. falciparum* drives other immune changes which might promote its survival. The half-lives of anti-malarial antibodies are estimated to be considerably shorter than for other pathogens[104,115,116]. Markers of phenotypic exhaustion have been seen to be upregulated on B and T cells in individuals chronically exposed to malaria[117] and atypical B and T follicular helper cells with impaired function are expanded in malaria-exposed individuals[118,119]. The role of immunoregulation, Tregs and the balance of pro- and anti-inflammatory responses to malaria constitutes a significant focus of this thesis so will be reviewed in greater depth separately.

The adaptive immune response to *P. falciparum* malaria is summarised in Figure 1.4.

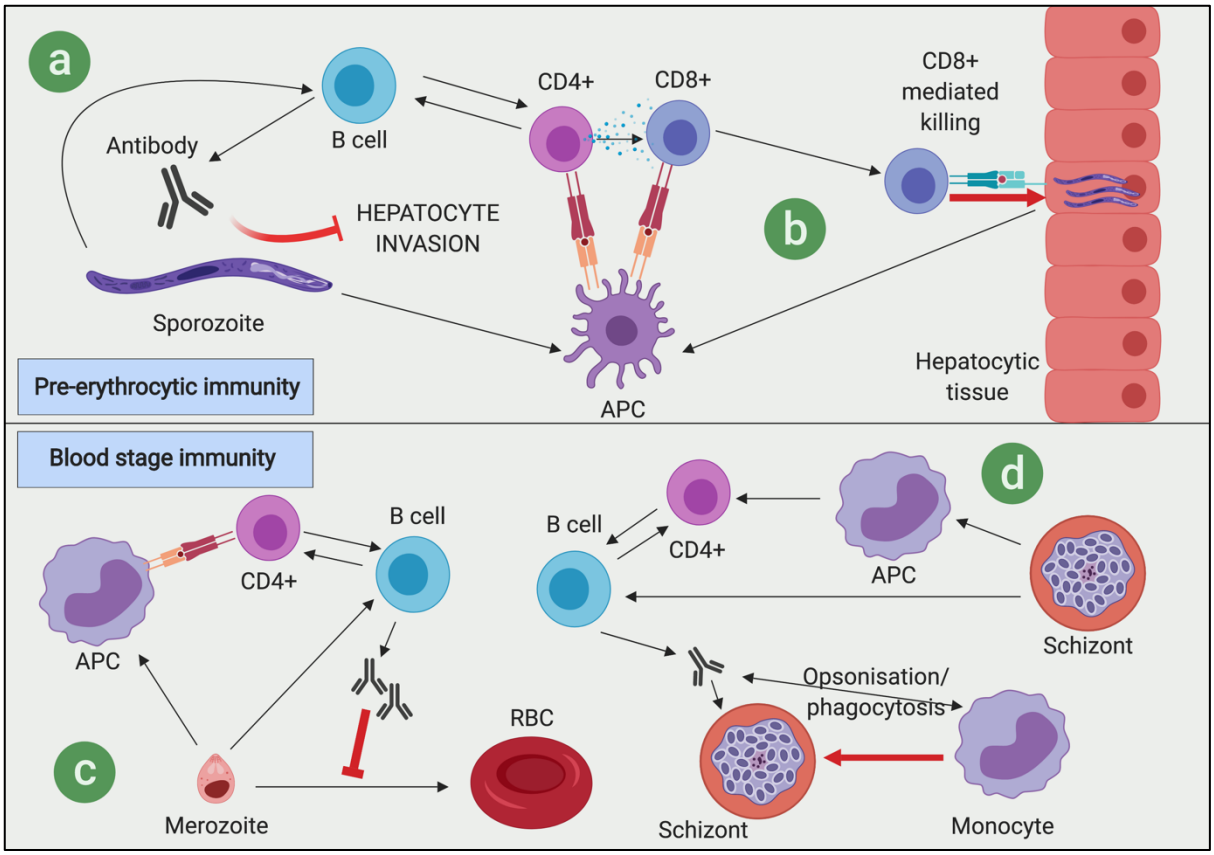

Figure 1.4: Adaptive immunity to malaria ***(a)*** *humoral response to sporozoite invasion.* ***(b)*** *cellular response to hepatocyte infection.* ***(c)*** *humoral response to block merozoite invasion.* ***(d)*** *response to clear infected red blood cells. (Figure by R. Morter, designed in BioRender.com).*

1.3. Malaria – vaccines

1.3.1. Current approaches and progress

Owing to the complexity of the parasite life cycle and the challenges in understanding the mechanisms of NAI to malaria, progress in developing an efficacious vaccine has been slow. Nevertheless, numerous strategies are currently being developed and tested in clinical trials.

1.3.1.1. Whole sporozoite vaccines

The first vaccine developed against *P. falciparum* malaria was a whole sporozoite vaccine (PfSPZ). Here, sporozoites are viable but attenuated by radiation which arrests their development in the liver. This approach potently induces both cellular and humoral immunity against pre-erythrocytic infection. As early as 1973, this regimen was shown to be efficacious in malaria-naïve humans, providing >90% protection against homologous CHMI[120,121]. Since then, the whole sporozoite approach has been advanced further by Hoffman and colleagues[122]. Numerous regimens have been tested with different doses, intervals and routes of administration, but efficacy appears lower in Phase II trials when tested in malaria-endemic settings such as Mali compared to the USA[123,124]. The whole sporozoite approach has also been advanced by attenuating the parasites genetically (GAP) or using unattenuated parasites with chloroquine cover (CVac), which prevents blood-stage infection but not liver-stage. The advantage of these approaches is that parasites arrest later in liver stage infection which increases their immunogenicity and decreases the dose required. Both products are in early stages of development but the chemoattenuated vaccine has been assessed in clinical trials in the USA where 100% sterile efficacy was achieved with considerably fewer sporozoites than are required for irradiated sporozoite approaches[125]. To date the whole sporozoite approach has achieved the highest efficacy of any malaria vaccine, but issues with scalability of production and the complex logistics needed for its deployment as well as the reduced efficacy in target populations has hindered its advance.

1.3.1.2. Subunit sporozoite vaccines

The most clinically advanced vaccine for malaria, RTS,S, was first developed in the 1980s and recently received approval from the WHO for pilot implementation in 3 African countries[126]. RTS,S is a virus-like particle (VLP) encoding 18 copies of the NANP repeat region of the main sporozoite surface protein CSP fused to a Hepatitis B surface antigen (HBsAg) backbone adjuvanted in AS01[127]. It induces humoral immunity against CSP which prevents infection by preventing sporozoite gliding motility, invasion and traversal of hepatocytes[128,129]. The time taken from sporozoite injection to hepatocyte invasion is relatively short meaning high antibody titres are required for efficacy. Despite receiving pre-licensure status, the vaccine only induces partial protection which quickly wanes. Over a 38 month follow-up, field efficacy against clinical malaria in 5-17 month-old infants was 36% following a standard 4-dose regime in a large Phase III trial[130]. Recently, a modified version of RTS,S called R21 has been developed at the Jenner Institute, University of Oxford[131]. R21 has an improved ratio of CSP to HBsAg particles compared to RTS,S (of 1:1 rather than 1:4), and is adjuvanted in Matrix M. The aim of this is to improve vaccine immunogenicity and reduce the dose required. Clinical trials of this vaccine are currently underway including Phase II trials in malaria-endemic settings.

1.3.1.3. Liver stage vaccines

Another major approach currently in development at the Jenner Institute uses viral vectors encoding pre-erythrocytic antigens[132]. Vaccines of this type will be studied in this thesis. The most commonly used viral vectors are replication-deficient viruses that can still infect somatic human cells. They are engineered to encode antigens of interest which are translated and transcribed by infected cells and expressed on MHC

molecules. This potently induces both cellular and humoral immunity, particularly CD8+ T cell responses[133]. Viral vectored vaccines have been successfully developed for a range of diseases including Ebola[134] and Hepatitis C[135] as well as certain cancers including prostate cancer[136] and demonstrate good safety profiles in clinical trials. For malaria vaccines, two vectors are commonly used, chimpanzee Adenovirus, strain 63 (ChAd63) and modified vaccinia Ankara (MVA). ChAd63 can infect human cells, but does not circulate in the environment naturally meaning anti-vector immunity is minimised. It is rendered replication deficient through deletion of the E1 genomic region and is manufactured in HEK293T cells[137]. MVA was rendered replication-deficient by serial passage through chick embryo fibroblasts. ChAd63 and MVA are commonly administered in combination in a prime-boost regimen with an 8-week interval. They encode the same antigen but using heterologous vectors mitigates the effects of anti-vector immunity which would impact immunogenicity of the second dose[138]. The most advanced viral vectored vaccine for malaria encodes the TRAP antigen of the T9/96 strain of *P. falciparum*, plus a multi-epitope string (ME-TRAP)[133]. TRAP has been shown to be essential for hepatocyte invasion and the motility of sporozoites[139]. The ME string contains mainly CD8+ T cell epitopes as well as some CD4+ T cell and B cell epitopes from potentially protective antigens including CSP, TRAP and LSA1[140]. So far, this vaccine has progressed to Phase IIb field efficacy trials in both adults and infants in sub-Saharan Africa with a good record of safety[141]. In UK adults, sterile efficacy was achieved in 21% [3/14] individuals undergoing heterologous CHMI following vaccination[133]. A delay to patency was seen in a further 36% of volunteers. In Kenyan adults, efficacy against infection was 67% over an 8 week follow-up[142]. However, in 5-17 month-old Burkinabe infants the vaccine failed to induce any significant protection[143]. In both UK and Kenyan efficacy trials, the

magnitude of $CD8^+$ T cell responses was shown to correlate with protection[144]. Discovery and evaluation of other potentially protective antigens which could be used in viral vectors is still ongoing[145].

1.3.1.4. Blood stage vaccines

Current approaches to developing blood stage vaccines focus on the generation of antibodies which block merozoite invasion of erythrocytes. The most clinically-advanced candidates use the merozoite surface antigen 'Reticulocyte binding homolog 5 (PfRH5)' expressed either in viral vectors or as a VLP. PfRH5 is a conserved protein shown to be essential for red blood cell invasion by merozoites[146]. Results on the immunogenicity of the viral vectored regimen have already been published[147] and efficacy studies using the VLP are currently underway. A viral vectored regimen has also been tested for two other blood stage antigens, MSP-1 and AMA-1 but neither vaccine showed any impact on parasite growth rates[148]. The data from these trials suggested higher antibody titres might be more protective, meaning the VLP approach will be favoured in future trials over viral vectors for PfRH5. The main difficulties in designing vaccines for blood stage infection are the significant antigenic diversity of parasites infecting erythrocytes and redundancy in parasite invasion pathways[149]. It has also been shown that merozoite infection of erythrocytes is exceptionally fast meaning induction of antibodies with high titres and affinity is required[150]. Efforts continue to identify more conserved antigens which are essential for parasite function.

1.3.1.5. Transmission blocking vaccines

Finally, transmission blocking vaccines are also being developed for *P. falciparum* malaria. These do not confer protection in the vaccinee but should prevent transmission to another host, making them useful as a public health control measure. Transmission blocking vaccines have been designed to induce antibodies which are taken up by a feeding mosquito and inhibit the development of post-gametocyte life cycle stages. Numerous antigenic targets have been identified including Pfs25[151], Pfs47[152] and Pfs230[153]. Although transmission blocking vaccine efficacy was demonstrated in animal models many years ago[154], the challenge in human trials has been raising antibodies at high titres against these relatively non-immunogenic antigens. Clinical trials are still in the early stages and focus is on formulating the vaccines with appropriate adjuvants to increase immunogenicity.

Current approaches to malaria vaccine design are summarised in Figure 1.5.

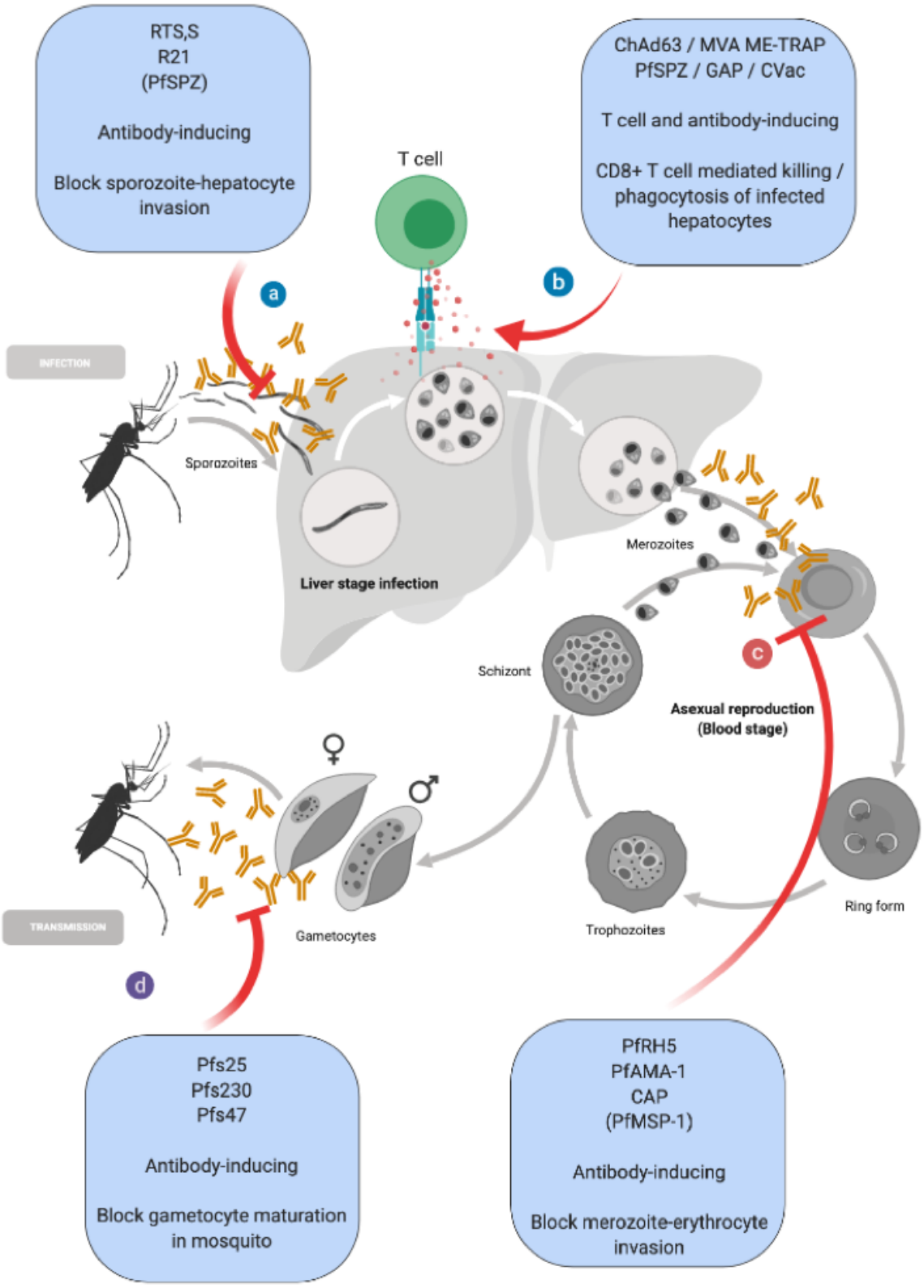

Figure 1.5: Current approaches to vaccine design for P. falciparum malaria ***(a)*** *Pre-erythrocytic invasion-blocking vaccines* ***(b)*** *Pre-erythrocytic cell-targeting vaccines* ***(c)*** *Blood-stage vaccines* ***(d)****Transmission-blocking vaccines. (Figure by R. Morter, designed in BioRender.com).*

1.3.2. Evidence for suppressed vaccine responses in malaria-endemic areas.

Few vaccines afford complete efficacy in any population. But crucially, many vaccines have been shown to perform considerably worse in developing countries where malaria is most common compared to developed countries. The most substantial reductions in efficacy in the developing world are seen in orally administered vaccines, such as those for polio and rotavirus infection. Second generation rotavirus vaccines show improved efficacy over their predecessors but are still less immunogenic in the tropics[155]. The only licensed tuberculosis (TB) vaccine, Bacillus Calmette-Guérin (BCG) is known to be less efficacious at lower latitudes, particularly in protecting against classical pulmonary TB in adults[156,157]. There is some evidence that protection against childhood TB is slightly worse in tropical regions too[158]. Measles vaccination results in lower seroconversion rates in developing countries[159] and the incidence of primary vaccine failure is higher[160]. Polysaccharide-based vaccines for pneumococcus and *Haemophilus influenzae* B appear to work well and have had significant impact on the reduction in acute respiratory infections in developing countries, however there is still evidence that responses to them can be negatively impacted and in these settings[161,162].

Overall, most routinely used childhood vaccines perform sub-optimally in populations who require them the most. It would be pertinent to investigate any similar effects for a malaria vaccine deployed in these communities as well. Limited data is available for experimental malaria vaccines, but in the data that does exist, there is consistent evidence of reduced responses when tested in malaria-endemic populations. The leading candidate vaccine for malaria, RTS,S/AS01B has shown efficacy in malaria-

naïve adults in Europe of greater than 80%, whilst field efficacy in Africa is consistently lower[163,164]. For ChAd63 / MVA ME-TRAP, antigen specific T cell frequencies reduced approximately two-fold in The Gambia and four-fold in Kenya, compared to the UK in Phase I and II clinical trials[165]. Whole sporozoite approaches tested by CHMI in both North America and Africa also experience reduced efficacy in malaria-endemic populations[123,124]. Further monitoring of reduced effectiveness of malaria vaccines, and the mechanisms behind it, should be undertaken.

It is possible to speculate on the reasons behind suppressed responses in malaria-endemic areas. Malnutrition is common in tropical settings and has been shown to negatively impact immune function[166]. Chronic viral and parasite infections as well as repeated episodes of malaria are also common in these locations. This may drive accelerated immune exhaustion and senescence[167,168]. Finally, some infectious diseases, including malaria are associated with an upregulation in suppressive and regulatory immune responses[105] which may impact responses to vaccines. The impact of regulatory responses on immunity to malaria and vaccination will be studied in this thesis.

1.4. Malaria and immunoregulation

1.4.1. Regulatory T cells

Regulatory T cells (Tregs) are an immunosuppressive subset of CD4+ T cells, normally associated with maintaining tolerance against self-antigens and preventing autoimmune and chronic inflammatory disorders[169]. Their function is to negatively regulate the activity of other immune cells, particularly other subsets of CD4+ T cells,

to prevent them making inappropriate immune responses that might be damaging to the host[170]. Tregs are defined by expression of the IL-2 receptor alpha (CD25)[171] and the transcription factor FoxP3[172,173].

Two separate mechanisms occurring in the thymus and the periphery respectively, are thought to lead to the differentiation of Tregs[174]. Thymic Treg development is a product of the process which generates diverse TCRs. Clonal TCR diversity is generated through the somatic recombination of segments of genes encoding the receptor recognition site. This is a random process and can create TCRs which bind to self-antigens, which would be damaging if released into the periphery[175]. T cells possessing TCRs specific to ubiquitously expressed self-antigens are removed in the thymus by apoptosis. However, TCRs can also bind to tissue-specific antigens which T cells might only encounter when they move to the periphery. In the thymus, medullary thymic epithelial cells can ectopically express tissue-restricted self-antigens via the transcription factor Aire[176]. If a precursor CD4+ T cell, called a thymocyte, recognises and binds to self-antigen under Aire expression, it begins to express CD25 and becomes a precursor Treg. Stimulation from the proximal secretion of IL-2 and IL-15[176] then drives expression of FoxP3 within the cell, causing it to become committed to the Treg lineage[177]. Bone marrow derived APCs can also take up blood borne antigen in the periphery and present it to thymocytes in the thymus to drive Treg development[178].

Thymocytes have to bind with high affinity to self-antigen in the thymus to drive Treg differentiation. If weak binding occurs, cells are released into the periphery as naïve CD4+ T cells. Conventional naïve CD4+ T cells can be driven towards a Treg

phenotype by exposure to anti-inflammatory cytokines such as Transforming growth factor beta (TGF-β) upon antigen recognition in tolerogenic environments such as the gut[179]. Chronic, low concentration exposure to antigens can also drive Treg commitment[180]. A large proportion of peripherally-induced Tregs are specific to the commensal microbiota[181]. Peripheral Tregs are functionally indistinguishable from thymically-derived cells.

Tregs possess multiple mechanisms enabling them to suppress the activity of other immune cells thereby potentially affecting vaccine responses. Not only can Tregs suppress the activity of T cells and B cells, they can also affect APCs which subsequently suppresses adaptive immune responses. Suppression occurs at all stages of activity from activation, proliferation and differentiation to effector function and is mediated by either contact-dependent mechanisms or via soluble factors. Firstly, Tregs produce large amounts of TGF-β and IL-10. TGF-β signalling via TGF-β receptors regulates the Smad family of transcription factors, which potently downregulate an array of genes involved in activation, proliferation and effector function in T cells, B cells and some myeloid cells[182]. IL-10 acts in a similar manner but signalling via its cognate receptor activates the transcription factor STAT3 which in T cells, negatively regulates the expression of pro-inflammatory cytokines, particularly TNFα[183]. It also limits activation of macrophages[184]. IL-10 signalling has also been shown to inhibit the maturation of monocytes into dendritic cells and suppress the MHC-II antigen presentation pathway[185,186].

Another suppressive mechanism used by Tregs involves signalling via the coinhibitory molecule CTLA-4. CTLA-4 is homologous to CD28 on effector T cells, which is

required for costimulation. CTLA-4 can out-compete CD28 in binding to CD80/CD86 on APCs thereby reducing cell-cell contact between effector T cells and APCs[187]. CTLA-4 is also thought to be able to capture CD80/CD86 from the surface of APCs targeting it for degradation within the Treg cell by endocytosis[188].

The final major mechanism used by Tregs is IL-2 starvation. Tregs constitutively express very high levels of CD25 on their surface. IL-2 is essential for the initial activation of naive CD4+ and CD8+ T cells upon antigen stimulation as well as for optimal differentiation into memory subsets[189]. Tregs consume available IL-2 via CD25 thus preventing effector T cell activation and differentiation.

All Treg mechanisms can suppress effector immune cells in a non-antigen specific manner leading to so-called 'bystander suppression'. Tregs primarily use these mechanisms to limit the activity of other immune cells against self-antigens, however there is increasing evidence that Tregs might also be involved in the immune responses to infectious diseases, including malaria.

1.4.2. Role of Tregs in immunity to malaria

The frequency of Tregs in blood has been observed to increase during malaria infection. In a study in The Gambia, Treg frequencies significantly increased in people exposed during the malaria transmission season compared to the dry season[105]. CD4+ CD25+ CD69- Treg frequencies and FoxP3 mRNA in blood also significantly increased during blood stage infection in malaria-naïve individuals undergoing

controlled human malaria infection (CHMI) in the UK[113]. Treg upregulation during malaria infection has also been replicated in multiple murine experiments[190–192] and *in vitro* cell cultures stimulating PBMC with parasite extract[111,112]. Similar findings have also been shown in human infections with *P. vivax*[193].

Despite good evidence that Treg responses are upregulated during infection, there is still uncertainty about what role they play in determining parasite growth outcomes and whether they limit effective anti-parasite immune responses. Murine studies paint a confusing picture with some showing Treg responses to be associated with protection[194,195], whilst in others they increase susceptibility of severe disease forms[191,196]. Other studies show Tregs have no effect on disease outcomes in mice[190,197,198]. In humans, most studies either show Treg responses increase susceptibility and severity of disease or have no effect on disease outcome. In a UK CHMI study, increased Treg responses as well as an early peak in plasma TGF-β concentration during blood stage infection were associated with faster parasite growth rates[113]. A follow-up study showed that higher pro-inflammatory cytokine concentrations over anti-inflammatory cytokines were associated with more rapid control of parasite growth[114]. Another study assessing susceptibility to natural infection in rural Kenya showed having high levels of CD25+ CD4+ T cells increased the risk of developing clinical malaria[94]. The Fulani people who live across West Africa are known to be partially resistant to clinical malaria and genetic studies show they have deficient Treg and TGF-β function[199,200]. Another study showed that a highly suppressive subset of Tregs expressing TNFRII was associated with severe malaria[201]. However other studies have shown no relationships between the magnitude of the Treg response and severity of disease[202,203].

Given that the pathology of malaria disease is associated with excessive inflammation and that Tregs might suppress this process, it cannot be ruled out that these cells might also have protective effects. Some studies speculate that the timing of a Treg response might be important whereby a response later on in infection might limit immunopathology whilst a response too early would cause hyperparasitaemia[110].

There is evidence that Tregs might limit the acquisition and function of protective anti-parasite immunity to malaria. In a study in The Gambia, depletion of CD25+ cells in *in vitro* culture of PBMC from exposed individuals caused significant increases in supernatant concentrations of IFNγ, IL-2 and IL-10 in response to parasite stimulation[204]. Other studies have also shown inverse relationships between Treg activity during infection and memory T cell responses up to 150 days post-infection[113,202,205]. A recent study demonstrated in both human and murine malaria infection that Tregs limited the acquisition of adaptive immunity primarily through CTLA-4 activity[206].

If Tregs are antagonistic to the acquisition of protective immunity and increase susceptibility and severity of infection, it is possible that through repeated infections the immune response might be trained to minimise the effects that Tregs have. One study in children in Uganda showed a marked decline in Treg frequencies in individuals with history of greater prior malaria incidence[207]. There was also a trend towards reduced risk of symptomatic infection in individuals with lower Treg frequencies. Two other studies in Indonesia found that children asymptomatically carrying *Plasmodium* parasites had lower Treg frequencies compared to uninfected

controls, however these cells also appeared to express greater levels of TNFRII and were more reactive[208,209].

The mechanism by which malaria parasites might cause Treg frequencies to increase has also been studied. Parasites were found to not have to interact directly with Tregs to do this[111,210,211]. Instead, APCs act as intermediaries, of which monocytes in particular probably have the greatest contribution. Small soluble components secreted by parasites are likely to alter the phenotype of monocytes which directs the upregulation of Treg activity[112]. The identity of the soluble components has not yet been defined. The parasite metabolic by product, haemozoin, was previously implicated, however one study excluded this on the basis of size[112]. It is thought the unidentified soluble component causes monocytes to become a suppressive phenotype which secretes IL-10 and TGF-β[111]. An anti-inflammatory cytokine milieu can cause the conversion of naïve CD25- CD4+ T cells into Tregs though induction of FoxP3 expression. Importantly, this process happens independently of TCR engagement, therefore converted T cells are not specific for blood-stage *P. falciparum* antigens. The consequence of this is that Treg mediated immune suppression from malaria infection may be broad and could dampen responses to heterologous antigens, including vaccines.

It is important to note that the immunoregulatory effects of malaria have been reported for other parasitic infectious diseases as well[212,213]. Many of these infections are co-endemic in areas of active malaria transmission[214,215]. Increased Treg frequencies have been observed during most helminth infections including schistosomiasis[216], filariasis[217], ascariasis and trichiuriasis[218]. Similar mechanisms behind the conversion

of naïve CD4+ T cells to Tregs are reported to exist for other parasitic infections as well[219,220].

Overall, evidence suggests that parasitic pathogens, such as *P. falciparum*, evolved mechanisms to induce Treg responses as a means to establish infection and promote survival by mitigating anti-parasite immune responses. However, it remains to be determined the extent to which Tregs might also be beneficial to the host by helping to limit excessive inflammation and consequential pathology. Questions also remain about how the Treg response changes with successive malaria exposures, how the response differs between adults and children and between areas with different transmission intensities. The effect that Tregs acquired from malaria infection might have on the suppression of responses to heterologous antigens also needs to be investigated.

A schematic summary of Treg upregulation by parasitic infections, and immunosuppressive Treg mechanisms is shown in Figure 1.6.

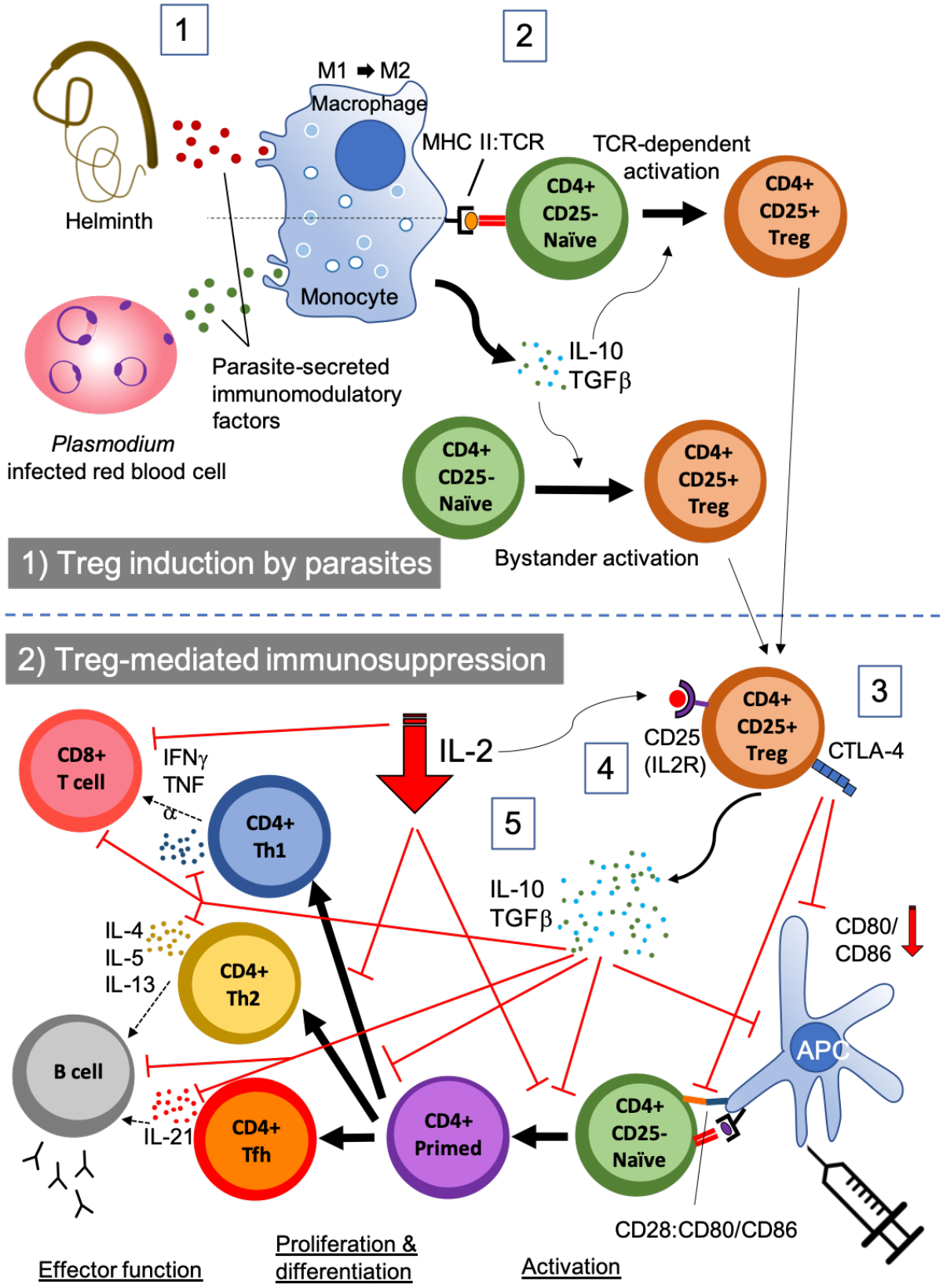

Figure 1.6: Possible mechanism of Treg conversion by parasites and mechanisms of immunosuppression. *(Figure by R. Morter).*

It is important to acknowledge that malaria infection has been implicated in other degenerative changes in immune phenotype as well, which may also contribute to the promotion of parasite survival and the reduction in responses to vaccination. As mentioned previously, accelerated immune senescence and T cell exhaustion has been seen following malaria infection[168]. A subset of T follicular helper cells with impaired capacity to help B cells are preferentially activated during malaria[118]. Atypical memory B cells are seen to expand in individuals in malaria-endemic areas[119] and these cells have reduced ability to proliferate and generate antibody[221]. Malaria has also been shown to inhibit the maturation of DCs[222], which in turn reduced their ability to activate T cells[223].

1.4.3. Tregs in the context of other regulatory immune mechanisms

Tregs exist as one component of many which serve to regulate immune responses and maintain immune homeostasis. Although Tregs have been predominantly described in relation to CD4+ T cells, there is evidence that regulatory CD8+ T cells exist as well[224]. CD8+ Tregs are able to recognise auto-reactive CD4+ T cells and are thought target them primarily by apoptosis through cytotoxicity[225] or to inhibit their activiation through expression of CTLA-4[226] and IL-10[227,228], in a smilar fashion to CD4+ Tregs. Regulatory B cells (Bregs) have also been identified[229]. These cells contribute to the control of inflammation by secreting IL-10[230] and TGF-β[231] and as such act upon multiple immune cell subsets. It is thought Bregs are activated by inflammation in situations such as auto-immunity and therefore act as a balancing mechanism[232].

Additionally, the innate immune system has regulatory components which contribute to the control of the immune system. Innate lymphoid cells (ILCs) are a group of innate immune cells which posess some properties of lymphocytes, but lack TCRs or BCRs[233]. NK cells, described in section 1.2.2 are a type of ILC. Regulatory ILCs have been recently identified[234]. These cells operate primarily in the intestine to regulate the activity of other ILCs. ILCregs are activated by local inflammation and produce IL-10 in response. This negatively regulates the activity of ILC1 cells (which includes NK cells) as well as ILC3 cells, to balance the inflammation to which these cells contribute.

Antigen presenting cells including macrophages can be polarised to become anti-inflammatory cells under certain conditions[235]. Classically, inflammatory macrophages have been described as M1 macrophages and anti-inflammatory macrophages as M2. M2 macrophages produce large amounts of IL-10 and TGF-β to modulate the activity of other immune cells locally, including Tregs[236]. Macrophages differentiate into M2 cells via many different stimuli, including IL-10 signalling and the presence of apoptotic cells. They are primarily thought to contribute to the resolution of inflammation towards the end of a pathological process[237] and to wound healing[238].

Finally, some metabolic factors also contribute to the regulation of the immune response. Expression of the enzyme indoleamine 2,3 dioxygenase-1 (IDO-1) catalyses the degradation of tryptophan as part of the kynureine pathway[239]. Activation of IDO-1 in different tissues has been shown to activate mature circulating Tregs, as well as drive FoxP3 expression in naïve CD4+ T cells, thus promoting a regulatory phenotype. Expression of IDO-1 can be upregulated by increasing concentrations of multiple cytokines, including both pro- and anti-inflammatory[240]. In particular, IFNγ and

TGF-β have been shown to be important in inducing IDO-1 expression in DCs[241,242]. IFNγ mediated induction promotes responses which balance inflammation, whilst TGF-β serves in a positive feedback loop to further increase Treg responses.

Overall, these regulatory responses work alongside CD4+ Tregs to prevent excessive inflammation and promote tolerance to self-antigen. The mechanisms also promote activation of each other, primarily through convergent signalling via IL-10 and TGF-β. It is important to recognise that any CD4+ Treg response to *P. falciparum* would occur alongside these other regulatory mechanisms, although exploration of them all was beyond the scope of this thesis.

1.5. Using CHMI to investigate naturally-acquired immunity to malaria

Despite ongoing efforts spanning more than 30 years, we still understand relatively little about the complex parasite-host interactions involved in *P. falciparum* infection. Because of this, there still remains no truly efficacious vaccine against infection. It is clear that efforts to design better vaccines will require more knowledge of the mechanisms underpinning protective immune responses to natural infection.
Methodological limitations have also played a part in slowing the progress made so far in this field.

Many infectious diseases have useful animal models in which infection can be carefully investigated and the data more easily translated into the human context. Malaria infection lacks an animal model which accurately reflects the infectious

process seen in humans. Wild-type *P. falciparum* cannot infect mice and outcomes from mouse infections with murine Plasmodial species can differ dramatically to human infections. The strain of mouse and the species of parasite used can also lead to different experimental outcomes. These factors have been attributed to the sometimes conflicting conclusions drawn from different animal studies[109] and the lack of relevance to human infection.

In human immunoepidemiological studies, investigators have traditionally opted for an approach combining cross-sectional surveys of antibodies followed by cohort study designs for episodes of malaria in order to identify immune correlates of protection. This approach can be confounded by numerous factors. For example, variation in exposure within a single endemic setting means some individuals may be classified as 'protected' when in fact they were never exposed[243]. Natural infections are also genetically heterogeneous[244] meaning different effector immune mechanisms which may act upon different parasite strains cannot be readily distinguished.

Controlled human malaria infection (CHMI) offers a method of investigating the human immune response to infection in a tightly controlled experimental setting. CHMI involves the deliberate infection of a volunteer, either by the bite of an infected mosquito, or the injection of sporozoites or infected erythrocytes[245]. Because exposure and strain diversity is controlled for, some of the confounding effects encountered in cross-sectional studies are controlled for. The first reported cases of humans being deliberately infected with malaria happened as early as 1920 as a treatment for neurosyphilis[246]. Since the 1940s, CHMI has been used as a method of testing the efficacy of anti-malarial drugs[247], vaccines[163] and diagnostic tools[248]. During CHMI,

infection is normally allowed to progress to blood stage infection where the density of parasitaemia is monitored, either by qPCR or microscopy. Infection is terminated at a pre-defined parasitaemia, usually well-below the density at which the onset of symptomatic infection occurs. Drug or vaccine efficacy is measured by the time taken to diagnosis or sterility.

Some studies have made use of samples from CHMI vaccine studies to perform secondary exploratory analyses characterising immune responses to infection[113,114]. However only recently have CHMI studies been purposefully designed to study mechanisms of natural immunity to infection. Performing CHMI studies in people with prior exposure to malaria allows measures of naturally acquired immunity to be associated with parasite growth outcome. This allows protective and non-protective naturally acquired immune mechanisms to be identified. Until recently, few CHMI studies have been undertaken at scale in malaria endemic locations. The principal concerns involve ensuring adequate clinical and laboratory facilities, difficulties accessing infectious reagents, preventing release of non-native parasite strains into endemic areas and protecting the interests of vulnerable study participants. Pilot studies have now been performed and have provided reassurance regarding safety and ethics whilst undertaking CHMI in resource-limited settings[249–251]. Another advance facilitating the conduct of CHMI studies in malaria-endemic areas has been the development of cryopreserved, purified sporozoites to infect volunteers (PfSPZ challenge)[252,253]. Transportation to research sites is easier and more secure than with infected mosquitos and administration does not require entomological facilities. Because of this, large-scale CHMI trials are now feasible in malaria-endemic countries

to better study naturally-acquired immunity to malaria. The data from which may be useful in informing vaccine design.

1.6. Mechanisms of suppression of vaccine-induced immunity

1.6.1. Evidence for suppression from malaria and other infectious diseases

In section 1.3.2, studies showing that the immunogenicity and efficacy of experimental malaria vaccines was reduced in trials in malaria-endemic settings compared to North America or Europe, were discussed. It has been observed both indirectly and through purposefully designed clinical trials that infection with certain pathogens at the time of vaccination can result in suppressed vaccine responses. This is most pronounced in parasitic infections with helminths and malaria-causing *Plasmodium sp*. Responses to BCG are known to be suppressed during intestinal nematode infection[254], filariasis and schistosomiasis[255]. *Schistosoma mansoni* infection has been shown to suppress responses to Hepatitis B and tetanus vaccination[256]. Lymphatic filariasis and onchocerciasis also caused reduced responses to tetanus vaccination[257,258]. Trichiuris infection was shown to reduce responses to a candidate malaria vaccine[259].

Malaria infection has also been shown to reduce the immunogenicity of some childhood vaccines, namely polysaccharide vaccines against group C meningococci, *Salmonella* Typhi*, Haemophilus influenzae* and possibly tetanus[161]. In this analysis, protein-based vaccines did not appear to be suppressed by malaria infection. Polysaccharide antigens are T-independent antigens meaning they stimulate antibody responses without B cells requiring T cell help. Protein-based vaccines on the other

hand are dependent on T cell responses. T-independent antigenic responses are generally weak in young children[260], so it may not be surprising that they appear most affected by malaria-driven immunosuppression.

Since both malaria and helminth infections are almost ubiquitous in the developing world and non-existent in developed countries, they could therefore explain some of the reduced vaccine efficacy and immunogenicity observed in developing nations. Understanding the suppressive mechanisms involved is necessary to help design better vaccination strategies. As discussed, both helminths and *Plasmodium sp*. are known to induce potent regulatory responses in the host as a mechanism of promoting survival and chronicity[110,261]. A consequence of this may possibly be suppression against heterologous antigen during parasite infections.

1.6.2. Evidence for suppression of vaccine responses from Tregs

So far, most evidence of Treg-mediated suppression of vaccine responses has come from studies on BCG. One long-standing hypothesis for reduced efficacy of BCG at tropical latitudes is pre-exposure to non-tuberculous mycobacteria (NTM) antigenically similar to BCG-strain mycobacteria. Antigen-specific Tregs are thought to be primed by exposure to NTM and might then be expanded by BCG vaccination to create a critical mass of Tregs that could limit both the immunogenicity of BCG and the direct effector response against invading *Mycobacterium tuberculosis*[262]. Tregs are known to be induced by both NTM[263] and BCG[264] and are associated with worsened clinical outcomes in TB infection[265]. A direct association between NTM-derived Tregs and

reduced BCG immunogenicity has been demonstrated in a mouse model[266]. However, field studies in humans have been more conflicting with one study in The Gambia finding no evidence for NTM-derived Tregs attenuating BCG immunogenicity[267].

More recently, the heterologous effects of helminth-derived Tregs on BCG efficacy have also become apparent. Helminth infections are known to modulate responses to a wide variety of vaccines[268]. Parasite-derived Tregs are now thought to possibly account for a much of this suppression. One study showed that deworming with albendazole before BCG administration resulted in significantly better vaccine responses and this was associated with decreased levels of TGF-β[269]. The study also showed that the levels of background Th2 cytokines IL-4 and IL-5 did not vary between the albendazole-treated and placebo groups. This is important because a parasite-induced skew towards Th2-type responses could inhibit the Th1 response required for BCG to protect against TB, however in this study hypo-responsiveness to BCG was only associated with increased Treg activity and not Th1/Th2 imbalance. A similar study has recently shown that helminth-derived Tregs might suppress responses to malaria too. Albendazole treatment resulted in reduced expression of CTLA-4 and this was associated with improved *in vitro* cytokine responses to stimulation with *Plasmodium falciparum* iRBC[270]. Functional experiments have also shown helminth-derived Tregs can suppress responses to heterologous antigens. When PBMC from helminth-infected and -uninfected children are cultured with either BCG or *P. falciparum* infected red blood cells, proliferation is seen to increase after Tregs are depleted in the helminth-infected group only[271].

Although most work on the role of helminth-derived Tregs has focussed on BCG, evidence that responses to malarial antigens are also be suppressed shows that the same mechanism could affect many antigens including vaccines. It is known that malaria induces Tregs and malaria infection has been associated with reduced immunogenicity of some vaccines[161]. However, to our knowledge, the role of malaria-induced Tregs in hypo-responsiveness to heterologous vaccines has not been studied. Malaria infection could contribute a significant amount of vaccine-suppressive Tregs, particularly in areas of high transmission where children experience multiple infections each year causing almost chronic infection and thus persistently high Treg frequencies. The age profile of malaria is also relevant in the context of EPI schedules where most vaccines are administered within the first 18 months of life. Likelihood of helminth infection is biased by risk-associated behaviours and peaks in school-age children at approximately 4 years of age[272]. In malaria, clinical disease can peak at 1 year in high transmission settings and parasite prevalence rates fluctuate minimally across different age groups[22]. Therefore, malaria infection may contribute more to the development of immunosuppressive Tregs at the peak age for EPI vaccine administration than helminths.

1.7. Thesis Objectives

1.7.1. Rationale

Relatively little is known about the role Tregs play in immunity to malaria. Tregs are thought to be upregulated during infection, but their impact on disease and their

potential role in suppressing responses to heterologous antigens, including vaccines, remains to be determined.

This thesis makes use of a large CHMI study in semi-immune adults to explore the impact of Treg responses and the balance between pro- and anti-inflammatory cytokine responses on the progression of parasite growth and effector immune mechanisms.

Secondly, malaria vaccines are known to perform significantly worse in target populations in malaria-endemic countries compared to in malaria naïve individuals. The impact that malaria-induced regulatory responses have on the suppression of vaccine immunogenicity has not been previously explored. Associations between Treg activity and vaccine immunogenicity are explored in malaria-naïve Adult populations before moving to investigate these relationships in Burkinabe infants in the context of malaria exposure.

1.7.2. Aims

- Measure systemic pro- and anti-inflammatory cytokine responses, Treg responses and antigen-specific effector T cell responses to CHMI and draw associations with parasite growth.
- Describe transcriptional phenotypes for Tregs and effector T cells taken during CHMI and investigate differential expression between individuals with different parasite growth outcomes.

- Investigate relationships between Treg responses and immunogenicity of the experimental vaccine regime for malaria, ChAd63 / MVA ME-TRAP in a malaria-naïve population.
- Assess observed associations between Treg responses and vaccine immunogenicity in infant populations highly exposed to malaria in Burkina Faso and examine associations with exposure intensity using serological correlates.
- Describe transcriptional phenotypes of Tregs at baseline in Burkinabe vaccinees and analyse differential expression between high and low vaccine responders and individuals with high and low prior exposure to malaria.

1.7.3. Outline

Chapter 2: Materials and methods used in the thesis.

Chapter 3: Analysis of cellular and cytokine immune responses to CHMI in semi-immune adults.

Chapter 4: Transcriptomic analysis of T cells subsets in response to CHMI.

Chapter 5: Associations between Treg responses and immunogenicity of ChAd63 / MVA ME-TRAP in malaria-naïve adults and exposed Burkinabe infants.

Chapter 6: Effect of malaria exposure on Treg activity and vaccine immunogenicity in Burkinabe infants.

Chapter 7: Summary and discussion of findings from the thesis, including implications and future directions.

Chapter 2

2. Materials and Methods

2.1. Materials and equipment

2.1.1. Reagents

A list of all commercially-available reagents and non-standard consumables used in these experiments is shown in Table 2.1.

Reagent / Consumable	***Supplier***	***Catalogue No.***
4-nitrophenylphosphate disodium salt hexahydrate (4NPP) tablets	Sigma-Aldrich	N2765
96.96 Dynamic Array IFC for gene expression	Fluidigm	BMK-M-96.96
AlbuMAX™ II Lipid-rich BSA	Thermo Fisher (Gibco)	11021037
Anti-human CD127, BV605	Biolegend	351334
Anti-human CD127, BV785	Biolegend	351330
Anti-human CD137, PE-Cy7	Biolegend	309818
Anti-human CD14, e450	Thermo Fisher (eBioscience)	48-0149-42
Anti-human CD154, BV711	Biolegend	310838
Anti-human CD19, e450	Thermo Fisher (eBioscience)	48-0199-42
Anti-human CD25, PE-Cy5	Biolegend	302608
Anti-human CD25, PE-Cy7	Biolegend	302612
Anti-human CD28 (functional grade)	Thermo Fisher (eBioscience)	16-0289-01
anti-human CD3 (functional grade)	Mabtech	3605-1-1000
Anti-human CD3, AF700	Thermo Fisher (eBioscience)	56-0038-82
Anti-human CD3, APC-Cy7	Thermo Fisher (eBioscience)	A15440
Anti-human CD4, APC	Thermo Fisher (eBioscience)	17-0049-42
Anti-human CD45RA, APC-Cy7	Biolegend	304128

Anti-human CD49d (functional grade)	Thermo Fisher (eBioscience)	16-0499-85
Anti-human CD8, APC-AF700	Thermo Fisher (eBioscience)	47-0088-43
Anti-human CD8, e450	Thermo Fisher (eBioscience)	48-0088-42
Anti-human FoxP3, PE	Biolegend	320208
Anti-human Ki-67, FITC	Thermo Fisher (eBioscience)	11-5699-42
Aqua LIVE/DEAD ™ for 405$_{nm}$ excitation	Thermo Fisher (Invitrogen)	L34957
ArC ™ Amine reactive compensation bead kit	Thermo Fisher (Invitrogen)	A10346
Benzonase® nuclease	Merck Millipore	70664
Beta mercaptoethanol (50 mM)	Thermo Fisher (Gibco)	31350010
Beta mercaptoethanol (99.0%)	Sigma-Aldrich	M6250-10ML
Bovine Serum Albumin, lyophilised (BSA)	Sigma-Aldrich	A9418-100G
Brefeldin A (1000X)	Thermo Fisher (eBioscience)	00-4506-51
Casein blocker 1% in PBS	Thermo Fisher	37528
Casyton fluid	OLS Omni Life Science	5651808
CFSE staining kit	Biolegend	423801
Diethanolamine buffer (5X)	Thermo Fisher	34064
Dimethyl Sulphoxide (DMSO)	Sigma-Aldrich	D2650
DNA binding dye & sample loading reagent kit	Fluidigm	BMK-M10-96.96-EG
ELISA diluent	Mabtech	3652-D2
Exonuclease I, (20 U/μl)	New England Biolabs	M0293L
Foetal calf serum (FCS)	Labtech International	FCS-SA/500
Foxp3 / Transcription Factor Staining Buffer Set	Thermo Fisher (eBioscience)	00-5523-00
Gentamycin (10 mg/ml)	Thermo Fisher (Gibco)	15710-049
Giemsa stain	Sigma-Aldrich	GS500-500ML
Glycerolyte 57 buffered glycerin	Baxter	4A7831
Goat anti-human IgG (γ chain)-Alkaline phosphatase	Sigma-Aldrich	A3187
HEPES buffer (1M)	Thermo Fisher (Gibco)	15630-106
Human Latent TGF Beta ELISA development kit	Mabtech	3550-1H-6
IFN alpha Human matched pair	Thermo Fisher (Invitrogen)	BMS216MST
IFN gamma Human uncoated ELISA kit	Thermo Fisher (Invitrogen)	88-7316-77
IgE Human uncoated ELISA kit	Thermo Fisher (Invitrogen)	88-50610-76
IL-1 beta Human uncoated ELISA kit	Thermo Fisher (Invitrogen)	88-7261-77
IL-10 Human uncoated ELISA kit	Thermo Fisher (Invitrogen)	88-7106-77
IL-17a Human uncoated ELISA kit	Thermo Fisher (Invitrogen)	88-7176-77
IL-2 Human uncoated ELISA kit	Thermo Fisher (Invitrogen)	88-7025-77
IL-4 Human uncoated ELISA kit	Thermo Fisher (Invitrogen)	88-7046-77
L-glutamine 200mM	Sigma-Aldrich	G7513-100ML
LEGENDplex™ HU Essential Immune Response Panel (13-plex)	Biolegend	740929
Lymphoprep ™	STEMCELL Technologies	07851
MACS-CS columns	Miltenyi Biotec	130-041-305

Monensin (1000X)	Thermo Fisher (eBioscience)	00-4505-01
Non-essential amino acids (100X)	Sigma-Aldrich	M7145-100ML
Nuclease-free water	New England Biolabs	B1500S
NUNC MaxiSorp ELISA 96-well plates	Thermo Fisher (Invitrogen)	44-2404-21
OneComp eBeads™ compensation beads	Thermo Fisher (Invitrogen)	01-1111-42
Paraformaldehyde (PFA) (16% w/v)	Alfa Aesar	43368
PBS bottle (500 ml)	Sigma-Aldrich	D8537-500ML
PBS powder	Thermo Fisher (Gibco)	21600-069
PBS tablets	Sigma-Aldrich	P4417-100TAB
Penicillin-Streptomycin solution (100X)	Sigma-Aldrich	P0781-100ML
Preamp mastermix kit	Fluidigm	100-5581
Reverse Transcription Master Mix	Fluidigm	100-6297
RNAprotect cell reagent	Qiagen	76526
RNase-free DNase set	Qiagen	79256
RNaseZap	Sigma-Aldrich	R2020-250ML
RNeasy mini kit	Qiagen	74106
RPMI-1640 cell culture medium	Sigma-Aldrich	R0883-500ML
Sodium Azide (NaN_3)	Sigma-Aldrich	S2002
Sodium Hypoxanthine	Sigma-Aldrich	H9636-25G
Sodium pyruvate (100 mM)	Sigma-Aldrich	S8636-100ML
SsoFast EvaGreen Supermix with low Rox	Bio-Rad Laboratories	172-5211
Staphylococcal enterotoxin B (SEB)	Sigma-Aldrich	S4881
TaqMan™ gene expression assay - human Beta-2-microglobulin	Thermo Fisher (TaqMan)	4331182 (Assay ID: Hs99999907_m1)
TaqMan™ Universal Master Mix II with UNG	Thermo Fisher (TaqMan)	4440038
TE Buffer	Thermo Fisher (Invitrogen)	12090015
TMB substrate kit	Biolegend	421101
TNF alpha Human uncoated ELISA kit	Thermo Fisher (Invitrogen)	88-7346-77
Trypan blue (0.4%)	Thermo Fisher (Gibco)	15250061
Tween-20	Sigma-Aldrich	P7949-500ML

Table 2.1: List of reagents and consumables used in experimental procedures

2.1.2. Buffers and solutions

R0 medium: RPMI-1640 cell culture medium (Sigma-Aldrich, St. Louis, Missouri) containing 1% Penicillin-Streptomycin (Sigma-Aldrich) and 2 mM L-glutamine (Sigma-Aldrich).

R10 medium: as R0, plus 10% FCS (Labtech Intl, Heathfield, UK).

sR10 medium: as R10, plus 1% non-essential amino acids (Sigma-Aldrich), 1 mM sodium pyruvate (Sigma-Aldrich), 25 mM HEPES buffer (Thermo Fisher, Waltham, Massachusetts), 30 μM β-mercaptoethanol (Thermo Fisher), 1 μg/ml anti-CD28 (Thermo Fisher) and 1 μg/ml anti-CD49d (Thermo Fisher).

PBS/Tween: 1X PBS, plus 0.05% Tween-20 (Sigma-Aldrich).

FACS Buffer: 1X PBS, plus 0.1% BSA (Sigma-Aldrich) and 0.01% NaN_3 (Sigma-Aldrich).

'Yellow' incomplete parasite culture medium: RPMI-1640, plus 37.5 mM HEPES, 2 mM L-glut, 25 μg/ml gentamycin (Thermo Fisher), 0.2% w/v glucose, 6 mM sodium hypoxanthine (Sigma-Aldrich).

'Blue' complete parasite culture medium: As for 'yellow' parasite culture medium, plus 10% AlbuMAX™ II (Thermo Fisher).

2.2. Clinical trials

The data presented in this thesis utilises samples taken as part of CHMI and vaccine clinical trials and includes secondary analysis of data collected as objectives of the parent studies. Data from the CHMI-SIKA trial is presented in chapters 3 and 4. Data from vaccine trials is presented in chapters 5 and 6. Summaries of the clinical trials are provided below.

All trials were performed under guidelines set by Good Clinical Practice (GCP) and the Declaration of Helsinki (2008). Ethical approval was sought from relevant UK committees and boards local to the study site for international trials. All studies were registered on the clinicaltrials.gov registry. Written informed consent was given by all participants or their responsible adult for enrolment in the trial and use of their samples in laboratory analyses. Independent monitoring of safety and regulatory compliance was sought for each trial.

2.2.1. CHMI-SIKA

Controlled human malaria infection in semi-immune Kenyan adults (CHMI-SIKA) received ethical approval from the Oxford Tropical Research Ethics Committee (OxTREC, 2-16) and by the Kenya Medical Research Institute Scientific and Ethics Review Board (ref. KEMRI/SERU/CGMR-C/029/3190). The trial is registered on the clinicaltrials.gov registry under study no. NCT02739763. The full clinical trial protocol has been published elsewhere[273]. Details pertaining to the recruitment, screening and

consent of participants as well as the production and administration of the PfSPZ Challenge product (Sanaria Inc., Rockville, Maryland) is contained within the published protocol. A description of clinical and experimental procedures relevant to the exploratory immunology analyses presented in this thesis are included in section 3.2. Recruitment to CHMI-SIKA began in April 2016 and is currently ongoing.

2.2.2. ME-TRAP vaccine trials

The ChAd63 ME-TRAP vaccine was manufactured to good manufacturing practice (GMP) standard at the Clinical Biomanufacturing Facility, University of Oxford. MVA ME-TRAP was manufactured by Impfstoffwerk Dessau-Tornau GmbH, Rosslau, Germany under GMP.

Vaccines were administered to adult participants intramuscularly (IM) to the deltoid muscle of the arm. Infants (<2 years old) were vaccinated IM into the anterolateral thigh.

UK volunteers were recruited at either the Centre for Clinical Vaccinology and Tropical Medicine (CCVTM), Churchill Hospital, University of Oxford; National Institutes for Health Research (NIHR) Southampton Clinical Research Facility, University Hospital Southampton or NIHR Imperial Clinical Research Facility, Hammersmith Hospital, London. Infant volunteers in the VAC50 trial were recruited at Unité de Recherche Clinique de Banfora (URC-B), Banfora, Burkina Faso by the study team from Centre National de Recherche et de Formation sur le Paludisme (CNRFP), Ouagadougou, Burkina Faso. Volunteers in the VAC47 trial were recruited at Roi Badouin Hospital,

Guédiawaye, Dakar, Senegal by the study team from Université Cheikh Anta Diop (UCAD), Dakar, Senegal.

A summary of regulatory approvals for the ChAd63 / MVA ME-TRAP trials included in this thesis is shown in Table 2.2.

Trial code	*Dates*	*UK ethical approval*	*Local ethical approval*	*NCT registration*
VAC43[274]	Jul 2011 – Jan 2013	NRES Committee South Central - Oxford A 10/H0604/96	n/a	NCT01364883
VAC45[144]	Apr 2012 – Oct 2012	NRES Committee South Central - Oxford A 12/SC/0037	n/a	NCT01623557
VAC47[275]	Jun 2012 – Mar 2013	OxTREC 05-12	Conseil National d'Ethique pour la Recherche en Santé SEN12/02	NCT01658696
VAC48[276]	Oct 2012 – Oct 2014	NRES Committee South Central - Oxford A 12/SC/0036	n/a	NCT01669512
VAC50[143]	Dec 2012 – Mar 2014	OxTREC 41-12	National Ethics Committee for Health Research, Burkina Faso – CERS 2012-6-37	NCT01635647

Table 2.2: Summary of ChAd63 / MVA ME-TRAP clinical trials included in thesis

Clinical and experimental procedures relevant to the analyses presented in this thesis; including the trial groups included in sub-analyses, vaccine dosing and blood sampling timepoints, are presented in Section 5.2.

2.2.3. EBL06 Ebola vaccine trial

EBL06[277] was a clinical trial of the vaccine regimen against Ebola, ChAd3 / MVA EBO-Z. The trial was conducted at the Centre Hospitalier Universitaire le Dantec (CHUD), Dakar, Senegal. Regulatory approval was sought from OxTREC (27-15) and Conseil

National d'Ethique pour la Recherche en Santé (SEN15/19). The trial was registered under NCT02485912.

Volunteers were vaccinated with viral vectors encoding the surface glycoprotein of the Mayinga strain of the Ebola Zaire virus (EBO-Z). Prime vaccination was by a chimp adenovirus (serotype 3) manufactured under GMP by the Vaccine Research Center, Bethesda, Maryland, USA. Boost was with an MVA encoding the same antigen manufactured under GMP by Emergent BioSolutions, Gaithersburg, Maryland, USA.

Further clinical and experimental details relevant to the analysis in this thesis are presented in Section 5.2.

2.3. Clinical trial lab assays

Some assays were performed as part of parent clinical trial procedures from which data is incorporated in this thesis. Brief descriptions of the procedures are outlined below. The division of responsibility for performing these assays is outlined in the statement of authorship.

2.3.1. Malaria qPCR

qPCR was performed in real-time as the main diagnostic tool during CHMI. Blood was collected in EDTA vacutainers at required timepoints and DNA extracted on a

QiaSymphony automated DNA extraction robot. The qPCR assay was set up as previously described[148].

2.3.2. ELISA (anti-schizont)

An ELISA assay was performed to measure anti-schizont IgG in plasma at screening as a correlate of prior exposure and immunity to malaria in CHMI volunteers, as previously described[278]. Coating antigen was prepared in-house from the lysate of cultured *P. falciparum* (3D7 strain) erythrocytic schizonts.

2.3.3. ELISpot (ME-TRAP[274] and EBO-GPZ[277,279])

Ex vivo IFNγ ELISpot assays were performed on fresh PBMC as the primary readout of cellular immunogenicity in clinical vaccine trials. Cells were plated in triplicate at 2.5 x 10^5 cells / well and stimulated with peptide pools of 20mer peptides overlapping by 10 amino acids spanning the length of the ME-TRAP or EBO-GPZ antigenic insert. Peptides were pooled at 10 peptides per pool to a concentration of 10 µg/ml. Negative (media only) and positive (0.04 µg/ml staphylococcal enterotoxin B and 10µg/ml phytohaemagglutinin-L) controls were also included for each sample. Stimulations were left to occur for 18-20 hours before development.

2.3.4. Intracellular cytokine staining (ME-TRAP[274])

Intracellular cytokine staining (ICS) was also performed on fresh, peptide-stimulated PBMC at selected timepoints following vaccination. All 20mer peptides spanning the ME-TRAP insert were pooled in a single megapool at 10μg/ml each, to which 2 x 10^6 PBMCs were added. Media was supplemented with 1 μg/ml anti-CD28 and anti-CD49d. Negative (media only) and positive (10 μg/ml staphylococcal enterotoxin B) controls were included for each sample. Stimulations were left to occur for 16-20 hours with brefeldin A and monensin added at 1 μg/ml each after 2 hours. Washed cells were stained and acquired by flow cytometry as described in section 2.4.6.

2.3.5. ELISA (TRAP & EBO-GPZ)

ELISA was performed to measure anti-TRAP and anti-GP IgG responses following vaccination. Assays were performed on thawed serum samples as previously described for TRAP[274] and EBO-GPZ[277,279].

2.3.6. Plasma & PBMC separation and storage

Plasma and PBMC samples taken as part of the CHMI and vaccine clinical trials were processed and stored until required for use in the laboratory procedures described in section 2.4. Blood was collected in heparinised blood collection tubes and plasma and PBMC were fractioned by established density gradient centrifugation methods[280] using

Lymphoprep™ (STEMCELL Technologies, Vancouver, Canada). Plasma was collected and stored in aliquots at -80°C until required. PBMCs were isolated and resuspended in FCS containing 10% DMSO (Sigma-Aldrich) at 5-10 x 10^6 cells / ml and frozen down by slow cooling and stored in liquid nitrogen until required.

2.4. Laboratory assay methods

2.4.1. Cytokine ELISAs

Kits for performing ELISAs to quantify IL-1β, IL-2, IL-4, IL-10, IL-17a, IFNα, IFNγ and TNFα were used which only varied by the specificity of coating and detection antibodies (ThermoFisher/Invitrogen). Assays were performed as per manufacturer's instructions. 50 µl of neat thawed plasma was plated out per well alongside 8 serial dilutions of standard and incubated overnight at 4°C. Samples and standard were ran in duplicate. 100 µl of 1X room temperature TMB solution was added, followed by 100 µl of 1M H_2SO_4 after exactly 15 mins, without washing. Plates were read immediately on a BioTek Synergy HTX ELISA reader at OD_{450} (BioTek Instruments, Winooski, Vermont). Data were analysed using Gen5 software (BioTek) and concentrations inferred from the standard curve by five parameter logistic curve fit.

2.4.2. Cytokine ELISA (TGF-β1)

A human latent TGF-β1 ELISA development kit was purchased from Mabtech, (Stockholm, Sweden) and used as per manufacturer's instructions. Thawed plasma

samples were diluted in ready-to-use ELISA diluent (Mabtech) at a concentration of 1:100 and 100 μl plated out per well. Plates were developed using TMB substrate (Biolegend, San Diego, California) for 20 mins, after which 100 μl of 1M H_2SO_4 was added to stop the reaction. Plates were read immediately on a BioTek ELx800 microplate reader at OD_{450}. Data were analysed using Gen5 software and concentrations inferred from the standard curve by five parameter logistic curve fit.

2.4.3. AMA-1 and MSP-1 ELISAs

Standardised ELISAs to quantify anti-AMA-1 and anti MSP-1 IgG in plasma were developed in-house. NUNC Immuno Maxisorp plates (Thermo Fisher) were coated with 2 μg/ml of either recombinant PfAMA-1 (3D7 strain) or PfMSP-1 in PBS overnight at 4°C. Plates were washed and blocked with 1% Casein in PBS (Thermo Fisher) for 1 hour. A standard curve was prepared from pooled hyperimmune serum from Kilifi, Kenya. The top standard was diluted 1:900 in 1% casein in PBS for MSP-1 ELISAs and 1:1000 for AMA-1 and a 1:2 dilution set prepared. 50 μl of sample and standard were plated out per well and incubated for 2 hours. Samples were diluted to a minimum of 1:300 in 1% casein in PBS. Samples were plated in triplicate and standards in duplicate. 50 μl of goat anti-human IgG (γ chain) secondary antibody (Sigma-Aldrich) diluted 1:1000 in 1% casein in PBS was added per well and plates incubated for 1 hour. Development buffer was prepared using diethanolamine buffer (Thermo Fisher) diluted 1:5 in 18.5MΩ deionised water and 4NPP tablets (Sigma-Aldrich) added at a final concentration of 1 mg/ml. Plates were washed 6 times between each step with PBS/Tween. Plates were read on a BioTek ELx800 microplate reader at OD_{405} after 25 mins for MSP-1 and 15 mins for AMA-1. Data were analysed using Gen5 software

and concentrations inferred from the standard curve by five parameter logistic curve fit.

2.4.4. Total IgE ELISA

A IgE human uncoated ELISA kit was purchased from Invitrogen and procedures performed as per manufacturer's instructions. These were similar to the Invitrogen cytokine ELISAs described in 2.4.1, except, samples were diluted 1:10 in blocking buffer before plating out and plates were read on a BioTek ELx800 microplate reader at OD_{450}. Data were analysed using Gen5 software and concentrations inferred from the standard curve by five parameter logistic curve fit.

2.4.5. PBMC thawing and preparation

9 ml of R10 was dispensed into 15 ml falcon tubes for each thawed sample. Frozen PBMC vials were partially thawed by submersion in a 37°C water bath and the liquid transferred to the falcon tube. Remaining cells were rinsed out of cryotubes by transfer of R10. Falcon tubes were centrifuged at 1000 x g for 5 mins, supernatants discarded and cells washed once more in 10 ml R10. All samples except those intended for cell sorting and RNA analysis were rested with Benzonase® nuclease (Merck Millipore, Darmstadt, Germany) diluted 1:5000 in R10 and placed in an incubator at 37°C with 5% CO_2 at a concentration of 2.5 x 10^6 cells / ml. Samples for cell stimulations were rested overnight and those for cell phenotyping for 2 hours. Samples for cell stimulations were rested overnight to increase the sensitivity of assays to detect

antigen-specific cells, following published data[281]. Cells were counted using a Casy® Counter (OLS Omni Life Science, Bremen, Germany) programmed to count human cells or manually using a haemocytometer and trypan blue before downstream handling. Cell numbers used varied by experiment. Cell viability was estimated prior to downstream analysis. Any sample with a viability <50% was discarded.

2.4.6. Treg phenotyping by flow cytometry

Tregs were phenotyped immediately following thawing and resting in Benzonase® (as described in 2.4.5) or following antigen-specific stimulation assays (section 2.4.7), depending on experimental design. In most experiments, 2 x 10^6 PBMC were used for phenotyping, unless insufficient material were available. Cells were centrifuged at 1000 x g for 5 min, resuspended in FACS buffer and transferred to a 96-well V-bottom tissue culture plate for staining. Cells were pelleted and 5 μl of a 1:40 dilution of Aqua Live/Dead stain in FACS buffer was added per well and incubated for 15 min in the dark. Cells were then stained with the surface staining cocktail described in Table 2.3 for 20 min. Fixation/permeablisation was then performed using 200 μl of FoxP3 / Transcription Factor Fix/Perm Kit (eBioscience/Thermo Fisher) for 30 min. Cells were washed twice with 200 μl of the permeblisation buffer provided and stained for intracellular markers with the cocktail listed in Table 2.4 for 30 min. After a final wash with FACS Buffer, cells were resuspended in 100 μl of 1% w/v PFA in PBS for acquisition. Cells were acquired within 24 hours, either on a BD LSRII or BD LSRFortessa flow cytometer (depending on location), running FACSDiva v6.2 software (all BD Biosciences, Franklin Lakes, New Jersey). Analysis was performed

in FlowJo v10. Quality control for staining and acquisition was performed and a minimum of 5 x 10^5 lymphocyte events were required for inclusion in analysis. Compensation was performed using single stained controls – OneComp beads (eBioscience/Thermo Fisher) were used for mAbs and ArC amine reactive beads for AQUA Live/Dead stain (Thermo Fisher).

Marker	*Fluorochrome*	*Clone*	*Vol. per reaction (µl)*
CD3	AF700	UCHT1	2
CD4	APC	RPA-T4	1
CD8	e450	RPA-T8	0.5
CD14	e450	61D3	1
CD19	e450	HIB19	1
CD25	PE-Cy5	BC96	1
CD127	BV605	A019D5	1
CD45RA	APC-Cy7	HI100	1
FACS buffer	-	-	41.5

Table 2.3: Surface staining cocktail for Treg phenotyping by flow cytometry

Marker	*Fluorochrome*	*Clone*	*Vol. per reaction (µl)*
FoxP3	PE	259D	2.5
Ki-67	FITC	20Raj1	0.5
CD137	PE-Cy7	4B4-1	0.5
CD154	BV711	24-31	1
Perm buffer	-	-	45.5

Table 2.4: Intracellular staining cocktail for Treg phenotyping by flow cytometry

2.4.7. Antigen-specific Treg stimulation assay

PBMCs were set up for stimulation after overnight rest in Benzonase® as described in 2.4.5. After washing off Benzonase in fresh R10, cells were resuspended at a concentration of 2 x 10^6 PBMC / ml in R10 supplemented with anti-CD49d and anti-

CD28 at 1 μg/ml each (both Thermo Fisher). 4 tubes each of 2 x 10^6 PBMC were made per sample; one tube was stimulated with a megapool of oligomeric peptides spanning the TRAP (T9/96 strain) antigen at 2 μg/ml and another with either 1.76 x 10^8 ChAd63-AMA-1 or 6 x 10^5 MVA-PvDBP (*P. vivax* Duffy binding protein) (courtesy of Nick Edwards, Jenner Institute) as vaccine vectors encoding irrelevant antigens. TRAP peptide sequences are as described previously[274]. Two final tubes were prepared with either no stimulant added, or staphylococcal enterotoxin B (SEB) (Sigma-Aldrich) at 1μg/ml as a positive control. Samples were left to incubate for 4 hours, after which brefeldin A and monensin (both Thermo Fisher) were added at 1μg/ml each. Stimulation was left to occur for a further 2 hours. Cells were then stained and acquired by flow cytometry as described in 2.4.6. Analysis and quality control were as described in 2.4.6 with the additional criteria of 1) positive control passing if >15% of cells were activated (CD137+ Treg or CD154+ Teff) in the SEB condition and 2) <0.5% of cells activated in the unstimulated condition.

2.4.8. Parasite culture

P. falciparum parasites were cultured by established methods[282] for the schizont stimulation and PBMC proliferation assay described in 2.4.9. Blood from a parasitaemic individual undergoing CHMI was drawn and prepared for cryopreservation of viable *P. falciparum* ring-stage parasites. Red blood cells were obtained from whole blood by centrifugation (1000 x g, 5 min) and washed two times in 10 x volume of 'yellow' parasite culture media. Cells were prepared for freezing by slowly adding 0.33 x V of glycerolyte solution (Baxter, Mississauga, Ontario, Canada)

with gentle agitation and then left to stand for 5 min. A further 1.33 x V of glycerolyte was then added. Cells were frozen at -80°C overnight and transferred to liquid nitrogen for long-term storage.

To begin culture, a 1 ml glycerolyte stock vial was thawed in a 37°C waterbath, transferred to a 50 ml falcon tube and resuspended by dropwise addition of 200 μl 12% w/v NaCl in distilled water, 10 ml 1.8% w/v NaCl and 10 ml 0.9% w/v NaCl with continuous agitation throughout. The pellet was washed 2 times with 'yellow' media and resuspended in 'blue' media at a 2% haematocrit. Tissue culture flasks were gassed with 92% N_2, 3% O_2 and 5% CO_2 and incubated at 37°C. Cultures were monitored on thin blood films with Giemsa staining and media changed at least every 48 hours. Cultures were split with fresh red blood cells as required. When sufficient parasite quantities were reached, late stage trophozoites and schizonts were isolated from uninfected cells by magnetic separation by passing through a MACS-CS column (Miltenyi Biotec, Bergisch Gladbach, Germany). Purified late trophozoites and schizonts were washed off the column in 'yellow' parasite culture media and resuspended at a concentration of 2.4 x 10^8 cells / ml. Schizont extract was prepared by immersing cells in liquid nitrogen for 2 min, followed by a 37°C waterbath for 2 min. This was repeated 3 times. Extract was stored at -80°C until required. Autologous uninfected red blood cells used to split parasite cultures were mock purified on MACS-CS columns and lysed by freeze-thaw as for infected cells to use as uRBC controls in stimulations.

2.4.9. Schizont stimulation and PBMC proliferation assay

PBMC were thawed and rested overnight as described in section 2.4.5. 2 x 10^6 PBMC were resuspended in 500 μl PBS with 5% FCS containing 5 μM Carboxyfluorescein succinimidyl ester (CFSE) (Biolegend). Cells were stained for 5 min and then washed twice with 10X volume R10. Cells were then resuspended at a concentration of 2 x 10^6 PBMC / ml in sR10 and 200 μl dispensed per well in a U-bottom tissue culture flask. To each well either 5 μl of uninfected red blood cells (uRBC) (prepared as per section 2.4.8), 5 μl schizont extract (PfSE) (prepared as per section 2.4.8) or 1 μg / ml anti-CD3 antibody (Mabtech) were added. A fourth condition had no stimulant added. The volume of uRBC and PfSE extract added was equivalent to 1.2 x 10^6 cells, for an effector:target ratio of 3:1. Cultures were left to incubate for 6 days. Remaining cells not stained with CFSE cells were used for Treg phenotyping as described in section 2.4.6.

At the end of culturing, plates were centrifuged at 1000 x g for 5 min. Supernatants were carefully removed by pipetting to a fresh U-bottom plate and stored at -80°C until required for the LEGENDplex™ assay described in 2.4.10. Cells were resuspended in FACS buffer and transferred to a V-bottom plate for staining. Cells were firstly stained with 5 μl of a 1:40 dilution of AQUA Live/Dead for 15 min. Cells were then stained with surface staining cocktail described in Table 2.5 for 20 min. Cells were acquired immediately on a BD LSRFortessa flow cytometer running at 'low' speed with FACSDiva v6.2 software. Analyses were performed in FlowJo v10. Percentage proliferation calculated as the proportion of cells with CFSE fluorescence intensity less

than the undivided population. QC criteria were: >50% proliferation in anti-CD3 condition and <5% proliferation in unstimulated condition to pass.

Marker	*Fluorochrome*	*Clone*	*Vol. per reaction (μl)*
CD3	AF700	UCHT1	2
CD4	APC	RPA-T4	1
CD8	APC-AF780	RPA-T8	3
CD14	e450	61D3	1
CD19	e450	HIB19	1
FACS buffer	-	-	42

Table 2.5: Cocktail for surface staining of PfSE stimulated cells

2.4.10. Cytokine LEGENDplex™ assay

A pre-defined 13-plex LEGENDplex™ kit was purchased from Biolegend to measure the concentrations of IL-4, IL-2, CXCL10 (IP-10), IL-1β, TNF-α, CCL2 (MCP-1), IL-17A, IL-6, IL-10, IFN-γ, IL-12p70, CXCL8 (IL-8) and TGF-β1 in cell culture supernatants from stimulations described in 2.4.9. Supernatants were stored at -80°C in 96-well U-bottom polypropylene plates and thawed before use. The assay setup was performed as per manufacturer's instructions using filter plates. Samples were read immediately on a BD LSRFortessa flow cytometer using FACSDiva v6.2 acquiring 5000 beads per sample. The cytometer was set up without compensation using control fluorescent beads to manually set detector voltages as per Biolegend protocol. Analysis was performed using proprietary LEGENDplex analysis software using recommended settings. Supernatants were diluted 1:2 initially and then the assay re-ran at 1:50 to analyse CCL2, CXCL8 and CXCL10 only.

2.4.11. Treg and Teff cell sorting

PBMC were thawed as per section 2.4.5 without resting in Benzonase. A total of 4 x 10^6 cells were stained for cell sorting and the remaining cells were used for Treg phenotyping as described in section 2.4.6. Cells were washed with FACS buffer and stained with 5 μl of a 1:40 dilution of AQUA Live/Dead for 15 min. After washing, cells were surface stained with the cocktail outlined in Table 2.6 for 20 min. Cells were washed and resuspended in 300 μl FACS buffer for cell sorting. Tubes were kept on ice before sorting to prevent clumping and were strained through a cell strainer with a 35 μm mesh immediately before sorting.

Marker	*Fluorochrome*	*Clone*	*Vol. per reaction (μl)*
CD3	APC-Cy7	UCHT1	2
CD4	APC	RPA-T4	1
CD8	e450	RPA-T8	0.5
CD14	e450	61D3	1
CD19	e450	HIB19	1
CD25	PE-Cy7	BC96	2
CD127	BV785	A019D5	2
FACS buffer	-	-	40.5

Table 2.6: Staining cocktail for Treg and Teff cell sorting

Up to 20 000 cells per population were sorted directly into 200 μl RNAprotect cell reagent (Qiagen, Hilden, Germany) on a BD FACSMelody cell sorter fitted with a 70 μm nozzle running BD FACSChorus software for CHMI-SIKA samples or a BD FACSAriaII cell sorter fitted with a 70 μm nozzle running FACSDiva v6.2 software (all BD biosciences) for VAC50 samples. Cells in RNAprotect were stored at -80°C until required for RNA extraction. For each daily run, the cytometer configuration and drop

delay was QCd. A control sample was run with each batch to confirm purity of cell sorts. Compensation was set up manually each day using OneComp beads for mAbs and ArC reactive beads for AQUA Live/Dead.

2.4.12. RNA extraction and cDNA synthesis

The workspace for RNA extractions was thoroughly decontaminated with RNaseZAP™ (Sigma-Aldrich) before use. Sorted cells from Section 2.4.11 were thawed and spun in a microfuge at 14 000 rpm for 15 min to pellet cells. The RNAprotect supernatant was carefully removed by pipetting and RNA extraction carried out using RNeasy mini spin columns (Qiagen). Extraction was performed as per the manufacturer's instructions for 'purification of total RNA extractions from animal cells using spin technology'. Buffer RLT was supplemented with 1% β-mercaptoethanol (Sigma-Aldrich). An on-column DNase digestion step was included as per the manufacturer's instructions using an RNase-free DNase set (Qiagen). RNA was eluted in 30 μl RNase-free water and stored at -80°C until required. No-template extraction controls were ran with each batch.

cDNA synthesis from extracted RNA was carried out using a reverse transcription master mix kit (Fluidigm, San Francisco, California). 1 μl of reverse transcription master mix, 1 μl of extracted RNA and 3 μl nuclease-free water (New England Biolabs, Ipswich, Massachusetts) were added per reaction in a 96-well PCR plate. Thermocycling conditions were as follows: 25°C for 5 min, 37°C for 30 min, 85°C for

5 min. cDNA was then stored at -20°C until further use. No-reverse transcriptase and no-template controls were run with each batch.

The presence of human cDNA in samples was confirmed by amplification of the human Beta-2-microglobulin (B2M) gene by qPCR. A TaqMan™ gene expression assay was used with primers spanning exons of the human B2M gene (Assay ID: Hs99999907_m1,Thermo Fisher). Reactions were set up with: 5 μl TaqMan™ Universal Master Mix II with UNG (Thermo Fisher), 1 μl human B2M TaqMan™ gene expression assay, 3 μl nuclease-free water and 1 μl cDNA. Thermocycling was performed in a StepOne real time PCR machine (Thermo Fisher) with the following conditions: 2 min at 50°C, 10 min at 95°C and 40 cycles of 95°C for 15 secs and 60°C for 1 min. Confirmation of cDNA was obtained from a positive PCR amplification curve for human B2M. No template controls were ran with each batch.

2.4.13. Fluidigm gene expression assay

The expression of 96 target genes, consisting of 90 genes of interest and 6 reference genes for normalisation, was analysed using Delta Gene assays for multiplex qPCR (Fluidigm). Forward and reverse primers for the 96 target genes were designed, validated and synthesised by Fluidigm. A list of the 96 target genes and primer sequences is shown in Table 2.7.

The cDNA processed in section 2.4.12 was pre-amplified before gene expression analysis. Separate Delta Gene™ assay combined forward and reverse primer sets

were pooled at a concentration of 500 nM in TE buffer (10 mM Tris-HCl, Ph 8.0, 0.1 mM EDTA; Thermo Fisher). 0.5 μl of pooled primers, 1 μl of preamp mastermix (Fluidigm), 2.25 μl of nuclease-free water and 1.25 μl of template cDNA were mixed per reaction in an 96-well PCR plate. Amplification was then allowed to occur in a standard thermocycler under the following conditions; 2 mins at 95°C followed by 18 cycles of 95°C for 15 secs and 60°C for 2 mins. Unincorporated primers were then digested by the addition of 0.4 μl of Exonuclease I, 0.2 μl ExoI reaction buffer (both New England Biolabs) and 1.4 μl of nuclease-free water per reaction. Digestion was then allowed to occur in a standard thermocycler under the following conditions; 37°C for 30 mins, and 80°C for 15 mins for one cycle each. The pre-amplified and exonuclease-digested cDNA was diluted 5-fold in TE buffer before use.

Multiplex qPCR was performed on a 96.96 dynamic array integrated fluidic circuit chip (Fluidigm) which can perform reactions for 96 genes on 96 samples simultaneously. The chip was primed by as per manufacturer's instructions. Samples were prepared by mixing 2.5 μl of SsoFast EvaGreen Supermix with low Rox (Bio-Rad Laboratories, Hercules, California) with 0.25 μl EvaGreen™ DNA binding dye (Fluidigm) and 2.25 μl of pre-amplified, ExoI-treated cDNA. Samples were loaded onto the 96.96 IFC as per manufacturer's instructions. Each sample was ran in duplicate. Assays were prepared by mixing 2.5 μl of assay loading reagent (Fluidigm), 2.25 μl TE buffer and 0.25 μl of Delta Gene™ assay combined forward and reverse primers. The 96 assays were loaded onto the chip as per manufacturer's instructions. Mixing of samples and assays on the chip was performed using a HX IFC controller machine (Fluidigm) and samples were then loaded onto a BioMark machine (Fluidigm) for thermocycling. Real time PCR and melt-curve analysis was performed using the manufacturer-defined protocol

'GE 96x96 PCR+Melt v2' for a total of 30 cycles. No-template control samples were included on each plate. Analysis of amplification curves was performed using the Fluidigm Real Time PCR analysis software. QC methodology is described in section 2.5.2: Transcriptomic data analysis.

Gene	*Gene Name*	*Fwd Primer*	*Rev Primer*
BCL2	BCL2, apoptosis regulator	ATGTGTGTGGAGAGCGTCAA	GTGCCGGTTCAGGTACTCA
CCL4	C-C motif chemokine ligand 4	GTAGCTGCCTTCTGCTCTCC	TCTACCACAAAGTTGCGAGGAA
CCL5	C-C motif chemokine ligand 5	TATGACTCCCGGCTGAACAA	AGAGTTGATGTACTCCCGAACC
CCR1	C-C motif chemokine receptor 1	ACGGACAAAGTCCCTTGGAA	TCTGTGGTCGTGTCATAGTCC
CCR2	C-C motif chemokine receptor 2	GCTGAGAAGCCTGACATACCA	GGGAAATGCGTCCTTGTTCAA
CCR3	C-C motif chemokine receptor 3	GGACACCCTACAATGTGGCTA	TCCGCTCACAGTCATTTCCA
CCR4	C-C motif chemokine receptor 4	CCTGGCATTGCCTCACAGA	GCTCCTCAAGGCAGGTCTG
CCR5	C-C motif chemokine receptor 5 (gene/pseudogene)	TGAGACATCCGTTCCCCTACA	TGGCAGGGCTCCGATGTATA
CCR6	C-C motif chemokine receptor 6	AGGCAGCGATGTCTGTGAA	AGCTCAAGCCCCAACATCA
CCR7	C-C motif chemokine receptor 7	TGAGGTCACGGACGATTACA	CGTCCTTCTTGGAGCACAAA
CD27	CD27 molecule	CACTACTGGGCTCAGGGAAA	CCGGTATGCAAGGATCACAC
CD274	CD274 molecule	ACCAGCCGCGCTTCTGT	TCAGCAAATGCCAGTAGGTCATGAAT
CD28	CD28 molecule	GTGGAGTCCTGGCTTGCTATA	GAGCCTGCTCCTCTTACTCC
CD3G	CD3g molecule	GCCCAATGACCAGCTCTA	TTCCTCCTCAACTGGTTTCC
CD40LG	CD40 ligand	GAGGCCAGCAGTAAAACAAC	AGTTGTTGCTCATGGTGTAGTA
CD69	CD69 molecule	TCACCCATGGAAGTGGTCAA	ACACACTTGTCAGACCCTGTA
CTLA4	cytotoxic T-lymphocyte associated protein 4	CATGGACACGGGACTCTACA	AATCTGGGTTCCGTTGCCTA
CXCL13	C-X-C motif chemokine ligand 13	GGACCCTCAAGCTGAATGGATA	ACACTGGAACTGGTAGAGTTGAA
CXCR3	C-X-C motif chemokine receptor 3	AACTGTGGCCGAGAAAGCA	TTGAGGCAGCAGTGCATGTA
CXCR5	C-X-C motif chemokine receptor 5	ATCTTCTTCCTCTGCTGGTCAC	GGTATTGTCCACGGCCTTCA
CXCR6	C-X-C motif chemokine receptor 6	TCTCTGGAACAAACTGGCAAA	CTGGCTGCTGTCATTGAAAC
DPP4	dipeptidyl peptidase 4	TGCGCTTGTCACCATCA	TTTGCGACTGTCAGCTGTA
EGR2	early growth response 2	CCATCTTTCCCAATGCCGAAC	ACGACCTCTTCTCTCCAGTCA
ENTPD1	ectonucleoside triphosphate diphosphohydrolase 1	AGGTGCCTATGGCTGGATTAC	GTCCAAAGCTCCAAAGGTTTCC
FAS	Fas cell surface death receptor	GCATCTGGACCCTCCTACC	CCTTGGAGTTGATGTCAGTCAC
FASLG	Fas ligand	CTGAGGAAAGTGGCCCAT	ACAAAGTACAGCCCAGTTTCA
FOXP3	forkhead box P3	TGTGGGGTAGCCATGGAAA	GGGTCGCATGTTGTGGAA
GFI1	growth factor independent 1 transcriptional repressor	AGCCTGGAGCAGCACAAA	TGACCTCTTGAAGCTCTTCCC
GZMA	granzyme A	CCTCCGAGGTGGAAGAGAC	GTGACCCCTCGGAAAACAC

GZMB	granzyme B	CTTCTCCAACGACATCATGCTAC	CTGGGCCTTGTTGCTAGGTA
HLA-DRA	major histocompatibility complex, class II, DR alpha	CGCTCAGGAATCATGGGCTA	CGCCTGATTGGTCAGGATTCA
HLA-DRB1	major histocompatibility complex, class II, DR beta 1	GGGGTTGTGGAGAGCTTCA	CAGGGGCTGGGTCTTTGAA
ICOS	inducible T cell costimulator	GCCAACTATTACTTCTGCAACC	GAACTTCAGCTGGCAACAAA
IFNAR1	interferon alpha and beta receptor subunit 1	AGTGACGCTGTATGTGAGAAAA	ACGGGAGAGCAAATAATGCA
IFNG	interferon gamma	ACTGCCAGGACCCATATGTAA	GTTCCATTATCCGCTACATCTGAA
IFNGR1	interferon gamma receptor 1	AAGCCAGGGTTGGACAAAA	GATATCCAGTTTAGGTGGTCCAA
IKZF2	IKAROS family zinc finger 2	AGGAAAGTCCAGGAGCTTCAA	AGAAGCTCCACACTGGTTACA
IL10	interleukin 10	CCGTGGAGCAGGTGAAGAA	GTCAAACTCACTCATGGCTTTGTA
IL10RA	interleukin 10 receptor subunit alpha	TGGACACCCATCCCAAATCA	TGGAGATGGAGTTCCAGGAC
IL13	interleukin 13	CTCATTGAGGAGCTGGTCAACA	TGTCAGGTTGATGCTCCATACC
IL17A	interleukin 17A	ACTACAACCGATCCACCTCAC	ACTTTGCCTCCCAGATCACA
IL17F	interleukin 17F	CGCGTTTCCATGTCACGTA	CTGTACAACTTCCGAGGGGTA
IL18R1	interleukin 18 receptor 1	GGGAGGCACAGACACCAAAA	TGAAGACGTGGCCTGGGATA
IL1RL1	interleukin 1 receptor like 1	GGCGACCAGGTCCTTCAC	AGGGGCTCCGATTACTGGAA
IL2	interleukin 2	ACCCAGGGACTTAATCAGCAA	GCATATTCACACATGAATGTTGTTTCA
IL21	interleukin 21	CTGAATTTCTGCCAGCTCCA	TTGTTTCCTGTATTTGCTGACTTTA
IL21R	interleukin 21 receptor	TGCATCCTGGAAATGTGGAAC	CCTCGTCCTTCAGCTCTTCATA
IL23R	interleukin 23 receptor	TCAATGGGATGCAGTAATAGCC	GATGTGGCCAGAGCAGTTTA
IL27RA	interleukin 27 receptor subunit alpha	TCTGTTGTGGGTGCTTTTCCA	AGGGTCCAACTCCGTAGCA
IL2RA	interleukin 2 receptor subunit alpha	TCCTGGGACAACCAATGTCA	GTCACTTGTTTCGTTGTGTTCC
IL2RB	interleukin 2 receptor subunit beta	ATGGCCATCCAGGACTTCA	TTGCATCTGTGGGTCTCCA
IL9	interleukin 9	GGGATCCTGGACATCAACTTCC	ACTGCAGTGGCACTTGGAA
IRF1	interferon regulatory factor 1	AACAAGGATGCCTGTTTGTTCC	TGGGATCTGGCTCCTTTTCC
IRF4	interferon regulatory factor 4	CGGGCAAGCAGGACTACAA	TGTCGATGCCTTCTCGGAAC
ITGB2	integrin subunit beta 2	TCAACGAGATCACCGAGTCC	CTTATCAGGGTGCGTGTTCAC
ITK	IL2 inducible T cell kinase	CAGCCGAGACAAAGCTGAA	TGCAGTCCTGGAATCCCTTA
JAK3	Janus kinase 3	TCCTGTACGAGCTCTTCACCTA	CATCCCATCATCCGCAGGAA
KLRB1	killer cell lectin like receptor B1	GGACATTCAACAGAGCAGGAA	CTCGGAGTTGCTGCCAATATA
KLRG1	killer cell lectin like receptor G1	TGGAGGTGGGAAGATGGATCA	CACCGCATGTCTGCACAAA
LAG3	lymphocyte activating 3	TGGAGCCTTTGGCTTTCAC	GAGGGTGAATCCCTTGCTCTA
LAMP1	lysosomal associated membrane protein 1	TCCAGGCTTTCAAGGTGGAA	CCACAGCGATGGGGATCA
LCK	LCK proto-oncogene, Src family tyrosine kinase	ACCCACTGGTTACCTACGAA	TAGCTGTGCAGAGCGATAAC
LRRC32	leucine rich repeat containing 32	CTAGGCCTGGCTGCACAA	CCAGAACCTGGCACGAGAC
MAF	MAF bZIP transcription factor	TCGACGACCGCTTCTCC	ATCACCTCCTCCTTGCTGAC
MKI67	marker of proliferation Ki-67	AGAGTAACGCGGAGTGTCA	CTTGACACACACATTGTCCTCA
NFATC2	nuclear factor of activated T cells 2	TGGAAGCCACGGTGGATAA	TGTGCGGATATGCTTGTTCC
NFKB1	nuclear factor kappa B subunit 1	CTACCTGGTGCCTCTAGTGAAA	ACCTTTGCTGGTCCCACATA
NRP1	neuropilin 1	ACATGGTGCAGGATTTTCCA	GGTGTTGTGTAGTTCTGGGAA
NT5E	5'-nucleotidase ecto	ATGAACGCCCTGCGCTAC	GTGGCTCGATCAGTCCTTCC
PAK2	p21 (RAC1) activated kinase 2	CTACGACTCCAACACAGTGAA	GCTGGTGTTCCAGAAGGAA
PDCD1	programmed cell death 1	GCAGCCTGGTGCTGCTA	GTGCGCCTGGCTCCTA

PRDM1	PR/SET domain 1	CCTGGTACACACGGGAGAAAA	TTGAGATTGCTGGTGCTGCTA
PRF1	perforin 1	GTACAGCTTCAGCACTGACAC	CTGGGTGGAGGCGTTGAA
RORC	RAR related orphan receptor C	CAAGACTCATCGCCAAAGCA	TTTCCACATGCTGGCTACAC
SELL	selectin L	ACTATGGGCCCCAGTGTCA	GTGAGTACAGTCCATGGTACCC
SOCS1	suppressor of cytokine signaling 1	CATCCGCGTGCACTTTCA	GCTCGAAGAGGCAGTCGAA
SOCS3	suppressor of cytokine signaling 3	TTCAGCTCCAAGAGCGAGTA	TCACTGCGCTCCAGTAGAA
SOCS5	suppressor of cytokine signaling 5	TGTGCCACAGAAATCCCTCA	AGTCTTGTTCCTGGGGTAACAC
STAT5A	signal transducer and activator of transcription 5A	CCCAGGCTCCCTATAACATGTA	ATGGTCTCATCCAGGTCGAA
STAT5B	signal transducer and activator of transcription 5B	AACAGAGGTTGGTCCGAGAA	GTTTCTGGGACATGGCATCA
TBP	TATA-box binding protein	TGCCCGAAACGCCGAATATA	CGTGGTTCGTGGCTCTCTTA
TBX21	T-box 21	GGGCGTCCAACAATGTGAC	CCGTCGTTCACCTCAACGATA
TGFB1	transforming growth factor beta 1	CTACTACGCCAAGGAGGTCAC	GCTGTGTGTACTCTGCTTGAAC
TIGIT	T cell immunoreceptor with Ig and ITIM domains	GTGGTGGTCGCGTTGACTA	TCCTGTCCAGCTGATTTTCTCC
TNF	tumor necrosis factor	CTTCTCGAACCCCGAGTGAC	ACTGGAGCTGCCCCTCA
TNFRSF18	TNF receptor superfamily member 18	GCTGCTGCCGCGATTA	GAATTCAGGCTGGACACACA
TNFRSF1B	TNF receptor superfamily member 1B	ACATACACCCAGCTCTGGAAC	AGTGCAGGCTTGAGTTTCCA
TNFRSF4	TNF receptor superfamily member 4	AACGACGTGGTCAGCTCCAA	CACAGCTGCTTCCGCTCAC
TNFRSF9	TNF receptor superfamily member 9	GGGGCAGAAAGAAACTCCTGTA	TCTGGAAATCGGCAGCTACA
TNFSF10	TNF superfamily member 10	AGAAGGAAGGGCTTCAGTGAC	CCTGGACCTCCATCATAGCC
Normalisation genes			
ACTB	actin beta	GCCGTCTTCCCCTCCA	CTCGTCGCCCACATAGGAA
B2M	beta-2-microglobulin	TTAGCTGTGCTCGCGCTAC	CTCTGCTGGATGACGTGAGTAA
GAPDH	glyceraldehyde-3-phosphate dehydrogenase	GAACGGGAAGCTTGTCATCAA	ATCGCCCCACTTGATTTTGG
GATA3	GATA binding protein 3	CACGGTGCAGAGGTACCC	AGGGTAGGGATCCATGAAGCA
HPRT1	hypoxanthine phosphoribosyltransferase 1	GCTTTCCTTGGTCAGGCAGTA	ACTTCGTGGGGTCCTTTTCAC
UBC	ubiquitin C	TCGGCCTTAGAACCCCAGTA	GAAAACCAGTGCCCTAGAGTCA

Table 2.7: List of genes and primers used in Fluidigm Delta Gene assay for gene expression analysis by multiplex qPCR

2.5. Data analysis

2.5.1. Immunology data analysis

All data were tested for normality by the D'Agostino-Pearson normality test. All immunology data sets were non-normally distributed and therefore non-parametric statistical tests were applied. Unless otherwise stated, all lines and error bars displayed on graphs represent geometric means with 95% confidence intervals. All *p* values displayed are two tailed and an alpha value of 0.05 was set as the threshold for statistical significance. Unless otherwise specified, differences were tested by Mann-Whitney U tests between two groups and Kruskal-Wallis with Dunn's correction for multiple comparisons when more than two groups were tested. Differences between timepoints for matched samples were tested by Wilcoxon matched pairs. Spearman's rho was used for all correlations. Where >3 correlations were performed in one analysis, *p* values were corrected by the Holm-Sidak method. All analyses were performed in Prism version 8.1.2 (GraphPad Software, San Diego, California). The PCAs shown in Chapter 3 were performed in SPSS v26.0 (IBM, Armonk, New York).

2.5.2. Transcriptomic data analysis

Data from the Fluidigm multiplex qPCR gene expression assay were firstly analysed in proprietary real time PCR analysis software v4.5.2 from Fluidigm. Poor amplification curves and melt curves were flagged by the software and were inspected visually. Curves that did not appear normal (i.e non-exponential amplification or melt curves with multiple products) were omitted. Samples with C_T values >25 in one replicate and

negative in a second were called as negative on the basis the positive sample was likely non-specific amplification. In samples with C_T values <25 in one replicate and negative in a second replicate, the negative replicate was omitted (unless the amplification looked abnormal in the positive, in which case the sample was called as negative). Replicates with %CV >5% were omitted.

Log_2 Fold change was inferred from the qPCR C_T values by the $2^{-\Delta\Delta Ct}$ method[283]. Differential gene expression analysis was performed in RStudio v1.2.1335 using Limma (Linear models for microarray data) packages[284]. PCA was performed in SPSS v26.0.

Chapter 3

3. Parasite growth kinetics following controlled human malaria infection in semi-immune Kenyan adults and the cellular and cytokine response to infection.

3.1. Introduction

To address the paucity in knowledge of naturally-protective immune responses to malaria[285], novel methods of investigation are required for human studies, as discussed in Section 1.5[286,287]. Here, data are presented from a controlled human malaria infection study in semi-immune Kenyan adults (CHMI-SIKA) – the largest such *P. falciparum* malaria challenge study to have been carried out in sub-Saharan Africa to date.

CHMI studies have been carried out extensively in malaria-naïve individuals in European and North American settings in the past, mainly in the context of drug and vaccine efficacy trials[286,287]. However, few studies have used CHMI as a model to investigate natural immune mechanisms against infection which could inform vaccine

design. In malaria-naïve volunteers, the infectious parasite dose has been titrated to induce infection resulting in patent parasitaemia in up to 100% of volunteers[253,288]. The first CHMI studies used mosquito-based challenge models whereby 5 infectious mosquito bites were required to reliably infect 100% of malaria-naïve individuals. In CHMI studies using cryopreserved sporozoites administered by different routes including IM and ID, doses have been titrated to match the infectivity of mosquito-based models. Here, cryopreserved sporozoites administered by direct venous inoculation (DVI) were used, requiring considerably fewer sporozoites per dose than would have been with either ID or IM. A previous dose-finding study found that 3200 sporozoites administered by DVI successfully infected 9/9 malaria-naïve individuals with pre-patent periods similar to those seen after 5 infectious mosquito bites[288]. Subsequent studies have also replicated 100% infectivity in malaria naïve adults using this method[124]. It was hypothesised that in a semi-immune cohort with historical exposure to natural infection, increased heterogeneity in clinical outcomes might be observed compared to that seen in malaria-naïve individuals. This heterogeneity can be exploited by linking infectious outcomes with immune readouts to identify correlates of protection and susceptibility.

The focus of this chapter is on understanding innate cytokine and $CD4^+$ T cell responses, and testing whether they correlate with protection or susceptibility to infection. This builds on work by M. Walther and colleagues[114,113] who investigated the relationships between pro- and anti-inflammatory cytokine responses, Treg responses and parasite multiplication rates in a malaria-naïve cohort undergoing CHMI.

This chapter firstly describes the parasite growth outcomes observed following CHMI in this semi-immune cohort.

An analysis is then presented on the kinetics of the systemic pro- and anti-inflammatory response during the course of CHMI including analysis of plasma concentrations of different cytokines, acute phase proteins and liver function markers.

An analysis of the phenotype and frequency of Tregs at different timepoints during CHMI is then described to determine if this cell subset plays a role in controlling parasite growth rates and effector CD4+ T cell responses in this cohort.

Finally, this chapter includes data from an *in vitro* proliferation assay to quantify the magnitude of the baseline antigen-specific T cell response to blood-stage *P. falciparum* parasites to determine whether T cell memory is predictive of CHMI outcome or is affected by Treg phenotype or abundance.

3.2. Study-specific methods

A detailed protocol for the CHMI-SIKA clinical trial is published elsewhere[273]. Briefly; healthy adult volunteers were enrolled from 2 separate areas in Kilifi County, east Kenya with varying levels of malaria transmission intensity (from low to moderate) and a region in south-western Kenya, Ahero, with high transmission intensity. Volunteers were pre-screened to measure anti-schizont IgG titres and enrolled to include volunteers with a range of anti-schizont IgG levels (and thus a range of prior exposure

intensities and levels of naturally acquired immunity). Volunteer exclusion criteria included (but were not limited to): being positive for sickle-cell trait and alpha thalassaemia by PCR genotyping, systemic use of antibiotics with antimalarial activity within 30 days prior to challenge and being parasite positive by qPCR the day before challenge.

Volunteers were infected with 3200 fresh cryopreserved *P. falciparum* sporozoites by DVI. Volunteers remained as inpatients in Pwani University accommodation, close to the KWTRP research laboratories for the duration of the study. Blood was sampled for real-time monitoring of parasitaemia by qPCR[27] at the timepoints indicated in Fig 3.1 The diagnostic criteria are shown in Table 3.1. Volunteers reaching the diagnostic criteria, or 21 days post-challenge (whichever came first) were treated with Artemether-Lumefantrine before discharge.

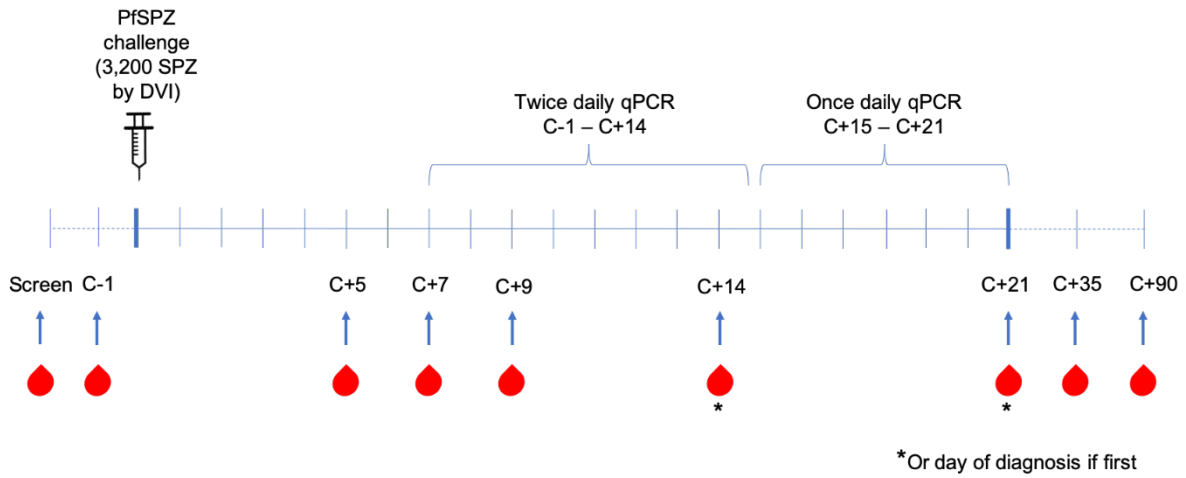

Figure 3.1: Malaria challenge and blood sampling schedule in the CHMI-SIKA trial *Timepoints for immunology blood sampling indicated by red droplets.*

>500 parasites / μl blood with or without symptoms	Symptoms and RDT +ve and microscopy +ve	Any other clinical indication at clinician's discretion	Asymptomatic and <500 parasites / μl blood
Diagnosed and treated			Not diagnosed (treated and discharged at C+21)

Table 3.1: Diagnosis criteria
Parasitological criteria for diagnosis and treatment of volunteers undergoing CHMI.

Blood was also drawn at indicated timepoints for processing and storage of samples for immunological assays (Fig 3.1). Plasma and PBMCs were isolated from heparinized blood using standard Ficoll-Paque density gradient centrifugation and stored by standard methods[289]. All immunological assays were performed on thawed, cryopreserved samples.

3.3. Results

3.3.1. Patient characteristics

116 volunteers who underwent CHMI were included in the sub-group for immunological analysis. The sub-group was selected to include all individuals undergoing CHMI in 2016 and 2017 (Kilifi only, *n* = 101) plus only the Ahero cohort (*n* = 15) from 2018. The participant characteristics of this sub-group are summarised in Table 3.2.

Characteristic	*Immunology sub-group (n = 116)*
Sex – no. (%)	
Male	85 (73.3)
Female	31 (26.7)
Age - years	
Median (Interquartile Range)	27 (23 – 33)
Range	18 – 45
Location of residence (Malaria transmission intensity) – no. (%)	
Ahero (High)	15 (12.9)
Kilifi North (Low)	24 (20.7)
Kilifi South (Moderate-High)	77 (66.4)

Table 3.2: Participant characteristics

Descriptive characteristics of n = 116 volunteers included in the immunology sub-group.

3.3.2. CHMI in semi-immune Kenyan adults induces four different growth phenotypes.

Parasitaemia was measured by qPCR between day 7 (coinciding with the release of merozoites from the liver into the blood) until the end of follow-up at day 21. Of the cohort selected for immunological analyses [*n* = 116], only 39 [33.6%] reached the treatment threshold (treated group) (Fig 3.2a). The median time to treatment in this group was 14 days post-inoculation [95% CI: 12.5-15, range: 11-21 days] (Fig 3.2b). Of the remaining 77/116 (66.3%) which did not meet the diagnostic criteria, their parasite growth kinetics could be defined by three further distinct phenotypes (Fig 3.2c). The first group exhibited slowed parasite growth whereby positive parasite growth was observed throughout follow-up, but the growth was slow and parasitaemia never reached a concentration above the treatment threshold (slow growth group). The second group had PCR-detectable levels of parasitaemia between days 7 to 10 but then cleared their infection and were qPCR-negative for parasitaemia for the remainder of follow-up (cleared group). The third group were highly immune, having no detectable parasitaemia by qPCR at any timepoint measured during the follow-up period (highly immune group).

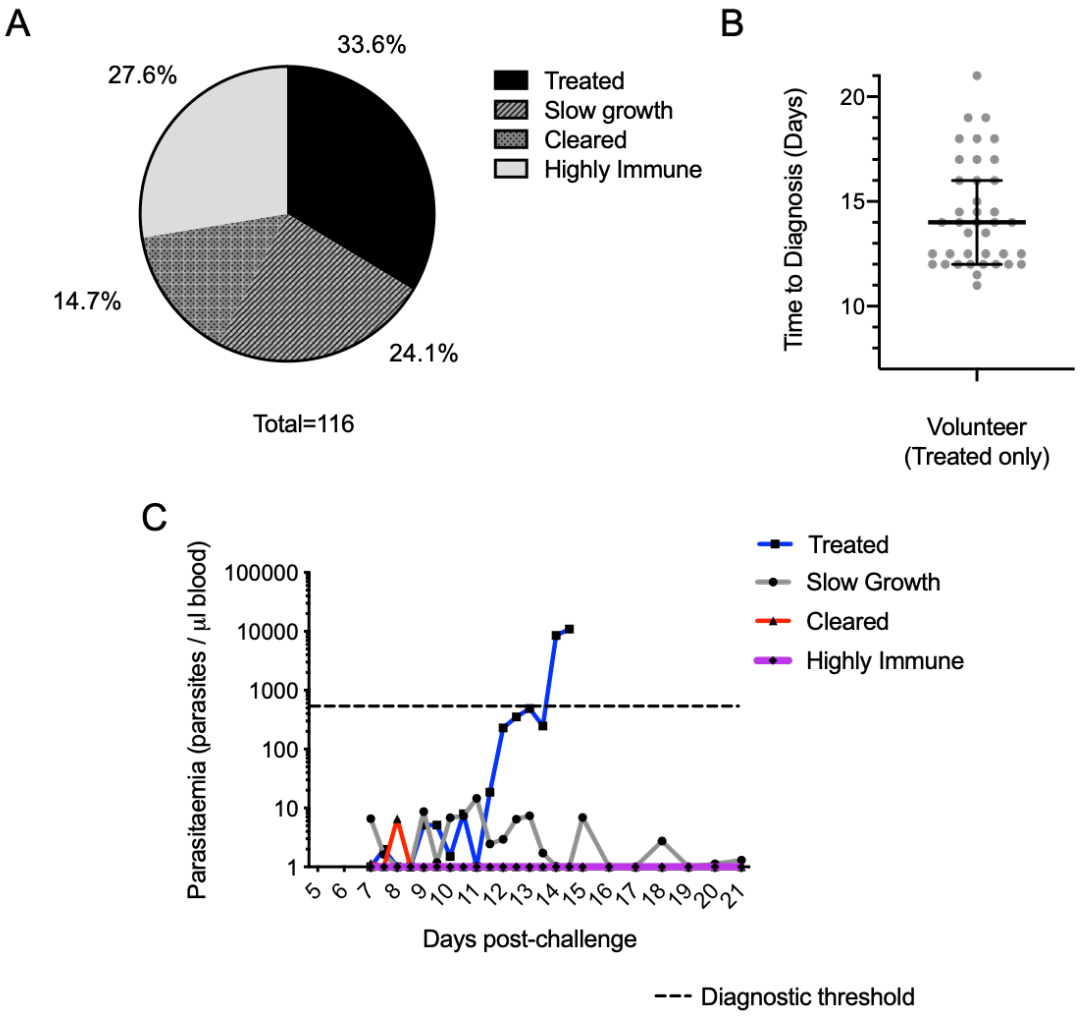

Figure 3.2: Parasite growth outcomes and kinetics
(a) *proportions of volunteers in the immunology sub-group with each parasite growth outcome. n = 116 individuals.* ***(b)*** *time to diagnosis in the treated group. Lines and bars represent the median and interquartile range. n = 39 treated individuals.* ***(c)*** *representative parasite growth lines over time of 4 selected volunteers, measured by qPCR for each of the four parasite growth outcomes observed.*

Subsequent immunological analyses will be primarily stratified by the four parasite growth outcome groups described above. In some analyses limited by sample size, groups are classified as ‘controllers’, combining those in the highly immune and cleared group, and ‘non-controllers’ combining the treated and slow growth groups, in order to increase statistical power.

3.3.3. Protection during CHMI is associated with prior malaria exposure

The proportions of volunteers within each parasite growth outcome group varied between locations of residence from which volunteers were recruited (Fig 3.3a). Volunteers living in Ahero, the region of high transmission intensity, mostly displayed slowed growth *n* = 8/15 [53%]. Notably there were no highly immune volunteers in this group. In the low transmission setting, Kilifi North, the vast majority of volunteers were treated, *n* = 20/23 [87%] and there were no highly immune volunteers. In the moderate transmission setting, Kilifi South, the largest group were the highly immune [*n* = 27/77, 35%] and there were similar numbers of treated [14/77, 18%], slow growth [19/77, 25%] and cleared [17/77, 22%] volunteers. There were no differences in growth outcome between males and females (Fig 3.3b) or based on volunteer age at the time of screening (Fig 3.3c). Anti-schizont antibody titres, as a correlate of prior malaria exposure, were significantly lower by Kruskal-Wallis between the treated group and the three non-treated groups (Fig 3.3d). There were no significant differences observed between the three non-treated groups. Age was only weakly associated with increasing anti-schizont IgG titre with location of residence being a greater determining factor (Fig 3.3e and 3.3f). Titres in the Kilifi South group were significantly higher than both the Kilifi North and Ahero groups.

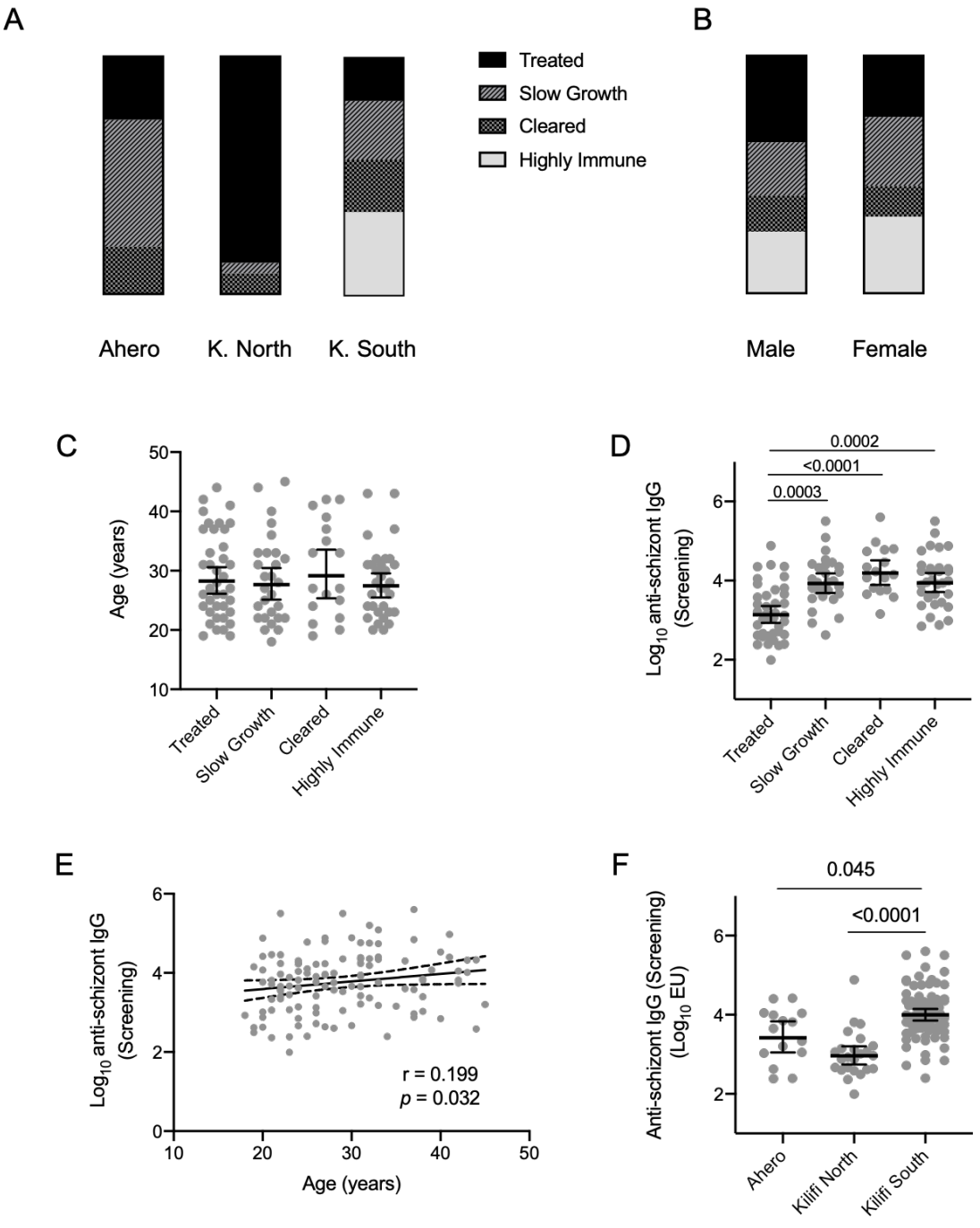

Figure 3.3: Associations between parasite growth outcome and participant demographics (a) *proportions of each parasite growth outcome between individuals living in different study recruitment areas.* ***(b)*** *proportions of each parasite growth outcome between males and females.* ***(c)*** *effect of age on parasite growth outcome.* ***(d)*** *effect of anti-schizont antibody titres at screening on parasite growth outcome.* ***(e)*** *relationship between age and anti-schizont IgG titre.* ***(f)*** *relationship between anti-schizont IgG titre and location of residence. For A and B, coloured areas represent percentages of total. For C, D and F, differences measured by Kruskal-Wallis with Dunn's correction – only significant values shown. For E, association measured by Spearman's rho.*

3.3.4. Cytokine concentrations at baseline are not associated with parasite growth outcome following CHMI

Next, the systemic cytokine response to CHMI was investigated using a panel of ELISA assays to measure plasma concentrations of 7 pro-inflammatory and 2 anti-inflammatory cytokines in all 116 volunteers at all available timepoints.

It was firstly investigated whether the inflammatory profile at baseline (C-1) could predict parasite growth outcomes following CHMI. In only 69/116 (59.5%) of volunteers was at least one pro-inflammatory cytokine detectable above the lower limits of detection [range: 1.17 pg/ml – 9.38 pg/ml] of the ELISA assays, as determined by the manufacturer based on the linear range of the standard curve. Figure 3.4a shows the frequency distribution of the number of cytokines detected per sample. In volunteers where pro-inflammatory cytokines were detected, there was generally even distribution of between 1 to 6 detectable cytokines per individual. A relatively broad range of cytokine concentrations in positive samples was observed, except for IL-1b and IL-4 where most positive responses were grouped just above the lower limit of detection (Fig 3.4b). Cross correlation analysis of cytokine concentrations showed a high degree of correlation between all pro-inflammatory cytokines except IFNα (Fig 3.4c).

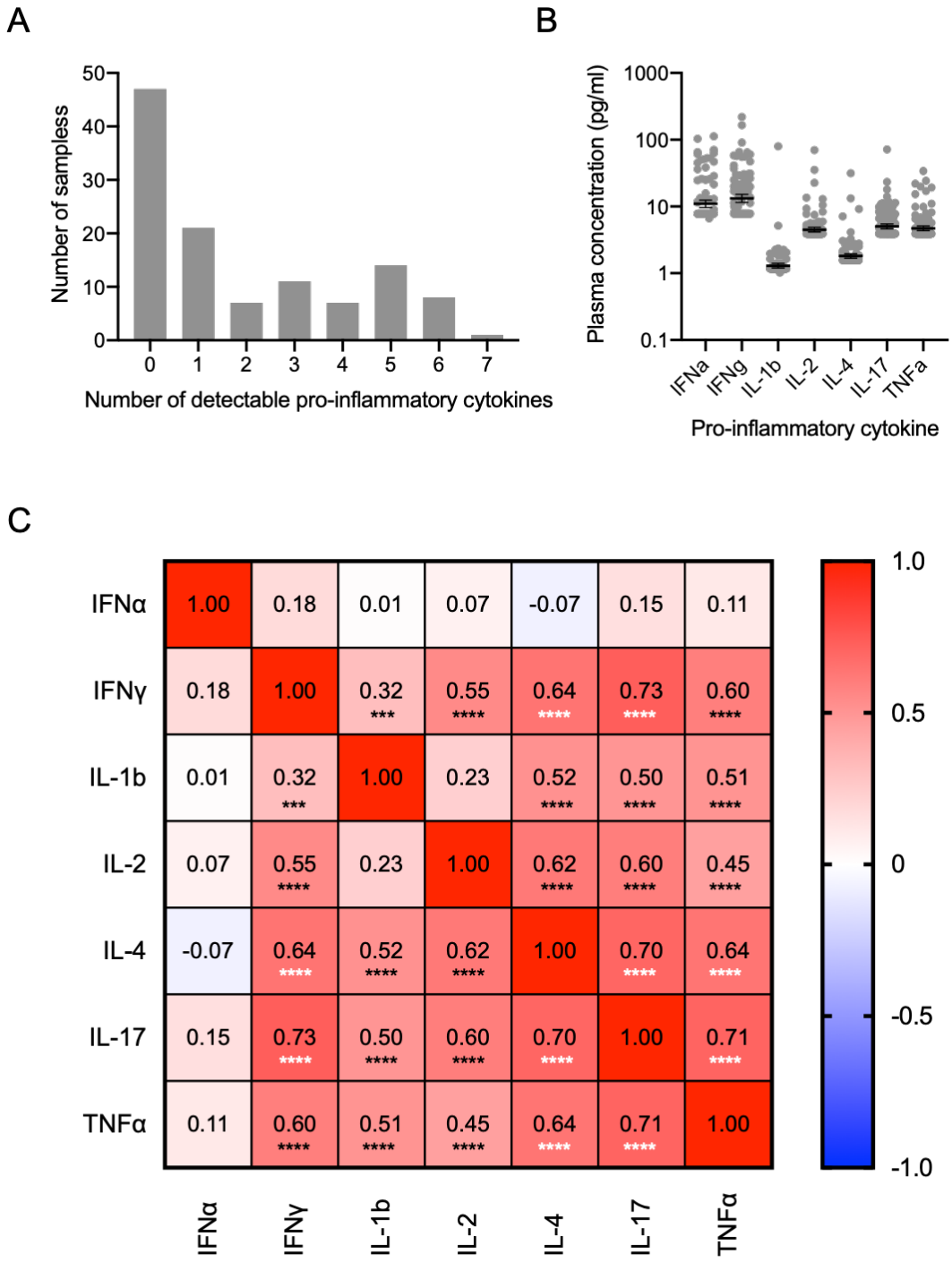

Figure 3.4: Distribution of baseline cytokine concentration data (a) *frequency distribution of the number of detectable positive cytokine measurements per sample.* ***(b)*** *distribution of cytokine concentrations.* ***(c)*** *correlation matrix of cytokine concentrations per sample. Numbers are r values derived from Spearman rho tests. *** p = <0.001, **** p = <0.0001, no asterisk p = >0.05.*

The concentrations of pro-inflammatory cytokines in plasma at baseline were compared across parasite growth outcome groups. There were no significant differences in concentration between groups for any pro-inflammatory cytokine when measured by Kruskal-Wallis tests, with the majority of responses being below the lower limit of detection across all four groups (Figure 3.5).

Combining data from all 7 pro-inflammatory cytokine concentration datasets, overall plasma cytokine profiles at baseline were analysed by principal component analysis (PCA). This analysis failed to separate samples by parasite growth outcome group (Figure 3.6). The discrete clustering along the second principal component was found to be primarily driven by differences in concentration of a single cytokine, IFNα. However, this was not associated with parasite growth outcomes.

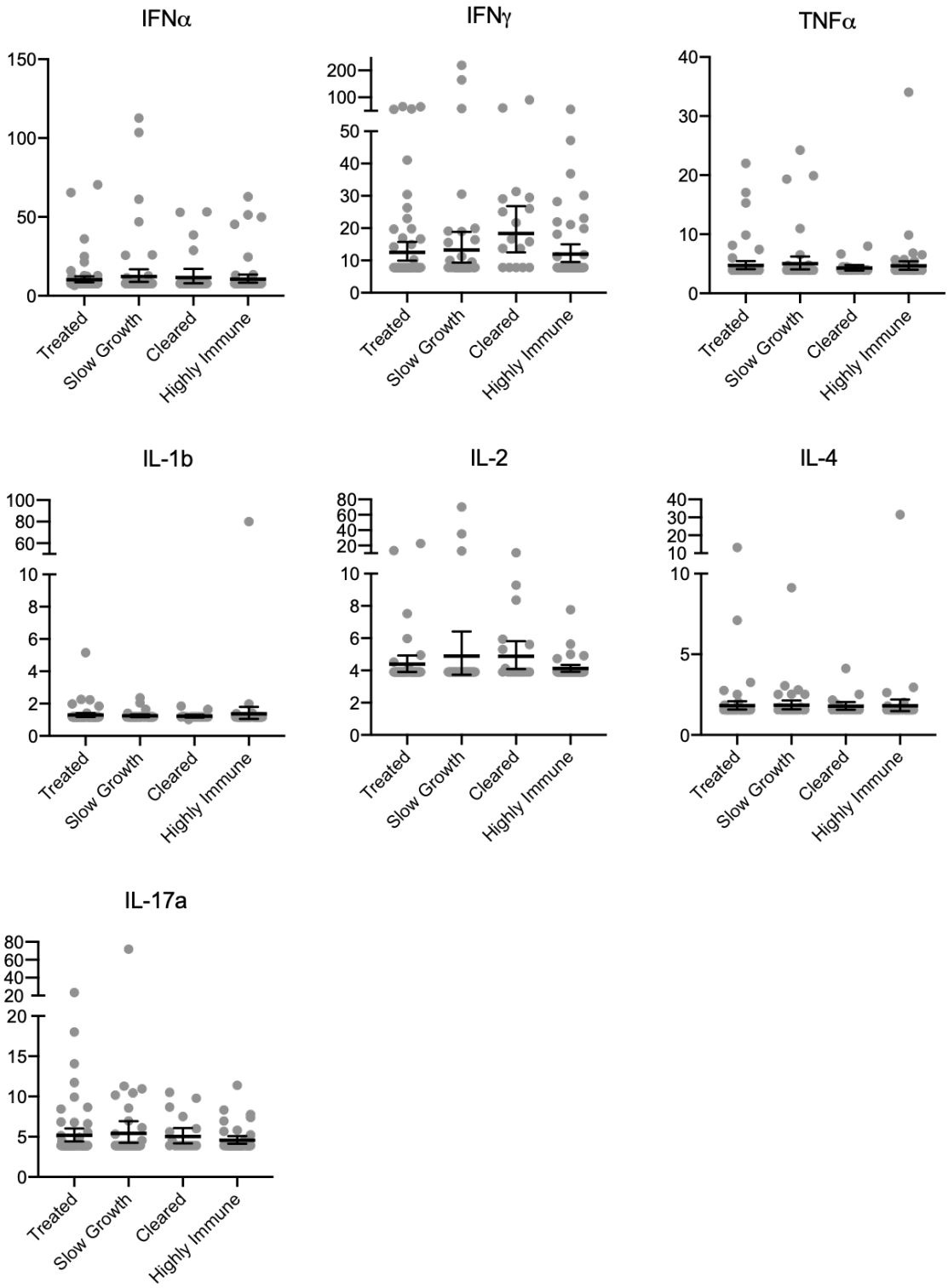

Figure 3.5: Association between pro-inflammatory cytokine concentration at baseline and parasite growth outcome during CHMI *All comparisons measured by Kruskal-Wallis tests with Dunn's correction for multiple comparisons – no significant differences observed for any cytokine. Concentrations adjusted to the manufacturer-defined lower limits of detection.*

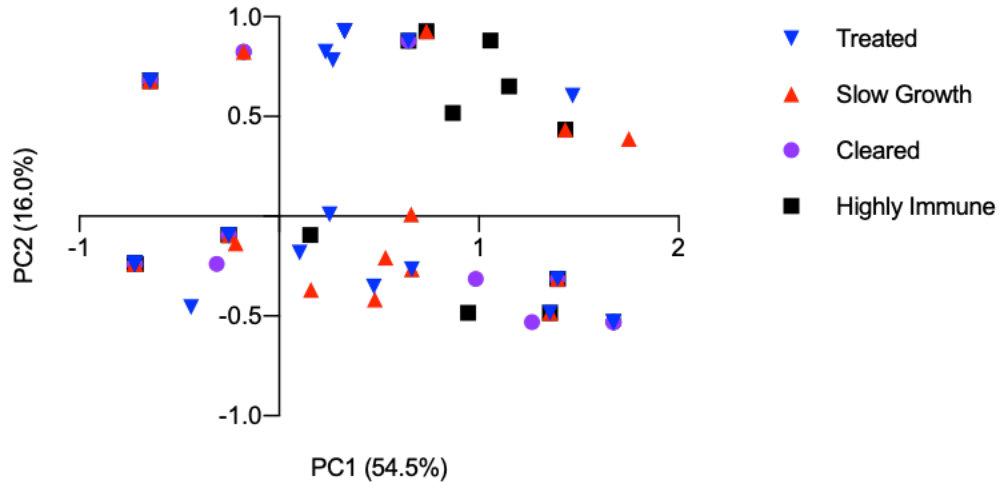

Figure 3.6: Baseline pro-inflammatory cytokine profiles tested by PCA *First 2 principal components shown accounting for 70.5% of variance.*

The plasma concentrations of two anti-inflammatory cytokines, IL-10 and latent TGF-β1 were also measured. At baseline (C-1), IL-10 was not detectable in the majority of volunteers 96/116 (82%). Latent TGF-β1 was however detectable in all volunteers; geometric mean concentration 4678 pM [95% CI:4115-5319, range: 547-14809]. Cytokine levels of TGF-β1 at C-1 were not associated with subsequent parasite growth outcome following CHMI (Fig 3.7a), and likewise neither were cytokine levels of IL-10 (Fig. 3.7b). I investigated whether anti-inflammatory cytokine concentrations were correlated with the concentrations of pro-inflammatory cytokines. No differences in the concentration of either TGF-β1 or IL-10 were observed when stratified by baseline pro-inflammatory cytokine status (where cytokine-positive is defined as having at least one detectable pro-inflammatory cytokine above the lower limit of detection and cytokine negative is having no detectable pro-inflammatory cytokines) (Fig 3.7c and 3.7d). However, the low numbers of samples positive for IL-10 may have limited power in this analysis.

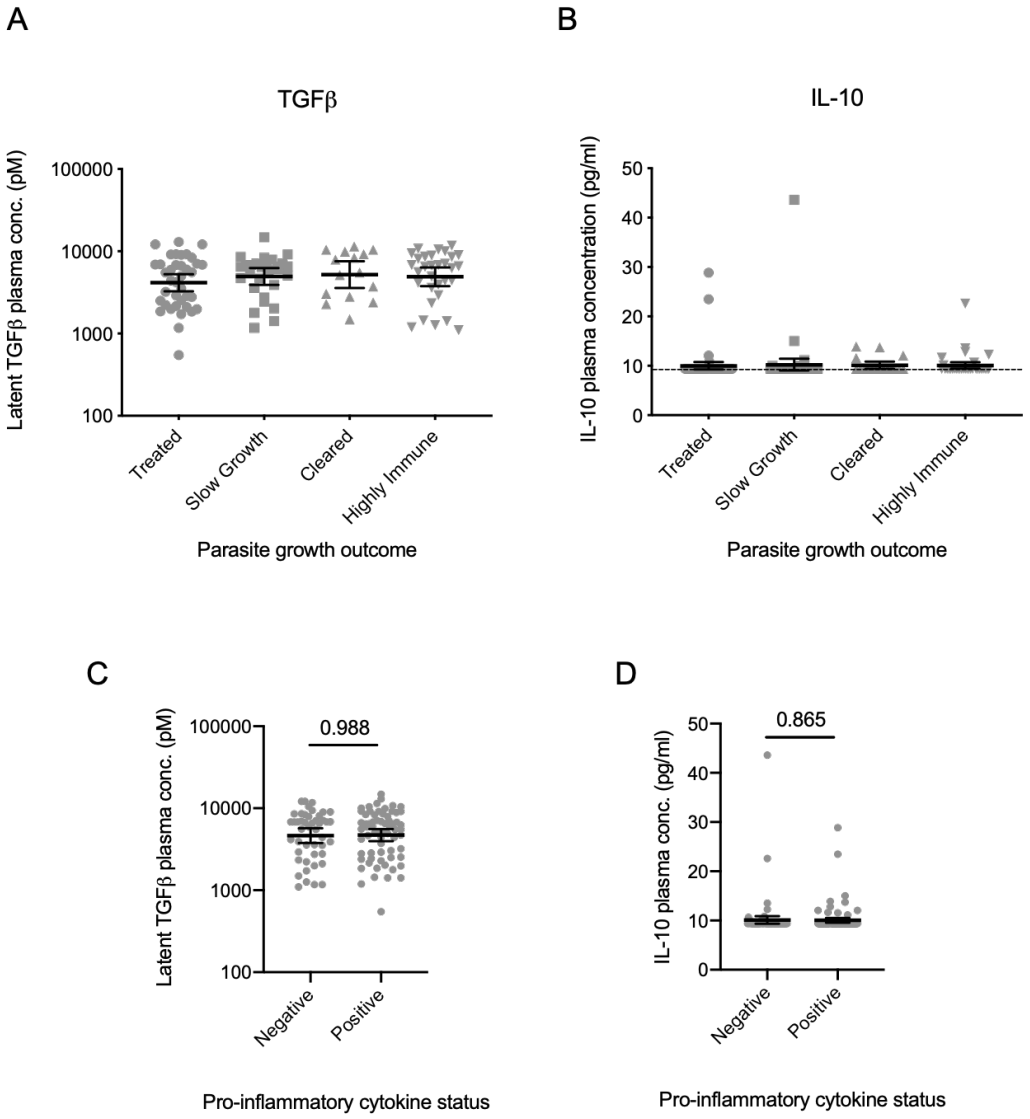

Figure 3.7: Association between anti-inflammatory cytokine concentrations and parasite growth outcomes following CHMI (a) *concentration of latent TGF-β1 in plasma at baseline (C-1) stratified by parasite growth outcome. No significant differences between groups by Kruskal-Wallis.* ***(b)*** *concentration of IL-10 in plasma at C-1 stratified by parasite growth outcome. Assay lower limit of detection was 10 pg/ml. No significant differences by Kruskal-Wallis.* ***(c)*** *concentration of latent TGF-β1 in plasma at C-1 stratified by baseline pro-inflammatory cytokine status (where cytokine-positive is defined as having at least one detectable pro-inflammatory cytokine above the lower limit of detection). No significant difference by Mann-Whitney U test, p = 0.998.* ***(d)*** *concentration of IL-10 in plasma at C-1 stratified by baseline pro-inflammatory cytokine status. No significant difference by Mann-Whitney U test, p = 0.865.*

3.3.5. Plasma cytokine kinetics reveal an IL-10 response in the treated group.

Next, the kinetics of the systemic cytokine response was measured at all available timepoints following CHMI. Individual participant time courses for all cytokines are shown in Figure 3.8. There were no significant increases observed in the concentrations of any pro-inflammatory cytokine at any timepoint during CHMI relative to C-1, measured by Kruskal-Wallis. This pattern was reflected across all parasite growth outcome groups, including in the treated group where cytokines were additionally measured on the day of diagnosis.

However, anti-inflammatory cytokine responses to CHMI were seen. For IL-10 there was a significant increase in concentration on the day of diagnosis in the treated group [GMC 19.34 pg/ml, 95% CI: 13.34-28.03] compared to baseline levels at C-1 [GMC 9.98 pg/ml, 95% CI: 9.26-10.76]. Conversely, for TGF-β1 there was a slight but statistically significant decrease in the concentration of latent cytokine in the treated group on the day of diagnosis (DoD) compared to baseline; C-1 GMC 4717 pM [95% CI: 3262-5427], DoD GMC 2549 pM [95% CI: 1993-3259]. There were no significant differences in the concentration of either IL-10 or TGF-β1 between any other groups or timepoints.

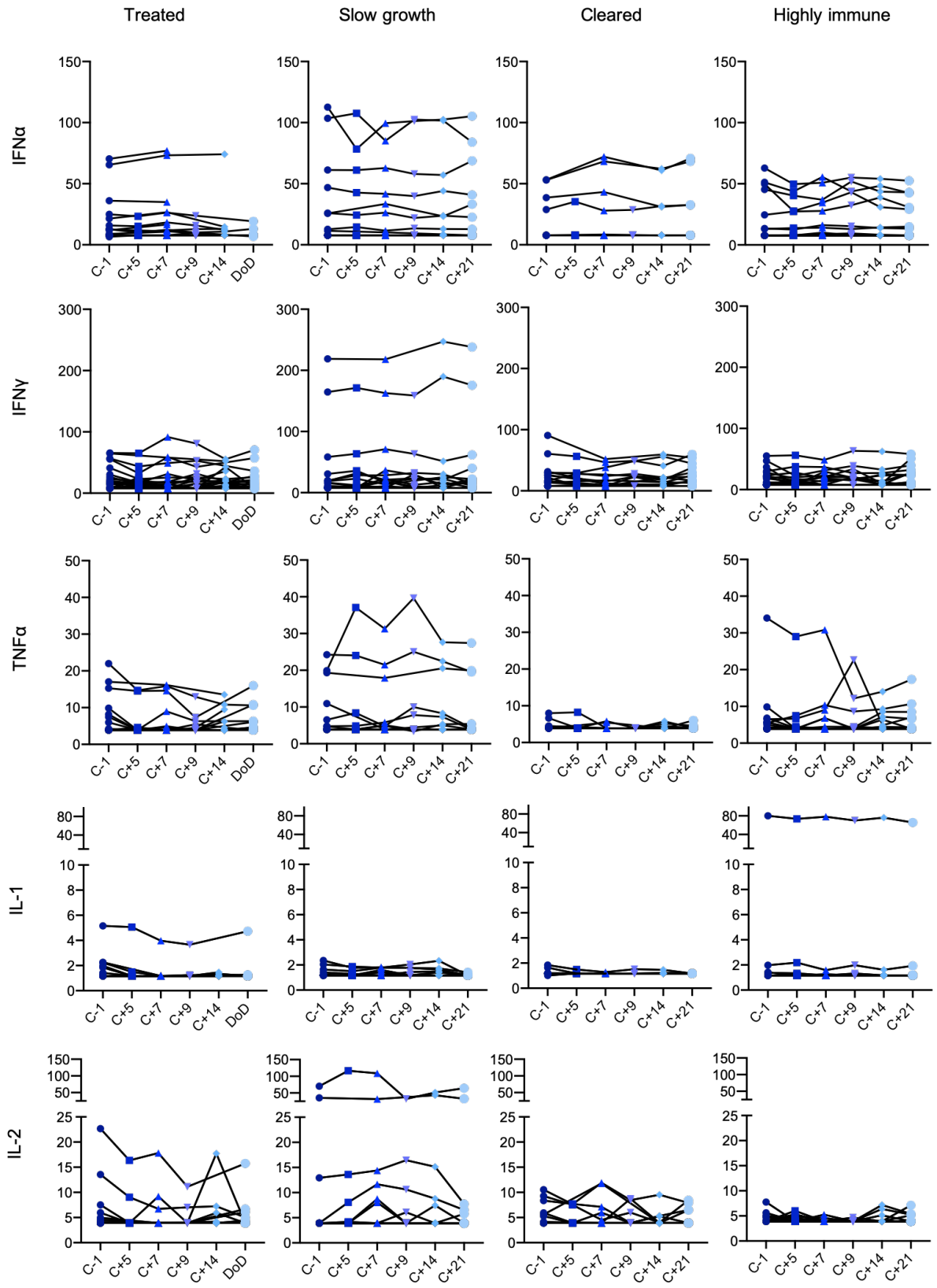

Figure 3.8: *(Continued below)*

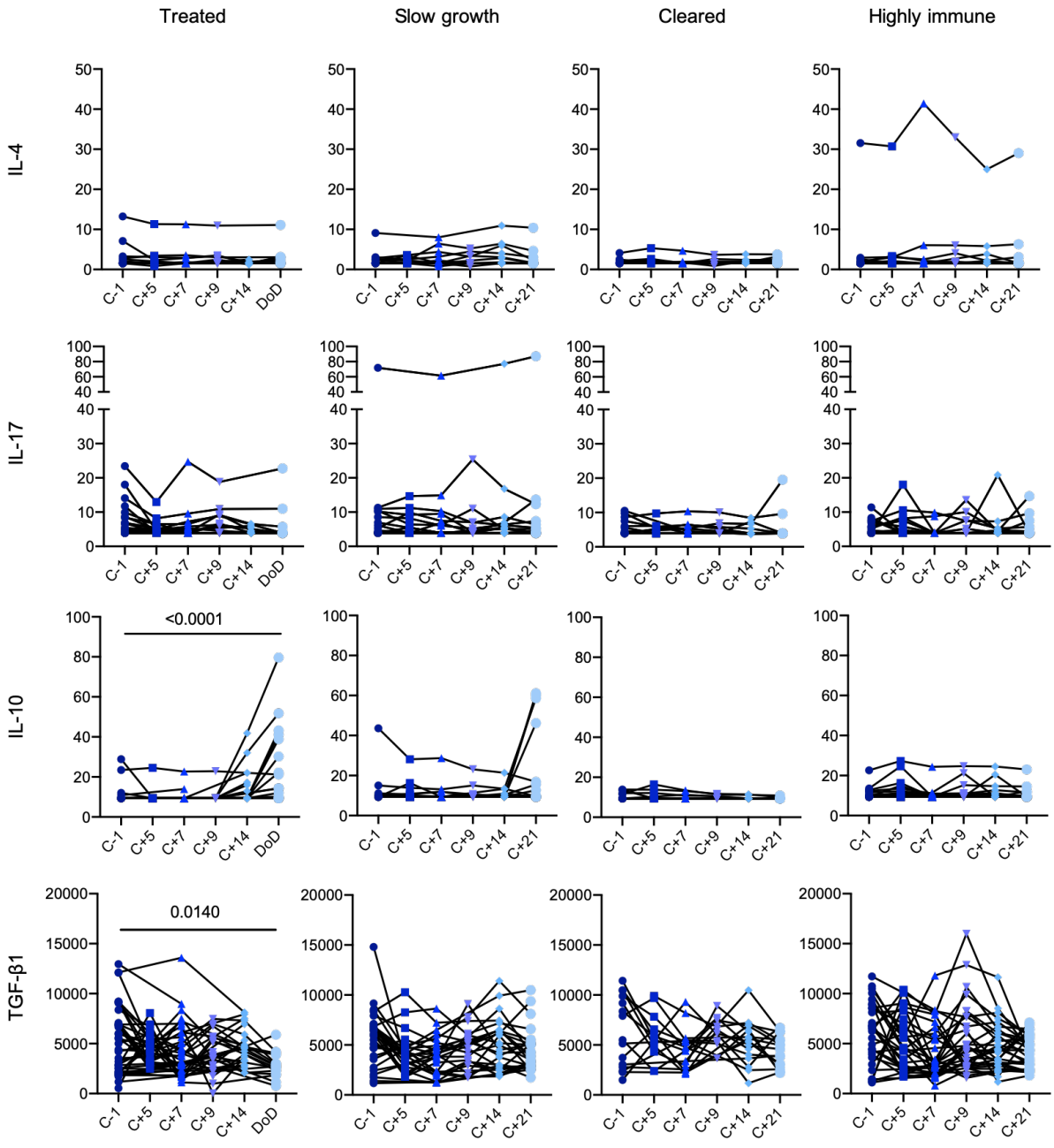

Figure 3.8: Individual volunteer kinetics for all cytokines throughout CHMI split by parasite growth outcome groups. *Differences between timepoints measured by Kruskal-Wallis with Dunn's correction for multiple comparisons. Only significant values shown. Cytokine concentrations measured in pg/ml, except for TGF-β1 which was measured in pM. X axis shows timepoints throughout CHMI. Timepoints along x axis indicate days post-challenge.*

Next, I investigated if anti-inflammatory cytokine responses were associated with parasite growth or clinical outcomes using body temperature as a proxy for fever. IL-10 concentration on the day of diagnosis in the treated group was not associated with time to diagnosis, parasitaemia on the day of diagnosis or body temperature at diagnosis (Fig 3.9a-c). Similarly, the increase in IL-10 concentration in some individuals in the slow growth group at C+21 did not correlate with parasitaemia at the same timepoint (Fig 3.9d). The decrease in TGF-β1 concentration was also not associated with any parasitological outcome, pro-inflammatory cytokine status or febrile illness.

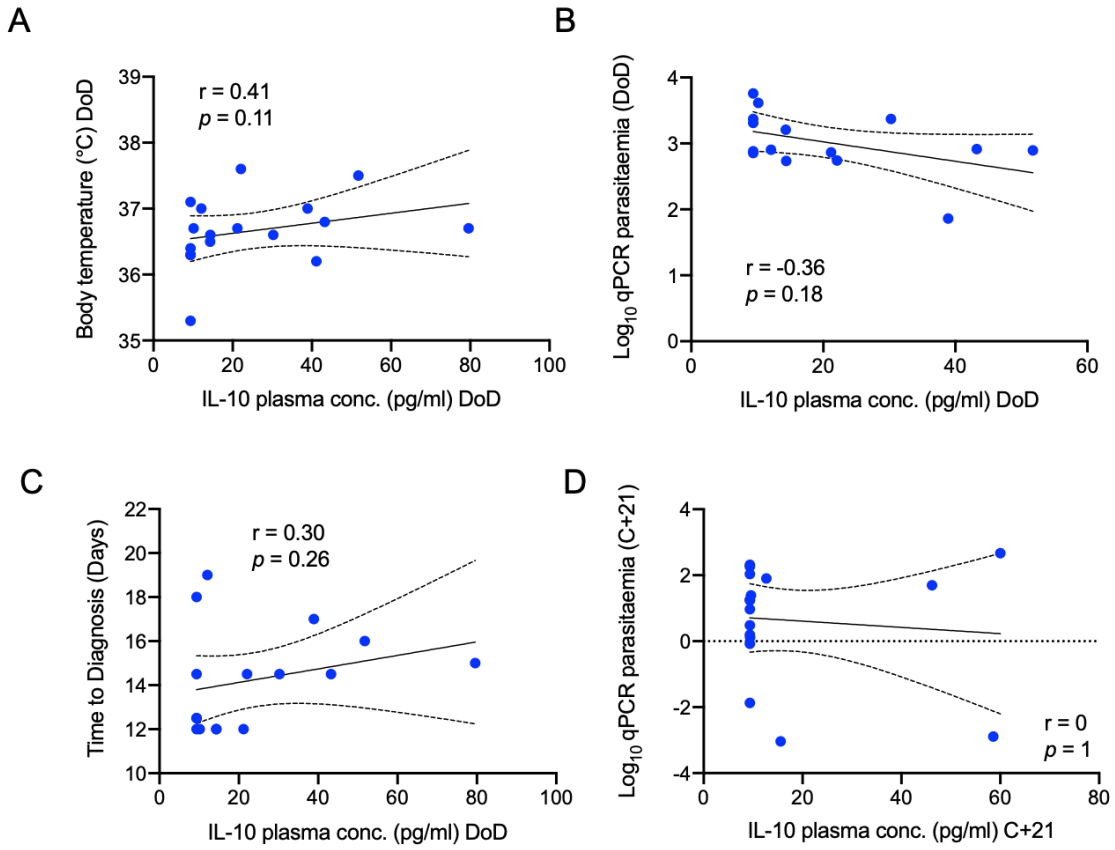

Figure 3.9: Association between fever, parasite growth and IL-10 plasma concentration (a) *association between IL-10 concentration and body temperature in treated volunteers on the day of diagnosis.* ***(b)*** *association between IL-10 concentration and parasitaemia measured by qPCR in treated volunteers on the day of diagnosis.* ***(c)*** *association between IL-10 concentration and the time to diagnosis in treated volunteers on the day of diagnosis (DoD).* ***(d)*** *association between IL-10 concentration and parasitaemia measured by qPCR in slow growth individuals at day 21 (C+21). No significant associations by Spearman rho in any comparison.*

There were also no associations between TGF-β1 concentration on the day of diagnosis and either parasite growth outcomes or fever in the treated group (Fig 3.10a-c) or between TGF-β1 concentration and parasitaemia at C+21 in the slow growth group (Fig 3.10d).

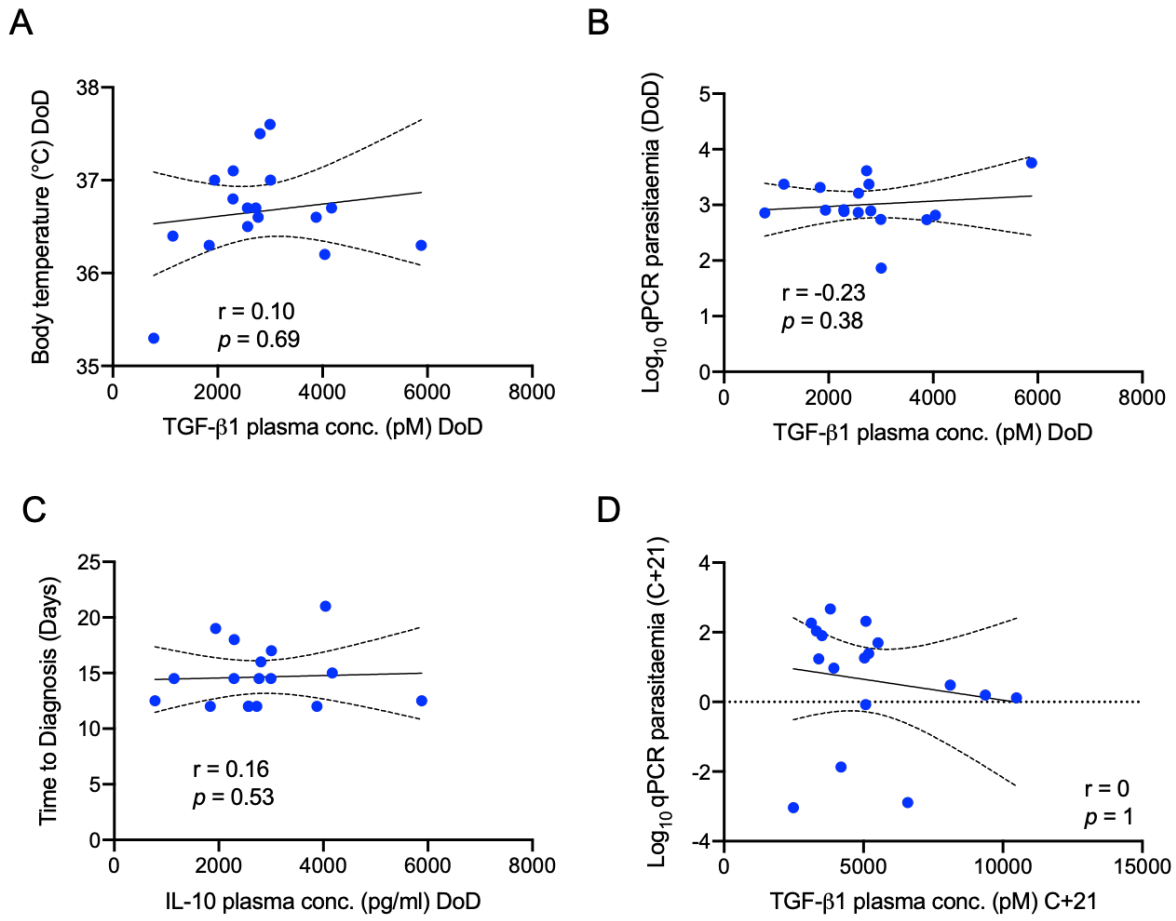

Figure 3.10: Association between fever, parasite growth and TGF-β1 plasma concentration (a) *association between TGF-β1 concentration and body temperature in treated volunteers on the day of diagnosis.* ***(b)*** *association between TGF-β1 concentration and parasitaemia measured by qPCR in treated volunteers on the day of diagnosis.* ***(c)*** *association between TGF-β1 concentration and the time to diagnosis in treated volunteers on the day of diagnosis (DoD).* ***(d)*** *association between TGF-β1 concentration and parasitaemia measured by qPCR in slow growth individuals at day 21 (C+21). No significant associations by Spearman rho in any comparison.*

3.3.6. Treg homeostasis is altered during CHMI

Considering the only cytokine seen to increase in concentration systemically during CHMI was IL-10, and this was only seen in the least immune group, it was considered whether an immunosuppressive cellular response might be associated with increased susceptibility to infection despite TGF-β1 concentration not following the same trend. The cellular origins of either cytokine during CHMI remain unknown and may differ between the two, reflecting separate mechanisms. Regulatory T cell activity was investigated as one potential cell type with an immunosuppressive role in CHMI. Treg frequency, memory phenotype and recent proliferative history were measured in PBMC by flow cytometry at C-1 and 14 days post-challenge (C+14) since this was 1 week into blood-stage infection and the latest timepoint available where the majority of volunteers remained undiagnosed.

Tregs were defined as being FoxP3+ CD25+ CD127lo CD4+ T cells. The frequency of Tregs as a proportion of total CD4+ T cells in PBMC was heterogeneous between volunteers at C-1; median 3.48% [IQR: 2.86-4.31%; range: 0.83-6.28%]. No differences in Treg frequency or in the proportions of Tregs expressing CD45RA or Ki-76 were found across parasite growth outcome groups at baseline by Kruskal-Wallis. However, considerable differences between groups in the Treg response to CHMI measured at C+14 compared to C-1 were found. Firstly, the frequency of bulk Tregs significantly increased at C+14 compared to C-1 in all but the treated group (Fig 3.11a). The increase by pairwise analysis was most significant in the highly immune group [p = <0.0001], with intermediate significance in the middle groups [slow growth p = 0.05, cleared p = 0.02] and no effect in the treated group [p = 0.10]. The increase

in bulk Treg frequencies coincided with an increase in the percentage of cells which expressed the naïve T cell marker CD45RA at C+14. Again, this occurred in all but the treated group and most-significantly so in the highly immune group (Fig 3.11b). Conversely, the proportion of Tregs expressing the proliferation marker Ki-67 were significantly reduced in all groups at C+14 timepoint, although again there was a trend towards increasing statistical significance in the highly immune group (Fig 3.11c).

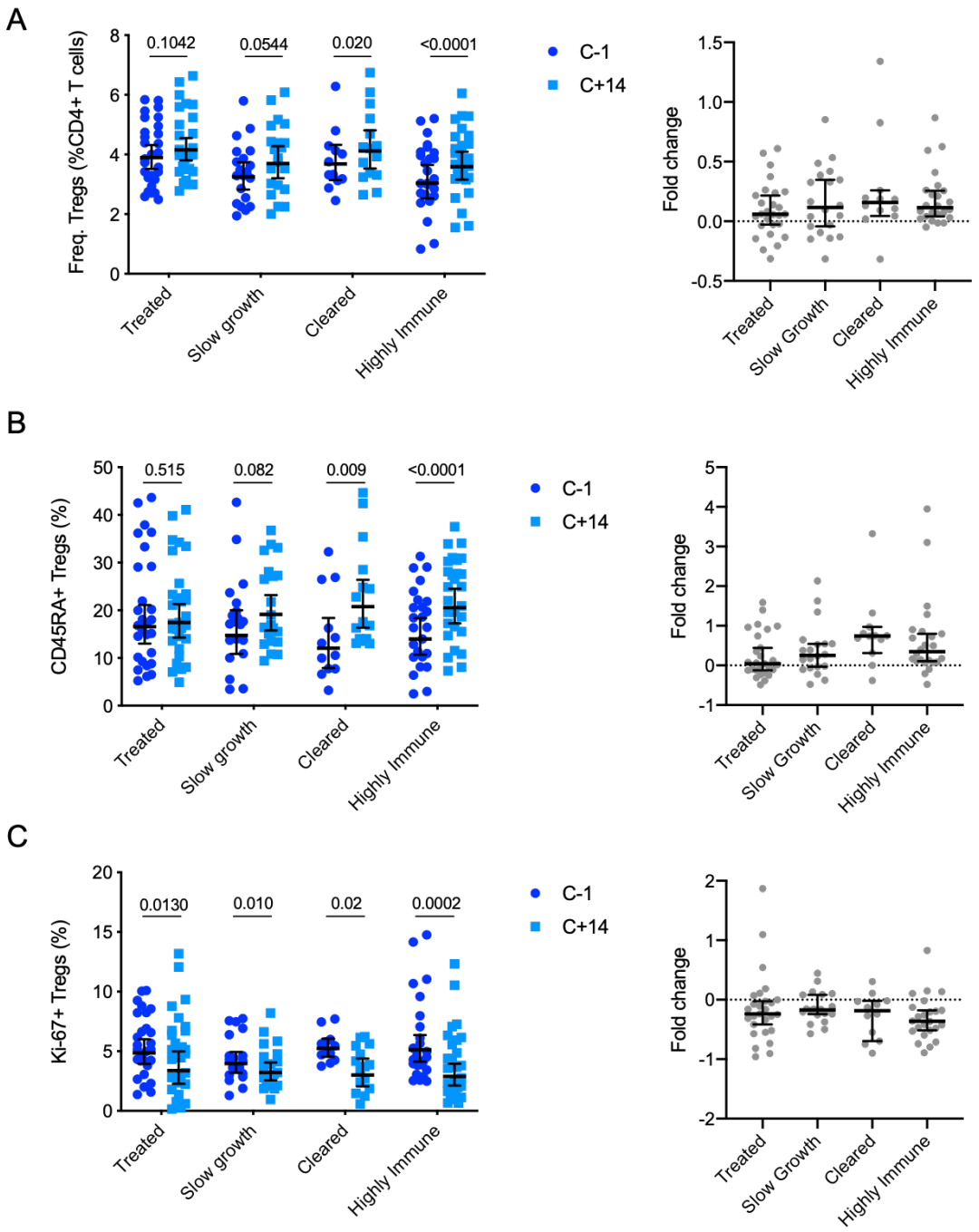

Figure 3.11: Change in Treg frequency and phenotype between baseline (C-1) and 14 days post-challenge (C+14)

Left-hand plots show comparisons between timepoints split by growth outcome group. p values between timepoints are derived from Wilcoxon matched pairs tests. Differences across groups at individual timepoints were also measured using Kruskal-Wallis tests with Dunn's correction for multiple comparisons and no significant differences were observed. Right hand plots show fold change from C-1 to C+14 for each measure indicating the direction and distribution of change between timepoints. Fold change calculated as: (frequency at C+14 / frequency at C-1) - 1. ***(a)*** *change in frequency of bulk Tregs, defined as the percentage of FoxP3+ CD25+ CD127lo cells as a proportion of total CD4+ T cells.* ***(b)*** *change in proportion of Tregs expressing CD45RA.* ***(c)*** *change in proportion of Tregs expressing Ki-67.*

A consolidated summary of the changes in Treg frequency and phenotype observed between groups at C+14 compared to C-1 is shown in Table 3.3.

Group	*Treg Frequency change*	*p =*	*CD45RA+ Treg change*	*p =*	*Ki-67+ Treg change*	*p =*
Treated	0.26 [-0.08 – 0.60]	0.104	1.47 [-1.65 – 4.60]	0.515	-0.86 [-1.94 – 0.21]	0.01
Slow Growth	0.46 [0.05 – 0.87]	0.054	2.54 [-0.47 – 5.56]	0.082	-0.67 [-1.23 – -0.10]	0.01
Cleared	0.77 [-0.14 – 1.68]	0.02	7.55 [2.98 – 12.12]	0.009	-1.57 [-3.06 – -0.08]	0.02
Highly immune	0.45 [0.27 – 0.63]	<0.0001	5.76 [3.18 – 8.33]	<0.0001	-1.96 [-2.89 – -1.03]	0.0002

Table 3.3: Treg response to CHMI*. 'Change' indicates the percentage of Tregs (as a proportion of CD4+ T cells) and CD45RA+ or Ki-67+ Tregs (as a proportion of Tregs) at C+14 minus values at C-1. Values in 'change' columns are means and 95% confidence intervals. p values are derived from Wilcoxon matched pairs tests for the change from C-1 to C+14.*

To confirm that the changes in frequency of Treg phenotypes represented an expansion or contraction of absolute cell number, relative cell counts were inferred by multiplying the frequency of CD45RA+ or Ki-67 positive cells (within the Treg subset) by the frequency of Tregs (as a proportion of CD4+ T cells). For CD45RA+ cells, the change in relative cell counts between C-1 and C+14 mirrored the change in frequency (Fig 3.12) – there were no significant differences for the treated and slow growth groups, but significantly higher counts in the cleared and highly immune groups. Again, the relationship was most significant in the highly immune group. For Ki-67+ Tregs, counts were only significantly reduced in the highly immune group.

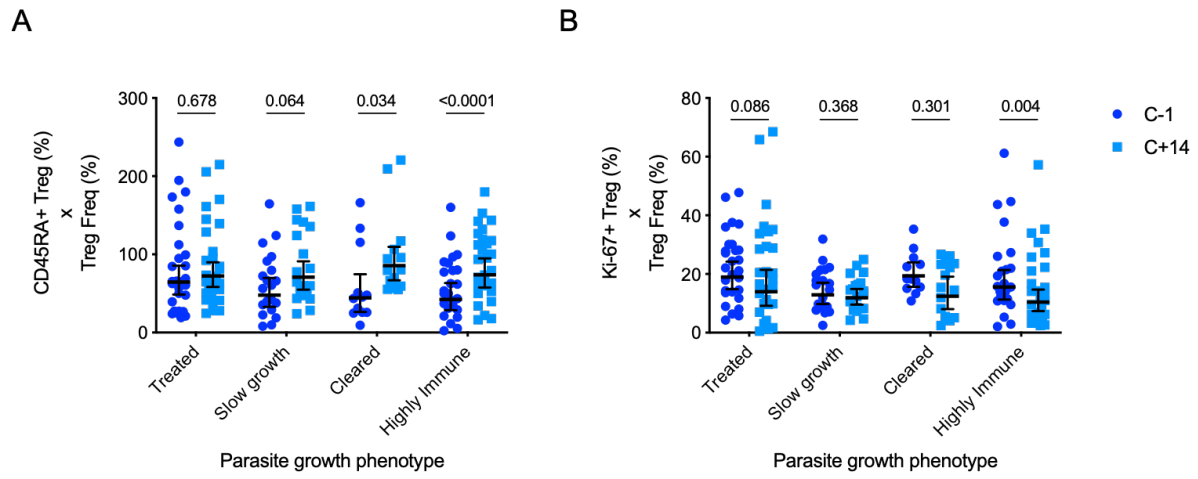

Figure 3.12: Change in relative counts of Treg subsets between C-1 and C+14 *Counts inferred by multiplying Treg phenotype subset frequency (as a proportion of all Tregs) by overall Treg frequency (as a proportion of all CD4+ T cells) at each timepoint.* ***(a)*** *inferred count of CD45RA+ Tregs.* ***(b)*** *inferred counts of Ki-67+ Tregs. Differences between timepoints measured by Wilcoxon matched pairs tests. Differences between groups also measured by Kruskal-Wallis and no significant differences observed.*

Changes in the frequency of different CD25-, CD127hi, FoxP3- effector CD4+ T cell (Teff) phenotypes following CHMI were also measured. Teff responses appeared to be different to the changes seen in Tregs (Figure 3.13). Firstly, there were significant increases in the frequency of CD45RA+ Teffs in all four groups, including those that were treated. These increases did not follow the same relationship of increasing significance in the most-protected groups. Unlike for Tregs, there were no changes in the proportions of Teffs expressing Ki-67 for any of the four groups.

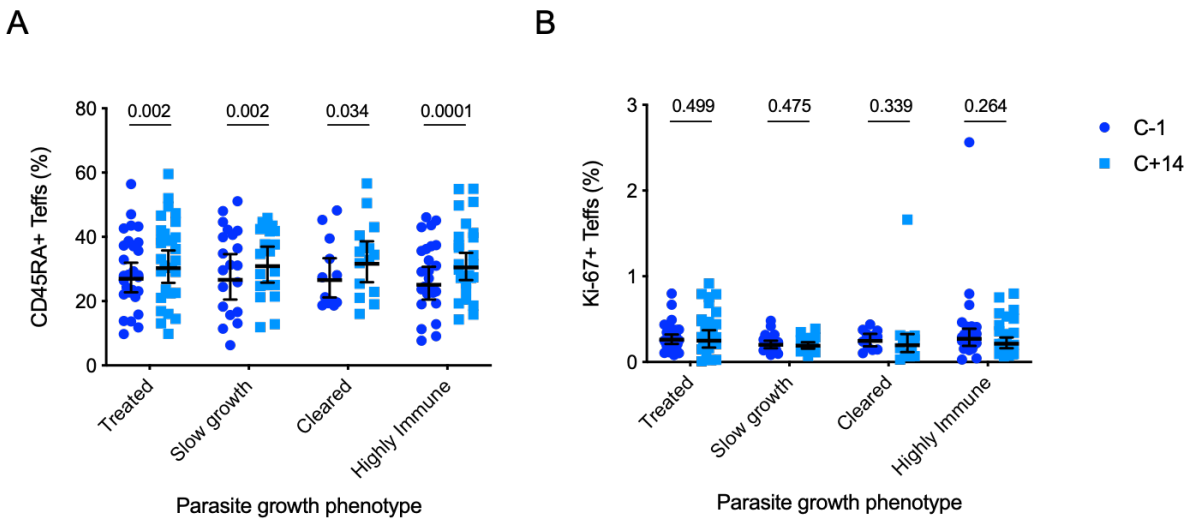

Figure 3.13: Change in Teff phenotype between C-1 and C+14 *Frequencies of different FoxP3- CD25- CD127hi Teff cell phenotype subsets measured by flow cytometry at C-1 and C+14.* ***(a)*** *frequency of CD45RA+ Teffs.* ***(b)*** *frequency of Ki-67+ Teffs. Differences between timepoints measured by Wilcoxon matched pairs tests. Differences between groups also measured by Kruskal-Wallis and no significant differences observed.*

Whilst the frequency of bulk Tregs was not significantly different between growth outcome groups at either C-1 or C+14, associations were observed with other immunological and demographic correlates and C-1 Treg frequencies. There was a negative association between Treg frequency at C-1 and the titre of anti-schizont IgG at screening (Fig 3.14a). Treg frequencies also declined with participant age (Fig 3.14b) and were also significantly lower in frequency in female participants than male (Fig 3.14c). Treg frequency was lower in participants from the moderately high transmission setting of Kilifi South [geomean: 3.31, 95% CI: 3.03-3.61] compared to Kilifi North [geomean: 4.13, 95% CI: 3.65-4.68], which experiences low transmission levels (Fig 3.14d). Treg frequency in Ahero [geomean: 3.16, 95% CI: 2.41-4.13] was not significantly different to either location in Kilifi however its geomean was less than in Kilifi South indicating a lack of statistical power to detect differences due to a smaller sample size.

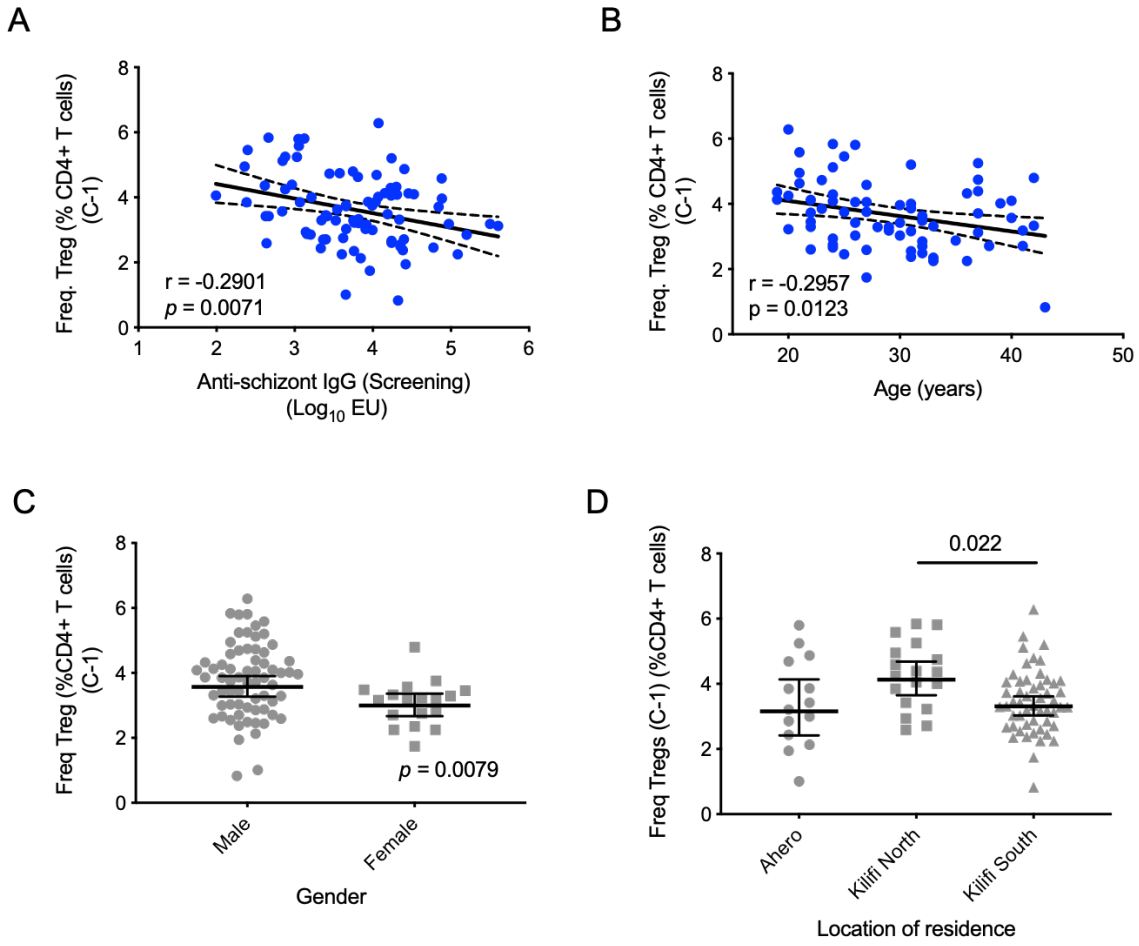

Figure 3.14: Associations between Treg frequency at baseline and immune and demographic correlates

(a) *association between Treg frequencies, defined as the percentage of FoxP3+ CD25+ CD127lo cells as a proportion of total CD4+ T cells in PBMC, at C-1 and the titre of IgG against schizont extract at screening. Spearman's Rho, r = -0.29 p = 0.007.* ***(b)*** *association between Treg frequencies at C-1 and participant's age at the time of trial. Spearman's Rho, r = -0.296 p = 0.01.* ***(c)*** *association between Treg frequencies at C-1 and participants gender. Mann-Whitney U, p = 0.008.* ***(d)*** *association between Treg frequency at C-1 and participants location of residence – differences measured by Kruskal-Wallis with Dunn's correction; only significant p values shown.*

3.3.7. CD4+ T cell proliferation in response to parasite stimulation is not associated with parasite growth outcome or Treg frequency

PBMCs were stimulated with schizont extract derived from *in vitro* culture of the parasite strain used for CHMI, isolated from the blood of an infected volunteer. PBMCs were cultured for 6 days and proliferation of the CD4+ T cell compartment monitored by CFSE staining. The rate of proliferation was heterogeneous between samples (Fig. 3.15a). After subtracting background stimulation with uninfected red blood cells and adjusting to the lower limit of detection (0.0032%; the detection rate if 1 in 31,315 CD4+ T cells proliferated, where 31,315 is the geomean number of CD4+ T cells acquired), the median rate of proliferation was 3.94% [IQR: 1.01-8.14%, range: 0.002-17.51%]. The rate of proliferation of PBMCs at C-1 following PfSE stimulation positively correlated with the fold change in the frequency of effector CD4+ T cells (CD25- FoxP3- CD127hi) expressing Ki-67 at C+14 compared to C-1 (Fig 3.15b) suggesting *in vitro* proliferation was predictive of the *in vivo* antigen-specific CD4+ T cell response to CHMI.

Despite this, there was not an association between the magnitude of CD4+ T cell proliferation to PfSE at C-1 and the parasite growth outcome following CHMI (Fig 3.15c).

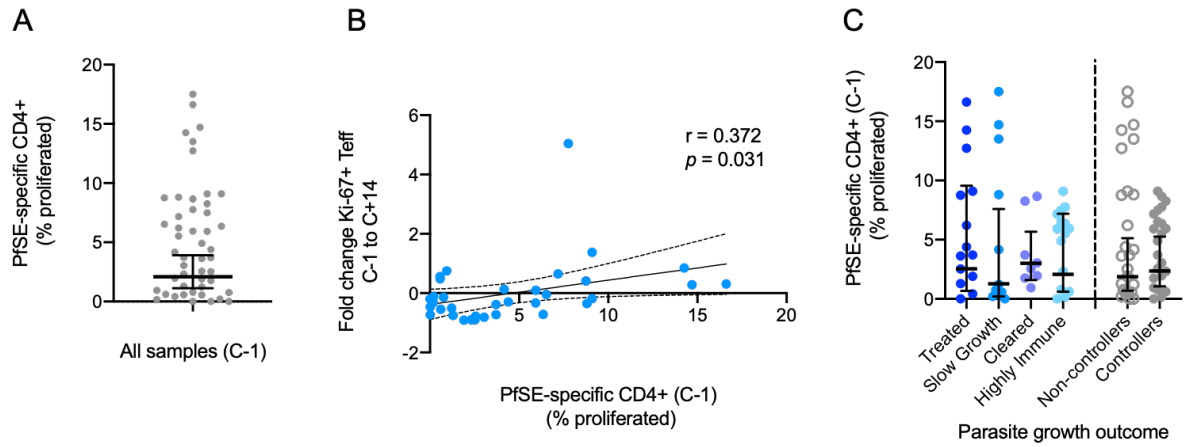

Figure 3.15: Association between in vitro CD4+ T cell proliferation following PfSE stimulation, the in vivo cellular response and parasite growth outcome following CHMI

Proliferative response of CD4+ T cells to PfSE stimulation measured as the percentage of cells having undergone at least one division, tracked by CFSE staining. Percentage proliferation of cells stimulated with autologous uninfected red blood cells is subtracted from the PfSE-stimulated condition and any values lower than the theoretical lower limit of detection were adjusted accordingly. ***(a)*** *distribution of data between individual samples.* ***(b)*** *association between in vitro CD4+ proliferation following PfSE stimulation and the fold change in CD25- FoxP3- CD127hi effector T cells which express Ki-67+ following CHMI. Spearman's rho, r = 0.372 p = 0.031* ***(c)*** *association between in vitro CD4+ T cell proliferation following PfSE stimulation and parasite growth outcome following CHMI split by four groups or combined as controllers (cleared and highly immune) or non-controllers (treated and slow growth). No significant differences by Kruskal-Wallis with Dunn's correction between the four outcomes or by Mann-Whitney for the controllers versus non-controllers.*

There was also no association between the magnitude of CD4+ T cell proliferation to PfSE stimulation and Treg frequency at C-1 or the titre of anti-schizont IgG present at screening (Fig 3.16a and 3.16b). There was a significant negative association between the rate of proliferation and the volunteer's age (Fig 3.16c). No association was observed between proliferation and the participants location of residence (Fig. 3.16d), however samples included in the subset analysed were not selected based on location meaning there were unequal numbers of samples per group for this analysis.

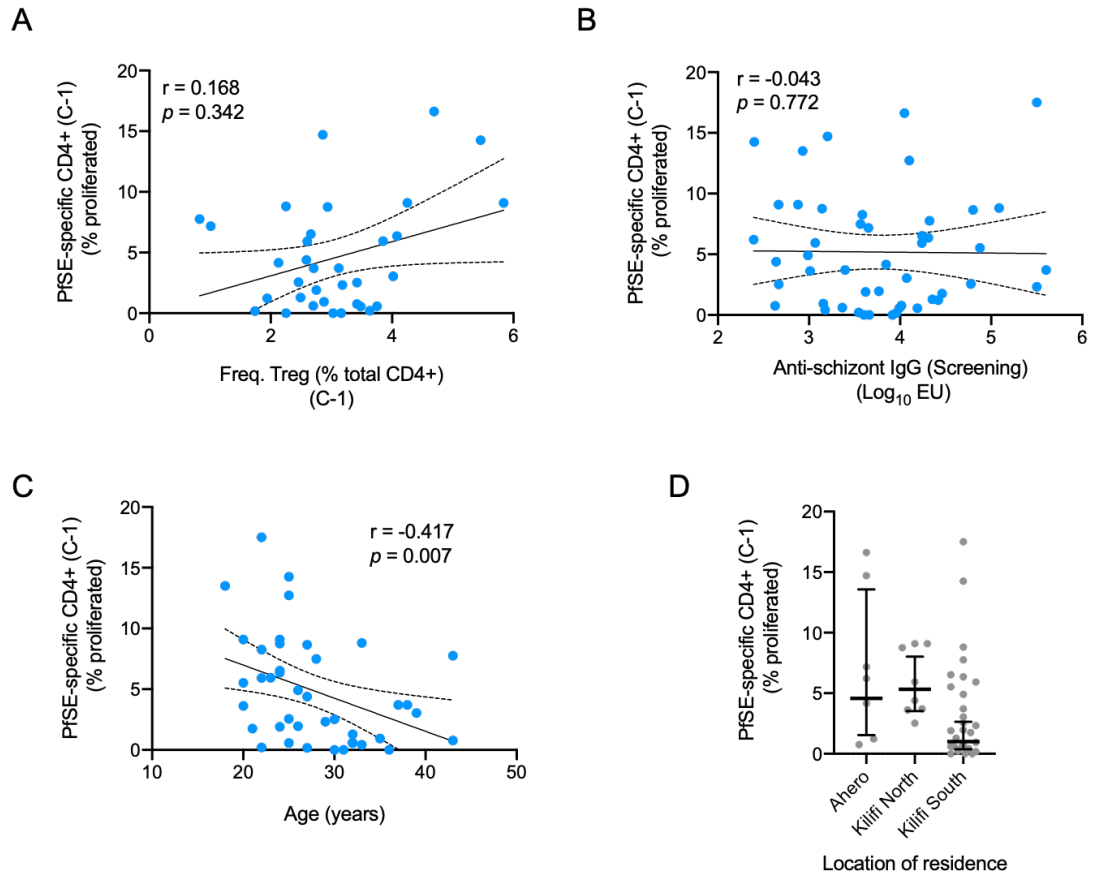

Figure 3.16: Association between in vitro CD4+ T cell proliferation to PfSE stimulation and Treg frequency, malaria exposure and age

(a) *association between in vitro PfSE-specific CD4+ T cell proliferation and the frequency of Tregs at C-1. Spearman's rho, r = 0.168 p = 0.342.* ***(b)*** *association between in vitro PfSE-specific T cell proliferation and the titre of anti-schizont IgG at baseline. Spearman's rho, r = -0.043 p = 0.772.* ***(c)*** *association between in vitro PfSE-specific T cell proliferation and participant's age. Spearman's rho, r = 0.417 p = 0.007.* ***(d)*** *association between in vitro PfSE-specific T cell proliferation and participant's location of residence. No significant differences between groups by Kruskal-Wallis with Dunn's correction for multiple comparisons.*

3.3.8. The concentrations of cytokines and chemokines in stimulation supernatants is not associated with CHMI parasite growth outcome

Supernatants were harvested from the 6-day-old stimulation cultures. The concentrations of 12 pro- and anti-inflammatory cytokines and chemokines were measured using a bead-based multiplex assay. Again, the antigen-specific response was calculated by subtracting cytokine concentrations in the autologous uninfected red blood cell stimulated condition from the PfSE-stimulated condition. In this analysis no significant differences in cytokine concentrations were seen by Kruskal-Wallis between the four parasite growth outcome groups. The only significant observation was for CCL2 which was higher in concentration in the controllers group than in non-controllers when groups were collapsed [$p = 0.045$] (Fig. 3.17). IL-4 showed a trend towards a lower concentration in controllers than non-controllers, but this relationship was not statistically significant [$p = 0.063$]. Considering the large number of comparisons made, these marginal p values are likely not significant findings.

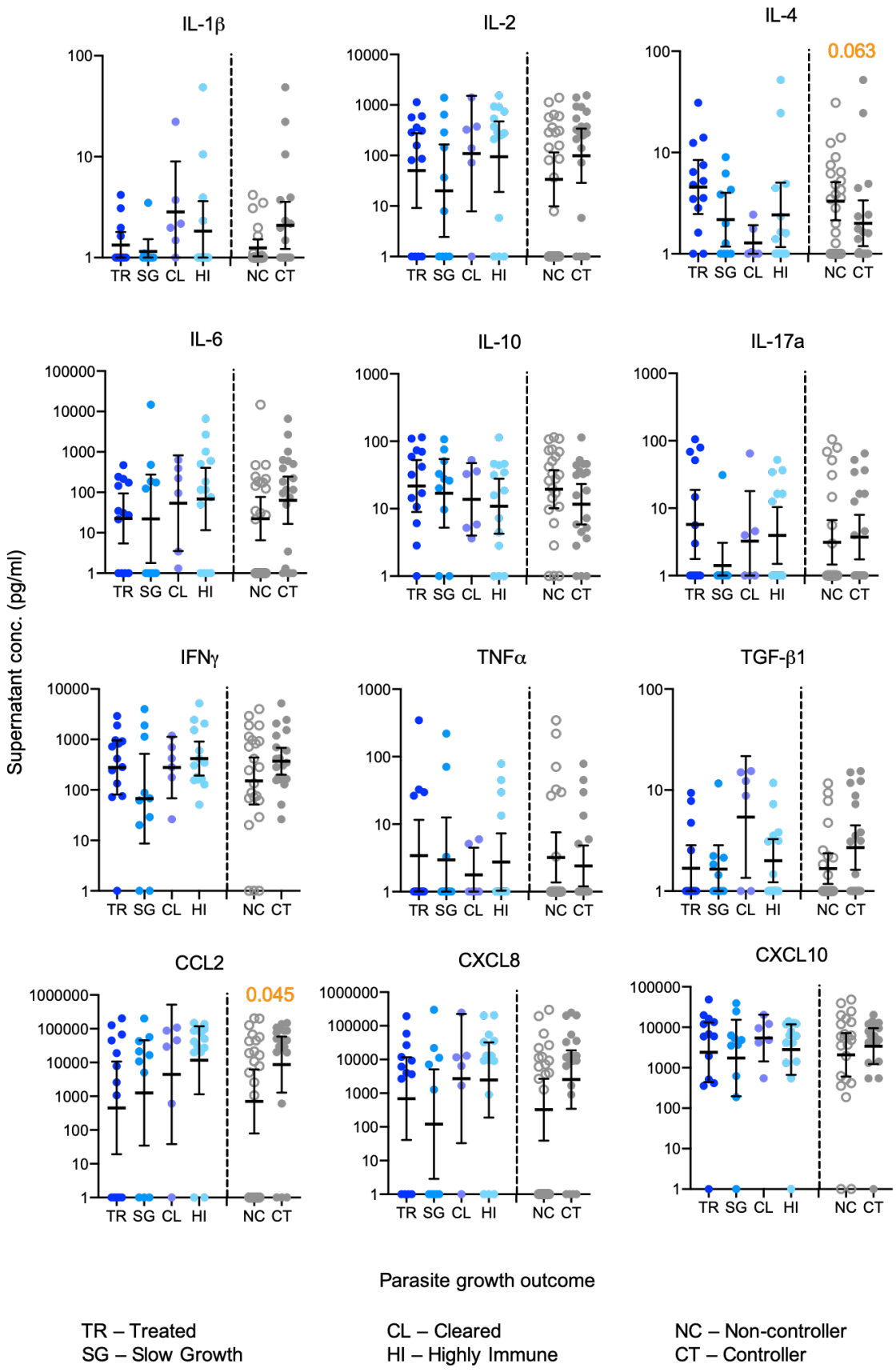

Figure 3.17: Supernatant cytokine and chemokine concentrations following PfSE stimulation of PBMC *(cont. below)*

Background concentrations of cytokine in uninfected red blood cell stimulated control conditions were subtracted values in the corresponding PfSE condition. Negative values corrected to a concentration of 1 pg/ml. Differences between four growth outcome groups measured by Kruskal-Wallis with Dunn's correction for multiple comparisons – no significant differences seen. Differences between controllers versus non-controllers tested by Mann-Whitney – only p values <0.1 shown for clarity.

The concentrations of the analytes were correlated against the magnitude of CD4+ T cell proliferation following PfSE stimulation. Concentrations of 5 of the 12 analytes including; CCL2, IFNγ, IL-2, CXCL8 and CXCL10 were associated with the magnitude of CD4+ T cell proliferation to PfSE stimulation (Fig. 3.18). No significant relationships were observed for the remaining 7 cytokines.

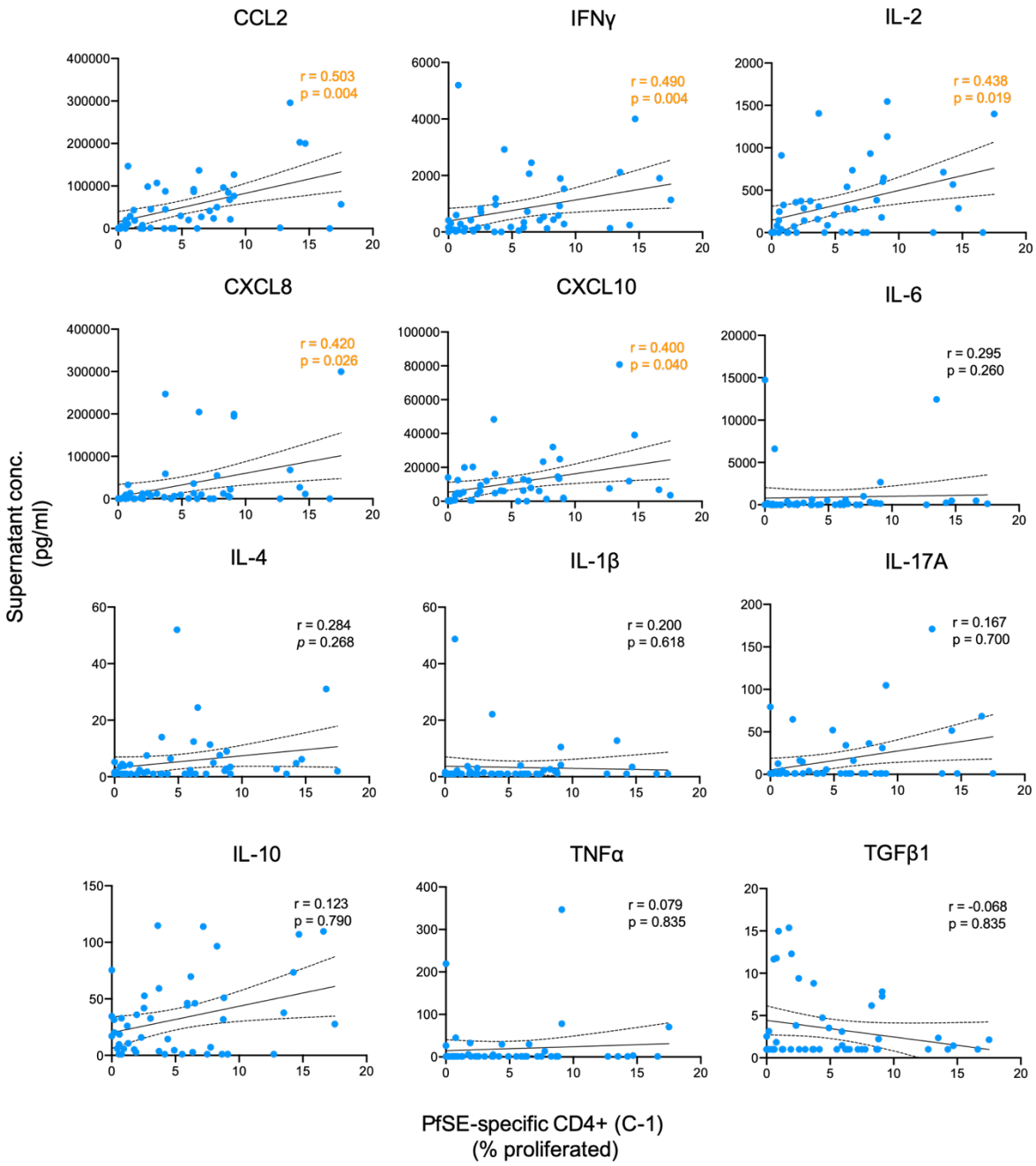

Figure 3.18: Correlation between CD4+ T cell proliferation upon PfSE stimulation and the concentration of cytokines in plasma

Associations measured by Spearman's rho correlation. Both CD4+ proliferation % and cytokine concentration plotted following background subtraction of values for uninfected red blood cell stimulated controls. Plots ordered by ranking of strength of associations – first 5 plots only show significant relationships. P values corrected for multiple correlations by the Holm-Sidak method.

The expression profiles of all cytokines measured following PBMC stimulation with PfSE were analysed together by PCA (Figure 3.19). No clustering of samples based on parasite growth outcome following CHMI was observed. The variance along PC1 was driven predominantly by elevated expression of CXCL8 only.

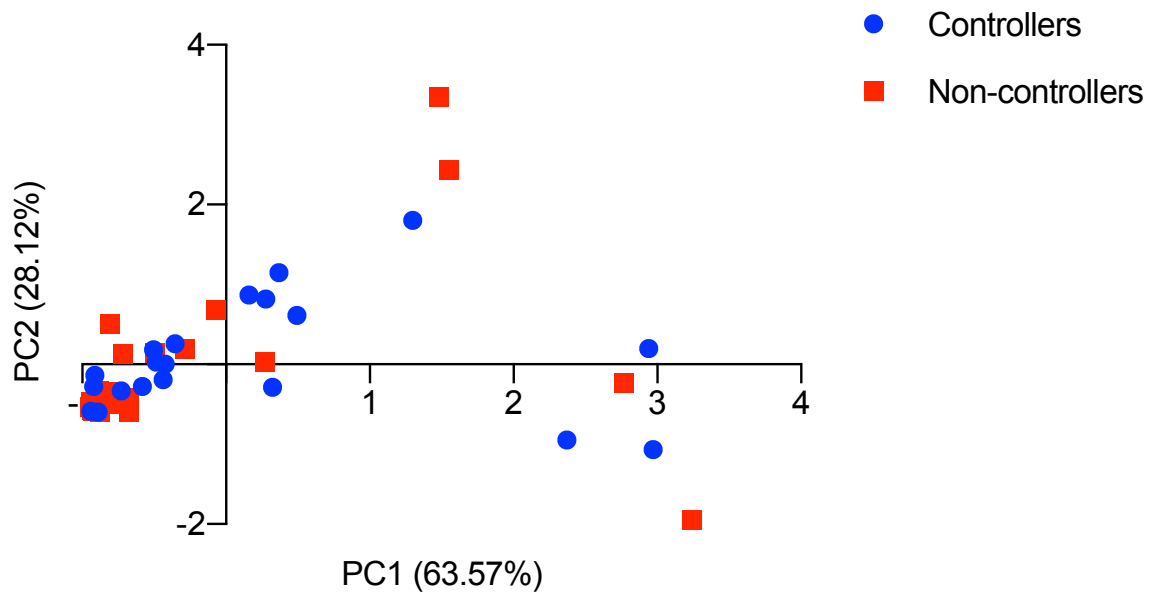

Figure 3.19: Principal component analysis of cytokine concentrations in culture supernatants following PfSE stimulation of PBMC *Only first two principal component dimensions shown, accounting for 91.7% of variance. PCA performed on a correlation matrix.*

Overall, there was no evidence that the magnitude of CD4+ T cell proliferation, nor the profiles of cytokines produced were predictive of parasite growth outcome following CHMI.

3.3.9. PCA on combined datasets does not reveal clustering by parasite growth outcome group

Finally, PCA was used to combine all data sets in order to assess whether overall responses can separate individuals by parasite growth outcome groups. PCA was conducted twice, using all available data at C-1 and C+14. Analysis of C-1 data is shown in Figure 3.20a. No clustering by parasite growth outcome groups was observed between individuals. Loadings analysis showed that anti-schizont IgG titre, CCL2 supernatant concentration and CXCL8 supernatant concentration accounted for the greatest variance along the first principal component. In the analysis conducted using C+14 data (Fig 3.20b), there was also no clustering by parasite growth outcome group observed either. Unlike for the analysis at C-1, loadings analysis did not reveal dominant variables accounting for the majority of variance.

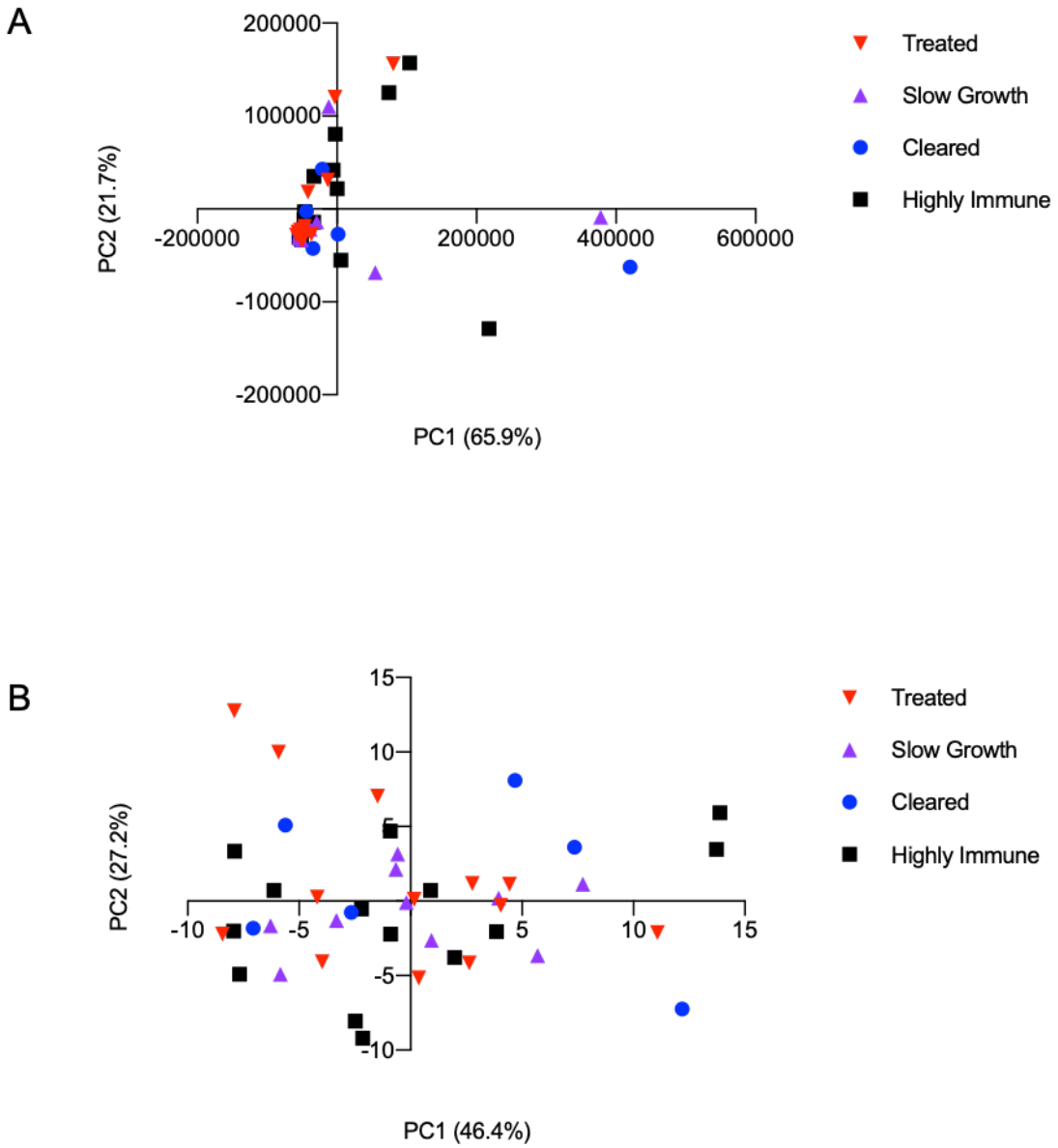

Figure 3.20: Principal component analysis of all data at C-1 and C+14 (a) *PCA at C-1 combining all demographic data (age, sex, location of residence), pro- and anti-inflammatory plasma cytokine concentrations at C-1, Treg frequency, CD45RA+ and Ki-67+ phenotype, Teff CD45RA+ and Ki-67+ phenotype, CD4+ T cell proliferation frequency following PfSE stimulation and supernatant cytokine concentrations. First two principal components shown accounting for 87.6% of variance.* ***(b)*** *PCA at C+14 combining all demographic data, pro-and anti-inflammatory cytokine concentrations at C+14, Treg frequency, CD45RA+ and Ki-67+ phenotype fold change over C-1. First two principal components shown accounting for 73.6% of all variance.*

3.4. Discussion

These data represent an initial understanding of both the immunological and parasite response to CHMI in semi-immune adults. Only 33.6% of individuals reached the treatment threshold and there was marked heterogeneity in parasite growth rates amongst this group. These findings contrast those of previous studies reporting more predictable parasite growth. In the study presented here, 3200 infectious sporozoites were delivered by DVI based on dose titrations in 9 malaria-naïve European adults which resulted in 100% infectivity[288], matching the gold-standard infection model using 5 infectious mosquito bites. A subsequent study in Tanzanian adults replicated 100% infectivity using the DVI method in 18 individuals[124]. Other studies in Africa have used used cryopreserved sporozoite challenges delivered by IM and ID routes, where doses have also been titrated to match the infectivity of mosquito-based challenge models. These studies also report high infectivity. In one study recruiting in Tanzania, 10/11 volunteers reached patent parasitaemia following ID inoculation of 25,000 sporozoites[290]. In a previous study in Kenya, volunteers received 125,000 sporozoites IM and 28/28 volunteers developed parasitaemia albeit with 1/28 volunteers exhibiting a reduced parasite multiplication rate[249]. It is most likely the differences seen in our study are down to higher levels of natural immunity acquired through natural exposure to the parasite. In both the Tanzanian study and first Kenyan study, participants were enrolled from the highly urbanized cities of Dar es Salaam and Nairobi respectively, with lower seasonal malaria transmission rates than in Kilifi[291,292]. The benefit of the heterogeneous parasite growth outcomes to CHMI observed in this study is that it provided variables by which protective and non-protective immune responses could be investigated[287].

Differences in parasite growth outcome between individuals recruited from different areas of residence were also observed and is most likely also reflective of the differences in transmission intensity between these locations. In Kilifi north, which has very low transmission levels[293], the majority of volunteers were treated, suggesting a lack of aquired immunity though lack of prior exposure. In Kilifi south, where higher transmission levels occur, most volunteers did not meet the threshold for treatment and the largest group were the highly immune. Interestingly, in Ahero, where the highest transmission rates occur, most volunteers had slow growth and there were no highly immune individuals. This suggests potentially different mechanisms of acquired immunity to malaria in very high transmission settings, however a larger cohort of volunteers from Ahero would be required to confirm this. Anti-schizont antibody titres as a correlate of exposure support the idea that higher prior exposure is protective in CHMI. Anti-schizont IgG was lowest in the treated group. Titres were similar between the three protected groups suggesting that further heterogeneity in the immune response is driving differences in parasite growth outcome and that this heterogeneity can occur in individuals who have had similar levels of prior exposure. The focus of the rest of this chapter was on whether differences in cytokine and T cell responses contribute to this heterogeneity.

The ELISA assays used here did not detect significant increases in the plasma concentrations of different pro-inflammatory cytokines during CHMI compared to C-1, nor did it show significant differences in cytokine concentration between parasite growth outcome groups at baseline. This is in disagreement with Walther and colleagues who observed increases in some pro-inflammatory cytokines, particularly IFNγ, at comparable parasitaemias to ours in a malaria-naïve UK cohort[114]. In this

study, they identified 3 groups based on cytokine upregulation. The first group upregulated IFNγ and IL-10 but not IL-12p70. The second group upregulated all 3 cytokines and the final group upregulated TGF-β1 early on in blood stage infection but none of the other 3 cytokines were significantly upregulated. The two groups with higher pro-inflammatory upregulation were better able to control parasite growth. Their cohort was malaria-naïve before CHMI and a multiplex Luminex assay was used to measure cytokines. In our study, similar increases in pro-inflammatory cytokine concentration at post-challenge timepoints were not detected using singleplex ELISA assays despite participants having comparable parasitaemias. For many volunteers, responses above the lower limits of detection of each assay were not detected. This disparity could reflect differences in sensitivity of these assays, or it could represent differences in the responses to malaria between naïve and pre-exposed individuals. As discussed in section 1.2.2, it is thought that at least some, if not the majority, of the pathology and symptomaticity behind malarial disease is driven by the host inflammatory response and not directly the parasite itself[20]. It is known that people living in malaria-endemic areas can harbour blood-stage parasites at medium-density parasitaemias and be completely asymptomatic[15,294]. The lack of detectable pro-inflammatory cytokines observed in plasma could reflect the training of the immune response through prior malaria exposure away from the over-exuberant systemic inflammation which leads to clinical illness. This is not a surprising find even in the low-transmission group from Kilifi North who are still semi-immune in that they very rarely display febrile malaria in the community. In contrast, malaria-naïve UK volunteers have a high rate of symptoms at considerably lower parasitaemias to those tolerated here[253].

The one cytokine which was observed to be significantly upregulated was IL-10 and this was only in the treated group. IL-10 was one of the cytokines significantly upregulated in Walther *et al*.'s analyses and upregulation highly correlated with that of IFNγ. It is interesting then that this cytokine was affected by CHMI without correlation to pro-inflammatory responses. This could fit with the hypothesis that the pro-inflammatory response is controlled to prevent pathology, whilst doing so to the anti-inflammatory response would be unnecessary and perhaps antagonistic to this process. A similar relationship for latent TGFβ-1 was not observed. Instead there was a slight decrease in plasma concentration in the treated group. It was not possible to measure free bioactive TGFβ-1 in this study. This data might have been helpful in forming conclusions on the activity of this cytokine even though it is likely free bioactive TGFβ-1 activity mirrors that of the latent isoform albeit with a slight delay. Walther and colleagues also did not show that TGFβ-1 activity was associated with IL-10. It is not known why TGFβ-1 concentration might have decreased in the treated group. Numerous cell types including T cells and monocytes can produce anti-inflammatory cytokines. The contrasting activity of IL-10 and TGFβ-1 in this study may reflect different cellular origins of the two cytokines whereby independent mechanisms are acting. Reduced TGFβ-1 production could result from switching to a pro-inflammatory state of the cell type of its origin in response to CHMI, or it could reflect the suppression of a particular compartment of immune response by the parasite. The number of Ki-67+ Tregs decreased following CHMI suggesting that parasite-mediated immunosuppression could act on anti-inflammatory responses as well.

This study only observed the upregulation of IL-10 late in the time course of infection in the treated group. One hypothesis might be that this signature indicated an unhelpful

anti-inflammatory response which is facilitating parasite growth. Determining this would require a detailed examination of the time course of IL-10 together with parasite growth dynamics early on in blood stage infection. This study did not detect significant increases in IL-10 until the day of diagnosis, making it difficult to evaluate small changes earlier on in infection. More sensitive tools would be required to facilitate this. The predominant source of IL-10 in malaria infection is likely either monocytes or Tregs[295]. Considering the findings of Walther *et al*., who identified an inverse relationship between CD4+ CD25+ Treg frequencies, FoxP3 mRNA in blood and time to parasitaemia in a malaria-naïve cohort, it was decided to focus on investigating this relationship in semi-immune adults as well. Here, Tregs were defined as being CD25+ FoxP3+ CD127lo CD4+ T cells – a more specific classification than was achievable at the time of the previous study[296]. In line with previous studies[105,113], our study observed increases in Treg frequency during blood-stage parasitaemia compared to pre-infection when the cohort was analysed as a whole. When the analysis was split by growth outcome, this increase was observable in all groups apart from those that were treated. Fold change analysis suggested there was considerable heterogeneity in Treg dynamics in this group with individuals experiencing both up- and down-regulation of Treg frequency. The increase appeared most significant in the highly immune group and certainty decreased through the other groups. The fact that a cellular immune response was seen in the absence of detectable parasitaemia in the highly immune group is plausible because even though qPCR is highly sensitive[297], it is still possible that active blood stage infection is ongoing in this group at extremely low parasitaemias below the lower limit of detection of the assay. To support this, reanalysis of blood samples using ultra-sensitive PCR methods is currently ongoing and preliminary data has identified parasitaemia in some individuals that had

previously been considered negative (M. Kapulu, personal communication). It is not yet known why greater Treg inflation was observed in the highly immune group – it could be that this is just reflective of an immune response overall that is greater in magnitude in the highly immune group and therefore not indicative of a functional relationship between Treg induction and protection from parasitaemia. Or it could indicate that control of inflammatory responses is protective of parasitaemia. The fact that in subsequent experiments, the proliferation of CD4+ T cells in PBMCs following *ex vivo* stimulation with PfSE was not higher in the highly immune group would indicate that this is not simply a consequence of a larger overall T cell response in the highly immune group. If functional, increased Treg activity in the highly immune group could be involved in the mechanism preventing over-exuberant inflammation and immune pathology whilst other factors such as functional antibody responses act alongside to control parasite growth.

Next, this study looked at the gross memory phenotype and proliferative history of Tregs. Expansion of Tregs that were CD45RA+ was proportional and of a greater magnitude to the expansion of overall bulk Treg frequencies. Again, there was no increase in the proportion of Tregs that were CD45RA+ following CHMI in the treated group. This suggests the Tregs accumulating during infection are from a naïve, rather than a memory pool of cells. The overall frequency of Tregs that were Ki-67+ actually decreased across all groups following CHMI. *P. falciparum* is known to cause reduced proliferative capacity of T cells, including those specific for heterologous antigens[298,299]. The expansion of the Treg pool in the absence of proliferation and the fact they are predominantly naïve cells would suggest that this is as a result of the conversion of circulating naïve CD25- FoxP3- T cells into Tregs. This is in line with a

mechanism proposed by Scholzen and colleagues who suggested Treg expansion in *P. falciparum* infection was caused by the increased secretion of immunosuppressive cytokines by monocytes whose phenotype had become anti-inflammatory following ingestion of infected red blood cells[111,112]. They found that the immunosuppressive milieu induced expression of FoxP3 in naïve CD4+ T cells which drove progression towards a Treg phenotype. This process was found not to require engagement of the T cell receptor and thus affected naïve CD4+ T cells in a non-antigen specific manner.

It was found that Treg frequencies at baseline were negatively correlated with the titre of anti-schizont antibody at baseline. This presents two possible scenarios; either Treg frequency and anti-schizont IgG titres do not directly interact meaning Treg frequencies decline with malaria exposure (as anti-schizont antibody titres increase), or Treg frequencies limit the acquisition of anti-schizont antibodies with the implication that this therefore limits acquisition of immunity to malaria overall. The data also showed that Treg frequencies were negatively associated with age and were more abundant in males than females. Anti-schizont antibody titres were only weakly associated with age meaning declining Treg frequencies through age might not simply be a consequence of the time taken for immunity to malaria to be acquired. Previous studies have reported increased Treg abundance and suppressive capacity through age in both mouse and human studies (in non-malaria endemic locations)[300,301]. The decline observed here is therefore unexpected and might reflect the perturbation of Treg homeostasis in areas endemic for malaria as well as other infectious pathogens such as helminths. The observation of males having higher Treg frequencies is known in the literature and is thought to underlie the increased propensity for females to develop autoimmune conditions[302].

Simply quantifying circulating Tregs and looking at only two surface markers by flow cytometry does not tell us much about the phenotype or function of these cells which might underlie further differences in parasite growth outcome. This will be addressed in the following chapter which seeks to analyse the transcriptional profile of Tregs and effector CD4+ T cells in more detail through multiplex qPCR and differential gene expression analysis.

Finally, the role the overall CD4+ effector response might play in determining outcomes from CHMI was investigated. Using an *ex vivo* proliferation assay of PBMCs taken at C-1 and stimulated with the CHMI parasite schizont extract, it was shown that proliferation *in vitro* correlated with the fold change in the proportion of CD4+ T cells that were Ki-67+ at C+14 compared to C-1. This indicates that this assay is predictive of the magnitude of the *in vivo* proliferative response of CD4+ T cells to CHMI. Despite this, no association with the overall magnitude of CD4+ T cell proliferation and parasite growth following CHMI was found. The data also showed that CD4+ T cell proliferation was not associated with Treg frequency or anti-schizont antibody titre but was negatively associated with age. Immunity at the blood stage of infection is primarily mediated by antibodies and not T cells[303]. Assessing the antibody response to CHMI was beyond the scope of this thesis. Nevertheless, large numbers of CD4+ T cells primed against blood-stage specific antigen were found and these cells are thought to be required to help B cells to make antibodies, so might still have some involvement in immunity to blood stage malaria. Simply quantifying the number of CD4+ T cells responding to PfSE does not inform us of the phenotype of these cells or the type of help they might be providing to B cells. To address some of this, the concentrations of a range of cytokines and chemokines present in the supernatants of the cell cultures

were measured. Considering the fact that cytokine concentrations were generally very low and difficult to detect in plasma, assessing their concentrations in cell culture supernatants is an alternative method of assessing the activity of responding immune cells which would otherwise require invasive sampling techniques such as lymph node, spleen or liver biopsies.

A basic analysis of singular cytokine and chemokine concentrations in supernatant stratified by growth outcome did not reveal clear relationships, but suggested trends for CCL2 being higher in concentration in controllers and IL-4 being lower in this group. A principal component analysis also confirmed that the overall profile of the cytokine response could not separate individuals based on parasite growth outcome. This study also looked to see if cytokine concentrations in supernatant correlated with CD4+ T cell proliferation. All chemokines as well as IL-2 and IFNγ concentrations correlated with CD4+ T cell proliferation, potentially indicating alternative sources for the remaining analytes.

The proliferation assay also incidentally found an association between increasing age and declining CD4+ T cell proliferation. The majority of volunteers in this study were between the ages of 20-40 years old. Although few studies have thoroughly detailed the long-term effect of ageing on T cell function in healthy populations, most studies on immune senescence describe effects in populations much older than our cohort. One study measured CD4+ T cell proliferation to anti-CD3 stimulation and found no significant differences between the young (average age 34.7 ± 2.8 years) and the middle-aged (45.3 ± 5.3 years) groups but significantly reduced proliferation in the elderly group (76.1 ± 3.6 years) compared to both the young and middle-aged

groups[304]. This raises the possibility that perhaps accelerated immune senescence is being observed in this population, likely through increased exposure to chronic infections, including malaria. Most work on ageing and immunity in humans has been done in the context of influenza vaccines[305]. Elderly populations are an important group to target for seasonal influenza vaccination, however efficacy has been shown to reduce to around 30-50% in >65 year olds compared to 70-90% in younger adults living in European and North American settings[306,307]. The hallmarks of immune aging are reduced chemotactic and phagocytic capabilities of innate immune cells, reduced proliferation and cytokine production in T cells and reduced immunoglobulin production by B cells[308]. These cells also express greater levels of markers of senescence like CD57 and KLRG-1[309]. Although it is beyond the scope of this thesis, this is an interesting finding and worthy of investigation. The lengths of telomeres, expression of markers of senescence and exhaustion and proliferation in response to heterologous antigens should all be investigated in malaria-exposed individuals compared to healthy controls.

3.5. Conclusions

This study presents initial data from the largest CHMI trial for *P. falciparum* in semi-immune adults to-date. This enabled identification of a range of parasite growth phenotypes which could be exploited to identify immunological correlates of protection and susceptibility to malaria. No increase in pro-inflammatory cytokine responses following CHMI were observed, in disagreement with findings in a malaria-naïve cohort – potentially suggesting a mechanism that is acquired through prior exposure which

reduces susceptibility to clinical illness following infection through reduced systemic inflammation. Increased Treg activity in the more highly immune groups was observed, again suggesting they may play a role in protection from inflammation with increased immunity though prior exposure. Overall CD4+ T cell proliferation was not associated with CHMI outcome, and analysis of supernatant cytokine concentrations did not identify particular cell phenotypes and subsets that might be important. PCA did not reveal clustering of individuals by parasite growth outcome group by combining all data presented here together.

These data also revealed some associations worthy of further investigation which are beyond the scope of this thesis. The association between Treg frequencies and anti-schizont antibody titres as well as Treg frequencies and age should be investigated to determine if Tregs are limiting long-term acquisition of immunity or if Treg homeostasis is altered through chronic exposure to malaria. Finally, the decreased proliferative capacity of CD4+ T cells suggests a mechanism of accelerated immune senescence through chronic malaria exposure should be investigated.

Further steps in this study are to profile the activity of Tregs and effector CD4+ T cells in greater detail through cell type-specific transcriptomics analysis of CD4+ T cell subsets. This will help to determine, with greater resolution than is possible by flow cytometry, if the phenotype of these cells is important in determining outcomes from CHMI.

Chapter 4

4. Transcriptional phenotyping of effector and Regulatory CD4+ T cells using multiplex qPCR – an analysis of cellular responses to CHMI

4.1. Introduction

Chapter 3 sought to investigate parasite growth outcomes to CHMI in semi-immune populations and began to assess associated immune responses. The magnitude of pro- and anti-inflammatory cytokine responses was measured and bulk Treg and antigen-specific effector CD4+ T cell responses were evaluated. Simply quantifying frequencies of cells in different CD4+ T cell subsets in the context of CHMI, as was carried out in the methods used in Chapter 3, does not capture diverse functional differences, which might be associated with the various infection outcomes. T cells may respond to CHMI by either expressing different effector functions (e.g. different cytokine profiles), or by upregulating these effector functions to a greater or lesser extent than in other individuals. It is important to assess whether differences in T cell effector functions exist between different parasite growth outcome groups.

Multiparametric flow cytometry does not allow analysis of a sufficient number of markers to properly evaluate heterogeneity of the many diverse functions of T cell subsets. To overcome this, a multiplex quantitative qPCR method was used in this chapter to assess the expression intensity of 90 genes, pre-selected for their specific roles in either Treg or effector CD4+ T cell function. Analysing the expression of different genes can help to infer the function of the cells sampled. In this study, cell subsets were isolated from PBMC by fluorescence activated cell sorting (FACS) at relevant baseline (C-1) and post-challenge (C+14) timepoints during CHMI. Sorting cells prior to gene expression analysis is necessary because it allows functions to be attributed directly to cell subsets of interest. If a whole blood transcriptomics approach was used, the cellular origin of a particular function would have to be inferred indirectly. Whilst analysis using multiplex qPCR is limited to a subset of specific genes, which might risk relevant hits being missed, this method facilitates greater throughput of a large number of samples from different volunteers than would be possible with other commonly used methods such as RNAseq. Overall, increasing the sample size increases the statistical power to detect differences in the genes that are analysed.

Two populations of cells were sorted from each sample, CD25+ CD127lo CD4+ Tregs and CD25- CD127hi CD4+ effector T cells 'Teffs'. CD25+ and CD127lo expression on CD4+ T cells highly correlates with FoxP3 expression and Treg phenotype[310] making these suitable cell surface markers for sorting Tregs for isolation of RNA when FoxP3 itself cannot be used[296]. Cells were collected at 2 timepoints, baseline (C-1) to assess baseline phenotype and 14 days post-infection (C+14) to assess cellular responses to blood stage infection. Gene expression was quantified in both cell subsets, either cross-sectionally at baseline or in response to CHMI at C+14. Differential expression

was primarily examined between different parasite growth groups in order to identify whether different phenotypes are associated with different CHMI outcomes.

4.2. Chapter-specific Methods

Detailed methods for the conduct of the CHMI-SIKA clinical trial are described in Chapter 2.2 and 3.2. Detailed laboratory methods for the isolation of CD25+ CD127lo CD4+ Tregs and CD25- CD127hi CD4+ Teffs and subsequent downstream processing for quantitative PCR are also described in Chapter 2.4.

Briefly, PBMCs were collected as part of the CHMI-SIKA trial and were thawed on the day of sorting. 3 x 10^6 cells per vial were stained for cell sorting. The remaining cells were stained for standard flow cytometric phenotyping in the data presented in Chapter 3. Cells were sorted using a BD FACSMelody™ into two populations – CD25+ CD127lo CD4+ Tregs and CD25- CD127hi CD4+ effector T cells, 'Teffs'. A maximum of 20, 000 cells were sorted per cell type and stored in RNA preservation buffer until further use.

RNA was extracted from bulk cells using Qiagen RNeasy mini spin columns. cDNA synthesis and PCR pre-amplification of target genes was carried out using standard reagents and workflow for the Deltagene assay from Fluidigm. Relative gene expression analysis was carried out on a panel of 90 genes selected for their role in CD4+ T cell function and immunity to malaria, using 6 housekeeping reference genes for normalisation, as listed in Chapter 2.4. Multiplex qPCR using the Deltagene

platform from Fluidigm was carried out on a Biomark HD thermocycler using the manufacturer's standard workflow. C_T values were normalised against housekeeping reference genes and processed into Log_2 fold change relative gene expression datasets by the $2^{-\Delta\Delta Ct}$ method for downstream analysis by the two methods described below. This method was chosen as it is the current best-practice standard for Log_2 fold change calculations from qPCR data[311]. Data were assessed for normal distribution before applying parametric statistical tests for differential gene expression analysis.

Data from the two timepoints were analysed by two methods:

- **C-1:** Normalised Log_2 fold change values were calculated per gene, relative to the mean expression of each gene across all samples at C-1. This analysis provided an estimate of the baseline resting phenotype of each cell subset.
- **C+14:** Normalised Log_2 fold change was calculated based on expression at C+14, relative to the expression in the matched C-1 sample. This analysis estimated the individual cellular response to CHMI.

Both datasets were used separately to analyse differential expression between samples in relation to CHMI outcomes as well as other immunological and demographic measures. Each cell type was also analysed separately.

One limitation of categorising Teffs as CD25- CD127hi CD4+ T cells, is that activated effector cells transiently express CD25[312]. This risks missing some activated Teffs which might have been important in this analysis. The priority here was to isolate as pure a population of Tregs as possible, making the use of CD25 as an isolation marker unavoidable. Teff data should be interpreted in the context of this caveat.

4.3. Results

4.3.1. Fluorescence activated cell sorting panel

A surface staining panel was designed to identify and sort CD25+ CD127lo CD4+ Tregs and CD25- CD127hi CD4+ Teffs simultaneously. A representative sample showing the gating strategy to sort the two populations of interest is shown in Figure 4.1. The strategy firstly gated on lymphocytes, followed by single cells and then live, CD14-/CD19- cells. Next, CD3+, CD4+ cells were gated on, followed by CD25+ CD127lo Treg cells and CD25- CD127hi Teff cells. The final gate was a second scatter gate to exclude non-single cells.

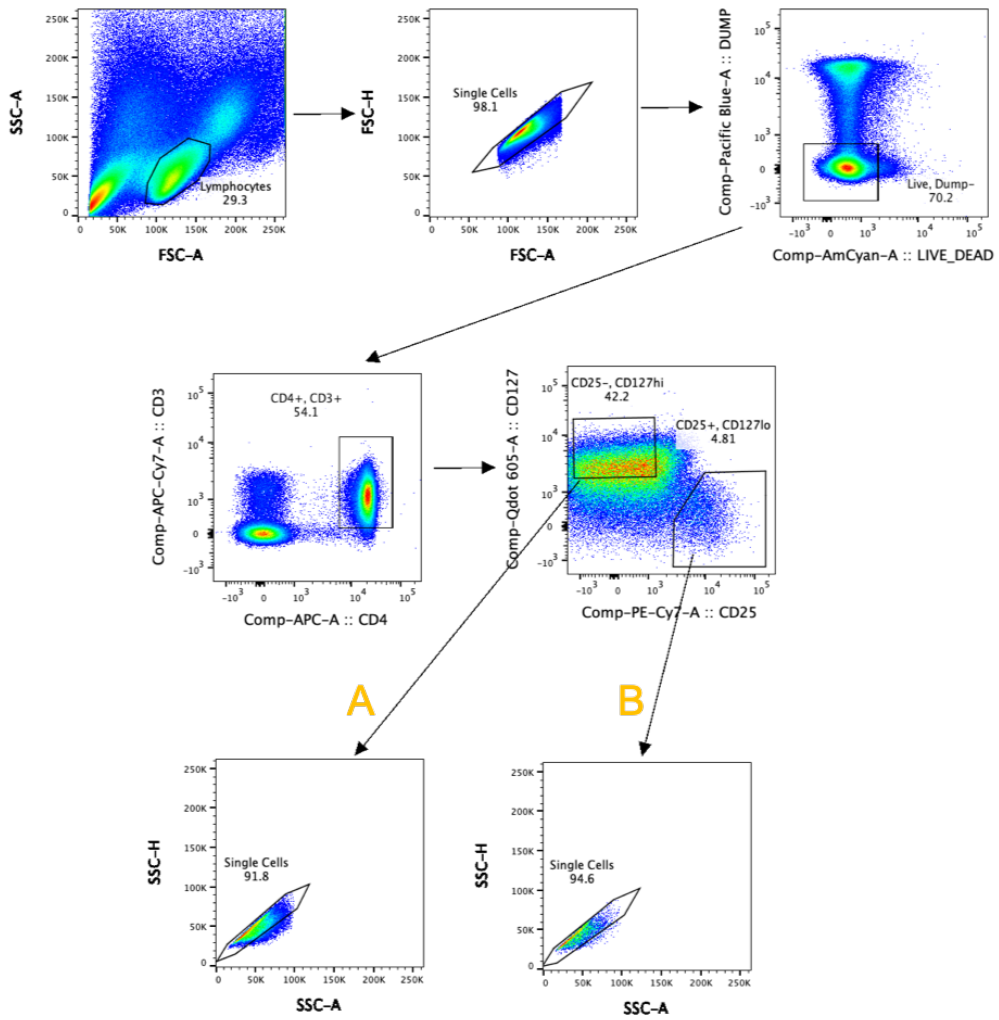

Figure 4.1: Gating strategy for sorting Teff and Treg cells from PBMC *(cont.)*

FACS plot for one single representative PBMC sample. ***(a)*** *sorted CD4+ CD25- CD127hi Teff population.* ***(b)*** *sorted CD4+ CD25+ CD127lo Treg population.*

A maximum of 20 000 cells per cell type were sorted per sample. Descriptive statistics for the number of samples and cells sorted are shown in Table 4.1.

Descriptive

Total volunteers – No.	53
Volunteers per timepoint – No.	
C-1	53
C+14	53
Cell types per volunteer – No.	2
Number of cells per sample (Tregs)	
Median (Interquartile range)	8476 [5726 – 11 631]
Range	2348 – 20 000
Number of cells per sample (Teffs)	
Median (Interquartile range)	20 000 [20 000 – 20 000]
Range	20 000 – 20 000

Table 4.1: Cell sample descriptive statistics

4.3.2. Sample quality control

The presence of cDNA in RNA-extracted and reverse transcribed samples was confirmed by qPCR targeting the human Beta-2-microglobulin gene using exon-spanning primers. cDNA was detected in 380/380 [100%] of extracted samples. All samples were then subjected to multiplex qPCR to amplify 90 genes of interest and 6 reference genes for normalisation.

Quality control of amplification data and calculation of relative fold gene expression by the $2^{-\Delta\Delta Ct}$ method was carried out as described in Chapter 2. The data were analysed by the two methods described previously, creating two foldchange datasets per cell type for expression at C-1 and C+14.

The frequency distribution of fold gene expression data was assessed to determine their suitability for downstream parametric analyses. Log_2 fold change values were pooled for all genes of interest and for all samples. This analysis was repeated for all four fold change datasets (Figure 4.2). The data were not markedly skewed in either direction, with mean Log_2 FC values close to 0. For C-1 Teff, C-1 Treg, C+14 Treg and C+14 Teff, mean Log_2 FC values were; -3.32×10^{-10} [95% CI: -0.088 – 0.088], -9.40×10^{-10} [-0.10 – 0.10], 0.04 [-0.07 – 0.16] and -0.008 [-0.15 – 0.13] respectively. A D'agostino-Pearson omnibus K2 normality test was used to assess if any of the 4 datasets followed Gaussian distribution. None of the datasets were normally distributed in this analysis [p = <0.0001 for all four]. This is likely due to the significant numbers of genes not differentially expressed leading to a large number of values at or near 0.

The parametric tool, Limma, was still applied for downstream differential gene expression analysis since it is the most established package for this type of analysis and is reported to be generally robust against minor violations of gaussian distributions[284].

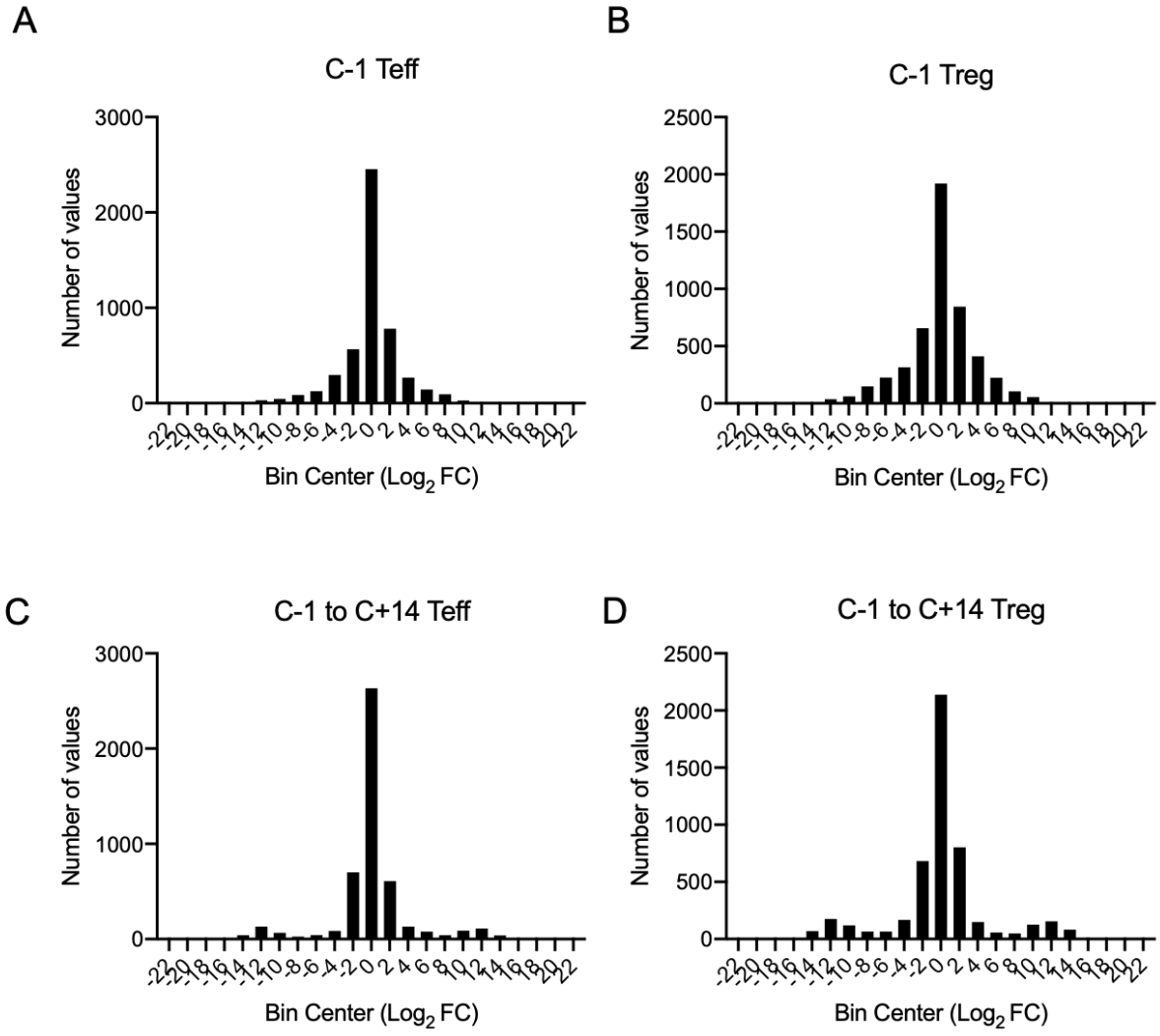

Figure 4.2: Frequency distributions of gene expression fold change values *Log_2 fold change values of all genes of interest plotted for **(a)** gene expression of Teff cells at C-1 (fold change relative to the mean per gene of all samples). **(b)** Treg cells at C-1. **(c)** Teff cells at C+14 relative to C-1 and **(d)** Treg cells at C+14 relative to C-1.*

Next, the effect of systematic variation induced by batch effects or from the input of different cell numbers was evaluated. Samples were analysed by multiplex qPCR on 5 separate assay plates. Each plate had an equal number of Teff and Treg samples from both timepoints. Batch effects were assessed by analysing ΔC_T values (normalised to 6 reference genes) of a single gene of interest across groups. Interferon gamma receptor 1 (IFNGR1) was used for this analysis because it was expressed in 100% of samples and at a medium intensity relative to other genes [geometric mean

C_T: 15.77, 95% CI: 15.57-15.98] Figure 4.3a shows no difference in ΔC_T values for IFNGR1 across the 5 batches. For Treg cells, different cell numbers were sorted and inputted into the assay because of variation in their frequencies in PBMC. Whilst normalisation to the reference gene controls for variation in input amounts, it was confirmed whether differences in ΔC_T values for IFNGR1 occurred depending on Treg cell counts in each sample. ΔC_T values for IFNGR1 were split by Treg cell count quartliles and no significant differences were observed between groups (Fig 4.3b).

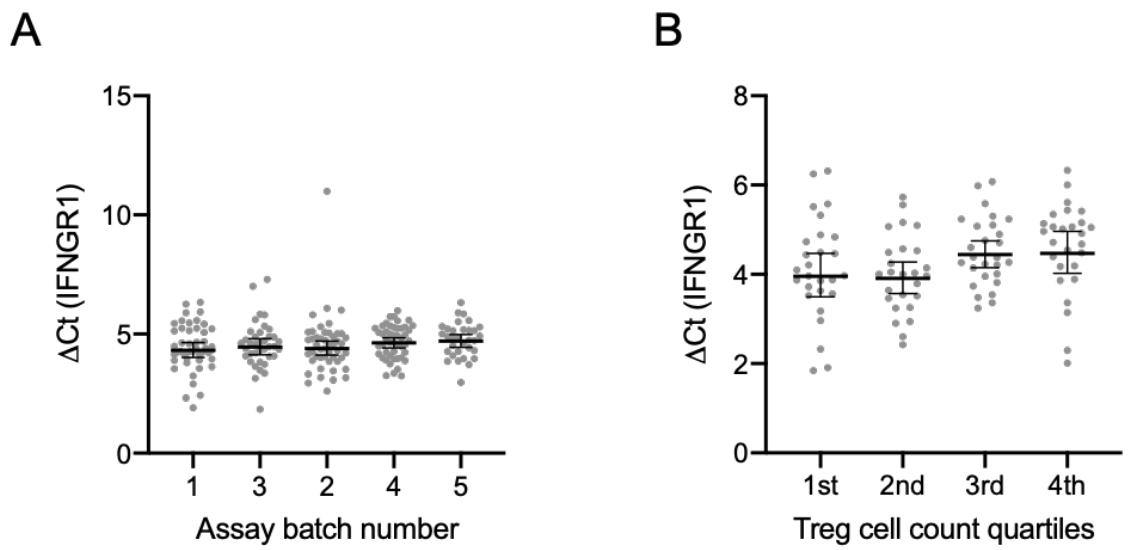

Figure 4.3: Analysis of systematic variation by analysis batch or number of cells per sample. (a) *ΔC_T values for IFNGR1 in both Teff and Treg samples split by assay plate batch.* ***(b)*** *ΔC_T values for IFNGR1 in Treg samples split by the number of cells sorted per sample where 1st quartile is the lowest input cell count and 4th the highest. Differences between groups compared by Kruskal-Wallis tests with Dunn's correction for multiple comparisons – no significant differences seen.*

Following the quality control procedures described in section 2.5.2 to remove poorly-amplified individual reactions, no samples had to be entirely removed from the analysis as no samples were observed to have significantly poor amplification across all genes. 2/6 reference genes were excluded in the normalisation calculation (Ubiquitin C and TATA box binding protein) as these were not amplified in every sample. No genes of

interest were removed entirely from analysis either despite some genes only having positive amplification in a small proportion of samples. All primers used were previously validated for human PBMC, therefore systemic reaction failures are unlikely and excluding potentially rarely activated genes may risk losing potentially important genes in this analysis.

4.3.3. Assessing differential gene expression in CD25+ CD127lo Tregs between CHMI parasite growth outcome groups

Variation in relative expression of genes from sorted Tregs was first assessed on heatmaps. Separate heatmaps were created for gene expression analysed at C-1 (Figure 4.4) and C+14 (Figure 4.5). In the C-1 cross-sectional analysis, the extent of differential expression was heterogeneous between genes, with some genes appearing stably expressed between individuals and other genes showing more marked differences. However, there were no obvious qualitative differences in phenotype between the four parasite growth outcome groups.

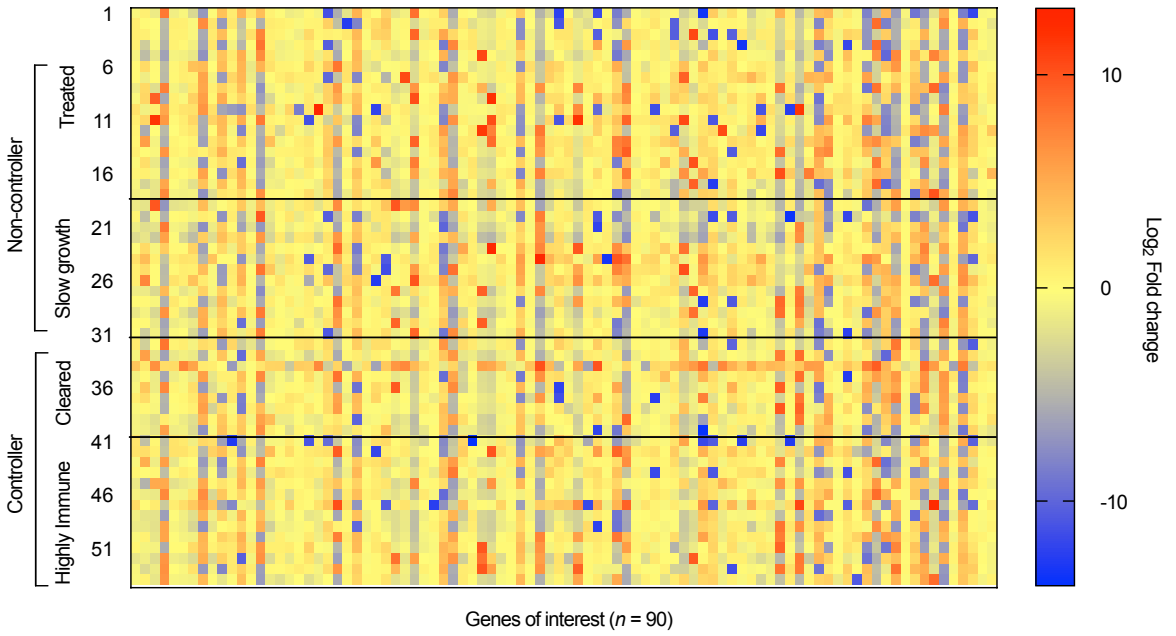

Figure 4.4: Heatmap of Log_2 FC in gene expression for Tregs at C-1. *FC for each gene calculated by $2^{-\Delta\Delta Ct}$ method relative to the mean of all samples.*

At C+14, there appeared to be a marginal downregulation of many genes in the cleared group, which was not apparent in the other 3 groups. The mean Log_2 FC across all genes in the cleared group was -0.42 [95% CI: -0.78 – -0.07], compared to 0.01 [-0.24 – 0.26] in the treated group, 0.09 [-0.20 – 0.39] in the slow growth group and 0.20 [-0.07 – 0.46] in the highly immune group. The difference between the cleared and highly immune groups was significantly different [p = 0.037] by ordinary one-way ANOVA with Tukey's correction.

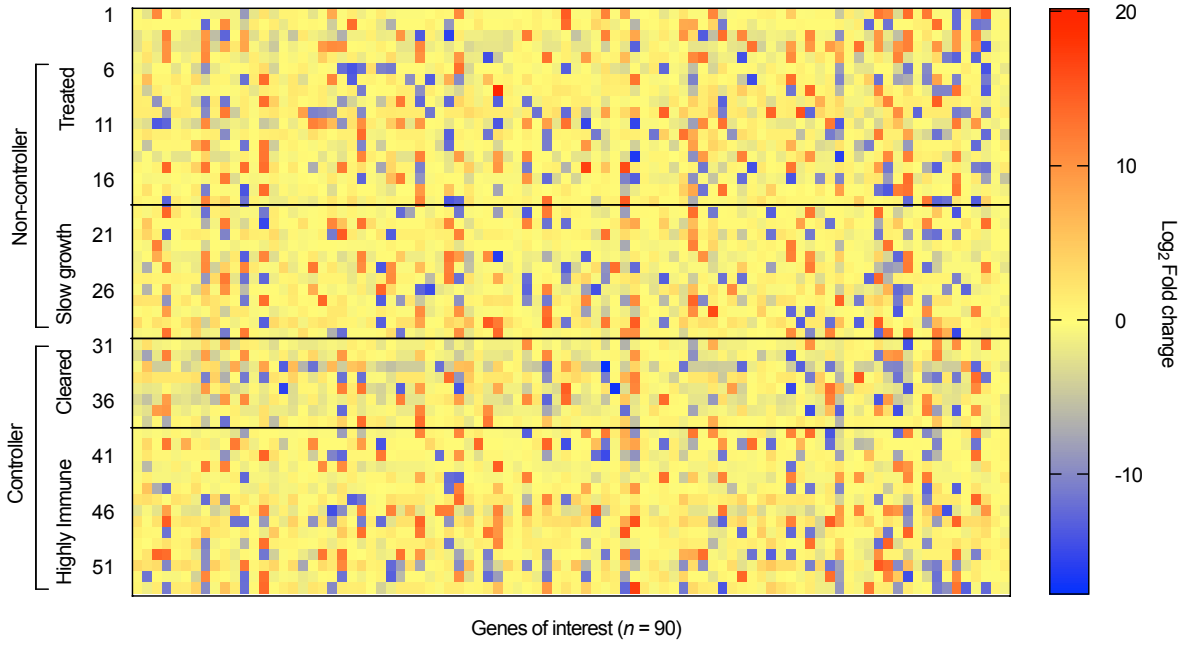

Figure 4.5: Heatmap of Log_2 FC in gene expression in Tregs at C+14. *FC calculated by $2^{-\Delta\Delta Ct}$ method for C+14 relative to C-1.*

Principal component analysis was then applied to the two Treg datasets to further examine whether samples clustered by parasite growth outcome based on gene expression profiles. Figures 4.6 and 4.7 show PCA plots for each dataset. PCA revealed similar findings between the two datasets. The majority of samples in the cleared group appeared to cluster separately from the rest of the samples. This was more apparent at C+14 compared to the C-1. The remaining three groups clustered more closely together, however the was some separation between the treated and slow growth groups with the highly immune group overlapping the two.

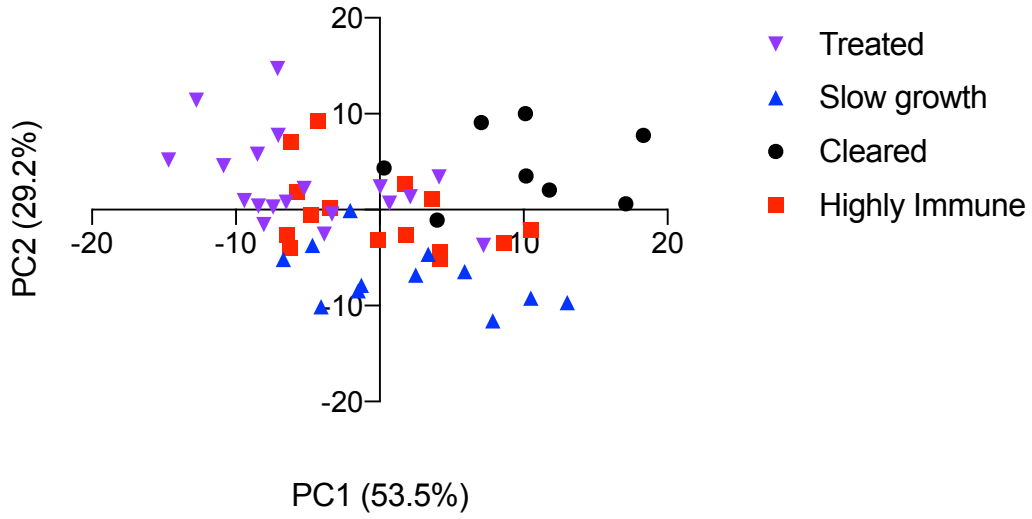

Figure 4.6: PCA of Treg gene expression profiles at C-1*. Log₂ FC values against the sample means at C-1 used. PCA applied to a variance-covariance matrix. Only first two dimensions shown, accounting for 82.7% variance.*

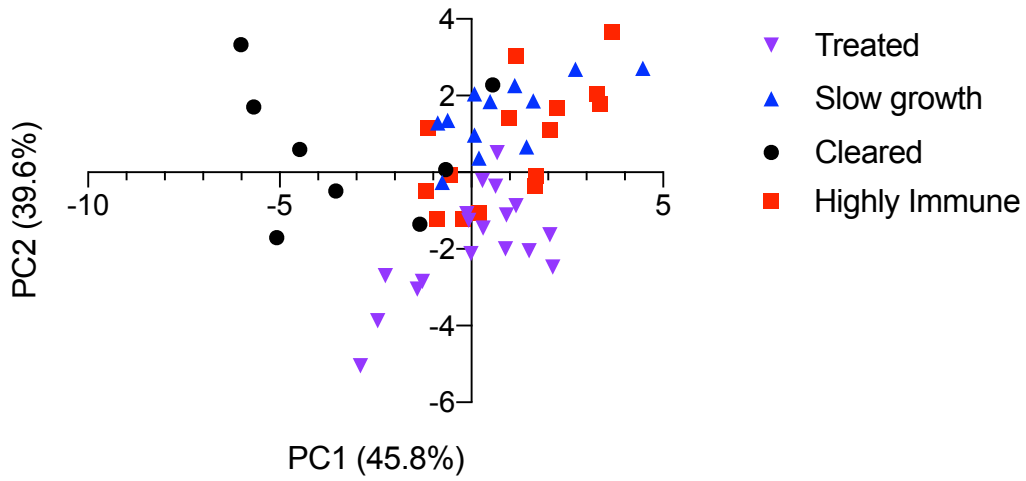

Figure 4.7: PCA of Treg gene expression profiles at C+14*. PCA applied to a variance-covariance matrix. Only first two dimensions shown, accounting for 85.4% of variance.*

Differential gene expression analysis (DGEA) was then conducted using 'Linear models for microarray data' (Limma) tools which measures differences in expression between two groups. In an initial analysis, samples were pooled into groups of

controllers (cleared and highly immune groups) and non-controllers (treated and slow growth) to facilitate analysis.

At C-1, 5 genes were identified as being differentially expressed. CCR3, CXCR6 and IRF1 were upregulated in controllers, whilst IRF4 and PAK2 were downregulated (Figure 4.8). However, once these genes were adjusted for multiplicity by false discovery rate (FDR), the relationships were found not to be significant (Table 4.2).

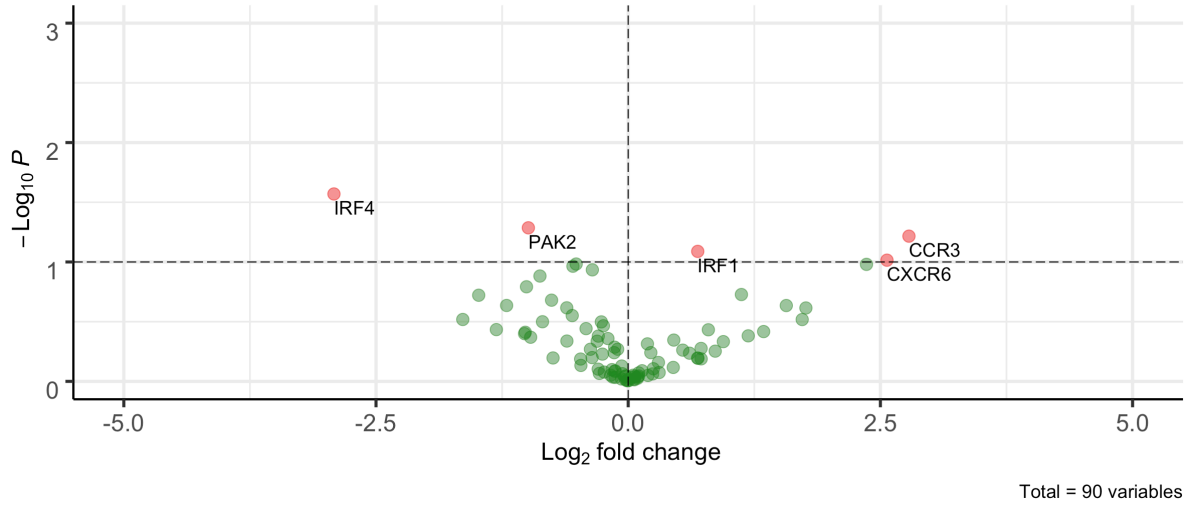

Figure 4.8: Volcano plot of differential expression between controllers and non-controllers in Tregs at C-1. *Positive Log_2 FC values indicate genes upregulated in controllers and vice versa. -Log_{10}P values not corrected for multiple comparisons.*

	Log_2 FC	*P Value*	*adj. P Val*
IRF4	-2.917	0.026	0.985
PAK2	-0.989	0.051	0.985
CCR3	2.783	0.060	0.985
IRF1	0.689	0.081	0.985
CXCR6	2.565	0.096	0.985

Table 4.2: Differentially expressed genes between controllers and non-controllers in Tregs at C-1. *P value adjusted by Benjamini-Hochberg procedure for an FDR of 5%.*

Similar findings were observed at C+14. 4 genes were found to be upregulated following CHMI in the controllers and 5 genes were downregulated (Figure 4.9).

Similarly, these were not significant following adjustment for multiple comparisons (Table 4.3).

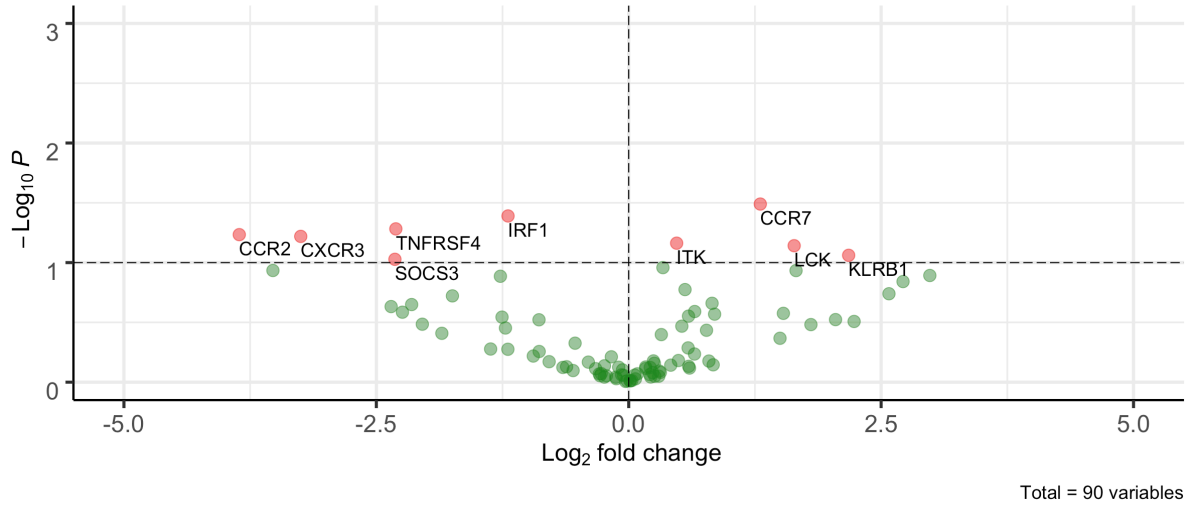

Figure 4.9: Volcano plot of differential expression between controllers and non-controllers in Tregs at C+14. *Positive Log_2 FC values indicate genes upregulated in controllers and vice versa. $-Log_{10}P$ values not corrected for multiple comparisons.*

	Log_2 FC	*P Value*	*adj. P Val*
CCR7	1.303	0.032	0.836
IRF1	-1.195	0.040	0.836
TNFRSF4	-2.306	0.052	0.836
CCR2	-3.857	0.058	0.836
CXCR3	-3.248	0.060	0.836
ITK	0.474	0.069	0.836
LCK	1.638	0.072	0.836
KLRB1	2.178	0.087	0.836
SOCS3	-2.315	0.094	0.836

Table 4.3: Differentially expressed genes between controllers and non-controllers in Tregs at C+14. *P value adjusted by Benjamini-Hochberg procedure for an FDR of 5%.*

Next, DGEA was repeated to analyse differences, splitting samples between the four growth outcome groups. Six separate DGEA analyses were performed with each parasite growth outcome group against every other.

In this analysis, no genes were significantly differently expressed at C-1 in any group compared to any other after adjustment for multiple comparisons. However, one gene, CXCR6 trended towards being significantly downregulated in the treated group compared to the cleared group [Log_2 FC = -6.92, adj. *P* = 0.1]. CXCR6 also appears as the top hit in the treated vs slow growth comparison, although this is not significant after adjustment [Log_2 FC = -4.84, adj. *P* = 0.75]. 3 other genes appeared on 3 separate lists, MAF, TNFSF10 and STAT5A, though none of the differences were significant. The top 5 hits from each analysis are shown in Table 4.4. A summary of the significant or near-significant [*p* = <0.1] results at C-1 is shown in Table 4.5.

Treg C-1		*Log_2 FC*	*P Value*	*adj. P Val*
Treated vs slow growth	*CXCR6*	-4.848	0.015	0.752
	TNFSF10	-4.060	0.026	0.752
	TNFRSF9	0.905	0.045	0.752
	BCL2	-1.594	0.047	0.752
	IL10	-2.324	0.059	0.752
Treated vs cleared	*CXCR6*	-6.922	0.002	0.107
	CCR3	-5.273	0.018	0.595
	IL2RB	1.034	0.030	0.595
	IL18R1	-4.912	0.034	0.595
	MAF	1.051	0.038	0.595
Treated vs Highly Immune	*PAK2*	1.416	0.031	0.855
	IRF4	3.322	0.051	0.855
	CCR1	2.600	0.075	0.855
	STAT5A	-2.252	0.090	0.855
	NFATC2	1.095	0.098	0.855
Slow growth vs Cleared	*MAF*	1.238	0.024	0.974
	STAT5A	3.459	0.041	0.974
	CCL4	1.588	0.060	0.974
	BCL2	1.724	0.068	0.974
	IL2RB	0.908	0.075	0.974
Slow growth vs Highly Immune	TNFSF10	3.957	0.036	0.947
	PAK2	1.274	0.077	0.947
	IRF4	3.016	0.108	0.947
	CD27	1.375	0.112	0.947
	IL17F	-2.873	0.114	0.947

Cleared vs Highly Immune	IL18R1	5.676	0.018	0.942
	STAT5A	-3.427	0.034	0.942
	LCK	0.705	0.065	0.942
	TNFSF10	3.713	0.070	0.942
	MAF	-0.924	0.076	0.942

Table 4.4: Top 5 differentially expressed genes in Tregs between parasite growth outcome groups at C-1

	Treated	*Slow Growth*	*Cleared*	*Highly Immune*
Treated				
Slow Growth	n/a			
Cleared	↓ CXCR6 [Log_2 FC = -6.92, adj. *P* = 0.1]	n/a		
Highly Immune	n/a	n/a	n/a	

Table 4.5: Summary of differentially expressed genes at C-1 between parasite growth outcome groups. *For clarity, only significant or near-significant [p = <0.1] differentially expressed genes reported. Direction of change is in the group in the column relative to the group in the row. n/a indicates no significant or near-significant results observed between groups.*

In the analysis at C+14, one gene was found to be significantly differently expressed and remained significant after adjustment, Suppressor of cytokine signaling 5 (SOCS5). This gene was downregulated in the treated group compared to the slow growth group [Log_2 FC = -8.69, adj. *P* = 0.03]. One further gene, CCR1, was found to trend towards being significantly upregulated in the slow growth group compared to the cleared group [Log_2 FC = 9.27, adj. *P* = 0.08]. There were no other significant or near-significant results between any of the other growth outcome groups following

adjustment for multiple comparisons. However, SOCS5 was also the top hit between the slow growth group and the highly immune group [Log_2 FC = 6.45, adj. *P* = 0.89]. The top 5 hits for each comparison are shown in Table 4.6. A summary of significant and near-significant [*p* = <0.1] results is shown in Table 4.7.

Treg C+14		*Log_2 FC*	*P Value*	*adj. P Val*
Treated vs slow growth	*SOCS5*	-8.694	0.0004	0.040
	NFKB1	-7.022	0.004	0.168
	CCR1	-5.723	0.011	0.282
	TNFSF10	6.255	0.013	0.282
	ENTPD1	6.859	0.016	0.296
Treated vs cleared	*IKZF2*	3.053	0.017	0.515
	CXCR3	6.370	0.017	0.515
	TNFRSF4	4.180	0.021	0.515
	CCR3	7.846	0.023	0.515
	TNFSF10	5.815	0.040	0.656
Treated vs Highly Immune	*NFKB1*	-5.666	0.012	0.648
	SOCS3	3.882	0.026	0.648
	IL21	-1.834	0.027	0.648
	TNFRSF4	2.954	0.046	0.648
	SELL	-0.518	0.055	0.648
Slow growth vs Cleared	*CCR1*	9.272	0.001	0.085
	STAT5A	-8.545	0.004	0.183
	IKZF2	3.238	0.018	0.502
	TNFRSF9	1.364	0.038	0.502
	FOXP3	2.936	0.038	0.502
Slow growth vs Highly Immune	*SOCS5*	6.435	0.010	0.899
	ENTPD1	-5.647	0.055	0.899
	IL18R1	-5.928	0.061	0.899
	CCR7	-1.480	0.085	0.899
	KLRB1	-3.062	0.086	0.899
Cleared vs Highly Immune	*IL1RL1*	-2.366	0.003	0.272
	TNFRSF9	-1.573	0.013	0.337
	IL21	-2.455	0.018	0.337
	TGFB1	-1.392	0.020	0.337
	CCR4	-1.480	0.025	0.337

Table 4.6: Top 5 differentially expressed genes in Tregs between parasite growth outcome groups at C+14

	Treated	Slow Growth	Cleared	Highly Immune
Treated				
Slow Growth	↓ SOCS5 [Log_2 FC = -8.69, adj. *P* = 0.03]			
Cleared	n/a	↑ CCR1 [Log_2 FC = 9.27, adj. *P* = 0.08]		
Highly immune	n/a	n/a	n/a	

Table 4.7: Summary of differentially expressed genes at C+14 between parasite growth outcome groups. *For clarity, only significant or near-significant [p = <0.1] differentially expressed genes reported. Direction of change is in the group in the column relative to the group in the row. n/a indicates no significant or near-significant results observed between groups.*

Overall these data are consistent with the PCA, in that differences in Treg phenotype are observed between the treated group and the slow growth group, and between the cleared group and either the treated or slow growth groups.

Because PCA showed that the cleared appeared to cluster separately to the three other parasite growth phenotype groups, DGEA was again repeated with each group against all other groups combined. A summary of adjusted *p* values of top hits for the C-1 and C+14 analyses are shown in Table 4.8 and Table 4.9 respectively. In summary, no significant differentially expressed genes were found when adjusted for multiple comparisons, either at C-1 or C+14. Of note, in the C+14 analysis, of the 13 genes identified as potentially differentially expressed in the cleared group, 12/13 were observed to be downregulated, in agreement with the heatmap analysis.

Treg C-1		*Log_2 FC*	*P Value*	*adj. P Val*
Treated	*CXCR6*	-4.619	0.004	0.320
	TNFRSF4	-1.869	0.035	0.775
	CCR3	-3.229	0.038	0.775
	TBX21	2.924	0.053	0.775
	IL23R	3.062	0.065	0.775
Slow Growth	*TNFSF10*	3.205	0.049	0.896
	IL17F	-2.988	0.049	0.896
	BCL2	1.306	0.062	0.896
	TNFRSF9	-0.718	0.069	0.896
	CTLA4	0.516	0.092	0.896
Cleared	*MAF*	-1.059	0.018	0.693
	IL18R1	4.739	0.021	0.693
	CXCR6	4.611	0.024	0.693
	IL2RB	-0.905	0.031	0.693
	CCR3	3.745	0.058	0.983
Highly Immune	*PAK2*	-1.273	0.023	0.998
	IRF4	-2.635	0.074	0.998
	LCK	-0.473	0.082	0.998
	NFATC2	-0.953	0.093	0.998
	CCR7	-1.073	0.094	0.998

Table 4.8: Summarised p values and adjusted p values for potentially differentially expressed genes in each group relative to the other three groups combined at C-1 *P value adjusted by Benjamini-Hochberg procedure for an FDR of 5%.*

Treg C+14		*Log_2 FC*	*P Value*	*adj. P Val*
Treated	*NFKB1*	-6.039	0.001	0.113
	SOCS5	-5.079	0.009	0.314
	TNFRSF4	3.142	0.010	0.314
	TNFSF10	4.575	0.019	0.427
	IL10	3.293	0.032	0.579
Slow Growth	*SOCS5*	6.903	0.002	0.140
	CCR1	5.645	0.006	0.249
	STAT5A	-4.761	0.027	0.600
	ENTPD1	-5.487	0.029	0.600
	PRF1	-2.823	0.050	0.600
Cleared	*IKZF2*	-3.033	0.008	0.409
	IL1RL1	-1.705	0.015	0.409
	CCR1	-5.777	0.016	0.409
	CCR3	-7.128	0.020	0.409
	STAT5A	5.726	0.023	0.409
Highly Immune	*IL21*	1.842	0.011	0.545
	SOCS3	-3.569	0.017	0.545
	IL1RL1	1.280	0.022	0.545
	TGFB1	0.930	0.024	0.545
	CCR7	1.273	0.059	0.820

Table 4.9: Summarised p values and adjusted p values for potentially differentially expressed genes in each group relative to the other three groups combined at C+14 *P value adjusted by Benjamini-Hochberg procedure for an FDR of 5%.*

4.3.4. Assessing differential gene expression in CD25- CD127hi effector CD4+ T cells between CHMI parasite growth outcome groups

Analysis of gene expression profiles was also carried out on Teff cells. A heatmap of gene expression between individuals at C-1 is shown in Figure 4.10 and at C+14 in Figure 4.11. Qualitatively, gene expression appears to be less heterogeneous than in Tregs at both C-1 and C+14. Again, no obvious differences in overall phenotype between parasite growth outcome groups is observed at either timepoint.

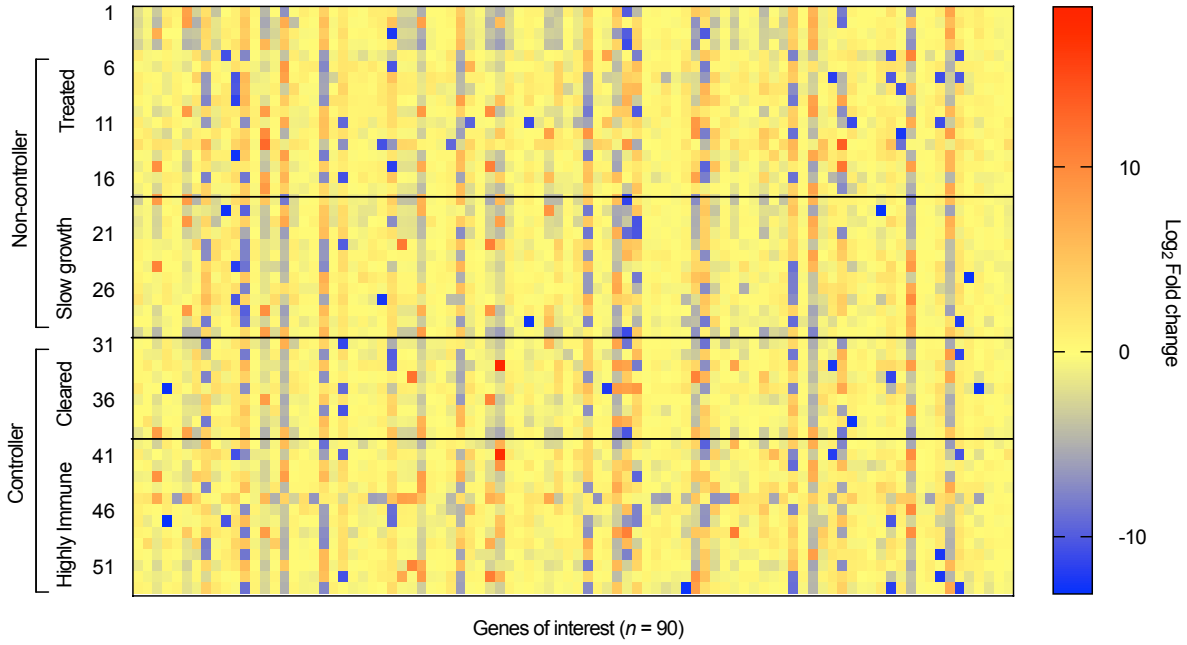

Figure 4.10: Heatmap of Log_2 FC in gene expression for Teffs at C-1. *FC calculated by $2^{-\Delta\Delta Ct}$ method relative to the mean of all samples.*

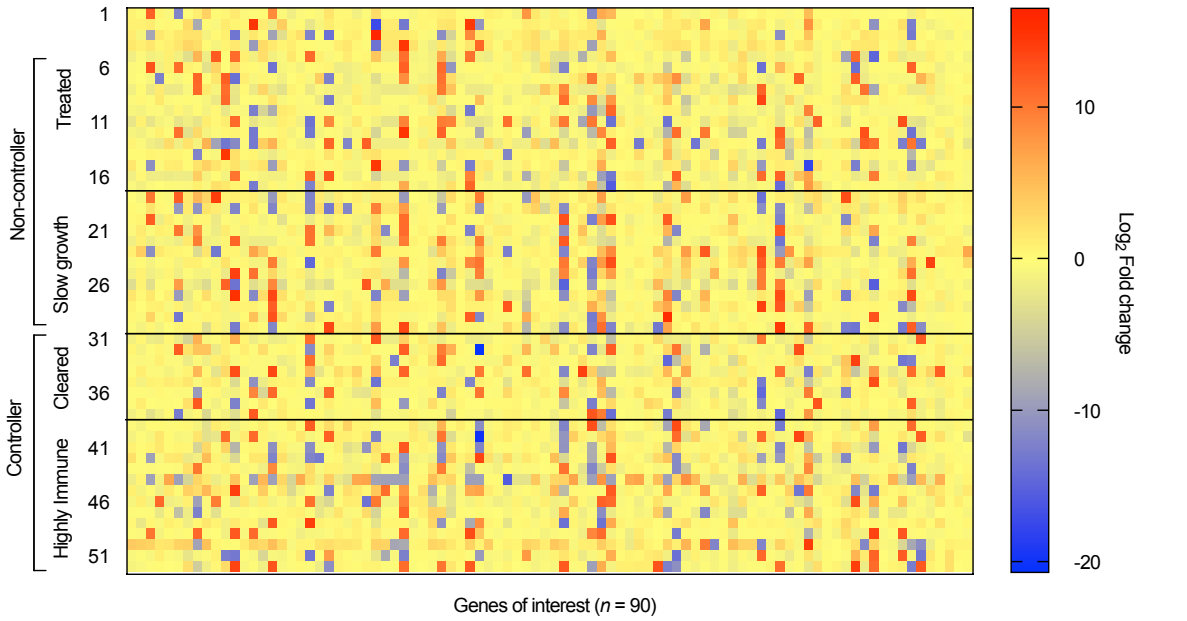

Figure 4.11: Heatmap of Log_2 FC in gene expression in Teffs at C+14. *FC calculated by $2^{-\Delta\Delta Ct}$ method for C+14 relative to C-1.*

PCA was then applied to the Teff analysis. Unlike for Tregs, PCA failed to cluster samples by parasite growth outcome group in either the C-1 cross-sectional analysis

(Figure 4.12) or at C+14 (Figure 4.13). At either timepoint, the cleared group was not clustered separately from the other three groups. Overlap was observed between the treated, slow growth and highly immune groups.

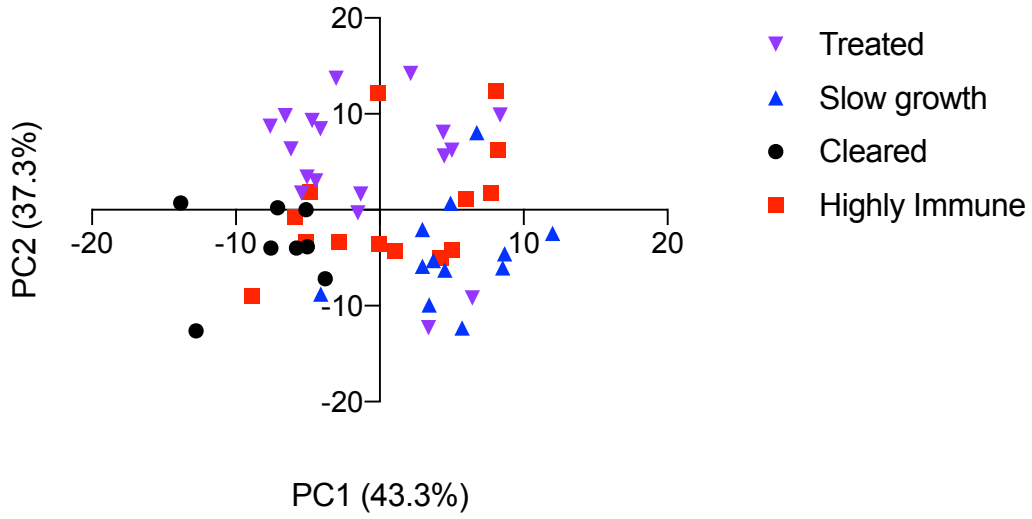

Figure 4.12: PCA of Teff gene expression profiles at C-1*. Log_2 FC values against the sample means at C-1 used. PCA applied to a variance-covariance matrix. Only first two dimensions shown, accounting for 80.6% variance.*

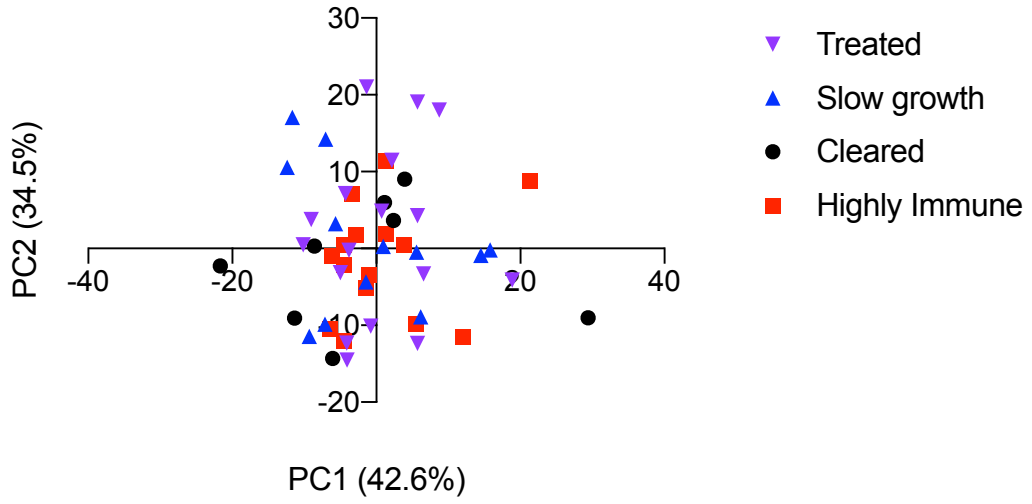

Figure 4.13: PCA of Teff gene expression fold change profiles at C+14*. PCA applied to a variance-covariance matrix. Only first two dimensions shown, accounting for 77.1% of variance.*

DGEA using Limma was applied to Teffs, firstly combining groups into controllers and non-controllers. Similar to the findings in Tregs, no genes identified as differentially expressed were statistically significant following adjustment for multiple comparisons at either timepoint. DGEA volcano plots for C-1 and C+14 are shown in Figures 4.14 and 4.15 respectively. Summarised *p* values and adjusted *p* values for the top flagged genes are shown in Table 4.10 and 4.11 for C-1 and C+14 analyses respectively.

Figure 4.14: Volcano plot of differential expression between controllers and non-controllers in Teffs at C-1. *Positive Log_2 FC values indicate genes upregulated in controllers and vice versa. -Log_{10}P values shown are not corrected for multiple comparisons.*

	Log_2 FC	*P Value*	*adj. P Val*
IL17A	1.676	0.028	0.881
TNFSF10	1.507	0.049	0.881
IL21	1.533	0.051	0.881
CXCR6	-2.854	0.055	0.881
CD40LG	0.418	0.075	0.881
ICOS	-0.598	0.079	0.881
CD28	0.274	0.089	0.881
KLRG1	-0.991	0.094	0.881

Table 4.10: Differentially expressed genes between controllers and non-controllers in Teffs at C-1. *P value adjusted by Benjamini-Hochberg procedure for an FDR of 5%.*

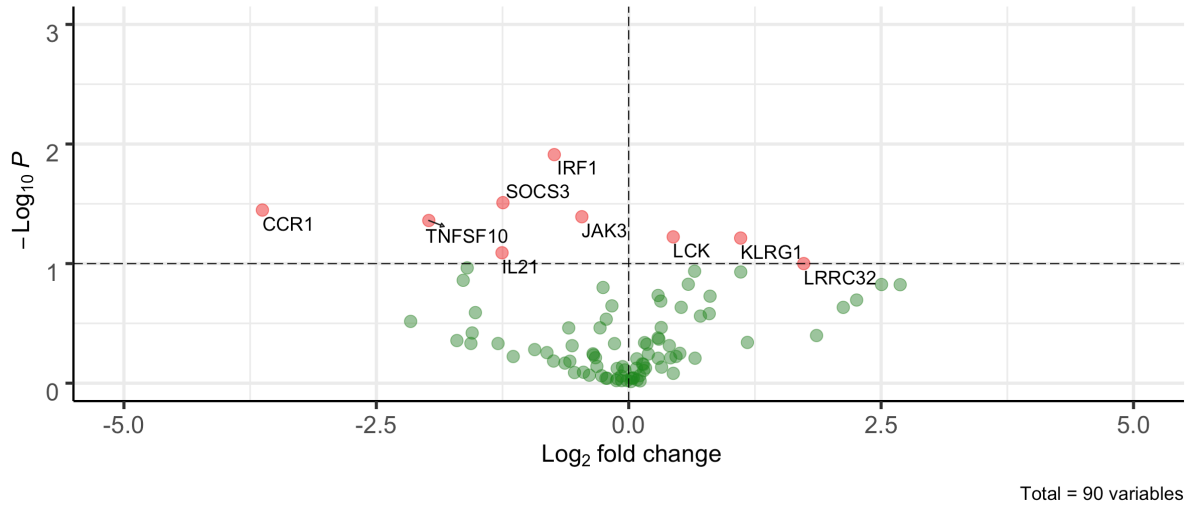

Figure 4.15: Volcano plot of differential expression between controllers and non-controllers in Teffs at C+14. *Positive Log_2 FC values indicate genes upregulated in controllers at C+14 and vice versa. $-Log_{10}P$ values not corrected for multiple comparisons.*

	Log_2 FC	*P Value*	*adj. P Val*
IRF1	-0.737	0.012	0.785
SOCS3	-1.246	0.031	0.785
CCR1	-3.629	0.036	0.785
JAK3	-0.464	0.041	0.785
TNFSF10	-1.980	0.044	0.785
LCK	0.441	0.060	0.786
KLRG1	1.108	0.061	0.786
IL21	-1.255	0.081	0.838
LRRC32	1.734	0.100	0.838

Table 4.11: Differentially expressed genes between controllers and non-controllers in Teffs at C+14. *P value adjusted by Benjamini-Hochberg procedure for an FDR of 5%.*

The four parasite growth outcome groups were then analysed against each other by separate DGEAs. Six separate analyses were carried out per timepoint, however no significant or near-significant differentially expressed genes were identified between parasite growth outcome groups in Teff cells at either C-1 corrected for multiple comparisons. 4 genes appeared 3 times in the top 5, CCR5, CXCR3, CXCR6 and

TNFSF10. Though none of the relationships were significant after adjustment, CCR5 was downregulated in the slow growth group relative to every other group, TNFSF10 was downregulated in the treated group and CXCR6 was downregulated in the cleared group. The top 5 flagged genes are shown in Table 4.12.

Teff C-1		*Log_2 FC*	*P Value*	*adj. P Val*
Treated vs slow growth	CCR5	6.127	0.004	0.243
	IKZF2	5.386	0.005	0.243
	BCL2	0.695	0.011	0.322
	TNFSF10	-2.094	0.041	0.747
	TGFB1	0.593	0.042	0.747
Treated vs cleared	CXCR6	6.534	0.003	0.273
	CXCR3	2.474	0.010	0.439
	IKZF2	4.942	0.018	0.547
	KLRG1	1.860	0.037	0.830
	TNFSF10	-2.157	0.053	0.963
Treated vs Highly Immune	TNFSF10	-2.504	0.010	0.629
	TNFRSF4	2.075	0.014	0.629
	BCL2	0.534	0.035	0.794
	IL17A	-2.079	0.036	0.794
	IKZF2	3.149	0.076	0.794
Slow growth vs Cleared	CCR5	-5.440	0.028	0.978
	IL23R	-4.679	0.032	0.978
	CXCR6	4.930	0.033	0.978
	TNF	3.808	0.056	0.990
	IL1RL1	2.906	0.085	0.990
Slow growth vs Highly Immune	IL17A	-2.115	0.050	0.948
	CCR5	-3.826	0.076	0.948
	RORC	-1.626	0.081	0.948
	MKI67	-1.753	0.081	0.948
	CCR1	-3.182	0.095	0.948
Cleared vs Highly Immune	CXCR6	-4.825	0.029	0.959
	CXCR3	-1.949	0.044	0.959
	IL23R	3.644	0.078	0.959
	IL2RA	-1.916	0.103	0.959
	TNFRSF4	1.527	0.122	0.959

Table 4.12: Top 5 differentially expressed genes in Teffs between parasite growth outcome groups at C-1

At C+14, again no significant or near-significant results were found following adjustment. However, 4 genes appeared in the top 5 hits 3 times, BCL2, IFNG, CXCR3 and KLRB1. BCL2 was downregulated in the treated group relative to all other groups albeit with only a slight negative Log_2 FC in each comparison. IFNG was downregulated in the treated group versus both the slow growth and cleared groups and was also downregulated in the highly immune group compared to the slow growth group.

Teff C+14		*Log_2 FC*	*P Value*	*adj. P Val*
Treated vs slow growth	BCL2	-0.826	0.013	0.664
	CXCR5	-2.635	0.027	0.664
	IFNG	-5.117	0.051	0.664
	TNFSF10	2.506	0.052	0.664
	CXCR3	-2.078	0.052	0.664
Treated vs cleared	KLRB1	0.643	0.020	0.981
	CXCR3	-2.766	0.024	0.981
	KLRG1	-1.908	0.038	0.981
	BCL2	-0.724	0.052	0.981
	IFNG	-5.150	0.083	0.981
Treated vs Highly Immune	TNFSF10	3.538	0.004	0.382
	IRF1	0.897	0.018	0.773
	ENTPD1	-4.839	0.028	0.773
	CD27	-1.093	0.035	0.773
	BCL2	-0.624	0.043	0.773
Slow growth vs Cleared	TNF	-5.907	0.042	0.981
	KLRB1	0.542	0.063	0.981
	SELL	0.410	0.069	0.981
	CCR2	6.482	0.073	0.981
	CD40LG	0.756	0.122	0.981
Slow growth vs Highly Immune	CCR1	7.217	0.002	0.223
	IRF1	0.830	0.043	0.855
	SOCS3	1.613	0.046	0.855
	IL17F	-4.601	0.064	0.855
	IFNG	4.804	0.074	0.855

Cleared vs Highly Immune	IL2RA	2.624	0.036	0.932
	TNFRSF4	-2.648	0.052	0.932
	KLRB1	-0.532	0.057	0.932
	CXCR3	2.287	0.066	0.932
	CD27	-1.134	0.074	0.932

Table 4.13: Top 5 differentially expressed genes in Teffs between parasite growth outcome groups at C+14

DGEA was next performed on Teff cells between each group and all three other groups combined. Again, no significant differentially expressed genes were found in Teffs for any parasite growth outcome group after adjustment of *p* values either at C-1 or C+14. Tables 4.14 and 4.15 show the top 5 hits in each comparison at C-1 and C+14 respectively.

Teff C-1		*Log_2 FC*	*P Value*	*adj. P Val*
Treated	*IKZF2*	4.343	0.004	0.196
	TNFSF10	-2.281	0.004	0.196
	BCL2	0.522	0.014	0.410
	TNFRSF4	1.484	0.034	0.755
	CCR5	3.173	0.061	0.848
Slow Growth	*CCR5*	-5.440	0.028	0.978
	IL23R	-4.679	0.032	0.978
	CXCR6	4.930	0.033	0.978
	TNF	3.808	0.056	0.990
	IL1RL1	2.906	0.085	0.990
Cleared	*CXCR6*	-5.514	0.004	0.384
	CXCR3	-2.022	0.016	0.724
	KLRG1	-1.523	0.051	0.978
	TNF	-2.940	0.071	0.978
	IL23R	3.241	0.072	0.978
Highly Immune	*IL17A*	1.862	0.027	0.889
	TNFRSF4	-1.488	0.040	0.889
	FASLG	3.124	0.056	0.889
	CD28	0.327	0.065	0.889
	STAT5A	0.473	0.077	0.889

Table 4.14: Summarised p values and adjusted p values for potentially differentially expressed genes in each group relative to the other three groups

combined at C-1 *P value adjusted by Benjamini-Hochberg procedure for an FDR of 5%.*

Teff C+14		*Log_2 FC*	*P Value*	*adj. P Val*
Treated	*TNFSF10*	2.842	0.005	0.243
	BCL2	-0.716	0.005	0.243
	ENTPD1	-3.865	0.034	0.704
	CXCR5	-1.927	0.036	0.704
	CD274	3.796	0.039	0.704
Slow Growth	*CCR1*	5.345	0.008	0.705
	CD40LG	0.716	0.040	0.977
	SELL	0.326	0.042	0.977
	IFNG	3.970	0.086	0.977
	CXCR5	1.738	0.093	0.977
Cleared	*KLRB1*	-0.578	0.018	0.990
	CXCR3	2.036	0.067	0.990
	TNF	4.407	0.068	0.990
	GFI1	-3.615	0.068	0.990
	KLRG1	1.418	0.083	0.990
Highly Immune	*IRF1*	-0.763	0.018	0.634
	CCR1	-4.365	0.021	0.634
	CD27	1.017	0.021	0.634
	TNFSF10	-2.284	0.033	0.705
	SOCS3	-1.306	0.040	0.705

Table 4.15: Summarised p values and adjusted p values for potentially differentially expressed genes in each group relative to the other three groups combined at C+14 *P value adjusted by Benjamini-Hochberg procedure for an FDR of 5%.*

4.3.5. Associations between Teff and Treg transcriptional phenotypes, participant demographics and immune variables

Finally, DGEA was used to assess whether Treg or Teff transcriptional phenotype at C-1 was associated with different demographic and immune variables. DGEA was performed between groups based on 5 variables, including:

- Low vs High transmission area of residence – Kilifi North volunteers compared to Kilifi South and Ahero
- Old vs young – volunteers aged 19 to 29 (young) and 30 to 42 (old)
- Male vs female
- Inflammatory cytokines vs non-inflammatory – volunteers expressing at least 1 pro inflammatory cytokine vs volunteers not expressing any pro-inflammatory cytokine (Chapter 3)
- High vs low anti-schizont IgG – top 50% based on titre vs bottom 50%

No significant differentially expressed genes were identified in Tregs at C-1 based on any of the five variables following adjustment. The top 5 gene hits for each variable are summarised in Table 4.16.

One gene was found to be differentially expressed after correction for multiple comparisons in Teffs at C-1. TNF superfamily member 10 (TNFSF10) was found to be significantly downregulated in Teffs in individuals from the low transmission setting in Kilifi north, compared to individuals from higher transmission settings in Kilifi South

and Ahero [Log_2 FC -3.33, p = 0.04]. A summary of the top five genes identified as potentially differentially expressed in each analysis are shown in Table 4.17.

Treg C-1		*Log_2 FC*	*P Value*	*adj. P Val*
Low vs High transmission area of residence	NRP1	1.009	0.047	0.800
	NFKB1	2.614	0.061	0.800
	PRF1	-1.772	0.063	0.800
	CXCL13	2.506	0.076	0.800
	TNFSF10	-3.088	0.076	0.800
Old vs young	DPP4	2.866	0.020	0.886
	ITGB2	0.536	0.040	0.886
	LCK	0.453	0.062	0.886
	RORC	2.439	0.090	0.886
	LAG3	-2.292	0.114	0.886
Male vs female	CXCL13	-3.346	0.006	0.495
	CCR3	-3.903	0.015	0.652
	FAS	2.149	0.028	0.652
	PRF1	1.691	0.038	0.652
	CXCR6	-3.099	0.064	0.652
Inflammatory cytokines vs non-inflammatory	CCR2	3.656	0.013	0.729
	HLA.DRA	2.141	0.016	0.729
	EGR2	1.510	0.070	0.993
	CD69	0.427	0.110	0.993
	PAK2	0.793	0.133	0.993
High vs low anti-schizont IgG	TNF	3.524	0.019	0.860
	CCR2	3.348	0.019	0.860
	IFNG	-2.069	0.042	0.949
	STAT5B	0.665	0.054	0.949
	CTLA4	0.484	0.057	0.949

Table 4.16: Top 5 differentially expressed genes in Tregs at C-1 based on demographic and immune variables

Teff C-1		*Log_2 FC*	*P Value*	*adj. P Val*
Low vs High transmission area of residence	TNFSF10	-3.333	0.0005	0.049
	ENTPD1	3.792	0.021	0.943
	CD28	-0.441	0.035	0.981
	CD27	0.878	0.054	0.981
	TGFB1	0.524	0.056	0.981
Old vs young	IL9	1.385	0.028	0.702
	PDCD1	1.399	0.034	0.702
	IL10	1.504	0.035	0.702
	TNFSF10	1.581	0.038	0.702
	IL17F	2.844	0.049	0.702
Male vs female	NT5E	-4.324	0.009	0.580
	GFI1	2.519	0.014	0.580
	CXCR6	3.586	0.025	0.580
	IRF4	-3.103	0.026	0.580
	IL27RA	0.770	0.032	0.583
Inflammatory cytokines vs non-inflammatory	IL27RA	-1.003	0.003	0.238
	IL17F	3.307	0.025	0.831
	CCL4	-1.464	0.031	0.831
	GZMB	0.853	0.045	0.831
	IL21R	-1.409	0.054	0.831
High vs low anti-schizont IgG	IKZF2	-3.343	0.019	0.928
	CCR3	3.555	0.027	0.928
	EGR2	2.048	0.038	0.928
	KLRG1	-1.094	0.063	0.928
	SOCS1	1.451	0.067	0.928

Table 4.17: Top 5 differentially expressed genes in Teffs at C-1 based on demographic and immune variables

4.4. Discussion

Analyses in this chapter utilised a multiplex qPCR method[313] to quantify the relative expression of a selection of relevant genes in sorted cell populations. The most advanced method for profiling the transcriptome is RNAseq[314,315]. This is a high-throughput sequencing method which requires complex computational methods to infer mRNA counts from reads of cDNA fragments. It generates a large dataset representative of the whole mRNA transcriptome of the sample, again requiring bespoke computational methods to analyse and perform differential gene expression analysis. The main advantage is that it is not limited by the number of genes that can be analysed, giving a global analysis of the function of population of cells. Because of this, it is now the most popular transcriptomic tool in use in biological studies[316].

Developed just before RNAseq were microarrays[317]. This method uses oligomeric probes complementary to the gene of interest bound to a solid substrate, to which cDNA molecules hybridise. The cDNA sample is pre-labelled with a fluorescent tag and gene expression is inferred by the intensity of fluorescence. The main advantages of this method are that it is higher throughput, requiring less labour and economic cost per sample. The less-complicated dataset also makes analysis more straightforward.

The multiplex qPCR method used in this study is analogous to microarrays. It is an adaptation of standard quantitative PCR where oligomeric primers are used to amplify a specific cDNA sequence and an intercalating DNA dye or fluorescently-labelled sequence-specific probe is used to quantify DNA. The reactions take place in microscopic chambers on a microfluidic chip meaning the number of reactions taking

place per run can be scaled up compared to conventional qPCR. In the setup used here, 96 genes from 96 samples can be analysed per chip. Its main advantage over microarrays is that the dynamic range is far superior and comparable to RNAseq. A major downfall of both microarrays and multiplex qPCR is that the number of genes that can be analysed is greatly reduced compared to RNAseq. This risks potentially relevant genes being missed from the analysis.

For this study, multiplex qPCR was chosen primarily because it can accommodate a higher throughput. CHMI in a heterogeneous population of semi-immune adults resulted in 4 growth phenotypes. This method allowed a larger sample size to be included in the experiment to increase the statistical power to detect differences between groups.

Because the gene targets have to be pre-defined in a multiplex qPCR experiment, they should be carefully selected to ensure they are functionally relevant and maximise the opportunity to identify meaningful correlates to parasite growth outcomes. To do this in this study, functional groups were firstly listed from which different genes should be included. The groups included; functional markers (including cytokines, chemokines and cell surface functional proteins), transcription factors, extracellular signalling molecules and activation markers. A shortlist of candidate genes was then drawn from other microarray and multiplex qPCR studies looking at Treg and CD4+ T cell gene expression in the context of other infectious diseases[318,319]. Other genes thought to be important in the cellular response to malaria specifically, were identified through literature searches and also included.

In this study, both Tregs and effector CD4+ T cells were analysed. Both subsets might be implicated in the control of inflammatory and pro-inflammatory responses to CHMI and this work is an extension to that explored in Chapter 3. Each analysis began by exploring overall differences in cellular phenotype using heatmaps and PCA between parasite growth outcome groups. This provided greater evidence for differences in phenotype in Tregs at both C+14 and C-1 between different parasite growth outcome groups than for Teffs. However, the exact functional differences driven by individual genes underlying this heterogeneity were not convincingly revealed by DGEA. Significant differentially expressed genes were identified between groups. However, when performing experiments with multiple comparisons, it is necessary to adjust *p* values to account for false-positive results which may be flagged as significant by chance alone. This is because the chances of identifying false-positive results (type I errors) increases as multiple comparisons are made[320], as in this experiment where 90 genes were analysed per sample. In microarray and multiplex qPCR experiments, a false discovery rate approach is usually used to adjust for multiple comparisons[321].

FDR was applied to all DGEA analyses performed here. Following this, only one gene was found to be significantly differently expressed in Tregs between parasite growth outcome groups. SOCS5 was downregulated in Tregs at C+14 in the treated group compared to the slow growth group. SOCS5 is a negative regulator of the JAK-STAT signalling pathway which in immune cells controls signalling from cytokine receptors[322]. In Tregs, negative regulation of JAK-STAT signalling has been shown to result in the downregulation of FoxP3 and thus a reduction in expression of proteins involved in Treg effector functions[323]. The implication of this finding, if valid, is that there is less inhibition from SOCS5 on Treg effector function in the treated group and

therefore Treg activity might be associated with increased parasite growth. It is not possible to draw a conclusion on the functional role of SOCS5 in CHMI from this result alone. Effector functions downstream of JAK-STAT signalling need to be investigated for both their associations with SOCS5 and parasite growth.

Finding a significant differentially expressed gene between the treated and slow growth group in Tregs at C+14, as was the case for SOCS5, is consistent with the PCA, which showed these two groups were phenotypically distinct and broadly clustered separately from each other. The group that appeared to cluster farthest from the other groups in the PCA was the cleared group. Although no significant differentially expressed genes were found by DGEA comparing the cleared to the three other groups, either individually or combined, there were two near-significant results between the cleared group and the slow growth and treated groups. PCA on Treg gene expression profiles found the highly immune group to broadly overlap with the treated and the slow growth groups. Consistent with this, no significant or near-significant differentially expressed genes were found between the highly immune group and the treated or slow growth groups. However, PCA also clustered the highly immune group away from the cleared group and DGEA revealed no differential expression between these groups either.

In Teffs, no significant or near-significant differentially expressed genes were observed following adjustment in any of the DGEA analyses carried out between parasite growth outcome groups on this cell type. Qualitative evaluation of heatmaps showed that gene expression was less heterogeneous than in Tregs and the PCA did not separate samples by parasite growth outcome. It is therefore not surprising to find

less evidence for differential expression in effector cells. One significant finding in Teffs was that expression of TNFSF10 was lower in Teffs at C-1 in volunteers from the low transmission setting of Kilifi north compared with those from high transmission settings. TNFSF10 is a small secreted signalling molecule which promotes the induction of apoptosis in cells when it binds to the surface receptor TNFRSF10B[324,325]. TNFSF10 also appeared in the top 5 hits in every analysis at C-1 when the treated group was compared to the 3 other protected groups, indicating its potential role in the Teff response to malaria. Its appearance as a differentially regulated gene between location settings may just reflect the fact that treated volunteers were over-represented in the Kilifi north group. Despite not being a significant result between any of the parasite growth outcome groups, the fact that this gene appears as a top hit across multiple analyses suggests it should be considered for further analysis.

Overall, DGEA did not provide good evidence identifying differentially expressed genes between different groups. The limited number of results that were significant following adjustment should be treated with caution considering the large number of comparisons made. Instead of drawing conclusions directly from DGEA data, instead it should be considered as a method to shortlist a set of genes, or functional groups of genes, which may be involved in a biological process. These candidates can then be followed-up in further experimental analyses. Therefore, genes that were flagged as differentially expressed, but lacked statistical significance are still important to this analysis. A disadvantage of adjusting for multiple comparisons is that too stringent an approach to false discovery might risk calling some candidate differentially expressed genes as false-negatives which would not then be followed up in further experiments. Genes that were not shown to be significantly differentially expressed following

adjustment, but appear across multiple analyses, or functional groups from which different members appear commonly, should be considered for further analysis. It is noteworthy that in both the Treg and Teff analyses, genes that frequently appeared in the list of top hits were chemokine receptors. These include CXCR6 and CCR1 which were near-significantly differentially expressed in Tregs between parasite growth outcome groups. Expressing different chemokine receptors will direct cells to different anatomical compartments[326]. The chemokine response to malaria is complex, and similarly to pro-inflammatory cytokines, there is evidence that responses can be helpful but can also direct immune cells to sites of inflammation and exacerbate pathology[327]. Whilst significant differences between groups were not found by DGEA for any chemokine or chemokine receptor, the frequency at which members of these families appeared as top hits is worthy of further investigation to understand whether compartmentalisation of T cell and Treg responses to malaria might contribute to protection and susceptibility.

It is difficult to contextualise the findings from this study with respect to the existing literature because of the limited number of studies which have performed similar analyses previously. One study performed RNAseq on whole blood samples from previously-exposed volunteers who underwent CHMI in Tanzania[328]. Analyses were performed during liver stage and early-blood stage infection. No differentially expressed genes were found at day 9, but at day 5, genes associated with ubiquitination, transcription factors, inositol phosphate pathways, cell cycle and intracellular transport were significantly downregulated in volunteers with short prepatent periods compared to those with longer prepatent periods. Considering this analysis was performed during pre-erythrocytic and early-blood stage infection and

was on whole blood rather than T cell subsets, the results are not directly comparable. The differentially expressed genes are also broadly unrelated to the Treg and Teff-associated genes analysed in the study presented in this chapter.

A limitation of the study presented here was that analyses were performed on bulk, non-antigen specific cells. Although changes in the phenotype of bystander T cells do occur during malaria infection and may contribute differing parasite outcomes[329], it is likely that greater and more-relevant changes in gene expression will occur in antigen specific cells. Analysing gene expression in bulk Teffs or Tregs, regardless of specificity, may have masked changes in expression occurring in antigen-specific subsets. The antigen specific response to malaria is against a very large and diverse repertoire of antigens and is very heterogeneous between individuals[330]. This makes isolating antigen specific cells challenging. One method might involve isolating cells against a small set of immunodominant blood-stage antigens using tetramers[331]. However, this would not be representative of the global T cell response against the parasite. Cell stimulations using recombinant antigen or parasite extract is also possible, however *in vitro* culture would change gene expression profiles and thus may not reflect phenotypes associated with the *in vivo* response.

The method used here also measured gene expression in bulk cell populations. Single cell transcriptomics is a rapidly growing field of bioinformatics[332,333]. Here, separate gene expression profiles are determined for individual cells from the same sample. The benefit of this is that in a heterogeneous population of cells, relevant expression changes occurring in only a subset of those cells can be detected. In malaria infection, it is perhaps likely that only certain phenotypic subsets of Teffs or Tregs may be

implicated in the immune response and a bulk transcriptomic approach may have masked this. Single cell sequencing might also counteract the problems associated with antigen specificity because a certain number of the cells sampled would be specific for parasite antigen, and analysis could be used to detect these[334,335].

A problem with single cell approaches is that wet lab workflow needs to be performed separately on hundreds or even thousands of cells from each individual patient sample[336]. This significantly increases the materials and costs required. Analysis is also more complicated and requires specialist input[337,338].

As previously discussed, another limitation of the study is using multiplex qPCR instead of transcriptome-wide RNAseq which might mean some relevant genes are missed.

4.5. Conclusions

Overall, this study provided evidence that Treg phenotype may differ between parasite growth outcome groups, but DGEA did not clearly reveal the functional gene signatures underlying these differences. For Teff cells, there was less evidence of bulk phenotypic differences between individuals with different parasite growth outcomes. DGEA did not provide robust evidence of individual genes which were differentially expressed between groups, however, the data from this analysis might be useful in providing evidence to select candidate genes and functional gene groups which may be involved in the T cell response to CHMI. In particular, the role chemokines play in

directing T cell subsets to anatomical compartments in response to CHMI should be investigated further. Other targets of interest which may contribute to parasite growth outcomes include SOCS5 in Tregs and TNFSF10 in Teffs. Further experiments to be considered might involve determining expression of these genes at the protein level by flow cytometry on PBMC. Functional experiments using chemotaxis assays would help to understand the role chemokines play in the cellular response to CHMI.

This work represents an initial analysis of transcriptomics data using routinely available tools. Further analysis of transcriptomics data using different bioinformatics pipelines is currently underway, but was unavailable for presentation at the time of submission – this work includes analysis of raw gene expression intensities and multivariate analysis also involving the data presented in Chapter 3. Genes which are flagged as potentially significant in this analysis and in any subsequent analyses will be validated with further experimental work as well. This will include analysis of expression at the protein level by flow cytometry and confirmation of expression at the mRNA level by singleplex qPCR.

Chapter 5

5. Investigating a role for Tregs in the suppression of immune responses to experimental malaria vaccines in adult and infant cohorts.

5.1. Introduction

The immunogenicity and efficacy of multiple vaccines has been shown to be reduced in malaria-endemic tropical locations compared to Europe and North America, as shown in Chapter 1.3.2. Malaria is thought to upregulate regulatory responses to evade anti-parasite immunity (Chapter 1.4.2). This chapter explores the potential relationships between Treg activity and the immunogenicity of vaccines against malaria. The experimental vaccine against pre-erythrocytic stage *P. falciparum* malaria, ChAd63 / MVA ME-TRAP was tested for safety and immunogenicity in healthy adult, non-malaria-exposed populations in the UK before moving to adult populations in malaria-endemic settings and age de-escalating to 5-17 month old infants. This chapter firstly describes the development of a Treg flow cytometry phenotyping panel to be used in all chapters of this thesis. The effect of Treg activity on the immunogenicity of ChAd63 / MVA ME-TRAP in healthy UK adults is then investigated,

to determine any effect when suppression from exposure to malaria is excluded as a factor. Data is then shown which seeks to reproduce observations between Treg activity and vaccine immunogenicity for an analogous vaccine against Ebola in an adult population before translating these findings into paediatric cohorts in malaria-endemic settings.

The overall frequency and phenotype of bulk Treg cells existing prior to vaccination is measured by flow cytometry and correlated with peak antigen-specific humoral and cellular responses to vaccination in all cohorts. In the UK adult cohorts, the induction of antigen-specific Tregs by vaccination will also be measured and any effect on effector vaccine immunogenicity measured.

5.2. Chapter-specific Methods

A summary of the clinical trials from which samples were derived and utilised in this chapter is described below in table 5.1 and further details are enclosed in Chapter 2.2.

	Phase	Location	Malaria-exposure status	Age	Prime vaccine dose	Boost vaccine dose	Prime-boost interval
VAC43[274]	Ia	Oxford, UK	Naïve	18-50 years	5 x 10^{10} vp ChAd63 ME-TRAP	2 x 10^{8} pfu MVA ME-TRAP	8 weeks
VAC45[144]	Ia	Oxford, UK	Naïve	18-50 years	5 x 10^{10} vp ChAd63 ME-TRAP	2 x 10^{8} pfu MVA ME-TRAP	8 weeks
VAC48[276]	Ia	Oxford, UK	Naïve	18-50 years	5 x 10^{10} vp ChAd63 ME-TRAP	2 x 10^{8} pfu MVA ME-TRAP	8 weeks
VAC50[143]	IIb	Banfora, Burkina Faso	Highly exposed	5-17 months	5 x 10^{10} vp ChAd63 ME-TRAP	1 x 10^{8} pfu MVA ME-TRAP	8 weeks
EBL06[277]	Ib	Dakar, Senegal	Very low / no current exposure	18-50 years (male only)	2.5 – 3.7 x 10^{10} vp ChAd3 EBO Z	1 x 10^{8} pfu MVA EBO Z	1 week

Table 5.1: Summary of clinical trial design characteristics for samples included in the analysis presented in Chapter 5.

A schematic timeline of vaccine administration and sampling schedules is shown in Figure 5.1.

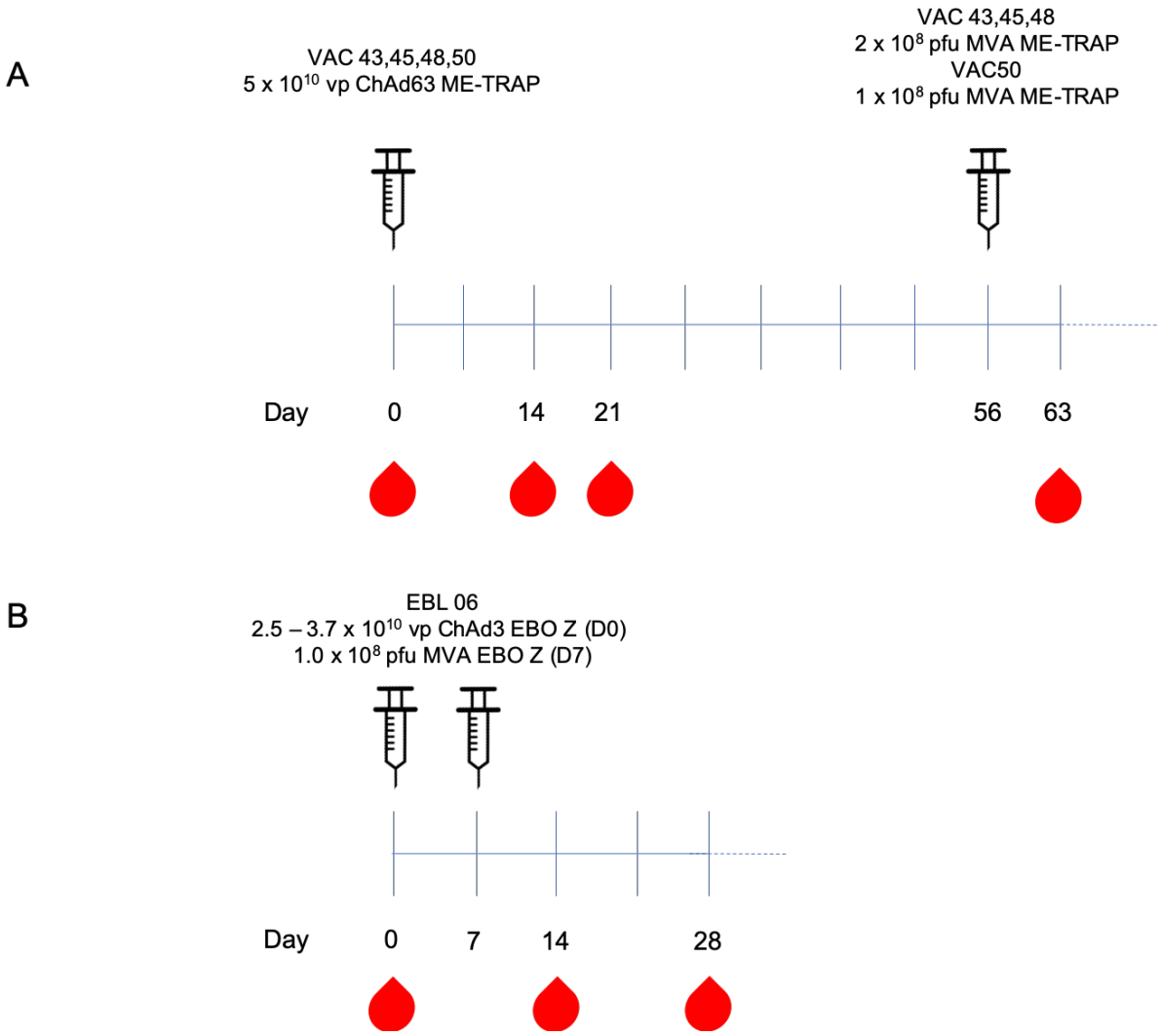

Figure 5.1: Schematic diagram of vaccination and sampling procedures for clinical trials (a) *procedures for ChAd63 / MVA ME-TRAP vaccination in VAC 43,45,48,50.* ***(b)*** *procedures for ChAd3 / MVA EBO Z vaccination in EBL 06. Syringes indicate timepoints for vaccination and red droplets timepoints for immunology blood sampling relevant to this analysis.*

All laboratory methods used in this chapter are as described in Chapter 2.

5.3. Results

5.3.1. Flow cytometry panel for quantification and phenotyping of Tregs

A flow cytometry phenotyping panel was developed for the quantification and phenotyping of Tregs in PBMC samples. Tregs were defined as FoxP3+ CD25+ CD127lo CD4+ T cells, in line with consensus recommendations by the Association for Cancer Immunotherapy[296]. Additional markers for minimum phenotyping were also included in line with the Association's recommendations. The fluorochromes were chosen such that the panel was universally compatible with different cytometers available at the Jenner Institute, University of Oxford and at KWTRP, Kilifi, Kenya. The panel was also designed so that it could be adapted for detecting antigen-specific activation markers following stimulation assays and for fluorescence activated cell sorting. Following titration of each antibody, the concentrations of reagents used were as described in Chapter 2.4.6.

A representative gating strategy for Treg quantification and phenotyping is shown in Figure 5.2. Cell viability was estimated by microscopy before staining for flow cytometry. Any sample with an estimated viability below <50% was discarded.

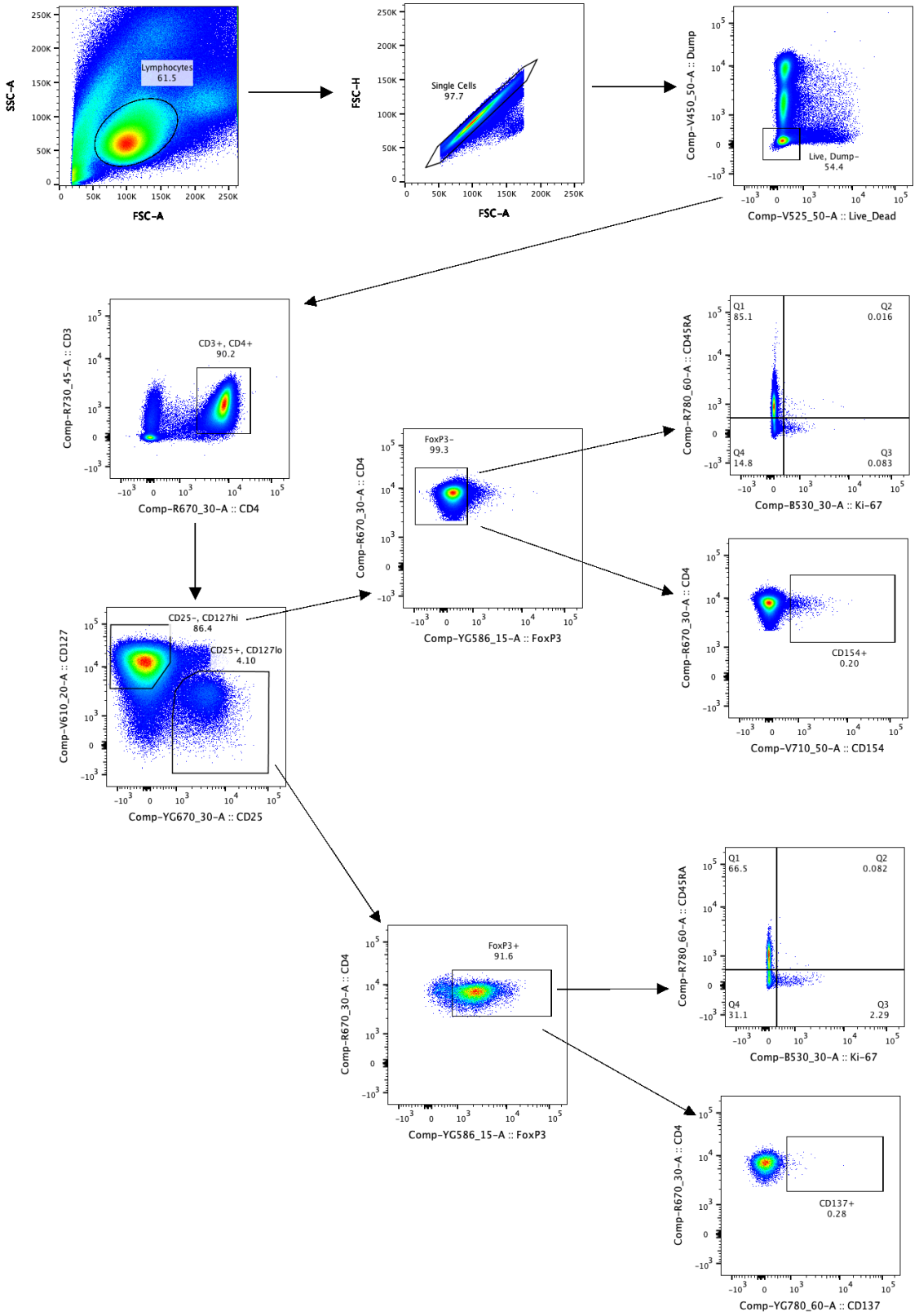

Figure 5.2: Gating strategy for Treg phenotyping and quantification *Tregs defined as FoxP3+ CD25+ CD127lo CD4+ T cells. Representative image from a single donor PBMC sample acquired on a BD LSRII cytometer. Where necessary to mitigate*

perturbations in cytometer flow, a time gate was also added immediately following the lymphocyte gate for some samples.

5.3.2. Vaccination with ChAd63 / MVA ME-TRAP induces potent cellular and humoral immune responses in healthy adult volunteers in Oxford

ChAd63 / MVA ME-TRAP is an experimental vaccine regimen which induces both cellular and humoral responses against the pre-erythrocytic stage *P. falciparum* antigen ME-TRAP. The most potent regimen in adults, defined by prior dose-escalation studies, is 5 x 10^{10} vp ChAd63 ME-TRAP prime followed by 2 x 10^{8} pfu MVA ME-TRAP boost 56-days later. Volunteers from three separate clinical trials of healthy adults based in the UK (Groups 4 and 7 of VAC 43, group 2 from VAC 45 and the control group from VAC 48) all received the same regimen of this vaccine and were combined into a single cohort to provide statistical power for analysis of Treg responses to vaccination (*n* = 24 volunteers). Clinical and laboratory procedures between trials were consistent and therefore immunogenicity between groups was comparable.

In order to assess the impact of Treg activity on the magnitude of the immune response to vaccination, timepoints measuring peak responses needed to be selected. Vaccine immunogenicity was determined by *ex vivo* IFNγ ELISpot to measure antigen-specific T cell responses and ELISA to quantify anti-TRAP IgG antibodies. The kinetics of both T cell and antibody responses to vaccination are shown in Figure 5.3. The peak cellular response following prime vaccination with

ChAd63 ME-TRAP is observed at day 14 [geomean 497 SFC / 10^6 PBMC, 95% CI: 310 – 797] whilst the peak following the MVA ME-TRAP boost vaccination is at day 63 (7 days after vaccination) [geomean 1582 SFC / 10^6 PBMC, 95% CI: 1182 – 2118]. The humoral response peaks considerably later than the cellular response following prime vaccination, such that titres were not routinely measured at Day 14. Antibody levels peaked at day 28 post-prime [29 GMT, 95% CI: 9.98 – 84.3]. Following MVA boost, antibody titres peaked at day 84 (28 days post-vaccination) [888 GMT, 95% CI: 428.1 – 1843.0], however a significant boost was also detectable earlier at day 63 [209 GMT, 95% CI: 60.7 – 719.9], coinciding with the peak cellular response. The antibody responses at day 63 and day 84 were not significantly different by Kruskal-Wallis tests. Therefore, to maintain comparability of data with paediatric data sets where more limited timepoints are available, day 63 was selected as the peak humoral immunogenicity timepoint.

A

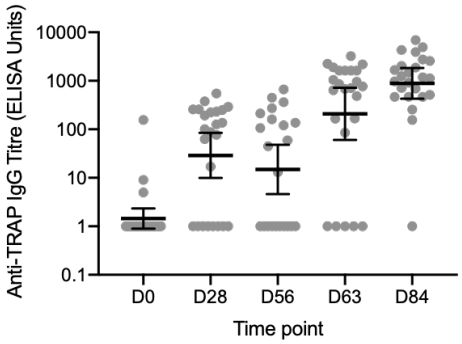

Dunn's multiple comparisons test	Summary	Adjusted P Value
D0 vs. D28	ns	0.1004
D0 vs. D56	ns	0.5216
D0 vs. D63	****	<0.0001
D0 vs. D84	****	<0.0001
D28 vs. D56	ns	>0.9999
D28 vs. D63	*	0.0480
D28 vs. D84	****	<0.0001
D56 vs. D63	**	0.0086
D56 vs. D84	****	<0.0001
D63 vs. D84	ns	0.9505

B

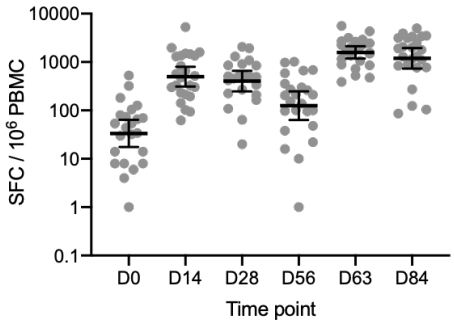

Dunn's multiple comparisons test	Summary	Adjusted P Value
D0 vs. D14	***	0.0001
D0 vs. D28	**	0.0013
D0 vs. D56	ns	0.7952
D0 vs. D63	****	<0.0001
D0 vs. D84	****	<0.0001
D14 vs. D28	ns	>0.9999
D14 vs. D56	ns	0.1737
D14 vs. D63	*	0.0429
D14 vs. D84	ns	0.3229
D28 vs. D56	ns	0.6057
D28 vs. D63	*	0.0127
D28 vs. D84	ns	0.1146
D56 vs. D63	****	<0.0001
D56 vs. D84	****	<0.0001
D63 vs. D84	ns	>0.9999

Figure 5.3: Kinetics of the immune response to vaccination with ChAd63 / MVA ME-TRAP *n = 24 volunteers from VAC 43, 45 and 48 each receiving 5 x 10^{10} vp ChAd63 ME-TRAP at day 0 and 2 x 10^{8} pfu MVA ME-TRAP at day 56. Differences between timepoints measured by Kruskal-Wallis with Dunn's correction for multiple comparisons.* ***(a)*** *anti-TRAP IgG antibody response to vaccination measured by ELISA.* ***(b)*** *antigen-specific T cell response to vaccination measured by ex vivo IFNγ ELISpot following stimulation of PBMC with ME-TRAP peptide pools (measured in spot forming colonies per 1 x 10^{6} PBMC).*

In summary, day 14 and day 63 were selected as timepoints measuring peak cellular responses post-prime and post-boost vaccination respectively whilst day 28 and day 63 were used for antibody responses.

5.3.3. Bulk Treg frequencies are not associated with vaccine immunogenicity following ChAd63 prime but memory phenotype may play a role.

Following the selection of day 14 for cellular responses and day 28 for antibody responses at which to correlate Treg activity with vaccine immunogenicity after priming, Treg frequencies at baseline were enumerated by flow cytometry. Treg frequencies were measured as a proportion of the total circulating pool of CD4+ T cells in PBMC. Treg frequencies were found to be relatively heterogeneous amongst this healthy adult population based in the UK [median 4.22% of CD4+ T cells, 95% CI: 3.69 – 5.32, range: 2.99 – 8.69].

There was no association, by Spearman rho, with the bulk frequency of Tregs at baseline and subsequent peak vaccine immunogenicity, either cellular or humoral, following prime vaccination with ChAd63 ME-TRAP (Figure 5.4). The phenotype of Tregs with respect to CD45RA+ memory status and Ki-67+ proliferation status was also analysed. This revealed a positive relationship between the proportion of Tregs that were positive for CD45RA and humoral vaccine immunogenicity at day 28 [Spearman r = 0.546, p = 0.0057] (Fig. 5.5a). There were no associations with CD45RA status and cellular immunogenicity (Fig. 5.5b), or between the frequency of Tregs that were positive for Ki-67 and either cellular or humoral vaccine immunogenicity (Fig 5.5c and 5.5d).

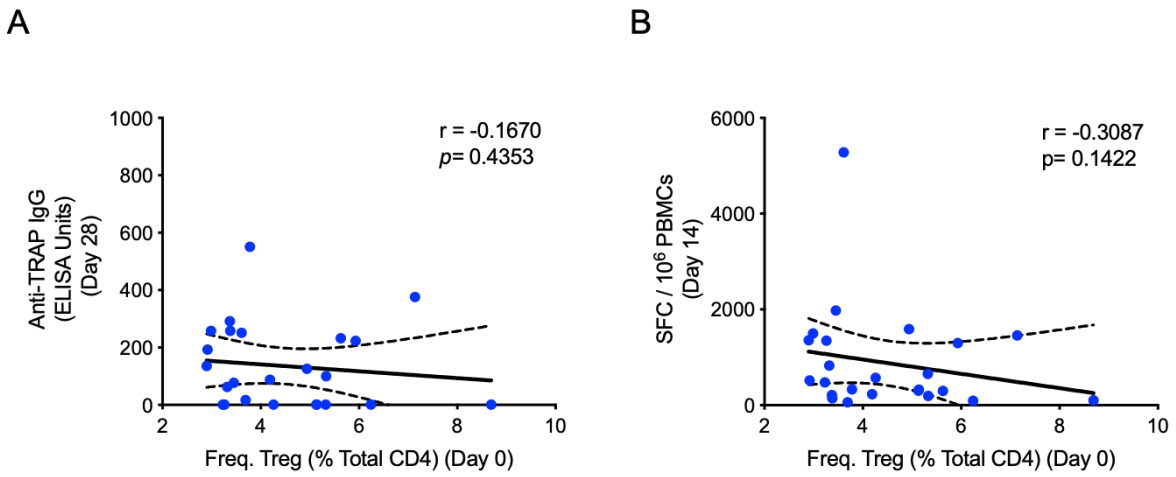

Figure 5.4: Association between baseline Treg frequencies and immunogenicity following ChAd63 ME-TRAP vaccination *FoxP3+ CD25+ CD127lo CD4+ Treg frequencies, expressed as a proportion of total CD4+ T cells, measured at baseline, correlated with* ***(a)*** *humoral vaccine immunogenicity at day 28 and* ***(b)*** *cellular vaccine immunogenicity by ex vivo IFNγ ELISpot at day 14. Correlations measured by Spearman rho with no significant associations observed; p = 0.44 and 0.14 for a and b respectively. n = 24 volunteers.*

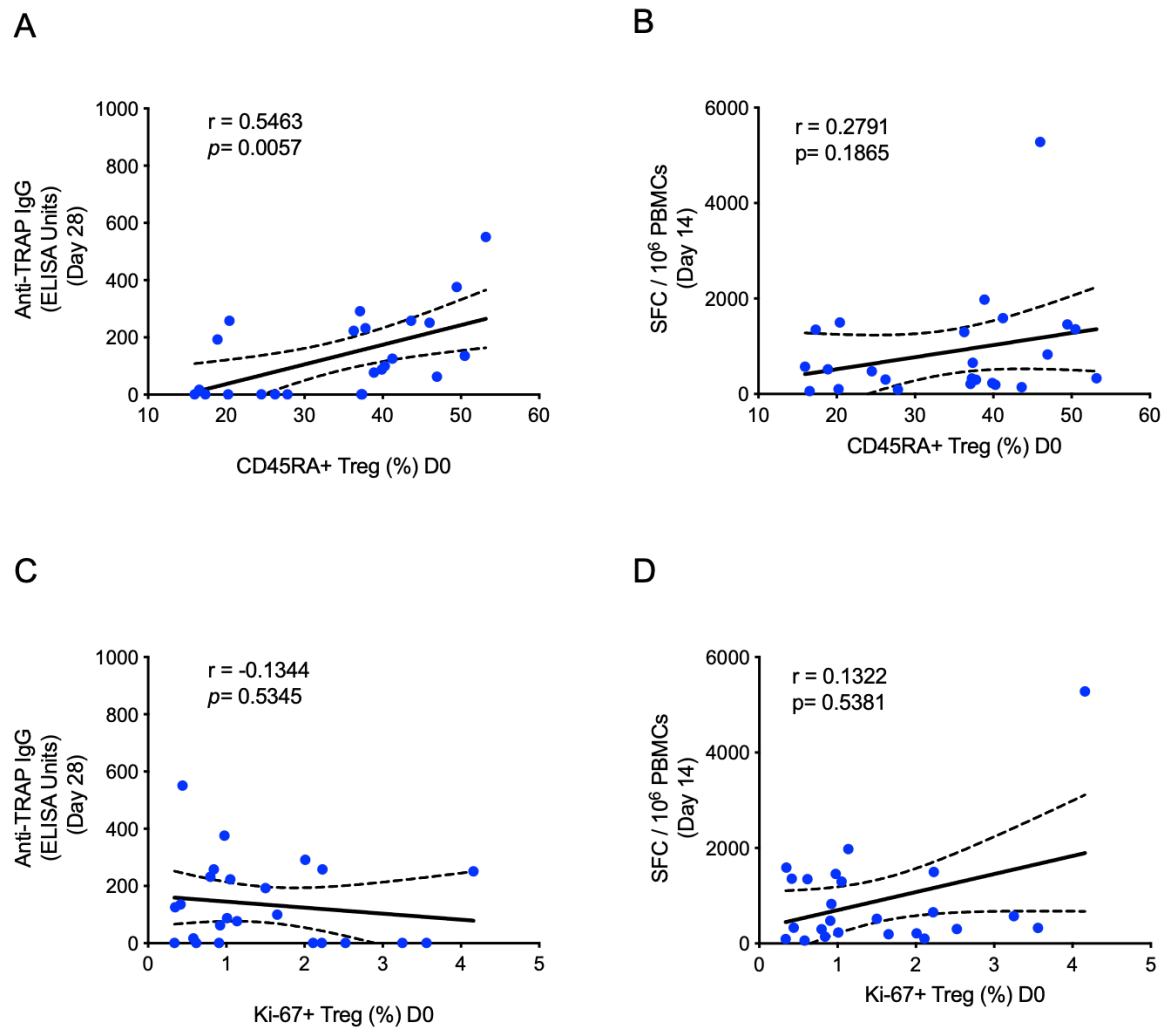

Figure 5.5: Association between vaccine immunogenicity following ChAd63 ME-TRAP prime and Treg phenotype at baseline. (a and b) *Proportion of Tregs at baseline expressing the naïve T cell marker CD45RA versus humoral and cellular vaccine immunogenicity at day 28 and day 14 respectively.* ***(c and d)*** *Proportion of Tregs at baseline expressing the marker of recent proliferation, Ki-67, versus humoral and cellular vaccine immunogenicity at day 28 and day 14 respectively. All correlations measured by Spearman rho. n = 24. P values corrected for multiple comparisons by the Holm-Sidak method.*

5.3.4. Bulk Treg frequencies are negatively associated with humoral vaccine immunogenicity following MVA ME-TRAP boost.

Next, associations between baseline Treg frequency and phenotype and vaccine immunogenicity following MVA ME-TRAP boost were assessed. Both humoral and

cellular vaccine responses were assessed at day 63, one week following boost vaccination. Both humoral and cellular responses were significantly increased compared to post-prime peak responses by Kruskal-Wallis [p = 0.048 and 0.043 respectively] (Figure 5.3). In contrast to that observed for post-prime responses, there was a significant negative relationship between the frequency of Tregs observed at D0 and subsequent peak vaccine immunogenicity post-boost at D63 (Figure 5.6). This relationship was significant for post-boost antibody titres [Spearman r = -0.58, p = 0.0029] and marginally non-significant for post-boost T cell responses [r = -0.38, p = 0.067].

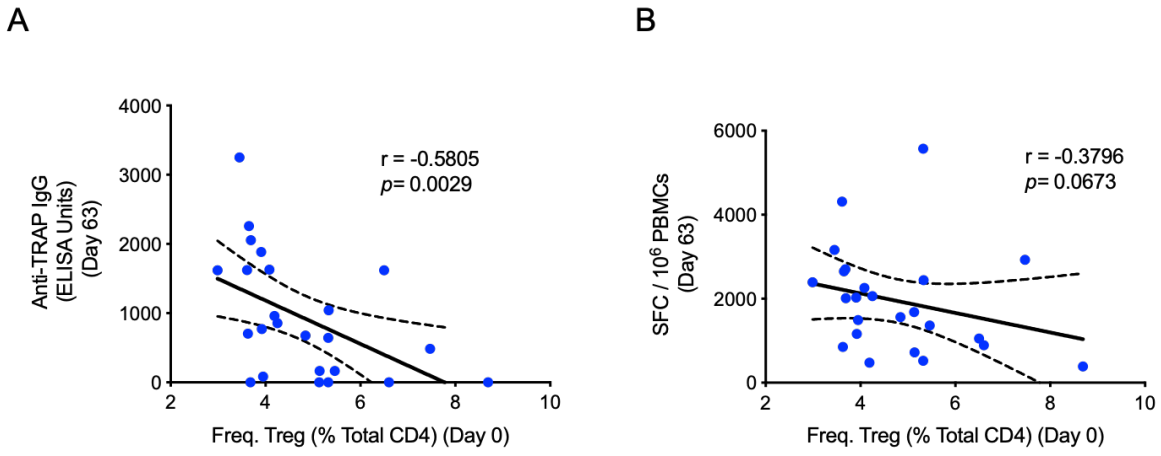

Figure 5.6: Association between baseline Treg frequency and post-boost vaccine immunogenicity (a) *frequency of Tregs at baseline correlated with the peak antibody response at day 63, one week after vaccination with MVA ME-TRAP.* ***(b)*** *frequency of Tregs at baseline correlated with the peak T cell response at day 63. Correlations by Spearman rho. n = 24.*

Again, in contrast to the relationships observed following prime vaccination, there was no association with the proportion of Tregs that were CD45RA+ and vaccine immunogenicity (Figures 5.7a and 5.7b). Tregs were also phenotyped and enumerated on day 63. Again, there was no association with the proportion of Tregs that were CD45RA+ at day 63 and vaccine immunogenicity (Figures 5.7c and 5.7d) or

between the fold change in CD45RA positivity between day 0 and day 63 and vaccine immunogenicity (Figures 5.7d and 5.7f).

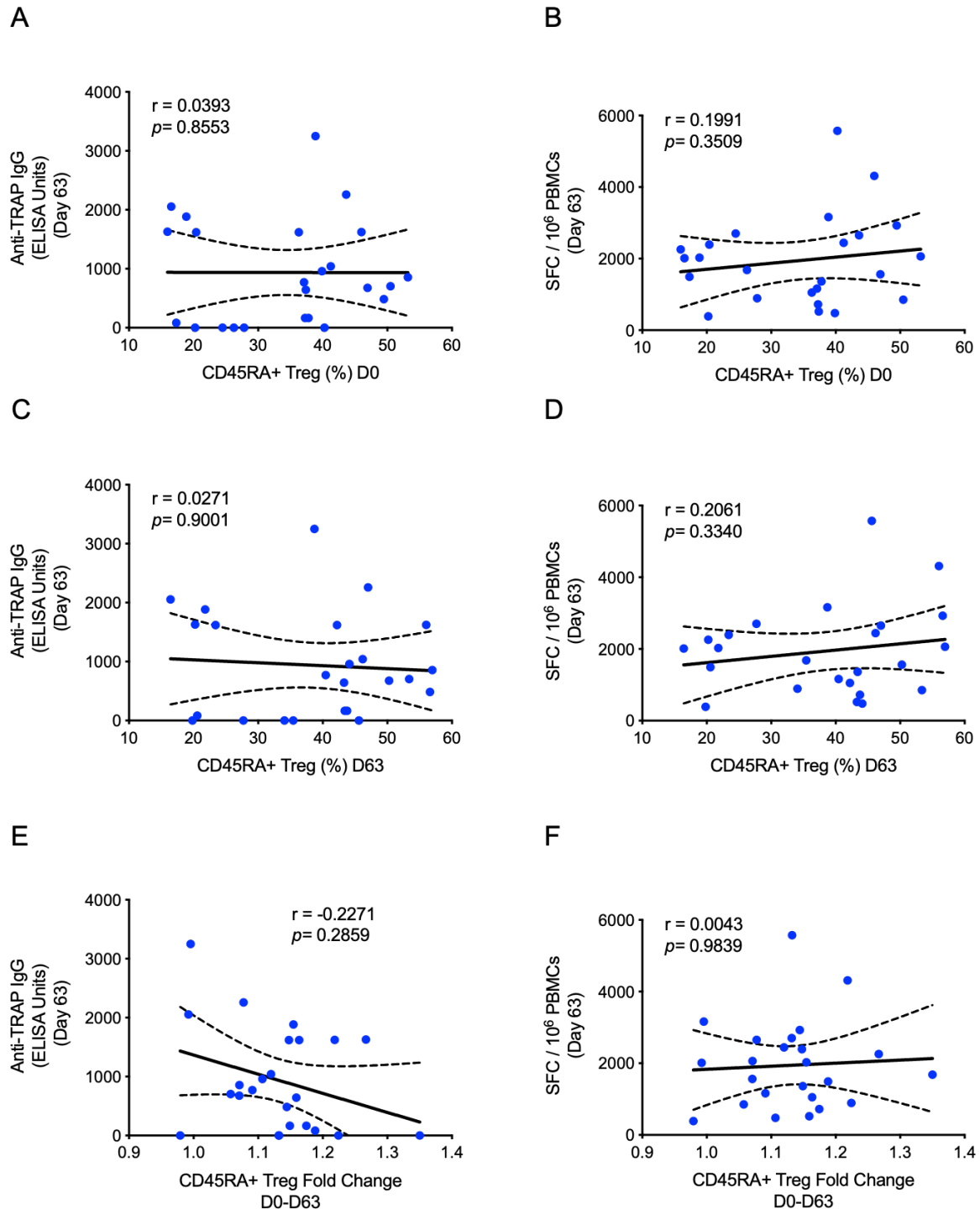

Figure 5.7: Associations between Treg CD45RA status and vaccine immunogenicity following boost (a and b) *association between the proportion of Tregs positive for CD45RA at baseline and post-boost vaccine immunogenicity.* ***(c and d)*** *association between CD45RA+ Treg proportions at day 63 and post-boost vaccine immunogenicity at the same timepoint.* ***(e and f)*** *association between the fold change*

in the proportion of Tregs positive for CD45RA at D63 compared to D0 and post-boost vaccine immunogenicity at D63. All correlations measured by Spearman rho and no significant associations observed. n = 24.

Similarly to the observations made between the proportion of Tregs expressing Ki-67 and post-prime vaccine immunogenicity, no significant associations were observed between Ki-67+ Tregs and post-boost vaccine immunogenicity. This was true for Ki-67+ Tregs at D0, D63 and D0-D63 fold change versus post-boost vaccine immunogenicity, both cellular and humoral (Figure 5.8).

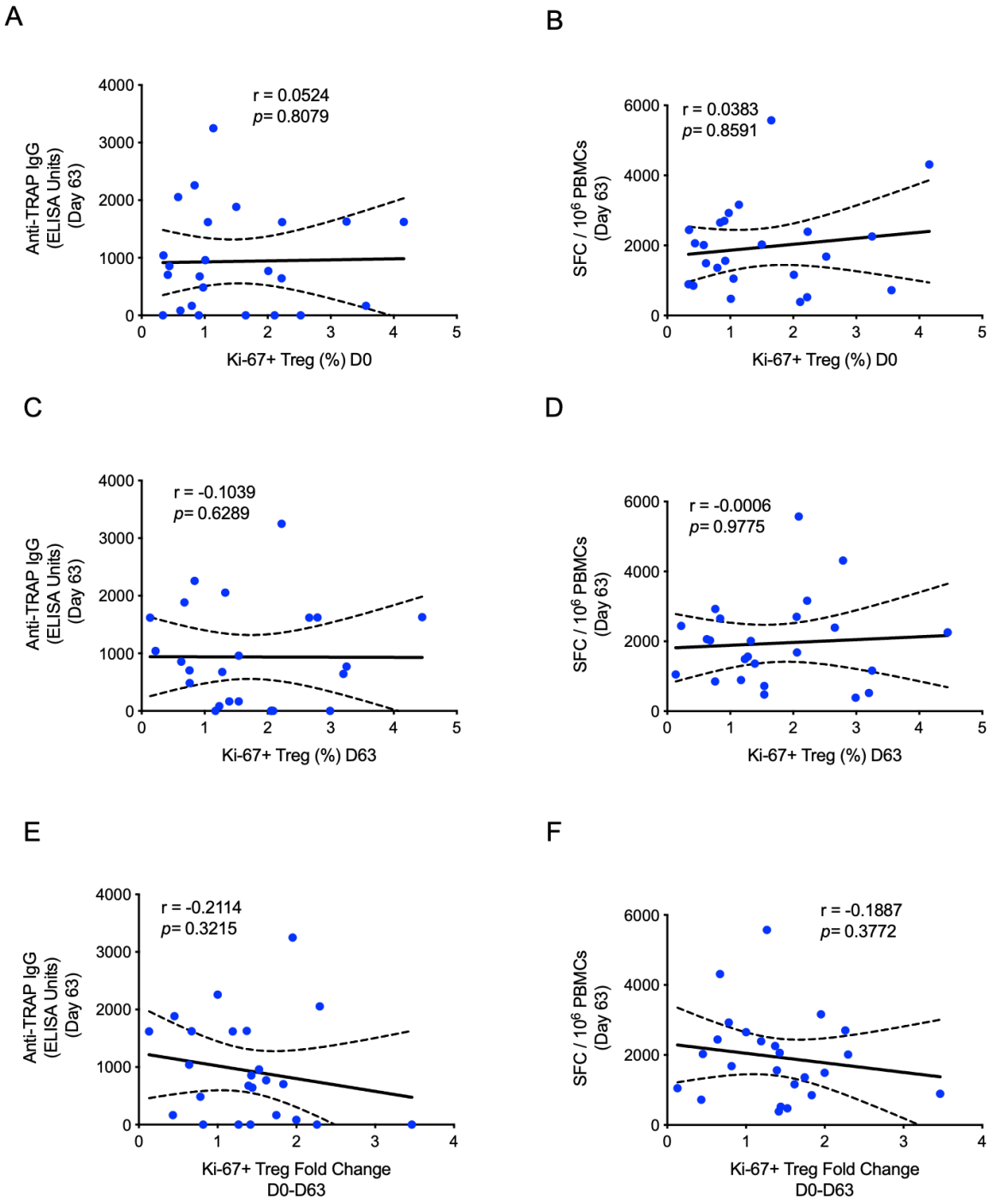

Figure 5.8: Association between Treg Ki-67+ status and vaccine immunogenicity following boost (a and b) *association between the proportion of Tregs positive for Ki-67 at baseline and post-boost vaccine immunogenicity.* ***(c and d)*** *association between Ki-67+ Treg proportions at day 63 and post-boost vaccine immunogenicity at the same timepoint.* ***(e and f)*** *association between the fold change in the proportion of Tregs positive for Ki-67 at D63 compared to D0 and post-boost vaccine immunogenicity at D63. All correlations measured by Spearman rho and no significant associations observed. n = 24.*

5.3.5. Treg frequencies at baseline are not associated with the cellular vaccine response post-boost, measured by intracellular cytokine staining

Figure 5.6 showed that baseline Treg frequencies were significantly negatively associated with post-boost vaccine humoral immunogenicity. There was a similar, but non-significant trend for the post-boost cellular response to vaccination measured by *ex vivo* IFNγ ELISpot. Cellular vaccine immunogenicity was also measured at the same timepoint by ICS which differentiates between antigen-specific CD4+ and CD8+ T cells and measures functionally distinct populations expressing either IFNγ, TNFα or IL-2 following peptide re-stimulation.

The association between Treg abundance at baseline and the quantity of different antigen-specific T cell subsets following boost vaccination was investigated. This revealed no associations between baseline Treg frequencies and either CD4+ or CD8+ antigen-specific T cell frequencies measured by ICS at D63 (Figure 5.9). This was true for all analyses for cells expressing either IFNγ, TNFα or IL-2.

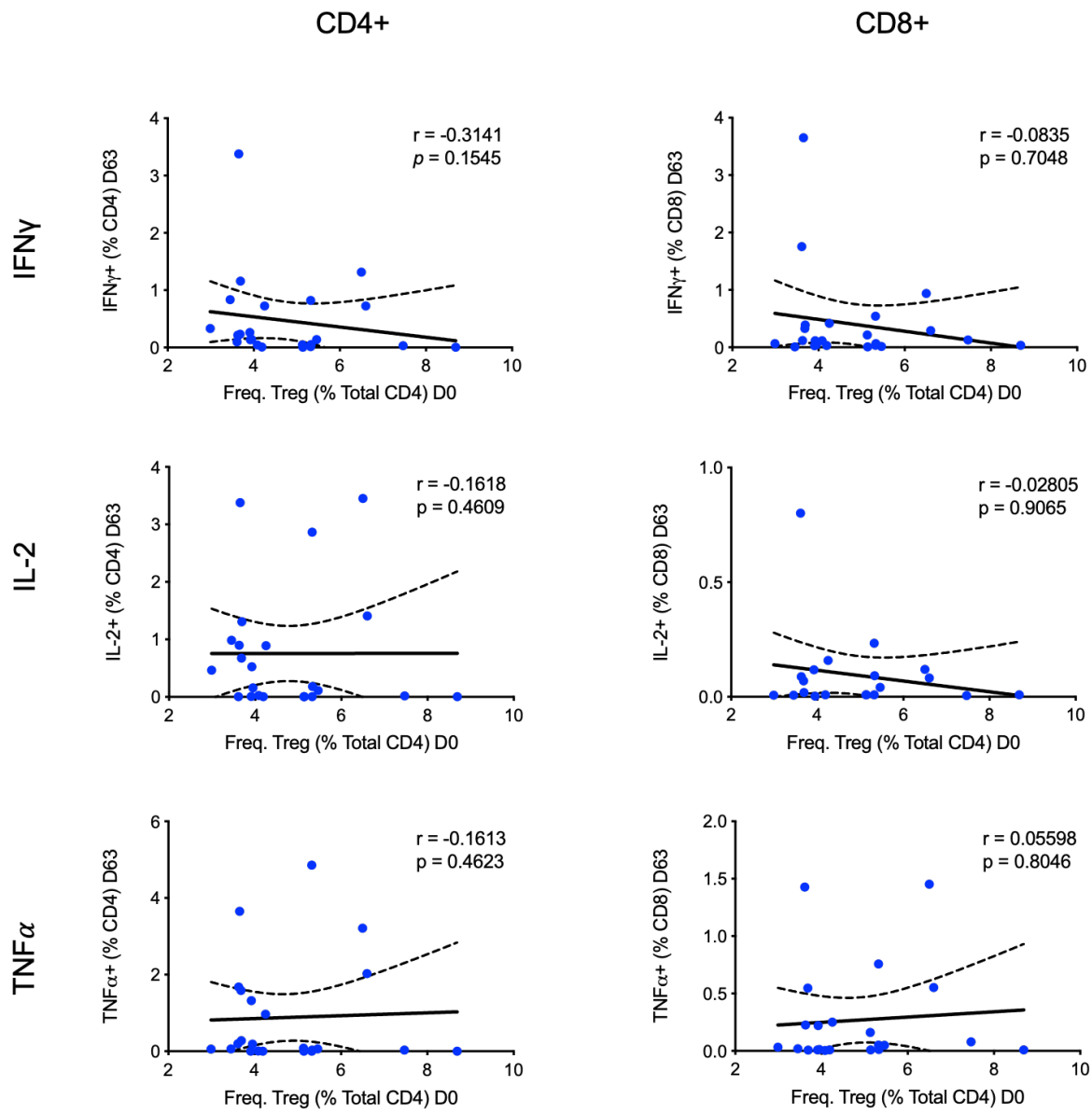

Figure 5.9: Associations between baseline Treg frequencies and antigen-specific T cell responses measured by ICS *CD4+ and CD8+ antigen-specific T cells expressing either IFNγ, TNFα or IL-2 were analysed and quantified separately. Antigen-specific cells were quantified at day 63 and Tregs at day 0. All correlations measured by Spearman rho and no significant associations observed. n = 24.*

5.3.6. Vaccination induces antigen-specific Tregs to ME-TRAP

As well as assessing the associations between antigen non-specific Tregs present at baseline with subsequent vaccine immunogenicity, the effect of antigen-specific Tregs induced by vaccination itself was also investigated. Using two activation induced

markers, CD137 (4-1BB) and CD154 (CD40L) which are present on the cell surfaces of activated FoxP3+ CD25+ CD127lo CD4+ Tregs and FoxP3- CD25- CD127hi CD4+ Teffs respectively at 6 hours following *in vitro* stimulation, antigen-specific cells were enumerated. PBMCs from D0, D14 and D63, representing baseline, post-prime and post-boost peak cellular immunogenicity timepoints, were stimulated with ME-TRAP peptide pools and ChAd63 and MVA viral vectors containing unrelated antigenic inserts. Following this, the proportions of cells expressing activation markers was measured by flow cytometry.

Firstly, the effect of vaccination on bulk Treg frequency and phenotype was assessed between D0 and D63. There was no significant change in the overall frequency of bulk Tregs between the two timepoints by pairwise analysis (Figure 5.10a). There was however a significant increase in the proportion of Tregs that were CD45RA+ at D63 compared to D0 (Fig. 5.10b). The proportion of Tregs expressing Ki-67 was not significantly different between D0 and D63 (Fig. 5.10c), however there appeared to be considerable fluctuation in positivity rates between the two timepoints in most volunteers.

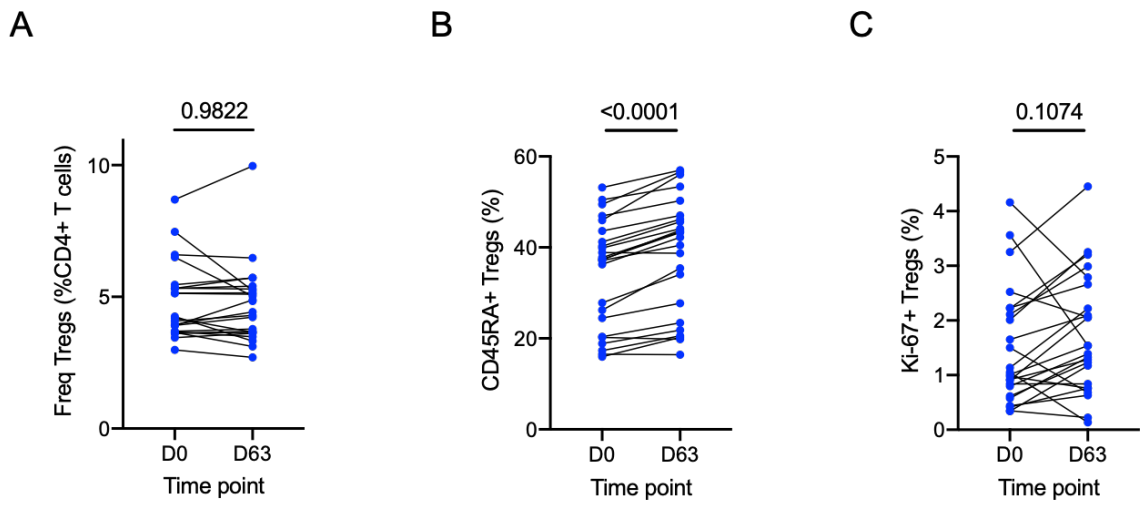

Figure 5.10: Changes in bulk Treg frequency and phenotype between D0 and D63 (a) *pairwise comparison of Treg frequencies between D0 and D63.* ***(b)*** *frequency of CD45RA+ Tregs between D0 and D63.* ***(c)*** *frequency of Ki-67+ Tregs between D0 and D63. Comparisons between timepoints measured by Wilcoxon matched pairs test. n = 24.*

The effect of vaccination on the frequency of antigen-specific Tregs and Teffs against ME-TRAP, ChAd63 and MVA was then measured. For Tregs specific to ME-TRAP, there was no significant increase at D14 compared to D0, however there was a significant increase by D63 (Figure 5.11). This mirrored the kinetics of the induction of effector T cells against ME-TRAP. The relative frequency of Tregs specific to ME-TRAP was greater at D63 than Teffs specific to ME-TRAP [1.8% CD137+ Treg, 95% CI: 1.27 – 2.56] and [0.13% CD154+ Teff, 95% CI: 0.04 – 0.34]. Detectable levels of ChAd63-specific Tregs and Teffs were measured in 7/13 (54%) volunteers at D0. These cells appeared to decline in frequency by D14 and were detected in 0/13 volunteers in the Teff subset (p = 0.03). No significant decline for Tregs was observed by pairwise analysis, (p = 0.16) despite only being detected in 2/13 volunteers by D14. For MVA-specific cells, there was a significant increase in CD137+ Tregs at D63 compared to D14 (p = 0.0005), but this was not reflected in the CD154+ Teff subset where no significant upregulation was observed (p = 0.19).

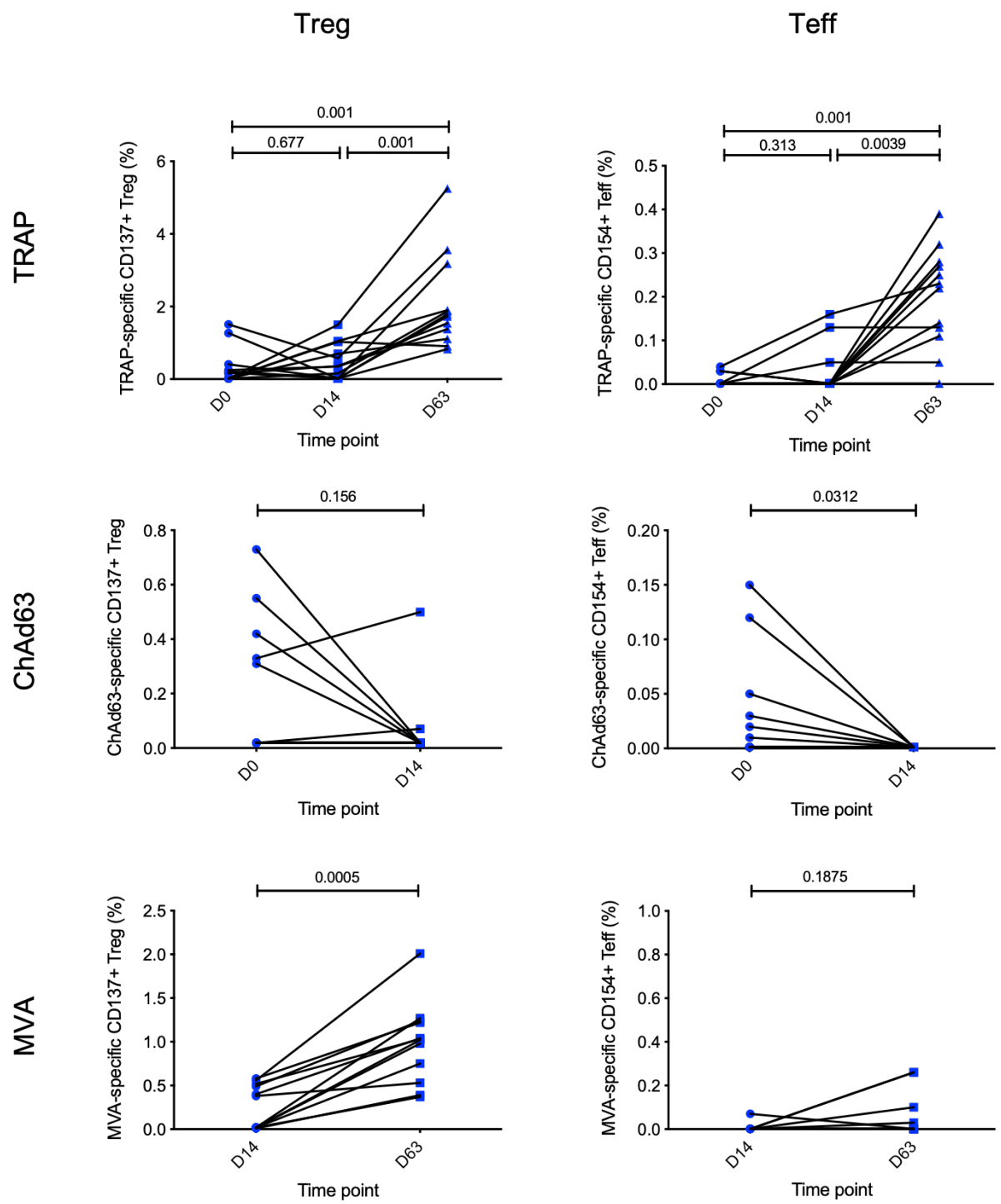

Figure 5.11: Quantities of antigen-specific Teffs and Tregs against ME-TRAP, ChAd63 and MVA measured using activation markers *n = 13 matched volunteers per timepoint. Differences between timepoints measured by Wilcoxon matched pairs tests with Holm-Sidak correction for multiple comparisons where analyses between 3 timepoints were made.*

Tregs induced by vaccination, either to ME-TRAP or to the viral vectors, were assessed to see if the magnitude of these responses had any impact on effector CD4+ T cell responses to ME-TRAP. Firstly, the titre of CD137+ Tregs against ME-TRAP observed at D63 correlated with the titre of CD137+ Tregs against MVA at the same timepoint (Figure 5.12a). Overall however, there was no evidence that the magnitude of anti-vector or anti-ME-TRAP Treg responses induced by vaccination were either negatively or positively associated with vaccine immunogenicity with respect to functional ME-TRAP specific effector CD4+ T cell responses. There was no association between the titre of CD137+ Tregs against ME-TRAP and the titre of CD154+ Teffs against the same antigen at D63 (Figure 5.12b). Since the frequency of CD137+ Tregs against ChAd63 reduced to undetectable levels in the majority of volunteers at D14 following prime vaccination, their association with CD154+ Teff responses to ME-TRAP was not assessable. Tregs were induced against MVA following boost vaccination but the frequency of these cells were not associated with the frequency of CD154+ Teffs against ME-TRAP at D63 (Figure 5.12c).

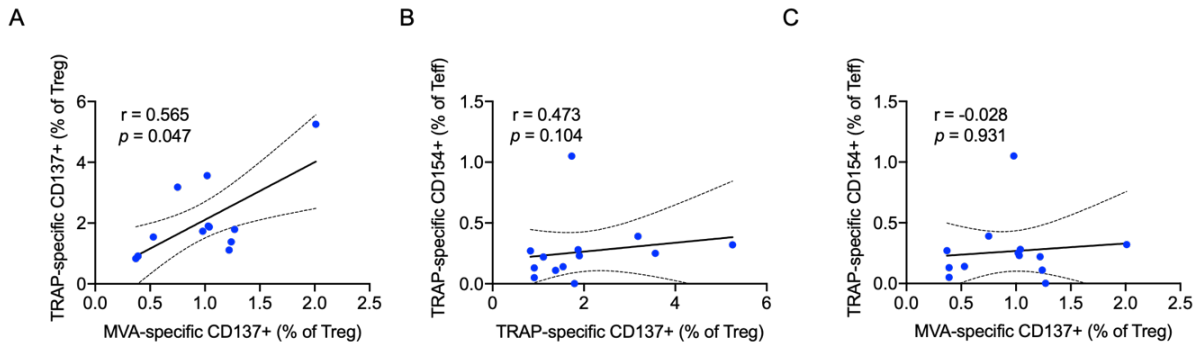

Figure 5.12: Associations between antigen-specific Tregs and Teffs against ME-TRAP and viral vectors *Antigen-specific responses to ME-TRAP peptide pools and MVA vector backbone measured using activation markers, CD137 for Tregs and CD154 for Teffs following 6 hour in vitro stimulation.* ***(a)*** *MVA-specific Tregs versus ME-TRAP-specific Tregs at D63.* ***(b)*** *ME-TRAP-specific Tregs versus ME-TRAP-specific Teffs at D63.* ***(c)*** *MVA-specific Tregs versus ME-TRAP-specific Teffs at D63. All associations measured by Spearman rho. n = 13.*

5.3.7. Baseline Treg frequencies are associated with humoral immunogenicity of an analogous vaccine against Ebola glycoprotein

Following findings observed in section 5.3.4 where baseline bulk Treg frequencies were negatively associated with peak humoral vaccine immunogenicity following a prime-boost regimen with ChAd63 / MVA ME-TRAP, it was investigated whether this could be replicated for an analogous viral vectored vaccine regimen expressing a different antigen. EBL06 was a Phase Ib clinical trial of the vaccine ChAd3 EBO Z / MVA EBO Z in healthy Senegalese adults. EBO Z is the glycoprotein of the Zaire strain of the Ebola virus. Dosing, routes of administration and laboratory procedures are comparable with trials of ChAd63 / MVA ME-TRAP, however this was an accelerated regimen whereby the boost dose is administered at 7 days post-prime. The timepoints for peak vaccine immunogenicity are therefore D28 for antibodies and D14 for T cells. Although the study was conducted in Senegal, the trial site was in the urban setting of Dakar where seasonal malaria transmission rates and prevalence of helminths are very low.

In agreement with the findings of section 5.3.4, there was a significant negative association between the frequency of Tregs at D0 and the peak antibody titre at D28 [r = -0.0474, p = 0.016] (Figure 5.13). Similarly there was no significant association between baseline Treg frequencies and peak ELISpot responses at D14 [r = -0.341, p = 0.103].

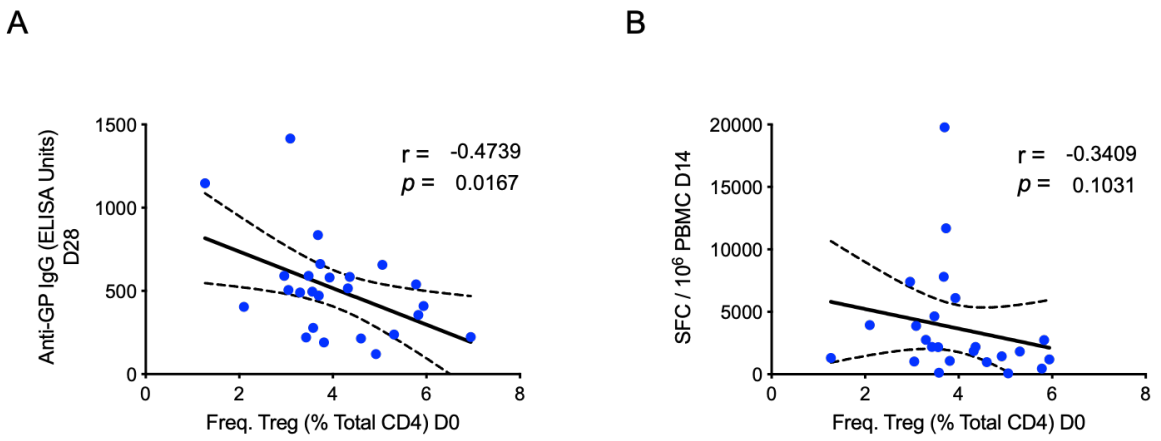

Figure 5.13: Associations between baseline Treg frequency and the immunogenicity of ChAd3 / MVA EBO Z in healthy Senegalese adults (a) *correlation between baseline Treg frequencies and the peak anti-Ebola glycoprotein IgG response at the peak titre timepoint at D28.* ***(b)*** *correlation between baseline Treg frequencies and peak anti-Ebola glycoprotein ex vivo IFNγ ELISpot response at the peak immunogenicity timepoint at D14. Associations measured by Spearman rho. n = 25 volunteers.*

In an effort to reproduce the findings of section 5.3.3 where the proportion of Tregs at baseline expressing CD45RA positively correlated with peak prime humoral vaccine immunogenicity, the responses at D7, before MVA boost were investigated. As expected with a very short prime-boost interval, antibody titres before boosting were very low [GMT 8.50, 95% CI: 3.68 – 19.60, range: 1 – 430] and undetectable in 10/25 [40%] volunteers. There was no association between the proportion of Tregs expressing CD45RA at D0 and the titre of anti-glycoprotein IgG at D7 [r = -0.167, p = 0.424] (Figure 5.14).

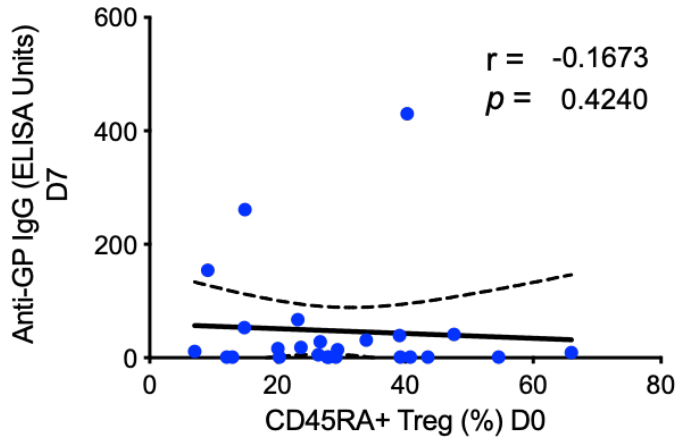

Figure 5.14: Association between frequency of Tregs expressing CD45RA at D0 and the titre of IgG against Ebola glycoprotein at D7 following ChAd3 prime vaccination *Associations tested by Spearman rho – no significant associations observed. n = 24.*

5.3.8. Immunogenicity of ChAd63 / MVA ME-TRAP differs in a malaria-exposed paediatric cohort and magnitude does not correlate with baseline Treg frequency

Finally, ChAd63 / MVA ME-TRAP was tested in a Phase IIb trial in 5-17 month old infants in Banfora, Burkina Faso (VAC 50) – an area of very high seasonal malaria transmission. The dose of ChAd63 ME-TRAP was the same as in UK adults (5×10^{10} vp) but the dose of MVA was reduced from 2×10^{8} pfu to 1×10^{8} pfu. The dose interval was 8 weeks and other clinical and laboratory procedures were comparable to the UK adults assessed in VAC 43, 45 and 48. Cell viability was checked following staining and was generally found to be high. *n* = 2/23 samples were discarded having an estimated viability <50%.

The immune response to ChAd63 / MVA ME-TRAP in Burkinabe infants differed to UK adults (Figure 5.15). The humoral response at D63 was superior in Burkinabe

infants [GMT 3170, 95% CI: 1731 – 5806] compared to UK adults [GMT 208.4, 95% CI: 60.6 – 717.4] (p = <0.0001). However the opposite was true for cellular responses. The geometric mean peak *ex vivo* IFNγ ELISpot response in UK adults was 1582 SFC / 10^6 PBMC [95% CI: 1182 – 2118] and 307.5 SFC / 10^6 PBMC [95% CI: 161.2 – 568.5] in Burkinabe infants (p = <0.0001).

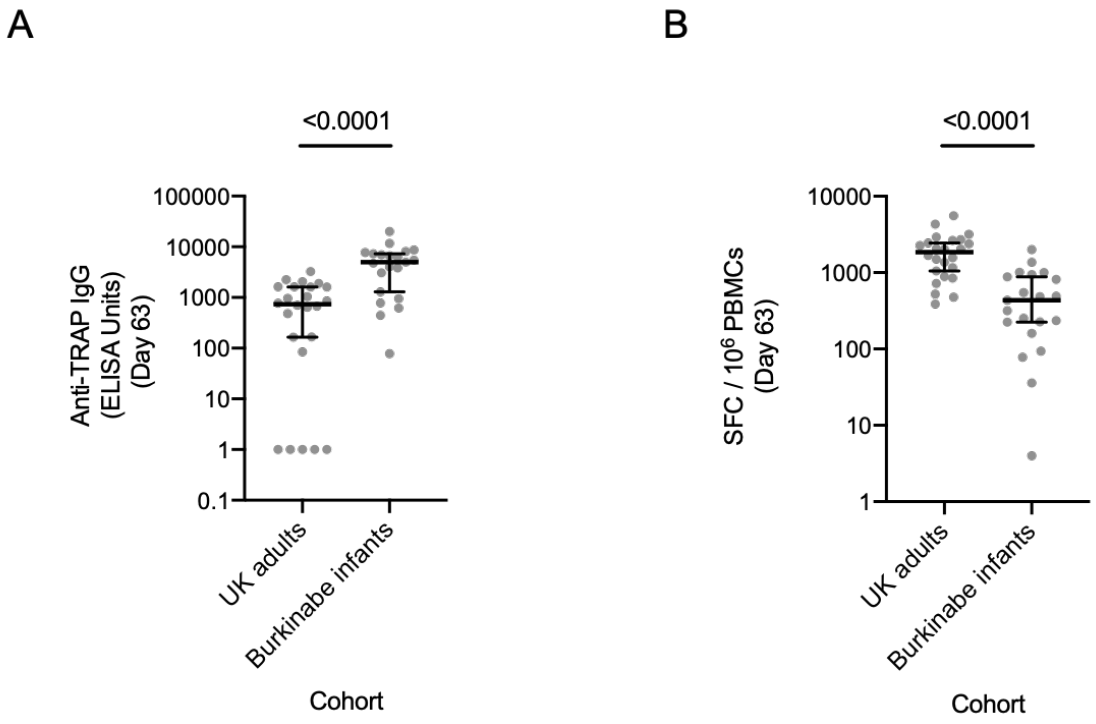

Figure 5.15: Humoral and cellular immunogenicity of ChAd63 / MVA ME-TRAP in UK adults and Burkinabe infants *Immunogenicity measured at D63, 1 week post-MVA boost. Differences between cohorts measured by Mann Whitney tests.* ***(a)*** *peak humoral anti-TRAP IgG response between the two cohorts measured by ELISA.* ***(b)*** *peak T cell response between cohorts measured by ex vivo IFNγ ELISpot assay. n = 24 UK adults and 21 Burkinabe infants.*

Baseline Treg frequencies were also measured in a subset of this cohort to test if there is a relationship with vaccine immunogenicity. Unlike in UK and Senegalese adults, there is no significant association between Treg frequency at D0 and peak humoral

vaccine immunogenicity at D63 [Spearman r = -0.018, *p* = 0.937] (Figure 5.16). There is also no relationship between baseline Treg frequencies and cellular vaccine immunogenicity measured by ELISpot [r = -0.103, *p* = 0.658].

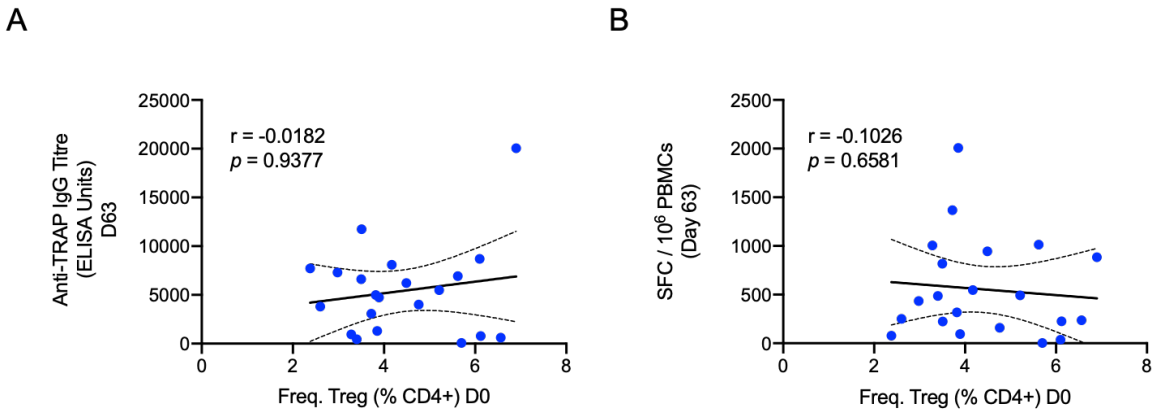

Figure 5.16: Association between Treg frequencies and immunogenicity of ChAd63 / MVA ME-TRAP in Burkinabe infants (a) *Treg frequencies at D0 correlated with peak antibody response at D63.* ***(b)*** *Treg frequencies at D0 correlated with peak T cell ELISpot response at D63. Correlations measured by Spearman rho correlation – no significant associations observed. n = 21 individuals.*

5.4. Discussion

This chapter explored the potential role of Tregs suppressing immunogenicity of the experimental vaccine regimen against pre-erythrocytic *P. falciparum* malaria, ChAd63 / MVA ME-TRAP. Although the principal hypothesis is that Treg homeostasis altered by exposure to malaria might impact immunogenicity, it was important to firstly assess if there were interactions between Treg activity and vaccine immunogenicity outside the context of malaria exposure. If malaria-induced immunosuppression is in part driven by an accumulation of bulk Tregs, then differences in immunogenicity could still be seen in non-malaria-endemic settings due to natural differences in Treg frequency.

Establishing a link between Treg activity and vaccine immunogenicity in malaria-naïve cohorts might also help to show if observations seen in malaria-endemic cohorts have the potential to be functional or are simply consequences of other malaria-induced immune changes which are not directly involved in suppression of vaccine-induced immunity.

To enumerate and provide some basic phenotypic data on Tregs in PBMC, a flow cytometry staining panel was designed. The definitive markers for human Tregs remain a contentious area of discussion, with no single protein having acceptable specificity to reliably identify these cells. FoxP3 is the master transcriptional regulator for Tregs, however it can also be transiently expressed in activated non-Treg CD4+ T cells as well. Much progress has been made in recent years in the availability of antibodies and buffers to stain for FoxP3, but its intranuclear location still makes it difficult to detect leading to much variability between studies[339]. Law *et al.* assessed optimal antibody clone and staining buffer combinations[340] in an effort to standardise panels across studies. Outcomes from this study were used to inform panel design in this project. Owing to the lack of a single definitive marker, combinations of markers are needed to reliably define CD4+ T cells as Tregs. An international workshop was set up by the Association for Cancer Immunotherapy in 2013 to rationally determine an appropriate combination of markers to be used across different studies and outline a flow cytometry gating strategy to isolate Treg cells[296]. In line with this, Tregs were defined in this study as FoxP3+ CD25+ CD127lo CD4+ Tregs. The workshop also listed a minimum set of essential phenotyping markers including CD45RA/RO and Ki-67 which were included accordingly. The method used in this study to quantify and

phenotype Tregs in PBMC therefore follows the currently accepted best practice guidelines.

These data appear to show a negative relationship between the activity of Tregs at baseline and the immunogenicity of ChAd63 / MVA ME-TRAP in adults. Following prime vaccination, the titre of anti-TRAP antibodies is reduced when the proportion of Tregs expressing CD45RA decreases, suggesting that having more Tregs of a memory phenotype is negatively associated with humoral vaccine immunogenicity. Following boost vaccination with MVA ME-TRAP, the frequency of total, rather than CD45RA+ Tregs, is associated with reduced humoral vaccine immunogenicity. No associations were identified between Tregs and cellular vaccine immunogenicity, measured either by ELISpot or ICS. Overall, this suggests that the greater the proportion of Tregs or the greater the proportion of Tregs that are memory cells, the less the antibody response to vaccination is.

This association does not prove a functional relationship between Tregs and antibody titres. However, it is possible to speculate on how Tregs might impact vaccine immunogenicity. The mechanisms of action of human Treg cells are described in detail in Chapter 1.4.1 and include the secretion of anti-inflammatory cytokines including IL-10 and TGF-β and the inhibition of costimulation by expression of CTLA-4[341,342]. All of these mechanisms could play a part in this interaction. The effect is seen at the level of bulk Treg cells, not just those that are responding in an antigen-specific manner, therefore this might suggest the cumulative basal activity of these cells at rest is enough to have a measurable effect on other immune cell types where the effect is proportional to the frequency of Tregs found in circulation. However, it is surprising that the effect is only observed with statistical significance on the antibody response

and not the T cell response, since Treg effector mechanisms affect T cell function as well. Viral vectors are known to be potent inducers of cellular immunity[343,344] so the T cell response might perhaps be dominant enough to counteract the bystander activity of Tregs. To limit the titre of antibodies, Tregs could act directly on B cells which are sensitive to IL-10 and TGF-β mediated signalling[345,346]. Although pro-inflammatory effector CD4+ T cell responses to ME-TRAP were not observed to be significantly affected by Treg activity in this analysis, B cell responses could still be indirectly affected by sub-optimal T cell help because of Treg activity. T follicular helper cells, which are important in providing B cell help, are also sensitive to Treg activity[347] and there is even a regulatory subset of Tfh which may play a role[348]. Future analyses should look at the interactions between Tregs, Tfh and B cells in response to vaccination.

There are very few other studies which have investigated the impact of Tregs on vaccine immunogenicity[349]. Ndure and colleagues found that the frequency of Tregs at the time of vaccination was negatively correlated with antibodies induced by measles vaccination but not diptheria-tetanus-pertussis vaccination in Gambian infants[350]. The fact that the effect was seen for one vaccine but not another suggests the suppressive influence of Tregs may vary depending on the mechanism of action of the vaccine. This paper was in infants, but in our study there was an effect for ChAd63 / MVA ME-TRAP in UK adults but not Burkinabe infants. This suggests a difference in immune response to ChAd63 / MVA ME-TRAP between adults and infants, which is different again to the response in infants to measles vaccine. It might also suggest a difference between the Gambian and Burkinabe cohorts. Age de-escalation studies of ChAd63 / MVA ME-TRAP have been conducted in the same

location in The Gambia as the measles vaccine trial, however PBMC samples were not available at the time of this study and these samples might have been useful to help determine site-specific differences.

One major difference between the Gambian and Burkinabe sites is malaria transmission intensity. Prevalence is very high at the site in Burkina Faso and relatively low in The Gambia (357.3 versus 19.6 clinical cases / 1000 person-years)[351]. The effect of malaria exposure on Treg homeostasis and vaccine immunogenicity is explored in greater depth in Chapter 6.

Further experiments are required to determine if the relationship between Tregs and vaccine immunogenicity observed here is causal. The gold standard method would be to suppress Treg activity *in vivo* at the time of vaccination, either through anti-CD25 therapy[352,353] or administration of cyclophosphamide[354], and measure subsequent immunogenicity. Manipulating Treg homeostasis in healthy volunteers is a difficult possibility because of the risk of inducing autoimmunity and is definitely not a feasible adjunct to vaccination if deploying post-licensure in a global health vaccine scenario. *In vitro* Treg suppression assays would be useful, however they require a large PBMC sample from which Tregs can be isolated and added back into PBMC at high fixed proportions. PBMCs are then stimulated and either proliferation or activation measured. Treg depletion assays have similar objectives and are an option here, however were not possible to complete within the timeframe of this project. This approach has been tried for an experimental HIV vaccine trial in HIV-1-infected individuals where *in vitro* Treg depletion significantly enhanced the proliferative T cell response upon restimulation following vaccination[355].

The HIV vaccine study also looked at the *in vivo* induction of Tregs following vaccination. Our study saw significant increases in the number of antigen-specific Tregs following vaccination. Similarly to our study, they observed an increase in the frequency of Tregs following vaccination (albeit not antigen-specific cells), and the magnitude of this increase did not correlate with vaccine immunogenicity. Taking into account the rest of the data in this chapter, this would suggest the activity of Tregs existing prior to vaccination is important in determining vaccine immunogenicity, whilst the Treg response induced by vaccination itself is not. This is not surprising since regulatory responses induced by vaccination are likely to be influenced by the same mechanisms as protective effector vaccine responses are.

The study presented in this chapter also saw interesting dynamics of the antigen-specific response to the viral vectors following immunisation. Antigen-specific Tregs and effector T cells against ChAd63 were detectable in some volunteers prior to vaccination, but these were undetectable 14 days later. Human adenoviruses circulate naturally in the environment and there may be some antigenic cross-reactivity with the chimpanzee adenovirus used in the vaccine, so finding pre-existing antigen-specific cells is not unexpected. The reduction in cell numbers observed peripherally following vaccination could represent trafficking of cells either to the site of vaccination or the local draining lymph node in response to infection. For MVA, antigen-specific Tregs but not effector CD4+ T cells were detected following vaccination. From searches of existing literature, this has not been shown in clinical trials using MVA as a vector before. Why MVA might induce antigen-specific Tregs but not effector T cells is currently unknown.

Finally, mouse models would also be useful to determine in greater detail the mechanistic basis of the associations between Tregs and vaccine responses observed in this chapter. For example, mouse models may be useful to investigate where antigen-specific Tregs and Teffs to viral vectors might traffic to following vaccination, as this type of study would not be possible in humans. Murine models may not necessarily always replicate human immune function, however it should be noted that the majority of murine studies investigating Tregs and vaccine responses have shown that these cells interfere with vaccine-induced immunity[349]. This includes one study showed that co-administration of anti-CD25 therapy and an adenoviral vectored vaccine in mice resulted in significantly increased immunogenicity[356].

5.5. Conclusions

This chapter has identified a relationship in UK adults between the frequency of Tregs in circulation before vaccination with ChAd63 / MVA ME-TRAP and the subsequent titre of antibodies induced against the vaccine antigen. There was however no relationship between Tregs and cellular immunogenicity. These findings were replicated in a second adult cohort of an analogous viral vectored vaccine. Despite this, there was no relationship between Tregs and vaccine immunogenicity in infants vaccinated in Burkina Faso. Further work needs to be done to understand the differences in immune response between UK adults and Burkinabe infants. The influence of malaria exposure on this cohort may play a part and this will be investigated in Chapter 6. Further experiments, either *in vitro* or in murine models, to determine a functional relationship between Tregs and vaccine immunogenicity are also necessary.

Chapter 6

6. Assessing the impact of malaria exposure and Treg activity on the immunogenicity of ChAd63 / MVA ME-TRAP in an infant cohort in Burkina Faso

6.1. Introduction

Chapter 5 explored a potential negative relationship between the frequency of Tregs at baseline and peak humoral immunogenicity of ChAd63 / MVA ME-TRAP in UK adults, which was not replicated in Burkinabe infants. This chapter explores exposure to malaria as a factor potentially linked to both the disruption of Treg homeostasis[207] and suppression of vaccine-induced immunity[161] (see sections 1.4.2 and 1.6.1 respectively). ChAd63 / MVA ME-TRAP was tested in a Phase 2b efficacy trial in 5-17 month-old infants in Banfora, Burkina Faso – an area highly endemic for malaria. During the study period in 2013, the estimated parasite prevalence rate in 2-10 year olds in southwestern Burkina Faso was 70.2% [95% CI: 61.6%-76.9%][351]. No protection against clinical infection following vaccination was observed, despite promising results in Kenyan adults previously[142].

Even within a single study setting, the intensity of exposure to malaria can be heterogeneous between individuals[357,358]. This heterogeneity can be exploited to explore relationships between cumulative malaria exposure and changes in immune phenotype. In the absence of being able to estimate malaria exposure by active case detection methods, as was the case in this retrospective study, serological markers have been shown to be a reliable correlate[359]. Here, two serological correlates were used, by measuring the titres of plasma IgG against the blood stage *P. falciparum* antigens, AMA-1 and MSP-1[359]. Malaria exposure was then analysed for its associations with both Treg activity and vaccine immunogenicity.

Helminth infections such as soil-transmitted helminths and schistosomiasis, which are co-endemic in the study population[360], are thought to have similar immunomodulatory mechanisms to malaria[261] and have also been implicated in reducing the immunogenicity and efficacy of other vaccines previously (see sections 1.4.2 and 1.6.1). Therefore this chapter also looks at their associations with the immunogenicity of ChAd63 / MVA ME-TRAP as well. The gold standard method to detect helminth infections is by microscopic examination of faeces and urine for parasite eggs[361], however these samples were not taken as part of the trial. Antigen-specific serological tests are also not well developed for these infections, which are considered to be neglected tropical diseases by the WHO[362]. Therefore, non-specific exposure to helminths was estimated by measuring the concentration of total IgE in plasma, which is upregulated following helminth infection[363].

Finally, the transcriptional phenotype of Tregs was assessed by multiplex qPCR and differential gene expression performed between high and low vaccine responders and

individuals with high and low exposure to malaria to understand whether the functional activity, rather than the quantity of Tregs, differs between those responding strongly or weakly to vaccination with ChAd63 / MVA ME-TRAP or differs following exposure to malaria. The multiplex qPCR gene expression analysis method developed in Chapter 4 for the analysis of Tregs and Teffs in the context of CHMI was adapted here for use in vaccine studies.

6.2. Chapter-specific methods

All samples analysed in this chapter were from VAC 50, except for section 6.3.1 where some data is also presented from VAC 43/45/48 and VAC47. VAC50 and VAC43/45/48 were as described in Chapter 2 and Chapter 5. VAC47 was a Phase IIb efficacy study of ChAd63 / MVA ME-TRAP prime-boost vaccination against *P. falciparum* infection in healthy Senegalese adult males. The experimental vaccine regimen and schedule in VAC47 was the same as for VAC43/45/48 as described in Chapter 5.

All experimental procedures were as described in the preceding chapters. The analysis of transcriptomic data in section 6.3.6 and 6.3.7 was as optimised and performed in Chapter 4.

6.3. Results

6.3.1. Differences in immunogenicity of ChAd63 / MVA ME-TRAP in Burkinabe infants are not related to age-related differences in Treg frequency

In Chapter 5, the association between Treg frequency and humoral vaccine immunogenicity between adults and infants differed following vaccination with ChAd63 / MVA ME-TRAP. To investigate this in more detail, differences in Treg frequency between these cohorts was firstly analysed. The 5-17 month-old Burkinabe infant cohort was split into three sub-groups of 4-month age intervals. This was done to detect differences resulting from the rapid maturation of the immune system that occurs in early life. There were no significant differences in Treg frequency by Kruskal-Wallis between adults in the UK [geomean 4.29% of CD4+ T cells, 95% CI: 3.77 – 4.88%], adults in Senegal [3.87%, 3.36 – 4.45%] and Burkinabe infants aged 5-8 months [4.43%, 3.49 – 5.63%], 9-12 months [4.36%, 3.55 – 5.35%] or 13-17 months [4.04%, 3.22 – 5.06%] (Figure 6.1a). Whilst differences in immunogenicity between UK adults and Burkinabe infants were seen previously (Chapter 5), there were no significant age-related differences between the three sub-groups in the Burkinabe infant cohort (Figure 6.1b and 6.1c).

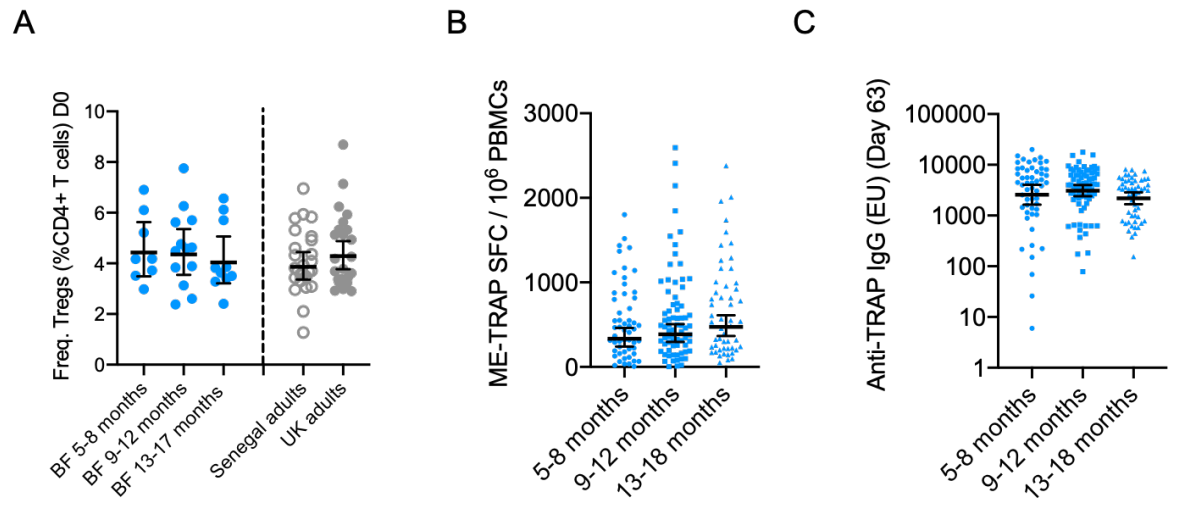

Figure 6.1: Differences in Treg frequency and vaccine immunogenicity between age groups. ***(a)*** *differences in Treg frequency between Burkinabe infants and adults in the UK and Senegal. The 5-17 month-old Burkinabe cohort was split into 3 age groups of 4-month intervals.* ***(b)*** *differences in cellular vaccine immunogenicity measured by ex vivo IFNγ ELISpot assay between the three Burkinabe infant age groups.* ***(c)*** *differences in humoral vaccine immunogenicity measured by ELISA between the three Burkinabe infant age groups. Differences between age groups measured by Kruskal-Wallis with Dunn's correction for multiple comparisons. No significant differences observed for any comparisons.*

6.3.2. Examining serological correlates as a method to estimate exposure to malaria

Prior exposure to malaria might suppress vaccine immunogenicity, which could underlie some of the differences observed between non-malaria-exposed UK adults and malaria-exposed Burkinabe infants in the interaction between Treg activity and vaccine immunogenicity. Entomological and parasitological methods of determining the intensity of exposure to malaria were not available in this retrospective study, therefore serological correlates were utilized for this purpose. IgG antibodies against two blood-stage *P. falciparum* antigens MSP-1 and AMA-1 were enumerated in *n* = 182 Burkinabe infants vaccinated with ChAd63 / MVA ME-TRAP. A positive IgG

antibody response against AMA-1 was detected in 145 / 182 [79.7%, 95% CI: 73.24 – 84.88%] infants and 134 / 182 [73.6%, 66.78 – 79.49%] for MSP-1. Antibody titres were measured in relative units, so are not directly comparable between antigens, however the mean response for anti-AMA-1 was 39.53 GMT [95% CI: 28.01 – 55.79, range: 1 – 4584] and for anti-MSP-1 was 39.55 GMT [95% CI: 27.12 – 57.69, range: 1 – 16718]. The distribution of responses are shown in Figure 6.2a. The per-individual anti-MSP-1 and anti-AMA-1 responses broadly correlated by Spearman rho [r = 0.423, *p* = <0.0001] (Figure 6.2b), however of the 62 individuals that were negative for IgG against either MSP-1 or AMA-1, only 23 were negative for both antigens [37.1%]. 25/62 [40.3%] individuals were negative for anti-MSP-1, but not anti-AMA-1 and 14/62 [22.6%] negative for anti-AMA-1 but not anti-MSP-1. When only those that had positive IgG responses against both AMA-1 and MSP-1 (*n* = 120) were analysed separately, the correlation was lost [r = 0.157, *p* = 0.088].

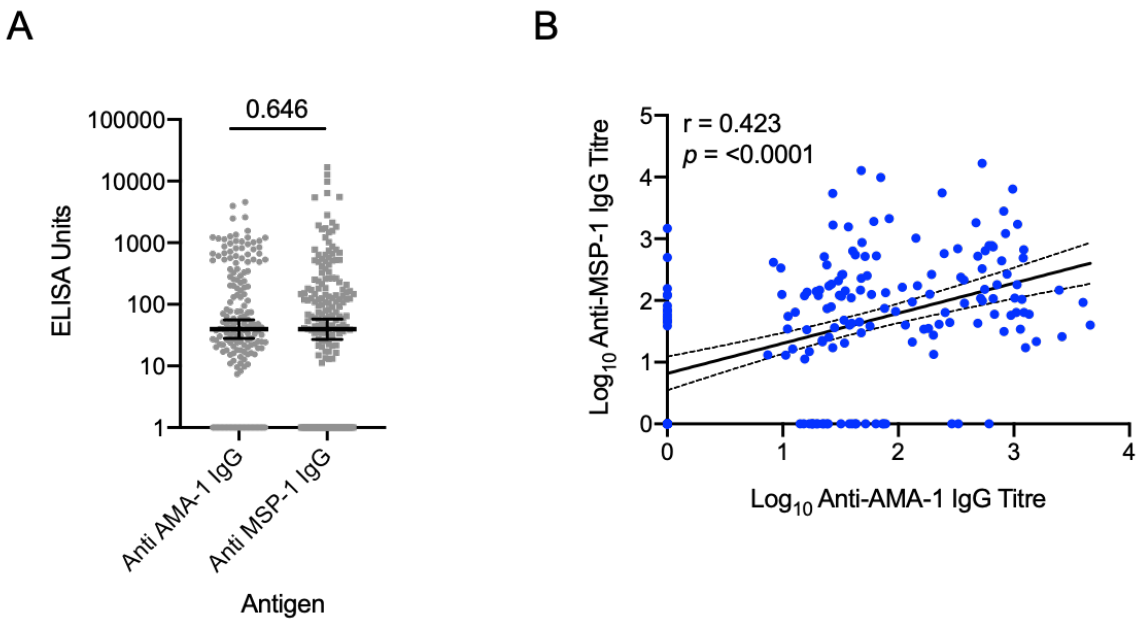

Figure 6.2: Association between anti-MSP-1 and anti-AMA-1 IgG responses in Burkinabe infants *Antibody responses measured by ELISA at D0 for two blood-stage P. falciparum antigens, AMA-1 and MSP-1, n = 182.* ***(a)*** *distribution of antibody titres against each antigen. No significant difference by Mann-Whitney, however titres not*

directly comparable across antigens as responses measured in relative units. ***(b)*** *association between responses against the two antigens by Spearman rho. [r = 0.423, p = <0.0001] for all n = 182 individuals and [r = 0.157, p = 0.088] for anti-MSP-1+ and anti-AMA-1+ double responders (n = 120).*

Neither the magnitude of IgG responses against MSP-1 or AMA-1 were associated with age (Figure 6.3). For AMA-1 the geometric mean titres were: 5-8 month-olds; 44.61 [95% CI: 25.48 – 78.10 GMT], 9-12 months; 39.65 [22.56 – 69.70] and 13-17 months; 34.89 [17.35 – 70.14]. For MSP-1 they were: 5-8 months; 26.20 GMT [12.85 – 53.42], 9-12 months; 39.24 [21.94 – 70.20] and 13-17 months; 60.36 [29.48 – 123.6]. The number of infants with a positive anti-AMA-1 response in the 5-8 month-old group was 46/54 [85.2%], in the 9-12 month-old group was 58/74 [78.4%] and in the 13-17 month-olds was 41/54 [75.9%]. The number of infants with a positive MSP-1 response in the 5-8 month-old group was 36/54 [66.6%], in the 9-12 month-old group was 55/74 [74.3%] and in the 13-17 month-olds was 43/54 [79.6%].

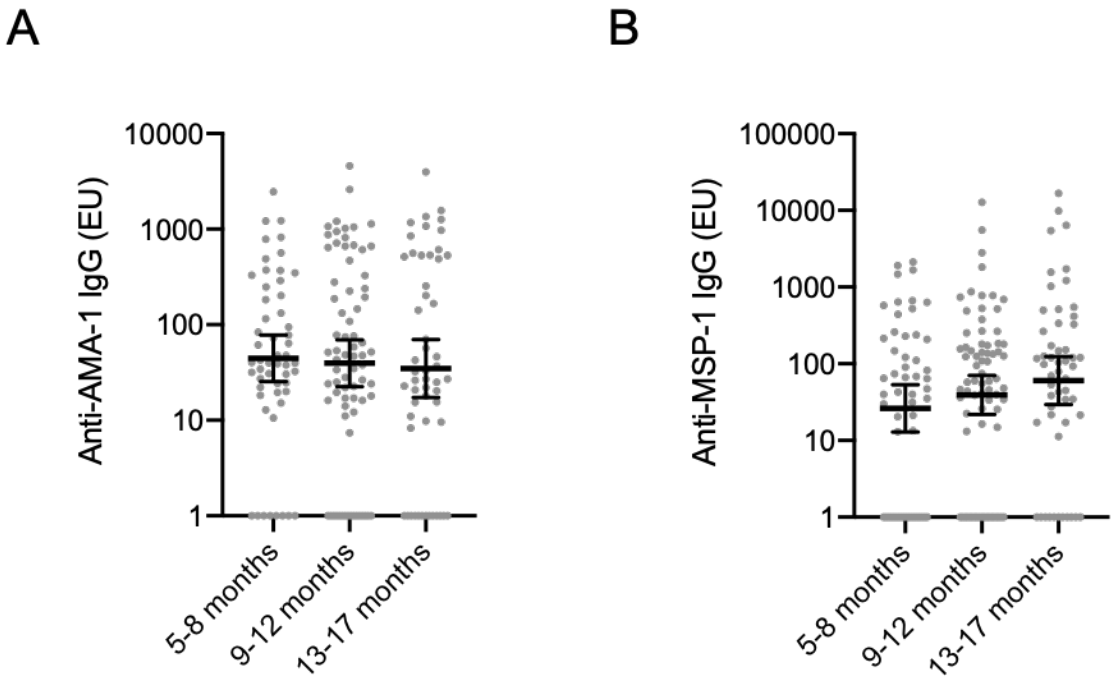

Figure 6.3: IgG responses to AMA-1 and MSP-1 in Burkinabe infants, split by age group *Antibody responses to AMA-1 and MSP-1 measured at D0. Differences*

between groups measured by Kruskal-Wallis test with Dunn's correction for multiple comparisons, no significant differences observed. n = 60 per age group.

Next, the frequency distribution of responses to each antigen were assessed. Neither the raw nor Log_{10} transformed data for either anti-AMA-1 or anti-MSP-1 were normally distributed (Figure 6.4). For AMA-1, the D'Agostino-Pearson normality test showed responses were positively skewed both as untransformed data [K^2 = 193.4, p = <0.0001] and when Log_{10} transformed [K^2 = 19.42, p = <0.0001]. This was also the case for MSP-1, both as untransformed data [K^2 = 257.0, p = <0.0001] and Log_{10} transformed [K^2 = 14.81, p = 0.0006]. Importantly, the lack of a negative skew suggested that IgG antibody responses to AMA-1 and MSP-1 in this cohort were not saturated meaning both antigens might be useful as serological correlates of exposure. Therefore both antigens were taken forwards to assess their associations with vaccine immunogenicity and Treg activity.

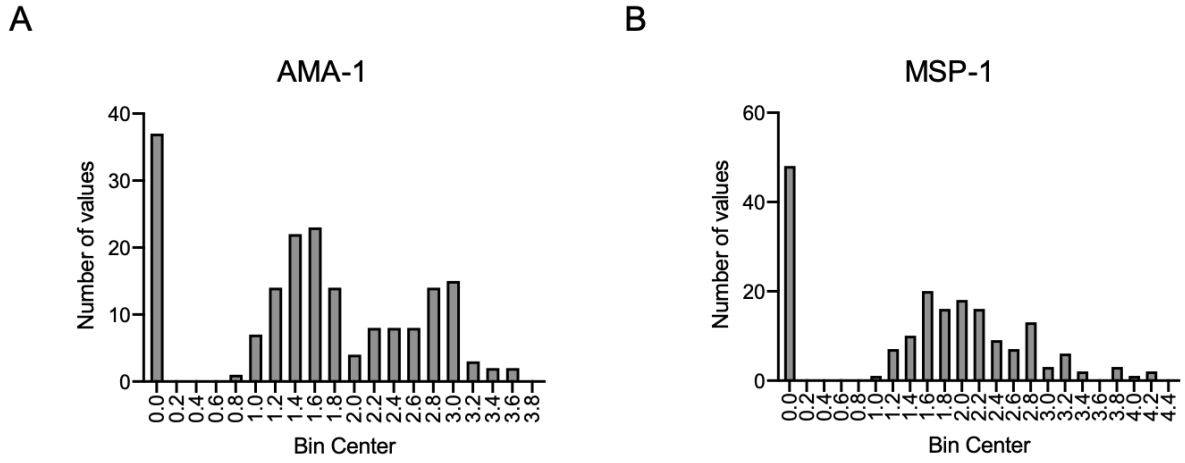

Figure 6.4: Distribution of antibody responses to AMA-1 and MSP-1 *Distribution of IgG responses measured by ELISA at D0 to blood-stage P. falciparum antigens AMA-1 and MSP-1. Log_{10} transformed values plotted and normality tested by D'agostino Pearson tests for* ***(a)*** *Anti-AMA-1 IgG [K2 = 19.42,* p *= <0.0001] and* ***(b)*** *Anti-MSP-1 IgG [K^2 = 14.81,* p *= 0.0006]. n = 182.*

6.3.3. Antibody responses against AMA-1, but not MSP-1 are associated with reduced cellular vaccine immunogenicity.

The magnitude of the anti-AMA-1 IgG response at baseline was plotted against vaccine immunogenicity readouts at D63 in Burkinabe infants aged 5-17 months vaccinated with ChAd63 / MVA ME-TRAP. There was a modest negative correlation between the titre of IgG antibodies against AMA-1 and the peak T cell response at D63 measured by ELISpot [r = -0.226, p = 0.002] (Figure 6.5a). This association was also demonstrated when ELISpot responses were analysed as quartiles of the anti-AMA-1 IgG titre (Figure 6.5b), where ELISpot responses were significantly lower in the top anti-AMA-1 quartile compared to the bottom [p = 0.0289 by Kruskal-Wallis]. For anti-TRAP antibodies induced by vaccination at D63, there was no association with baseline anti-AMA-1 IgG titres, either by Spearman rho or Kruskal-Wallis based on anti-AMA-1 IgG quartiles (Figure 6.5c and 6.5d).

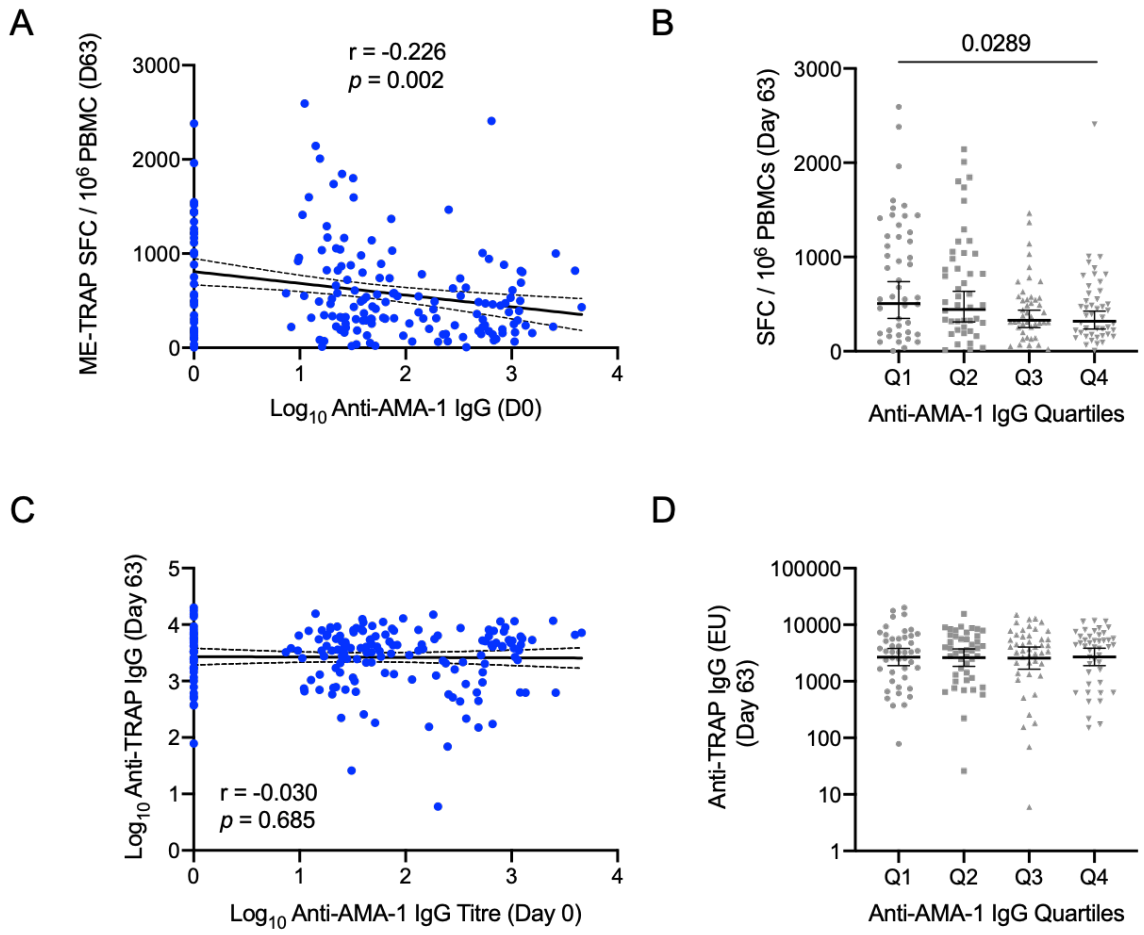

Figure 6.5: Association between baseline anti-AMA-1 antibody titres and immunogenicity of ChAd63 / MVA ME-TRAP in Burkinabe infants (a) *anti-AMA-1 response at D0 versus the antigen-specific T cell ELISpot response to ME-TRAP after vaccination at D63.* ***(b)*** *antigen-specific T cell ELISpot response split into quartiles by anti-AMA-1 response (Q1: lowest 25% anti-AMA-1 titre, Q4: highest 25%).* ***(c)*** *anti-AMA-1 response at D0 versus the anti-ME-TRAP IgG response after vaccination at D63.* ***(d)*** *anti-ME-TRAP IgG response split into quartiles by anti-AMA-1 response (Q1: lowest 25% anti-AMA-1 titre, Q4: highest 25%). Correlations tested by Spearman rho and comparisons between quartiles by Kruskal-Wallis with Dunn's correction for multiple comparisons (only significant results shown). n = 182.*

This analysis was repeated using antibody titres against MSP-1 as a correlate of exposure to *P. falciparum*. Contrary to the findings with anti-AMA-1, there was no association between anti-MSP-1 antibody titres at D0 and the peak T cell response at D63 measured by ELISpot [Spearman rho = -0.087, p = 0.249] (Figure 6.6a). There was also no difference in ELISpot response when split into anti-MSP-1 IgG quartiles (Figure 6.6b). In agreement with anti-AMA-1, there was also no association between

anti-MSP-1 IgG titres and the peak humoral response to ME-TRAP following vaccination (Figure 6.6c and 6.6d).

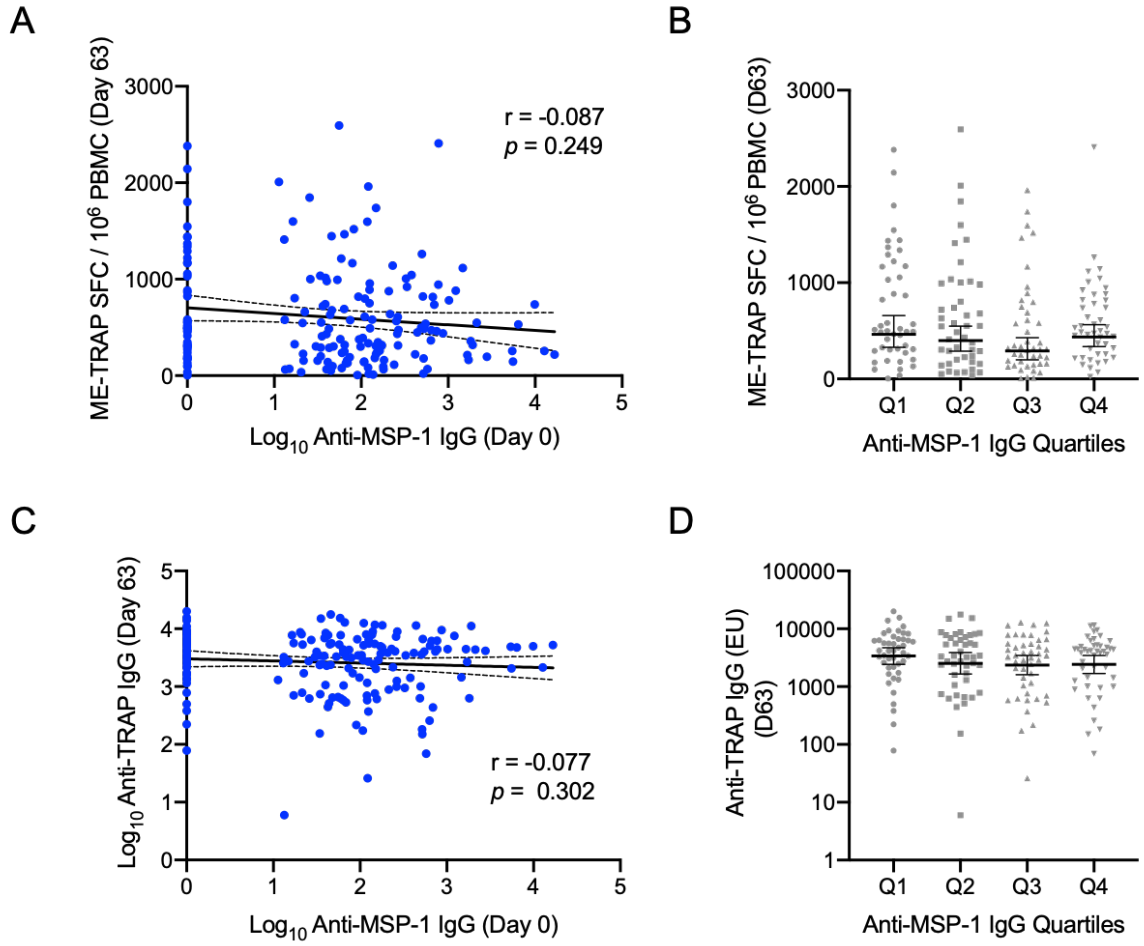

Figure 6.6: Association between baseline anti-MSP-1 antibody titres and immunogenicity of ChAd63 / MVA ME-TRAP in Burkinabe infants. (a) *anti-MSP-1 IgG response at D0 versus the antigen-specific T cell ELISpot response to ME-TRAP after vaccination at D63.* ***(b)*** *antigen-specific T cell ELISpot response split into quartiles by anti-MSP-1 response (Q1: lowest 25% anti-MSP-1 titre, Q4: highest 25%).* ***(c)*** *anti-MSP-1 response at D0 versus the anti-ME-TRAP IgG response after vaccination at D63.* ***(d)*** *anti-ME-TRAP IgG response split into quartiles by anti-MSP-1 response (Q1: lowest 25% anti-MSP-1 titre, Q4: highest 25%). Correlations tested by Spearman rho and comparisons between quartiles by Kruskal-Wallis with Dunn's correction for multiple comparisons (no significant differences observed). n = 182.*

6.3.4. Antibody response to blood-stage *P. falciparum* antigens is negatively associated with Treg frequency

The titres of IgG antibodies raised against MSP-1 and AMA-1 were correlated with Treg frequency at baseline (Figure 6.7). There was a negative association between Treg frequency and the titre of anti-AMA-1 antibodies [Spearman rho = -0.512, p = 0.01] as well as anti-MSP-1 antibodies [r = -0.445, p = 0.043].

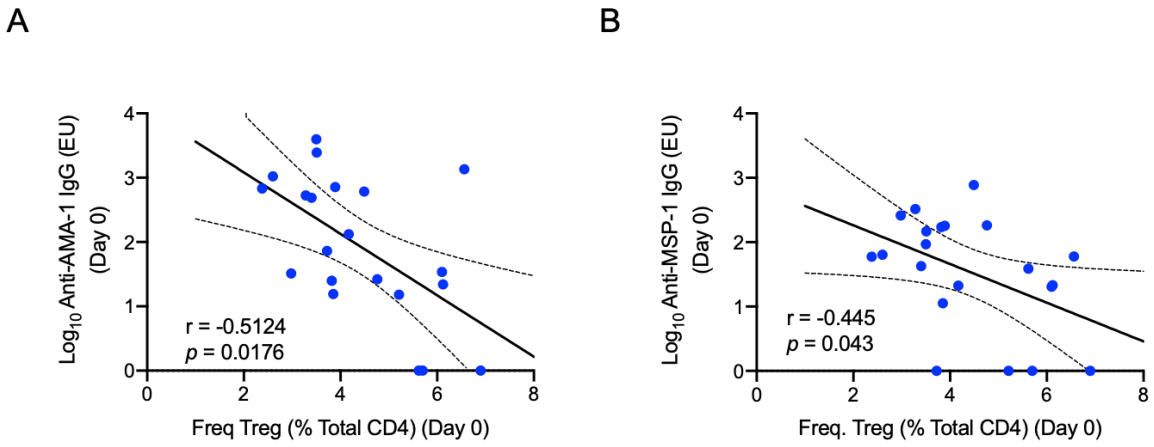

Figure 6.7: Association between Treg frequency and anti-AMA-1 and anti-MSP-1 antibody titre *Treg frequencies correlated against IgG antibody titres against* ***(a)*** *AMA-1 and* ***(b)*** *MSP-1 measured at D0. Associations measured by Spearman rho. n = 21.*

IgG titres against AMA-1 and MSP-1 were also analysed against phenotypic Treg markers. There were no associations between the titres of either anti-AMA-1 or anti-MSP-1 and the proportion of Tregs that express CD45RA or Ki-67 (Figure 6.8).

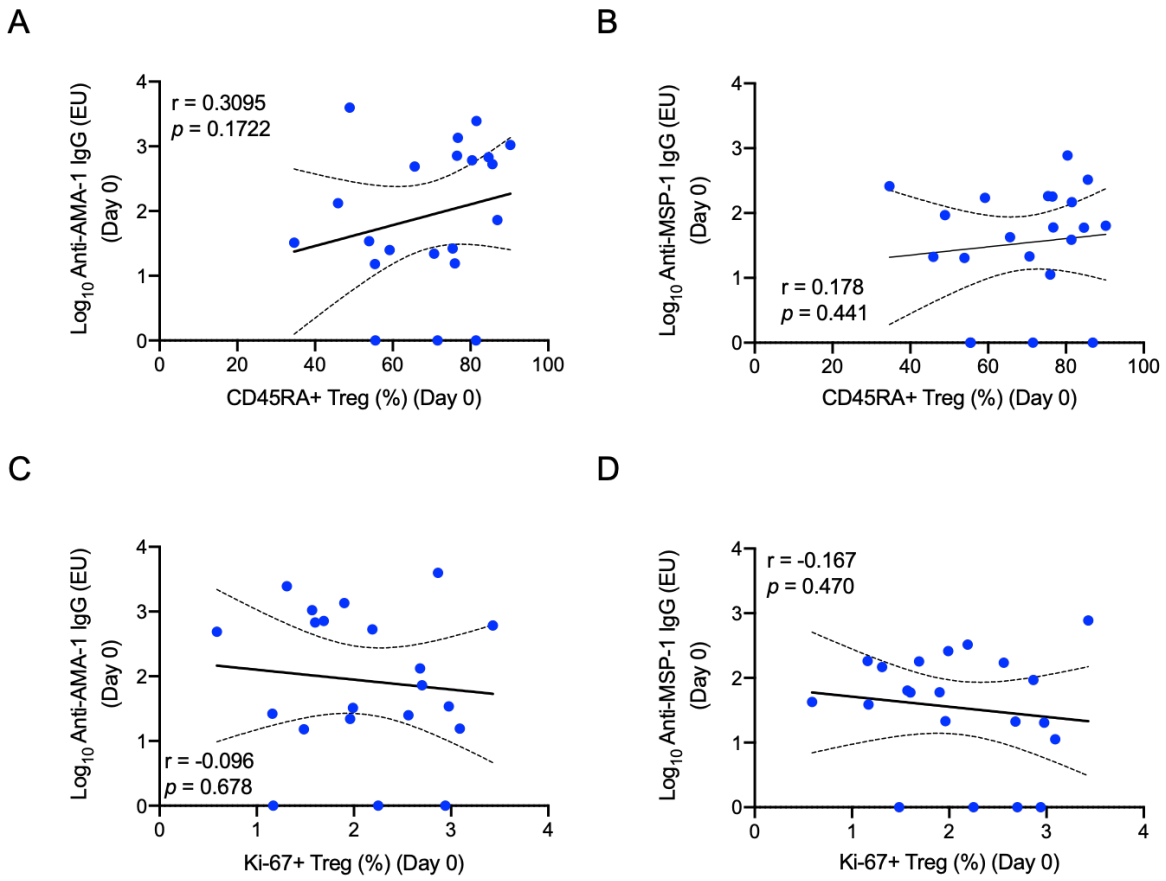

Figure 6.8: Association between anti-AMA-1 and anti-MSP-1 antibody titres and the frequency of Tregs expressing CD45RA and Ki-67 *Treg phenotype frequencies and IgG antibody titres against MSP-1 and AMA-1 measured at D0. Treg phenotype frequencies expressed as the proportion of total Tregs expressing either CD45RA or Ki-67.* ***(a)*** *anti-AMA-1 vs CD45RA+ Treg %,* ***(b)*** *anti-MSP-1 vs CD45RA+ Treg %,* ***(c)*** *anti-AMA-1 vs Ki-67+ Treg %,* ***(d)*** *anti-MSP-1 vs CKi-67+ Treg %. Associations measured by Spearman rho, no significant associations observed. n = 21 per graph.*

6.3.5. No association between total IgE concentration as a correlate of helminth exposure and vaccine immunogenicity.

Since the mechanisms by which malaria might suppress responses to vaccinations are most likely shared with different helminth infections, which are co-endemic in this study region, exposure to these pathogens was also investigated for their potential role in the suppression of vaccine-induced immunity in Burkinabe infants vaccinated with ChAd63 / MVA ME-TRAP. Since parasitological methods of determining helminth

infection status were not available in this retrospective study, Total plasma IgE concentrations were employed as a correlate of exposure. The overall geometric mean concentration of total IgE in plasma was 271.3 pg/ml [95% CI: 227.2 – 323.9, range: 78.13 – 4871] however there was also a significant age-related effect (Figure 6.9a). GMC in 5-8 month-olds was 154.2 pg/ml [95% CI: 119.6 – 198.8], 9-12 month-olds: 281.7 [219.6 – 361.4] and 13-17 month-olds: 477.5 [323.5 – 704.7]. There was no association with the frequency of Tregs at baseline and the concentration of total IgE in plasma at the same timepoint (Figure 6.9b).

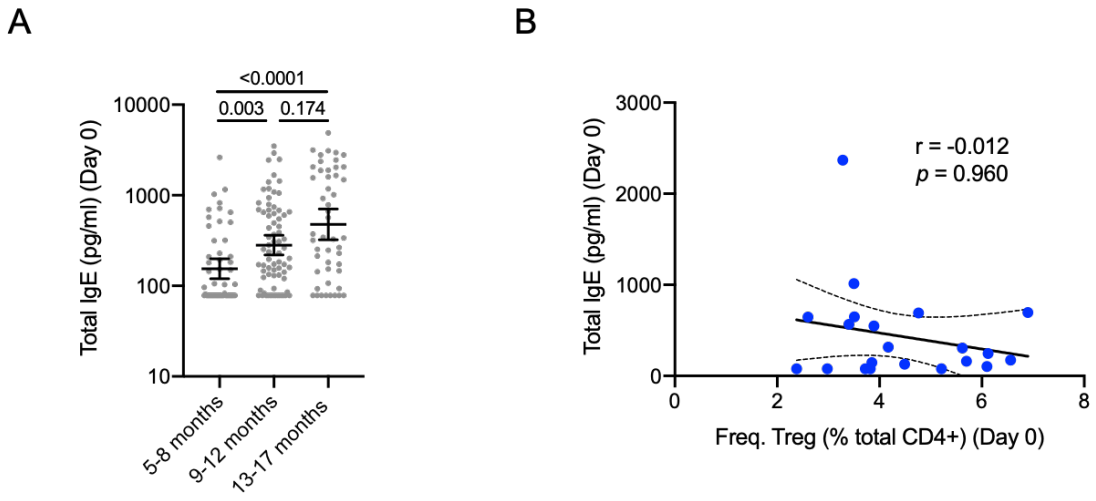

Figure 6.9: Total plasma IgE concentration associations with age and Treg frequency *Total plasma IgE concentration determined by ELISA and Treg frequency by flow cytometry at D0.* ***(a)*** *differences in IgE concentration between ages measured by Kruskal-Wallis with Dunn's correction for multiple comparisons. n = 60 per group.* ***(b)*** *association between total IgE concentration and Treg frequency measured by Spearman rho. n = 21.*

Next, total IgE concentrations were measured against vaccine immunogenicity following vaccination with ChAd63 / MVA ME-TRAP. There was no association between the concentration of total IgE at D0 and the peak cellular T cell ELISpot response at D63, when analysed either by Spearman rho [r = 0.075, *p* = 0.325] (Figure

6.10a) or Kruskal-Wallis based on total IgE concentration quartiles (Figure 6.10b). There was also no association between total IgE concentration and the antibody response to vaccination at D63 [Spearman rho = -0.123, p = 0.103] (Figure 6.10c and 6.10d).

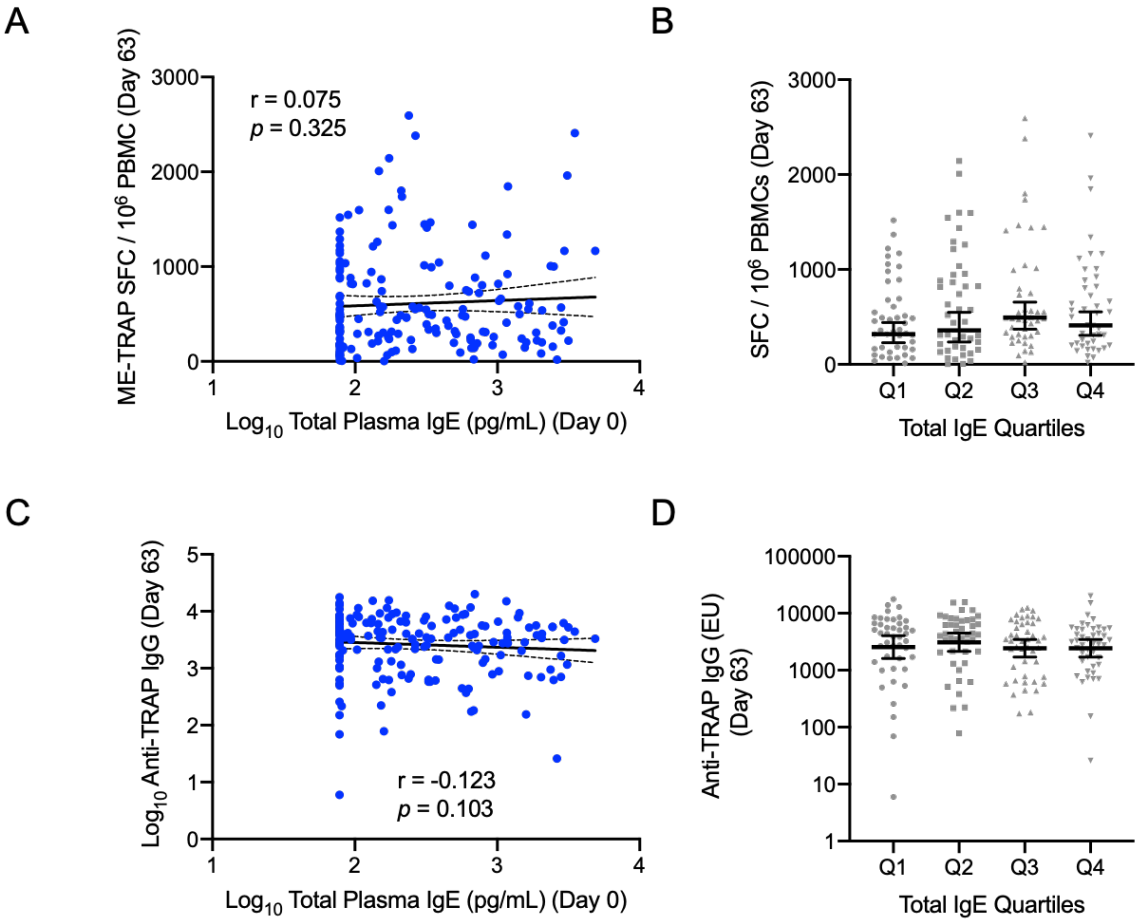

Figure 6.10: Association between total plasma IgE concentration and immunogenicity of ChAd63 / MVA ME-TRAP (a) *total IgE concentration at D0 versus the antigen-specific T cell ELISpot response to ME-TRAP after vaccination at D63.* ***(b)*** *antigen-specific T cell ELISpot response split into quartiles by total IgE concentration (Q1: lowest 25% total IgE concentration, Q4: highest 25%).* ***(c)*** *total IgE concentration at D0 versus the anti-ME-TRAP IgG response after vaccination at D63.* ***(d)*** *anti-ME-TRAP IgG response split into quartiles by total IgE concentration (Q1: lowest 25% total IgE concentration, Q4: highest 25%). Correlations tested by Spearman rho and comparisons between quartiles by Kruskal-Wallis with Dunn's correction for multiple comparisons (no significant differences observed). n = 182.*

6.3.6. No difference in transcriptional phenotype of Tregs between high and low vaccine responders

The transcriptional phenotype of Tregs sorted from PBMC of Burkinabe infants at D0 was measured by multiplex qPCR. PBMC samples from *n* = 21 randomly selected vaccinees were FACS sorted and 90 genes of interest were analysed and gene expression between samples measured as fold differences relative to the mean of all samples.

Sample quality control processes were performed as described previously in Chapter 2.5.2 and Chapter 4. Sample quality was found to be similar to that described in Chapter 4. Again Ubiquitin C and TATA box binding protein were excluded from the normalisation calculation as expression of these genes was not detected in all samples. No samples or genes of interest were removed entirely from analysis as there was no evidence of systemic reaction failures. Individual reactions were removed where there was evidence of non-specific amplification as described in 2.5.2.

Heat maps were firstly produced to observe qualitative differences in expression between genes and volunteers. Separate heat maps were produced with samples ordered by post-vaccination cellular and humoral responses to ME-TRAP. Figure 6.11 shows a heat map with samples ordered by the anti-TRAP IgG response. Qualitatively, the heat maps show that the majority of genes were expressed at similar levels between volunteers with Log_2 fold differences close to 0 indicating little deviation from the mean. Some genes showed greater variation in expression between samples,

[Log_2 FD range: 12.6 to -13], however there were no obvious differences between the low and high vaccine antibody responders.

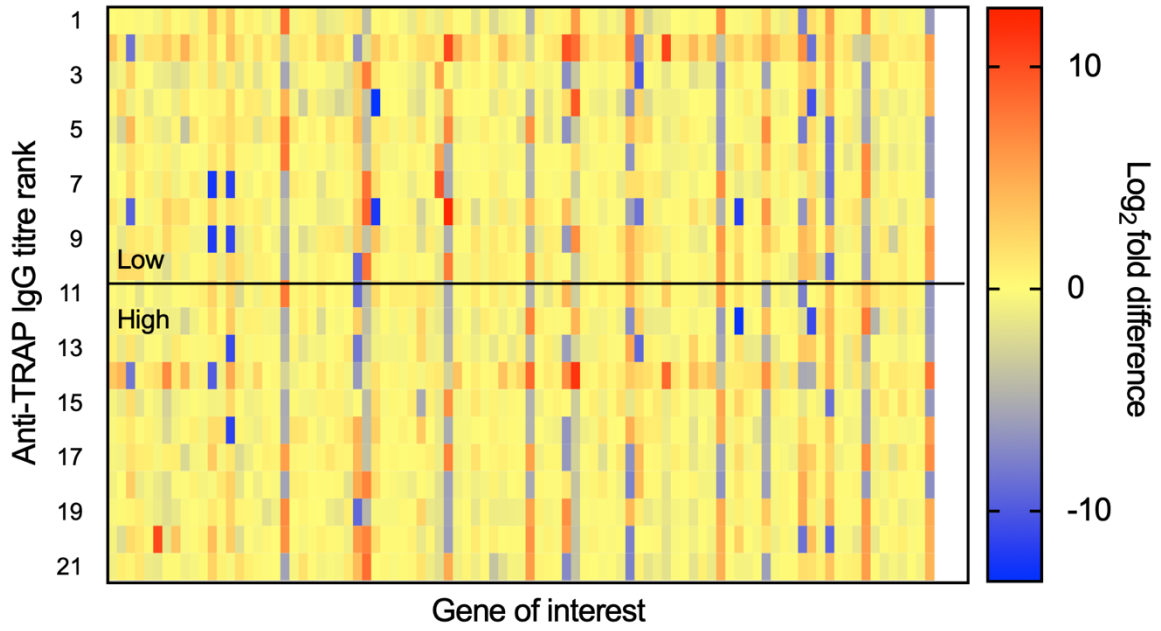

Figure 6.11: Heat map of gene expression in Tregs at D0 ordered by vaccine antibody response to ChAd63 / MVA ME-TRAP *Heat map representing the Log_2 fold difference in expression of a range of 90 Treg-associatied genes per individual relative to the mean expression across all individuals (n = 21). Volunteers are ranked along the y axis in order of their post-vaccination peak (D63) anti-TRAP IgG titre (where 1 is the lowest responder and 21 the highest). Volunteers were randomly selected and responses are representative of the range of responses in the parent cohort.*

Figure 6.12 shows a heatmap with samples ordered by ELISpot response to ME-TRAP. Again, there was no clear differences in gene expression in Tregs between those with high and low effector T cell responses to the vaccine antigen.

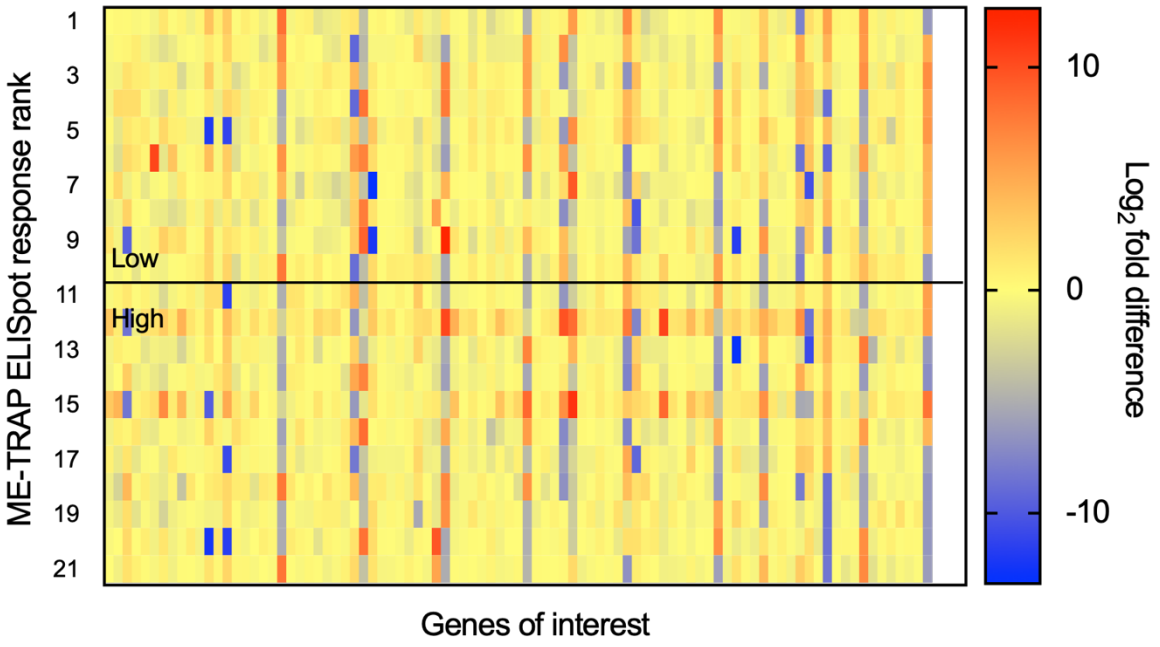

Figure 6.12: Heat map of gene expression in Tregs at D0 ordered by ELISpot response *Heat map representing the Log_2 fold difference in expression of a range of 90 Treg-associatied genes per individual relative to the mean expression across all individuals (n = 21). Volunteers are ranked along the y axis in order of their post-vaccination peak (D63) antigen-specific T cell response to ME-TRAP measured by ex vivo IFNγ ELISpot (where 1 is the lowest responder and 21 the highest). Volunteers were randomly selected and responses are representative of the range of responses in the parent cohort.*

Next, differential gene expression analysis was performed using the Limma package in R in order to identify any statistically significant differences in individual genes which might not have been obvious on the heatmaps. DGEA was performed twice for both T cell and antibody responses to vaccination, separating volunteers by high and low responses. A volcano plot stratified by high and low anti-TRAP IgG response is shown in Figure 6.13. This analysis identified two genes, IL-17F and CXCL13 which had lower expression in Tregs in the group which had higher antibody responses to vaccination. However when *p* values were adjusted by FDR, these results were not significant (Table 6.1).

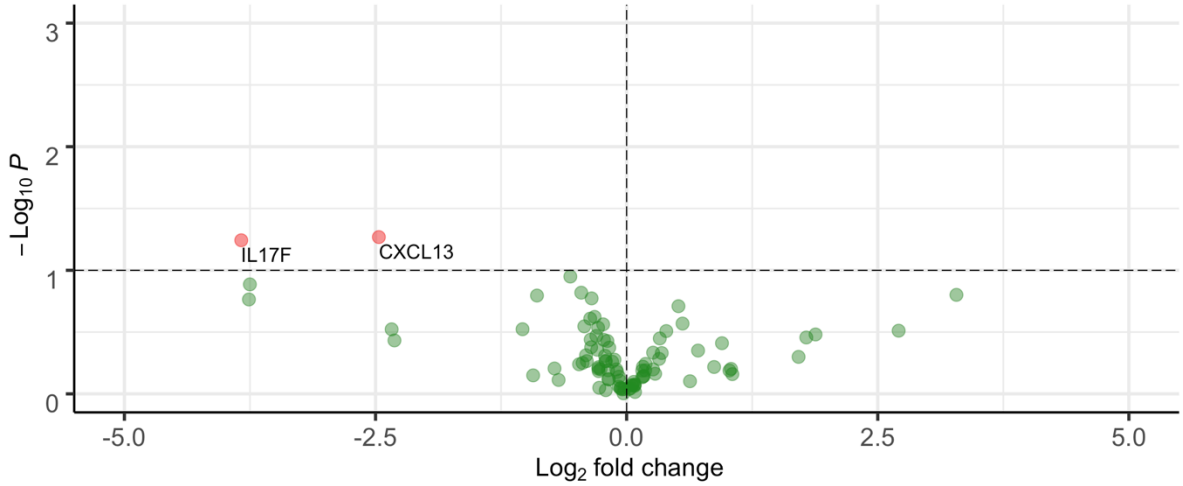

Figure 6.13: Volcano plot of differentially expressed Treg-associated genes between high and low antibody responders to ME-TRAP vaccination *Positive Log_2 fold change represents genes that were more highly expressed in Tregs in the group which had higher anti-TRAP IgG responses following vaccination (and vice versa for negative Log_2 FC). Cutoff for significant results was -Log_{10} P = 1.*

	Log_2 FC	*P. Value*	*adj. P. Val*
CXCL13	-2.466	0.053	0.950
IL17F	-3.836	0.057	0.950

Table 6.1: p values and adjusted p values for Treg genes flagged as differentially expressed between high and low antibody responders to ME-TRAP vaccination. *Adjustment made using the Benjamini-Hochberg procedure with an FDR of 5%.*

Differential gene expression analysis was repeated, but with samples stratified by high and low ELISpot response (Figure 6.14). This time, four Treg genes, PRDM1 (BLIMP-1), Granzyme B, Killer-like receptor B1 and Ki-67 were found to be upregulated in Tregs in the group with higher ELISpot responses. However again after FDR adjustment, these differences were not significant (Table 6.2).

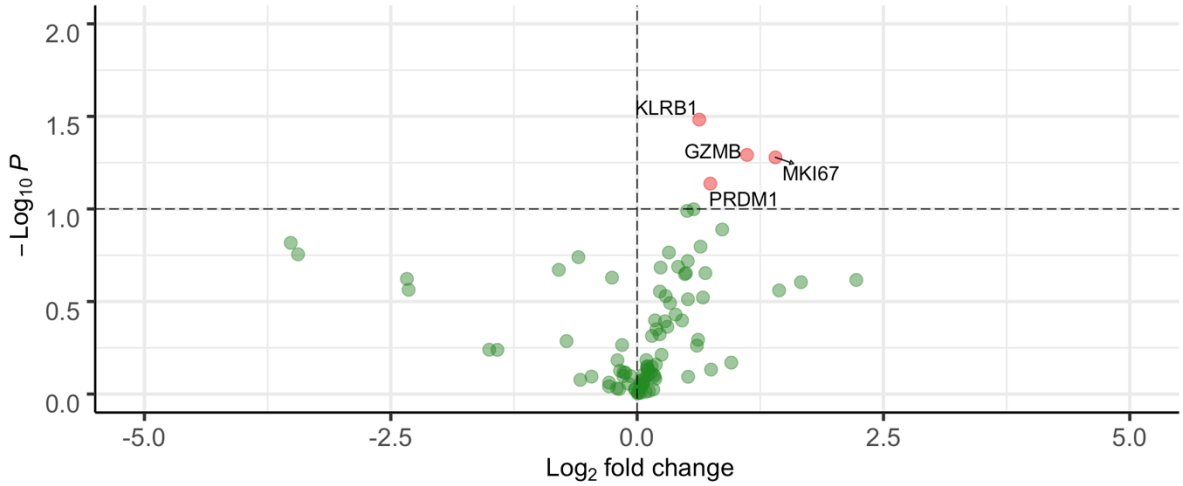

Figure 6.14: Differentially expressed Treg-associated genes between high and low T cell responders to ME-TRAP vaccination *Positive Log_2 fold change represents genes that were more highly expressed in Tregs in the group which had higher ELISpot responses following vaccination (and vice versa for negative Log_2 FC). Cutoff for significant results was -Log_{10} P = 1.*

	Log_{10} FC	*P. Value*	*adj. P. Val*
KLRB1	0.630	0.032	0.933
GZMB	1.114	0.051	0.933
MKI67	1.403	0.052	0.933
PRDM1	0.742	0.072	0.933

Table 6.2: p values and adjusted p values for Treg genes flagged as differentially expressed between high and low T cell responders to ME-TRAP vaccination. *Adjustment made using the Benjamini-Hochberg procedure with an FDR of 5%.*

Overall, this data does not show that the transcriptional phenotype of Tregs is different in infants who responded better to vaccination with ChAd63 / MVA ME-TRAP than those that responded worse.

6.3.7. No significant differences in Treg transcriptional signature when stratified by AMA-1 and MSP-1 titres

Since there were significant correlations between Treg frequency and IgG titres to MSP-1 and AMA-1 at D0 (Fig 6.7), it was investigated whether transcriptional differences in Tregs based on exposure intensity could be seen as well. Heatmaps were generated, this time ranking individuals by AMA-1 and MSP-1 IgG titre. Figure 6.15 shows the gene expression heatmap ordered by AMA-1 IgG titre and Figure 6.16 for MSP-1. Similarly to grouping by vaccine immunogenicity responses, the heatmaps do not show any obvious qualitative differences in Treg gene expression profile between individuals with high or low AMA-1 or MSP-1 antibody titres.

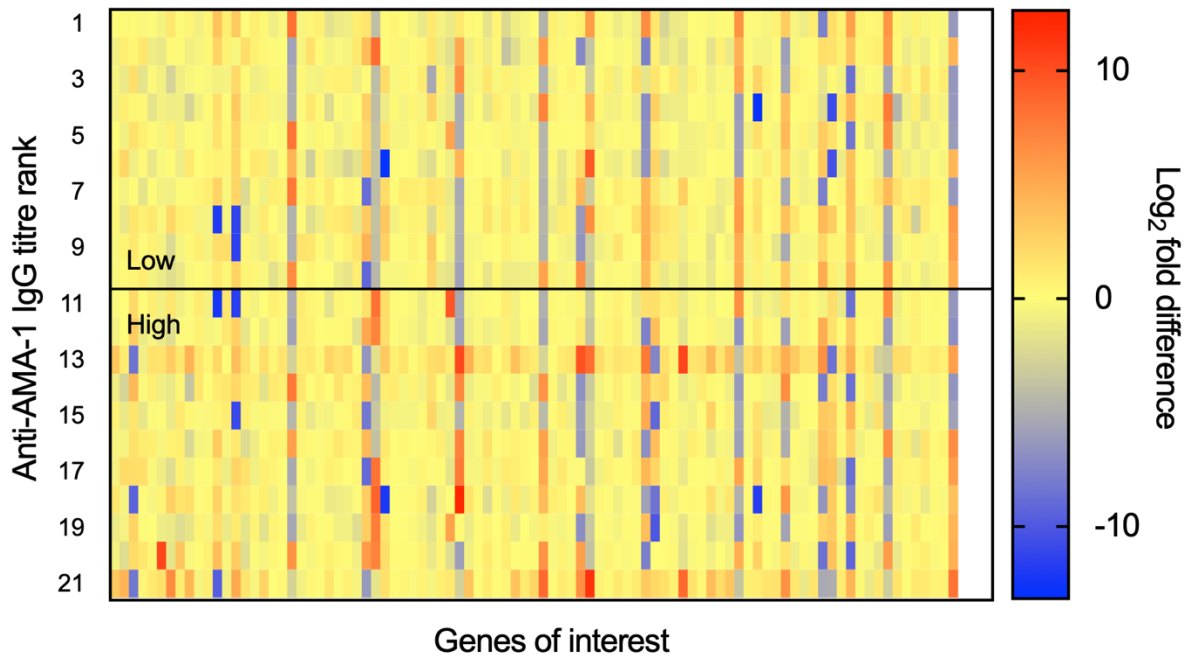

Figure 6.15: Heat map of gene expression in Tregs at D0 ordered by anti-AMA-1 IgG titre *Heat map representing the Log_2 fold difference in expression of a range of 90 Treg-associatied genes per individual relative to the mean expression across all individuals (n = 21). Volunteers are ranked along the y axis in order of their titre of IgG against AMA-1 at D0 (where 1 is the lowest titre and 21 the highest). Volunteers were*

randomly selected and titres are representative of the range of titres in the parent cohort.

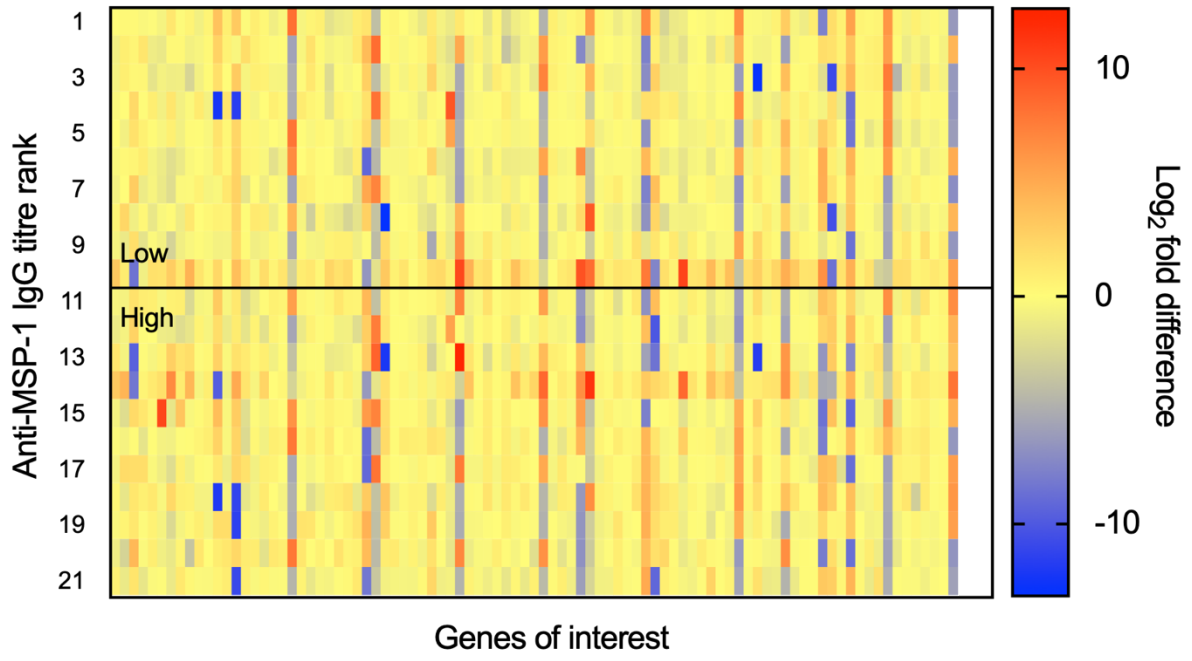

Figure 6.16: Heat map of gene expression in Tregs at D0 ordered by anti-MSP-1 IgG titre *Heat map representing the Log_2 fold difference in expression of a range of 90 Treg-associatied genes per individual relative to the mean expression across all individuals (n = 21). Volunteers are ranked along the y axis in order of their titre of IgG against MSP-1 at D0 (where 1 is the lowest titre and 21 the highest). Volunteers were randomly selected and titres are representative of the range of titres in the parent cohort.*

Differential gene expression analysis on Tregs using linear methods in the Limma package was then performed between volunteers with high and low titres of AMA-1 and MSP-1. Figure 6.17 shows the volcano plot for DGEA between high and low AMA-1 titre individuals. This analysis flagged 9 genes as being upregulated in individuals with high AMA-1 titres – LAG3, PDCD1 (PD-1), CXCR5, Ki-67, LAMP1, JAK3, CCL5, CCL6 and IL-21 and 3 genes which were downregulated – CCR2, CD274 (PDL1) and IFNγ. However none of the *p* values remained significant after adjustment (Table 6.3).

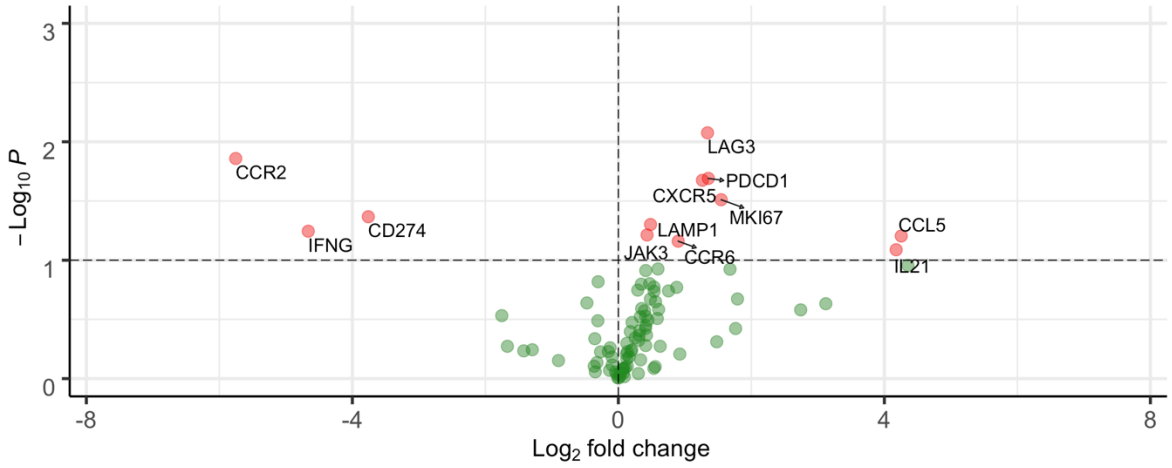

Figure 6.17: Differentially expressed Treg-associated genes between individuals with high and low titres of anti-AMA-1 IgG *Positive Log_2 fold change represents genes that were more highly expressed in Tregs in the group which had higher anti-AMA-1 IgG titres (and vice versa for negative Log_2 FC). Cutoff for significant results was $-Log_{10} P = 1$.*

	Log_{10} FC	*P. Value*	*adj. P. Val*
LAG3	1.341	0.008	0.481
CCR2	-5.754	0.014	0.481
PDCD1	1.353	0.020	0.481
CXCR5	1.264	0.021	0.481
MKI67	1.546	0.031	0.561
CD274	-3.760	0.043	0.568
LAMP1	0.484	0.050	0.568
IFNG	-4.663	0.057	0.568
JAK3	0.432	0.061	0.568
CCL5	4.254	0.062	0.568
CCR6	0.900	0.069	0.572
IL21	4.177	0.082	0.619

Table 6.3: p values and adjusted p values for Treg genes flagged as differentially expressed between individuals with high and low titres of anti-AMA-1 IgG. *Adjustment made using the Benjamini-Hochberg procedure with an FDR of 5%.*

When Treg gene expression was stratified by MSP-1 IgG titre (Figure 6.18), 3 genes were flagged as upregulated in the high titre MSP-1 group – LAG3, CXCR5 and CCR1 and 2 genes as downregulated – IFNγ and KLRB1. Again, all genes lost statistical significance following adjustment (Table 6.4).

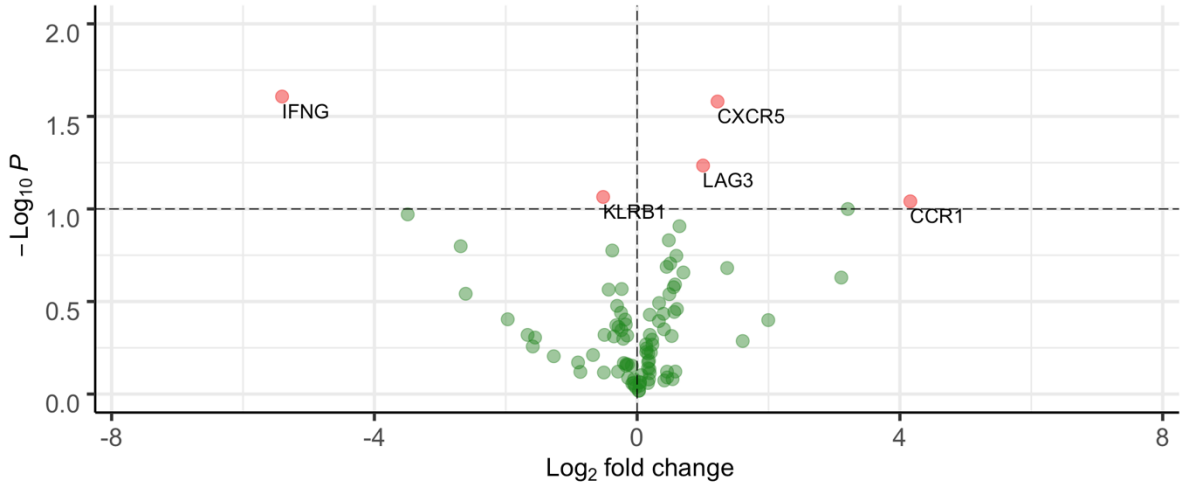

Figure 6.18: Differentially expressed Treg-associated genes between individuals with high and low titres of anti-MSP-1 IgG *Positive Log_2 fold change represents genes that were more highly expressed in Tregs in the group which had higher anti-MSP-1 IgG titres (and vice versa for negative Log_2 FC). Cutoff for significant results was $-Log_{10} P = 1$.*

	Log_2 FC	*P. Value*	*adj. P. Val*
IFNG	-5.405	0.025	0.928
CXCR5	1.224	0.026	0.928
LAG3	1.004	0.058	0.928
KLRB1	-0.517	0.086	0.928
CCR1	4.158	0.091	0.928

Table 6.4: p values and adjusted p values for Treg genes flagged as differentially expressed between individuals with high and low titres of anti-MSP-1 IgG. *Adjustment made using the Benjamini-Hochberg procedure with an FDR of 5%.*

From this data, there is no evidence that Treg phenotype differs between individuals with high and low IgG titres against MSP-1 and AMA-1.

6.4. Discussion

Malaria exposure has been shown to be associated with both the disruption of Treg homeostasis[207] and suppression of vaccine-induced immunity previously[161]. This chapter sought to understand whether these factors might be involved in the immune response to ChAd63 / MVA ME-TRAP in 5-17 month-old infant volunteers in Banfora, Burkina Faso. The overall prevalence of malaria in the community enrolled in the vaccine trial is very high, meaning these volunteers might have been susceptible to these mechanisms. Since malaria transmission hotspots[357,358] can cause the relative exposure intensity per individual to vary widely even within a single community, it is possible to investigate how differences in exposure are associated with different immunological outcomes to vaccination.

Gold standard methods of estimating an individual's exposure to malaria, such as calculating the entomological inoculation rate[364] is not possible in retrospect of the clinical trial, as was the case here. Therefore, serological correlates of exposure were evaluated for use, since these can be measured retrospectively requiring only a frozen serum or plasma sample. IgG antibodies against immunogenic and well studied blood-stage *P. falciparum* antigens AMA-1 and MSP-1 have been studied in detail previously and there is evidence that titres are proportional to the cumulative number of malaria episodes an individual has, meaning they correlate with exposure[359,365]. The dynamics of the IgG response to blood-stage antigens has been shown to be heterogeneous between individuals, with antibodies against AMA-1 seemingly requiring fewer infections to develop compared to MSP-1[365]. These factors can affect the suitability of each antigen for use as serological correlates of infection intensity. Considering the

high transmission rates in the study area, there is a chance that antibodies against AMA-1 might have saturated, skewing the distribution of data leftwards and limiting the ability to separate medium and highly exposed individuals. However given the young age of this cohort, the infants may not have had enough infections for this to have happened. Since antibodies against MSP-1 are more difficult to generate, it might have been possible that many younger individuals were IgG-negative despite having been exposed previously. Considering these factors, it was unknown which antigen would be the best correlate of exposure in this cohort, therefore both were measured.

To decide the appropriateness of IgG responses against AMA-1 and MSP-1 for use as serological correlates of malaria exposure, the distributions of data for each were assessed. Although the data were not normally distributed for either antigen, the responses looked to be neither saturated, nor were there a disproportionate number of individuals negative for one antigen over the other. Either of these scenarios would have over- or under-estimated the intensity of exposure to malaria respectively. It was then decided that both AMA-1 and MSP-1 IgG responses would be taken forward and used for correlations with vaccine immunogenicity readouts and Treg activity and the data between the two compared.

The only significant association between malaria exposure and vaccine immunogenicity was between anti-AMA-1 titre and the ME-TRAP-specific cellular response measured by ELISpot. There were no associations with AMA-1 and vaccine antibody responses or between MSP-1 and either cellular or humoral vaccine immunogenicity. The disparity between anti-AMA-1 and anti-MSP-1 IgG titres with respect to their associations with cellular vaccine responses might be explained by

differences in the dynamics of acquisition and retention of these antibodies following natural infection. Anti-MSP-1 antibodies are thought to be extremely durable whilst the longevity of anti-AMA-1 IgG is thought to be more moderate[359]. The major immunosuppressive mechanisms induced by malaria infection are most likely relatively short-lived[105] in comparison to the durability of antibodies, therefore a more short-lived antibody response which is reflective of more recent infection is likely to better correlate with these malaria-induced immunosuppressive mechanisms. This could be confirmed in further experiments by analysing relationships between anti-AMA-1 & MSP-1 titres and Treg frequencies between high and low malaria transmission seasons.

Anti-AMA-1 IgG titres were not associated with humoral vaccine immunogenicity in the study presented in this chapter. The findings in Chapter 5.3.8 that Burkinabe infant antibody titres to ME-TRAP were higher than in UK adults might suggest that the potency of the infant humoral response is reactive enough to overcome the immunosuppressive effects of malaria exposure, or it could suggest that malaria-mediated immunosuppression has less of an effect on the humoral arm over the T cell arm. Increased antibody responses in infants have been observed for other vaccines such as those against HIV[366] which is likely to be caused by the contrasting functionality of the immature infant immune system over adults[367]. To understand if there might be a relationship in adults between antibody responses and malaria exposure would require repeating this study in a population also exposed to malaria at a similarly high intensity. Unfortunately vaccination of adults with ChAd63 / MVA ME-TRAP has not been carried out in Banfora, Burkina Faso or any other site with such high transmission intensity, so this was not possible.

Similarly to the results presented here, a previous study[368] found that cellular responses measured by ELISpot were reduced following ME-TRAP vaccination in children aged 1-6 years in Kilifi, Kenya who had microscopy-detectable parasitaemia at basline. These individuals received a previous iteration of the ME-TRAP vaccine where the prime dose was encoded in a fowlpox vector instead of ChAd63. This study did not measure TRAP antibody responses so it is not possible to determine if this data would be comparable to ours as well. Patent parasitaemia at the time of vaccination has previously been associated with the suppression of antibody responses in children to some polysaccharide-based vaccines, such as the group C meningococcal vaccine[369,370], whilst little evidence exists for malarial suppression of protein-based vaccines[161] (see section 1.6.1). Polysaccharide antigens are largely T-independent antigens, meaning B cell responses do not require T cell help. The hypothesis from this might be that malaria-driven immunosuppression has a greater effect on B cells when they are not receiving T cell help. Similarly to protein-in-adjuvant vaccines, viral vectored vaccines are T-dependent antigens, so this finding fits with existing literature. However, in the study presented here, as well as in the previous ME-TRAP study[368], reduced T cell responses were associated with malaria exposure. Aside from these two studies, no other T cell inducing vaccines have been tested for their associations with malaria exposure. Further data might contextualise these findings and provide insight into the mechanism behind malaria-driven suppression of vaccine responses. More work needs to be done to understand the mechanism underlying why malaria infection might affect T cell function but not B cell function in the context of viral vectored vaccines. The potential role for Tregs in this mechanism will be discussed in chapter 7 as results from chapters 5 and 6 are consolidated.

Previous studies have shown that Treg frequencies increase following malaria infection[105], therefore this study investigated whether increased Treg activity in this cohort might contribute to increased suppression of responses to ChAd63 / MVA ME-TRAP. However a negative correlation between Treg frequency and both AMA-1 and MSP-1 titre was observed, although the association with MSP-1 was only marginally significant. This is similar to the findings in Chapter 3 between Treg frequency and anti-schizont antibody titres in Kenyan adults. This might suggest that Treg frequencies actually decline with exposure to malaria or that Tregs limit the acquisition of anti-malarial antibodies at higher frequencies. Given the young age of these infants and the small age interval from 5-17 months, it might be too short a time for such a dramatic alteration of Treg homeostasis to occur because of malaria exposure, making it seem more likely that Tregs might be limiting acquisition of anti-malarial antibodies. This is a limitation of using an immunological correlate of exposure to draw associations with other immune parameters since confounding interactions are a possibility. Estimating malaria exposure intensity is best done using entomological inoculation rates or by active monitoring. A future vaccine clinical trial should integrate these methods into its design so that malaria-driven immunosuppression of vaccine responses can be investigated in more detail.

It was necessary to determine the interactions between helminth infection and vaccine immunogenicity and Treg activity as well, since helminths and *P. falciparum* are thought to share many of the same immunomodulatory mechanisms[261,271]. *P. falciparum* and helminths are co-endemic in the study region[360]. Helminths are a diverse group of pathogens and due to their neglected status, serological diagnostic assays are not available for many of them. Instead of measuring exposure to a limited

set of helminths, this study used total plasma IgE concentrations as a broad correlate of helminth exposure. In a setting such as Burkina Faso where allergy and autoimmune conditions are a rare occurrence, total IgE is a useful correlate of helminth exposure[363]. This study found no associations between total IgE and vaccine immunogenicity or Treg frequency. This gives greater confidence over the interactions observed between malaria exposure and vaccine immunogenicity or Treg activity. The prevalence of helminth infection peaks in primary school-aged children[272], much older than our 5-17 month-old cohort. On the other hand, malaria infection, particularly clinical illness, is most prevalent in our age group. It is therefore expected that malaria is of greater relevance to vaccine immunosuppression than helminths in 5-17 month-olds. Different helminths also have different pathogenic mechanisms[371] and therefore potentially different immunomodulatory effects. Grouping all helminth infections together by measuring total IgE concentrations may miss some of the heterogeneity between different helminth species. Assessing exposure to different helminths is the most ideal option, but would only be possible when better serological diagnostic assays become available for these infections.

Finally, the transcriptional phenotype of Tregs was investigated through multiplex qPCR. There was generally very little differential expression between bulk Treg samples from different individuals. Differential gene expression analysis did not reveal any significantly differently expressed genes between individuals that responded better or worse, in terms of either cellular or humoral responses, to vaccination with ChAd63 / MVA ME-TRAP. This may not be surprising since no relationship was found between Treg frequency and vaccine immunogenicity either. There was also no difference in Treg transcriptional phenotype between individuals with high or low titres

of IgG against AMA-1 and MSP-1. Considering that associations were seen between the frequency of Tregs and both vaccine immunogenicity and anti-AMA-1/MSP-1 IgG titres, this might suggest that any effect exerted by Tregs on vaccine or anti-malarial immunological responses is largely dependent on the number of Tregs rather than differences in the activity of individual Tregs. However it is important to acknowledge that power to detect differences may have been limited by the small sample size analysed here and a larger cohort may have yielded different results. There may be differences in the phenotype of only certain subsets of Tregs which would be masked by bulk cell transcriptional analysis. Therefore single cell analysis might also be recommended for future studies.

6.5. Conclusions

This chapter found an association between exposure to malaria estimated by anti-AMA-1 IgG titres and cellular vaccine immunogenicity in Burkinabe infants. Anti-AMA-1 and MSP-1 antibody titres were negatively associated with Treg frequency – the first such study to do this analysis to our knowledge. No associations were observed between helminth exposure measured by total IgE concentration and vaccine immunogenicity or Treg frequency. No differences in Treg transcriptional phenotype were observed between high and low vaccine responders or between individuals with high and low titres of antibodies against blood-stage malaria antigens. Combined with the data from Chapter 5, it is clear that the interactions between vaccine responses, malaria exposure and Treg activity are complex and these will be discussed and summarised in greater detail in Chapter 7.

Future analyses should utilise different methods of estimating exposure to malaria in vaccine cohorts, such as active case detection instead of serological methods which might be causally linked with other immunological readouts. These would provide better certainty over determining the interactions between malaria exposure and either vaccine immunogenicity or Treg activity.

Chapter 7

7. Conclusions and future directions

7.1. Overview

This thesis investigated two themes – the role of Tregs in immunity to malaria and in response to vaccination. We know relatively little about either and increasing our understanding in these areas will inform the design of better vaccines against malaria. The work presented here confirms the involvement of Tregs in both processes and provides a basis upon which functional mechanisms can be studied. It also highlights the differences in responses observed between malaria-naïve and malaria-exposed populations, underlining the need to continue to carry out studies in malaria-endemic regions where data will be relevant to target populations for vaccination.

The key findings in each theme are discussed and contextualised below.

7.2. Summary of main findings, implications and recommendations

7.2.1. Regulatory immune responses to CHMI

Chapters 3 and 4 explored pro- and anti-inflammatory cytokine responses, regulatory T cell responses and effector CD4+ T cell responses to CHMI semi-immune Kenyan adults using immune phenotyping techniques including ELISA and flow cytometry as well as multiplex qPCR transcriptomics.

To summarise the findings of this work – there was an absence of a detectable inflammatory cytokine response to CHMI, even in individuals with parasitaemia levels where detectable cytokine concentrations would be expected in malaria-naïve individuals[114]. This may be reflective of a mechanism to control the inflammatory immune response in malaria-exposed individuals to prevent pathology. Pro-inflammatory responses detected at baseline did not predict parasite growth outcome following CHMI. Only one cytokine, IL-10, was significantly upregulated by blood stage parasite growth compared to baseline and this was restricted to the treated group, suggesting the potential involvement of regulatory immune mechanisms in susceptibility to infection.

Analysis of Treg responses by flow cytometry showed greater upregulation in cell number following CHMI in individuals with more-protective parasite growth outcomes. The largest Treg response was in the highly immune group, meaning it occurred in the absence of detectable parasitaemia. The accumulating Tregs appeared to be mostly of a naïve phenotype and formed without evidence of recent proliferation. This fits with existing literature suggesting Tregs accumulate during malaria infection through

conversion from naïve effector CD4+ T cells[111]. Overall the data suggests that if these Tregs are functional, they may be contributing to the control of inflammation and parasitaemia in highly immune individuals. These findings contradict those of Walther *et al*[113] who reported Treg activity to positively correlate with parasite growth rates in malaria-naïve individuals.

Effector CD4+ T cell responses did not seem to be associated with parasite growth outcome, either by phenotyping of PBMC or in *in vitro* proliferation assays. Transcriptomic analysis appeared to support these findings with PCA showing that Treg but not Teff phenotype differed between parasite growth outcome groups. DGEA did not reliably identify individual genes which may underlie the heterogeneity in Treg phenotype. Therefore, although this work does suggest that Tregs might contribute to determining parasite growth outcomes following CHMI, the mechanisms by which they act remain to be determined. Future work could involve investigating some of the mechanisms potentially flagged by DGEA, such as the activity of, and cellular responsivity to, chemokines. Optimising transcriptomic methods, such as through using single cell technologies or enriching antigen-specific or responsive cells to CHMI should also be considered.

Other interesting research questions were generated from this data which should also be investigated. These include investigating the effect of age on Treg dynamics and immune senescence in malaria-endemic settings and the role of co-infection with chronic viral or parasite infections on parasite growth outcomes following CHMI.

Using CHMI to investigate NAI offers numerous advantages over cross-sectional methods. However, it still has some limitations which are important to acknowledge to contextualise this data. Firstly, the parasite used for challenge is a laboratory-reared strain called Nf54. *P. falciparum* isolates have extreme genetic diversity which has implications for the adaptive immune responses the individuals acquire through exposure to different isolates. Using a single strain does not account for differences in strain-specific immunity. The strain was originally isolated from a patient in The Netherlands in the 1970s[372] and genomic analysis suggests it to be of African origin, most likely West African[373]. It may not be representative of strains naturally circulating in Kenya today to which volunteers have exposure. It is also likely that immune responses to malaria are highly heterogeneous between individuals, even against a single parasite strain due to numerous factors including host genetics and co-infection status. Although this study had one of the largest samples of any CHMI study undertaken today, it still may be insufficiently powered to detect meaningful differences.

It is likely that numerous mechanisms and immune subsets each contribute to pathologic and parasite growth outcomes following CHMI. It is important that the immune response to malaria is viewed holistically. The work presented in this thesis is part of a larger body of work looking at other aspects of the immunity to infection, including antibody, B cell and innate immune responses to CHMI. These data should eventually be considered in association with each other to build a unified evidence base determining which immune phenotypes are protective and non-protective.

7.2.2. The role of Tregs and malaria exposure on the immunogenicity of ChAd63 / MVA ME-TRAP

Chapters 5 and 6 focussed on investigating associations between Treg activity, malaria exposure and immunogenicity of the experimental pre-erythrocytic vaccine against malaria, ChAd63 / MVA ME-TRAP in an adult and a malaria-exposed infant cohort. Humoral and cellular vaccine immunogenicity was measured by ELISA and ELISpot respectively, Treg activity was measured by baseline phenotyping and in an antigen-specific stimulation assay and malaria exposure was estimated using serological correlates against blood stage *P. falciparum* antigens. Tregs were also transcriptionally phenotyped at baseline in the infant cohort using the method developed in chapter 4.

In brief, this work found a negative relationship between Treg frequencies at baseline and peak humoral immunogenicity to ChAd63 / MVA ME-TRAP in UK adults. There was also a trend towards a negative relationship for ELISpot responses, however this was not significant. Both relationships were replicated in an adult vaccine trial cohort in Dakar, Senegal receiving an analogous viral vectored vaccine against the Ebola virus glycoprotein. However, in 5-17 month-old infants living in an area of high malaria transmission in Burkina Faso, there were no relationships between Treg frequency and either ELISA or ELISpot responses to vaccination with ChAd63 / MVA ME-TRAP.

When malaria exposure was factored in, there was an association between higher anti-AMA-1 titres and lower T cell responses to vaccination by ELISpot in Burkinabe

infants. Treg frequency was also strongly negatively associated with anti-AMA-1 antibody titre. This raises two possibilities; that either the relationship between Treg frequency and vaccine immunogenicity differs in infants, or it differs in populations where Treg homeostasis has been perturbed by malaria exposure. To establish which might be true, it would be necessary to repeat the analysis in malaria-unexposed infants and malaria-exposed adults. ChAd63 / MVA ME-TRAP has not been tested in heavily-exposed adults, but samples from a smaller cohort of Gambian infants, who are estimated to have very low malaria exposure, are available for further analysis.

Overall this data does not support the hypothesis that malaria exposure might drive inflation of Treg frequencies which in turn contribute to suppressed vaccine responses. However, it does still provide evidence of interesting relationships between malaria exposure and Treg activity on vaccine immunogenicity when the two factors are considered separately in different populations.

This work also revealed that antigen-specific Tregs were induced by vaccination in UK adults against the ME-TRAP insert and the MVA vector, but not ChAd63. These responses did not appear to correlate with effector vaccine immunogenicity. Transcriptomic analysis of Tregs prior to vaccination in Burkinabe infants did not reveal any significant differences, either between high and low vaccine responders or individuals with high and low malaria exposure.

Improvements in malaria vaccination immunogenicity need to be made to achieve improvements in field efficacy. Depending on the context, this work shows that reducing the impact of either Tregs or malaria exposure may be helpful. Modulating

Treg activity is a theoretical possibility – anti-CD25 mAbs like Daclizumab and drugs which deplete Tregs such as cyclophosphamide are available which have been shown to be useful in improving the immunogenicity of viral vectors and numerous cancer vaccines in mouse studies[356,374]. But it is difficult to conceive how treatments which so dramatically skew immune homeostasis would be practical or indeed safe when used in low-resource clinical settings in developing countries. However, considering the findings in this study were correlative, a clinical trial administering a Treg-suppressing therapy alongside ChAd63 / MVA ME-TRAP in a controlled clinical setting could prove a functional relationship.

To address the problem of malaria related immunosuppression, administering vaccines under the cover of malarial chemoprophylaxis could be beneficial. Studies have shown that deworming with albendazole in Indonesian children resulted in improved inflammatory responses to heterologous antigens in vaccines[270], so a similar effect could be seen with malaria.

7.3. Final remarks

A highly efficacious vaccine against *P. falciparum* remains to be developed. The host-parasite interactions occurring during malaria infection are exceptionally complex in comparison to other infectious diseases. Some of the lack of progress in vaccine development can be owed to difficulties the field has faced in understanding these complex mechanisms. This thesis has described some findings which contradict each other or are difficult to contextualise with existing literature. The complexity of the immune response to malaria is a challenge and can frustrate efforts to study it. Nevertheless, research like this is important and contributes to a growing body of evidence which together may eventually contribute to the development of a highly efficacious malaria vaccine. This thesis provides a novel contribution to the expanding literature. In the future, it will be exciting to see how advanced methods of investigating human immune responses, such as CHMI and experimental interventional arms of clinical vaccine trials can be utilised to provide answers to outstanding questions in malaria immunology.

Chapter 8

8. References

1. World Health Organisation. World Malaria Report. (2018). Available at: http://www.who.int/malaria/publications/world-malaria-report-2018/en/. (Accessed: 30th June 2019)
2. Miller, L. H., Ackerman, H. C., Su, X. & Wellems, T. E. Malaria biology and disease pathogenesis: insights for new treatments. *Nat. Med.* **19**, 156–167 (2013).
3. World Health Organisation. The top 10 causes of death. (2014). Available at: https://www.who.int/news-room/fact-sheets/detail/the-top-10-causes-of-death. (Accessed: 30th June 2019)
4. Alkema, L., Chao, F., You, D., Pedersen, J. & Sawyer, C. C. National, regional, and global sex ratios of infant, child, and under-5 mortality and identification of countries with outlying ratios: a systematic assessment. *Lancet Glob. Heal.* **2**, e521–e530 (2014).
5. Snow, R. W. & Omumbo, J. A. *Malaria*. *Disease and Mortality in Sub-Saharan Africa* (The International Bank for Reconstruction and Development / The World Bank, 2006).
6. Flaxman, A. D. *et al.* Rapid Scaling Up of Insecticide-Treated Bed Net Coverage in Africa and Its Relationship with Development Assistance for Health: A Systematic Synthesis of Supply, Distribution, and Household Survey Data. *PLoS Med.* **7**, e1000328 (2010).
7. World Health Organisation. Seasonal malaria chemoprevention with sulfadoxine-pyrimethamine plus amodiaquine in children: A field guide. (2013).

Available at: https://www.who.int/malaria/publications/atoz/9789241504737/en/. (Accessed: 30th July 2019)

8. World Health Organisation. Intermittent preventive treatment in pregnancy (IPTp). (2018). Available at: https://www.who.int/malaria/areas/preventive_therapies/pregnancy/en/. (Accessed: 30th July 2019)
9. Bhatt, S. *et al.* The effect of malaria control on Plasmodium falciparum in Africa between 2000 and 2015. *Nature* **526**, 207–211 (2015).
10. Griffin, J. T. *et al.* Reducing Plasmodium falciparum Malaria Transmission in Africa: A Model-Based Evaluation of Intervention Strategies. *PLoS Med.* **7**, e1000324 (2010).
11. Coetzee, M., Craig, M. & le Sueur, D. Distribution of African malaria mosquitoes belonging to the Anopheles gambiae complex. *Parasitol. Today* **16**, 74–7 (2000).
12. Centers for Disease Control and Prevention. Malaria - About Malaria - Biology. (2019). Available at: https://www.cdc.gov/malaria/about/biology/index.html. (Accessed: 1st July 2019)
13. Autino, B., Corbett, Y., Castelli, F. & Taramelli, D. Pathogenesis of malaria in tissues and blood. *Mediterr. J. Hematol. Infect. Dis.* **4**, e2012061 (2012).
14. Ali, H. *et al.* Parasite density and the spectrum of clinical illness in falciparum malaria. *J. Coll. Physicians Surg. Pak.* **18**, 362–8 (2008).
15. Chen, I. *et al.* “Asymptomatic” Malaria: A Chronic and Debilitating Infection That Should Be Treated. *PLoS Med.* **13**, (2016).
16. Bartoloni, A. & Zammarchi, L. Clinical aspects of uncomplicated and severe malaria. *Mediterr. J. Hematol. Infect. Dis.* **4**, e2012026 (2012).
17. Perkins, D. J. *et al.* Severe Malarial Anemia: Innate Immunity and Pathogenesis. *Int. J. Biol. Sci.* **7**, 1427–1442 (2011).
18. Storm, J. & Craig, A. G. Pathogenesis of cerebral malaria--inflammation and cytoadherence. *Front. Cell. Infect. Microbiol.* **4**, 100 (2014).
19. Centers for Disease Control and Prevention. Malaria - About Malaria - Disease. (2019). Available at: https://www.cdc.gov/malaria/about/disease.html. (Accessed: 1st July 2019)
20. Clark, I. A., Budd, A. C., Alleva, L. M. & Cowden, W. B. Human malarial

disease: a consequence of inflammatory cytokine release. *Malar. J.* **5**, 85 (2006).

21. Clark, I. A. & Rockett, K. A. The cytokine theory of human cerebral malaria. *Parasitol. Today* **10**, 410–2 (1994).
22. Griffin, J. T. *et al.* Gradual acquisition of immunity to severe malaria with increasing exposure. *Proc Biol Sci* **282**, 20142657 (2015).
23. Ademolue, T. W. & Awandare, G. A. Evaluating antidisease immunity to malaria and implications for vaccine design. *Immunology* **153**, 423–434 (2018).
24. Fleischer, B. Editorial: 100 years ago: Giemsa's solution for staining of plasmodia. *Trop. Med. Int. Heal.* **9**, 755–756 (2004).
25. Wongsrichanalai, C., Barcus, M. J., Muth, S., Sutamihardja, A. & Wernsdorfer, W. H. *A Review of Malaria Diagnostic Tools: Microscopy and Rapid Diagnostic Test (RDT)*. (2007).
26. Krampa, F. D., Aniweh, Y., Awandare, G. A. & Kanyong, P. Recent Progress in the Development of Diagnostic Tests for Malaria. *Diagnostics (Basel, Switzerland)* **7**, (2017).
27. Hermsen, C. C. *et al.* Detection of Plasmodium falciparum malaria parasites in vivo by real-time quantitative PCR. *Mol Biochem Parasitol* **118**, 247–251 (2001).
28. World Health Organisation. Guidelines for the treatment of malaria. (2015). Available at: https://www.who.int/malaria/publications/atoz/9789241549127/en/. (Accessed: 25th July 2019)
29. Cui, L., Mharakurwa, S., Ndiaye, D., Rathod, P. K. & Rosenthal, P. J. Antimalarial Drug Resistance: Literature Review and Activities and Findings of the ICEMR Network. *Am. J. Trop. Med. Hyg.* **93**, 57–68 (2015).
30. Hamilton, W. L. *et al.* Evolution and expansion of multidrug-resistant malaria in southeast Asia: a genomic epidemiology study. *Lancet Infect. Dis.* **0**, (2019).
31. Prame Kumar, K., Nicholls, A. J. & Wong, C. H. Y. Partners in crime: neutrophils and monocytes/macrophages in inflammation and disease. *Cell Tissue Res.* **371**, 551–565 (2018).
32. Amulic, B., Cazalet, C., Hayes, G. L., Metzler, K. D. & Zychlinsky, A. Neutrophil Function: From Mechanisms to Disease. *Annu. Rev. Immunol.* **30**, 459–489 (2012).

33. Gordon, S. & Plüddemann, A. Tissue macrophages: heterogeneity and functions. *BMC Biol.* **15**, 53 (2017).
34. Mogensen, T. H. Pathogen recognition and inflammatory signaling in innate immune defenses. *Clin. Microbiol. Rev.* **22**, 240–73 (2009).
35. Flannagan, R. S., Heit, B. & Heinrichs, D. E. Antimicrobial Mechanisms of Macrophages and the Immune Evasion Strategies of Staphylococcus aureus. *Pathog. (Basel, Switzerland)* **4**, 826–68 (2015).
36. Götz, A. *et al.* Innate Immunity to Malaria. in *Malaria* 3–25 (Springer International Publishing, 2017). doi:10.1007/978-3-319-45210-4_1
37. Couper, K. N. *et al.* Macrophage-Mediated but Gamma Interferon-Independent Innate Immune Responses Control the Primary Wave of Plasmodium yoelii Parasitemia. *Infect. Immun.* **75**, 5806–5818 (2007).
38. Abdalla, S. H. Peripheral blood and bone marrow leucocytes in Gambian children with malaria: numerical changes and evaluation of phagocytosis. *Ann. Trop. Paediatr.* **8**, 250–8 (1988).
39. Mahanta, A., Kar, S. K., Kakati, S. & Baruah, S. Heightened inflammation in severe malaria is associated with decreased IL-10 expression levels and neutrophils. *Innate Immun.* **21**, 546–552 (2015).
40. Tangteerawatana, P., Krudsood, S., Kanchanakhan, N., Troye-Blomberg, M. & Khusmith, S. Low monocyte to neutrophil ratio in peripheral blood associated with disease complication in primary Plasmodium falciparum infection. *Southeast Asian J. Trop. Med. Public Health* **45**, 517–30 (2014).
41. Feintuch, C. M. *et al.* Activated Neutrophils Are Associated with Pediatric Cerebral Malaria Vasculopathy in Malawian Children. *MBio* **7**, e01300-15 (2016).
42. Steinman, R. M. Decisions About Dendritic Cells: Past, Present, and Future. *Annu. Rev. Immunol.* **30**, 1–22 (2012).
43. Bettiol, E., Van De Hoef, D. L., Carapau, D. & Rodriguez, A. Efficient phagosomal maturation and degradation of Plasmodium-infected erythrocytes by dendritic cells and macrophages. *Parasite Immunol.* **32**, 389–398 (2010).
44. Miller, J. L., Sack, B. K., Baldwin, M., Vaughan, A. M. & Kappe, S. H. I. Interferon-Mediated Innate Immune Responses against Malaria Parasite Liver Stages. *Cell Rep.* **7**, 436–447 (2014).
45. Artavanis-Tsakonas, K. *et al.* Activation of a Subset of Human NK Cells upon

Contact with *Plasmodium falciparum* -Infected Erythrocytes. *J. Immunol.* **171**, 5396–5405 (2003).

46. Roussilhon, C., Agrapart, M., Ballet, J.-J. & Bensussan, A. T Lymphocytes Bearing the T Cell Receptor in Patients with Acute Plasmodium falciparum Malaria. *J. Infect. Dis.* **162**, 283–285 (1990).
47. Ho, M., Webster, H. K., Tongtawe, P., Pattanapanyasat, K. & Weidanz, W. P. Increased gamma delta T cells in acute Plasmodium falciparum malaria. *Immunol. Lett.* **25**, 139–41 (1990).
48. Costa, G. *et al.* Control of Plasmodium falciparum erythrocytic cycle: T cells target the red blood cell-invasive merozoites. *Blood* **118**, 6952–6962 (2011).
49. Dinarello, C. A. Historical insights into cytokines. *Eur. J. Immunol.* **37 Suppl 1**, S34-45 (2007).
50. Taverne, J., Tavernier, J., Fiers, W. & Playfair, J. H. Recombinant tumour necrosis factor inhibits malaria parasites in vivo but not in vitro. *Clin. Exp. Immunol.* **67**, 1–4 (1987).
51. Clark, I. A., Hunt, N. H., Butcher, G. A. & Cowden, W. B. Inhibition of murine malaria (Plasmodium chabaudi) in vivo by recombinant interferon-gamma or tumor necrosis factor, and its enhancement by butylated hydroxyanisole. *J. Immunol.* **139**, 3493–6 (1987).
52. Deloron, P., Chougnet, C., Lepers, J. P., Tallet, S. & Coulanges, P. Protective value of elevated levels of gamma interferon in serum against exoerythrocytic stages of Plasmodium falciparum. *J. Clin. Microbiol.* **29**, 1757–60 (1991).
53. Shear, H. L., Srinivasan, R., Nolan, T. & Ng, C. Role of IFN-gamma in lethal and nonlethal malaria in susceptible and resistant murine hosts. *J. Immunol.* **143**, 2038–44 (1989).
54. Sam, H. & Stevenson, M. M. In vivo IL-12 production and IL-12 receptors beta1 and beta2 mRNA expression in the spleen are differentially up-regulated in resistant B6 and susceptible A/J mice during early blood-stage Plasmodium chabaudi AS malaria. *J. Immunol.* **162**, 1582–9 (1999).
55. Singh, R. P. *et al.* The Role of IL-18 in Blood-Stage Immunity Against Murine Malaria *Plasmodium yoelii 265* and *Plasmodium berghei ANKA*. *J. Immunol.* **168**, 4674–4681 (2002).
56. Angulo, I. & Fresno, M. Cytokines in the pathogenesis of and protection against malaria. *Clin. Diagn. Lab. Immunol.* **9**, 1145–52 (2002).

57. Kwiatkowski, D. *et al.* TNF concentration in fatal cerebral, non-fatal cerebral, and uncomplicated Plasmodium falciparum malaria. *Lancet* **336**, 1201–1204 (1990).
58. Yoshimoto, T. *et al.* A pathogenic role of IL-12 in blood-stage murine malaria lethal strain Plasmodium berghei NK65 infection. *J. Immunol.* **160**, 5500–5 (1998).
59. Amani, V. *et al.* Involvement of IFN-γ receptor-mediated signaling in pathology and anti-malarial immunity induced by Plasmodium berghei infection. *Eur. J. Immunol.* **30**, 1646–1655 (2000).
60. Mohan, K. & Stevenson, M. M. Dyserythropoiesis and severe anaemia associated with malaria correlate with deficient interleukin-12 production. *Br. J. Haematol.* **103**, 942–9 (1998).
61. Olsen Saraiva Camara, N., Lepique, A. P. & Basso, A. S. Lymphocyte differentiation and effector functions. *Clin. Dev. Immunol.* **2012**, 510603 (2012).
62. Zhu, J. & Paul, W. E. CD4 T cells: fates, functions, and faults. *Blood* **112**, 1557–69 (2008).
63. Zhang, N. & Bevan, M. J. CD8(+) T cells: foot soldiers of the immune system. *Immunity* **35**, 161–8 (2011).
64. LeBien, T. W. & Tedder, T. F. B lymphocytes: how they develop and function. *Blood* **112**, 1570–80 (2008).
65. Lu, L. L., Suscovich, T. J., Fortune, S. M. & Alter, G. Beyond binding: antibody effector functions in infectious diseases. *Nat. Rev. Immunol.* **18**, 46–61 (2018).
66. Schroeder, H. W., Cavacini, L. & Cavacini, L. Structure and function of immunoglobulins. *J. Allergy Clin. Immunol.* **125**, S41-52 (2010).
67. Stavnezer, J., Guikema, J. E. J. & Schrader, C. E. Mechanism and Regulation of Class Switch Recombination. *Annu. Rev. Immunol.* **26**, 261 (2008).
68. Di Noia, J. M. & Neuberger, M. S. Molecular Mechanisms of Antibody Somatic Hypermutation. *Annu. Rev. Biochem.* **76**, 1–22 (2007).
69. Sallusto, F., Lenig, D., Förster, R., Lipp, M. & Lanzavecchia, A. Two subsets of memory T lymphocytes with distinct homing potentials and effector functions. *Nature* **401**, 708–712 (1999).
70. Sallusto, F., Geginat, J. & Lanzavecchia, A. Central Memory and Effector Memory T Cell Subsets : Function, Generation, and Maintenance. *Annu. Rev.*

Immunol. **22**, 745–763 (2004).

71. Dame, J. *et al.* Structure of the gene encoding the immunodominant surface antigen on the sporozoite of the human malaria parasite Plasmodium falciparum. *Science (80-.).* **225**, 593–599 (1984).
72. Offeddu, V., Thathy, V., Marsh, K. & Matuschewski, K. Naturally acquired immune responses against Plasmodium falciparum sporozoites and liver infection. *Int. J. Parasitol.* **42**, 535–548 (2012).
73. Druilhe, P. *et al.* Levels of antibodies to Plasmodium falciparum sporozoite surface antigens reflect malaria transmission rates and are persistent in the absence of reinfection. *Infect. Immun.* **53**, 393–7 (1986).
74. Maleevan, O. *et al.* Anti-Sporozoite Antibodies Induced by Natural Infection *. *Am. J. Trop. Med. Hyg.* **32**, 1203–1208 (1983).
75. Hoffman, S. *et al.* Naturally acquired antibodies to sporozoites do not prevent malaria: vaccine development implications. *Science (80-.).* **237**, 639–642 (1987).
76. White, M. T. *et al.* A combined analysis of immunogenicity, antibody kinetics and vaccine efficacy from phase 2 trials of the RTS,S malaria vaccine. *BMC Med.* **12**, 117 (2014).
77. Dobaño, C. *et al.* Concentration and avidity of antibodies to different circumsporozoite epitopes correlate with RTS,S/AS01E malaria vaccine efficacy. *Nat. Commun.* **10**, 2174 (2019).
78. Hafalla, J. C., Silvie, O. & Matuschewski, K. Cell biology and immunology of malaria. *Immunol. Rev.* **240**, 297–316 (2011).
79. Doolan, D. L., Houghten, R. A., Good, M. F. & Pike, B. L. Location of human cytotoxic T cell epitopes within a polymorphic domain of the *Plasmodium falciparum* circumsporozoite protein. *Int. Immunol.* **3**, 511–516 (1991).
80. Doolan, D. L., Khamboonruang, C., Beck, H.-P., Houghten, R. A. & Good, M. F. Cytotoxic T lymphocyte (CTL) low-responsiveness to the *Plasmodium falciparum* circumsporozoite protein in naturally-exposed endemic populations: analysis of human CTL response to most known variants. *Int. Immunol.* **5**, 37–46 (1993).
81. González, J. M. *et al.* HLA-A*0201 restricted CD8+ T-lymphocyte responses to malaria: identification of new Plasmodium falciparum epitopes by IFN-gamma ELISPOT. *Parasite Immunol.* **22**, 501–14 (2000).

82. Hoffman, S. L. *et al.* Human lymphocyte proliferative response to a sporozoite T cell epitope correlates with resistance to falciparum malaria. *J. Immunol.* **142**, 1299–303 (1989).
83. Sedegah, M. *et al.* Naturally acquired CD8+ cytotoxic T lymphocytes against the Plasmodium falciparum circumsporozoite protein. *J. Immunol.* **149**, 966–71 (1992).
84. Fidock, D. A. *et al.* Plasmodium falciparum liver stage antigen-1 is well conserved and contains potent B and T cell determinants. *J. Immunol.* **153**, 190–204 (1994).
85. Luty, A. J. F. *et al.* Interferon-γ Responses Are Associated with Resistance to Reinfection with *Plasmodium falciparum* in Young African Children. *J. Infect. Dis.* **179**, 980–988 (1999).
86. Aidoo, M. *et al.* Identification of conserved antigenic components for a cytotoxic T lymphocyte-inducing vaccine against malaria. *Lancet (London, England)* **345**, 1003–7 (1995).
87. Flanagan, K. L. *et al.* Broadly distributed T cell reactivity, with no immunodominant loci, to the pre-erythrocytic antigen thrombospondin-related adhesive protein of Plasmodium falciparum in West Africans. *Eur. J. Immunol.* **29**, 1943–1954 (1999).
88. Flanagan, K. L. *et al.* Ex vivo interferon-gamma immune response to thrombospondin-related adhesive protein in coastal Kenyans: longevity and risk of Plasmodium falciparum infection. *Am. J. Trop. Med. Hyg.* **68**, 421–30 (2003).
89. Connelly, M. *et al.* T-cell immunity to peptide epitopes of liver-stage antigen 1 in an area of Papua New Guinea in which malaria is holoendemic. *Infect. Immun.* **65**, 5082–7 (1997).
90. Migot-Nabias, F. *et al.* Immune response to Plasmodium falciparum liver stage antigen-1: geographical variations within Central Africa and their relationship with protection from clinical malaria. *Trans. R. Soc. Trop. Med. Hyg.* **94**, 557–562 (2000).
91. Luty, A. J. *et al.* Parasite antigen-specific interleukin-10 and antibody reponses predict accelerated parasite clearance in Plasmodium falciparum malaria. *Eur. Cytokine Netw.* **9**, 639–46 (1998).
92. Kurtis, J. D., Lanar, D. E., Opollo, M. & Duffy, P. E. Interleukin-10 responses to

liver-stage antigen 1 predict human resistance to Plasmodium falciparum. *Infect. Immun.* **67**, 3424–9 (1999).

93. John, C. C. *et al.* Cytokine responses to Plasmodium falciparum liver-stage antigen 1 vary in rainy and dry seasons in highland Kenya. *Infect. Immun.* **68**, 5198–204 (2000).
94. Todryk, S. M. *et al.* Correlation of Memory T Cell Responses against TRAP with Protection from Clinical Malaria, and CD4+ CD25high T Cells with Susceptibility in Kenyans. *PLoS One* **3**, e2027 (2008).
95. Ong'echa, J. M. O. *et al.* Association of interferon-gamma responses to pre-erythrocytic stage vaccine candidate antigens of Plasmodium falciparum in young Kenyan children with improved hemoglobin levels: XV. Asembo Bay Cohort Project. *Am. J. Trop. Med. Hyg.* **68**, 590–597 (2003).
96. Cohen, S., McGregor, I. A. & Carrington, S. Gamma-Globulin and Acquired Immunity to Human Malaria. *Nature* **192**, 733–737 (1961).
97. Crompton, P. D. *et al.* Malaria immunity in man and mosquito: insights into unsolved mysteries of a deadly infectious disease. *Annu. Rev. Immunol.* **32**, 157 (2014).
98. Crompton, P. D., Pierce, S. K. & Miller, L. H. Advances and challenges in malaria vaccine development. *J. Clin. Invest.* **120**, 4168–4178 (2010).
99. Takala, S. L. & Plowe, C. V. Genetic diversity and malaria vaccine design, testing and efficacy: preventing and overcoming 'vaccine resistant malaria'. *Parasite Immunol.* **31**, 560–573 (2009).
100. Scherf, A., Lopez-Rubio, J. J. & Riviere, L. Antigenic Variation in *Plasmodium falciparum*. *Annu. Rev. Microbiol.* **62**, 445–470 (2008).
101. Pombo, D. J. *et al.* Immunity to malaria after administration of ultra-low doses of red cells infected with Plasmodium falciparum. *Lancet* **360**, 610–617 (2002).
102. Horowitz, A. *et al.* Cross-Talk between T Cells and NK Cells Generates Rapid Effector Responses to *Plasmodium falciparum* - Infected Erythrocytes. *J. Immunol.* **184**, 6043–6052 (2010).
103. Grau, G. E. *et al.* Tumor Necrosis Factor and Disease Severity in Children with Falciparum Malaria. *N. Engl. J. Med.* **320**, 1586–1591 (1989).
104. Portugal, S., Pierce, S. K. & Crompton, P. D. Young lives lost as B cells falter: what we are learning about antibody responses in malaria. *J. Immunol.* **190**, 3039–46 (2013).

105. Finney, O. C., Nwakanma, D., Conway, D. J., Walther, M. & Riley, E. M. Homeostatic regulation of T effector to Treg ratios in an area of seasonal malaria transmission. *Eur J Immunol* **39**, 1288–1300 (2009).
106. Omer, F. M. & Riley, E. M. Transforming Growth Factor β Production Is Inversely Correlated with Severity of Murine Malaria Infection. *J. Exp. Med.* **188**, 39–48 (1998).
107. Li, C., Corraliza, I. & Langhorne, J. A defect in interleukin-10 leads to enhanced malarial disease in Plasmodium chabaudi chabaudi infection in mice. *Infect. Immun.* **67**, 4435–42 (1999).
108. Dodoo, D. *et al.* Absolute Levels and Ratios of Proinflammatory and Anti-inflammatory Cytokine Production In Vitro Predict Clinical Immunity to *Plasmodium falciparum* Malaria. *J. Infect. Dis.* **185**, 971–979 (2002).
109. Finney, O. C., Riley, E. M. & Walther, M. Regulatory T cells in malaria--friend or foe? *Trends Immunol* **31**, 63–70 (2010).
110. Scholzen, A., Minigo, G. & Plebanski, M. Heroes or villains? T regulatory cells in malaria infection. *Trends Parasitol* **26**, 16–25 (2010).
111. Scholzen, A., Mittag, D., Rogerson, S. J., Cooke, B. M. & Plebanski, M. Plasmodium falciparum-mediated induction of human CD25Foxp3 CD4 T cells is independent of direct TCR stimulation and requires IL-2, IL-10 and TGFbeta. *PLoS Pathog* **5**, e1000543 (2009).
112. Scholzen, A., Cooke, B. M. & Plebanski, M. Plasmodium falciparum induces Foxp3hi CD4 T cells independent of surface PfEMP1 expression via small soluble parasite components. *Front Microbiol* **5**, 200 (2014).
113. Walther, M. *et al.* Upregulation of TGF-beta, FOXP3, and CD4+CD25+ regulatory T cells correlates with more rapid parasite growth in human malaria infection. *Immunity* **23**, 287–296 (2005).
114. Walther, M. *et al.* Innate immune responses to human malaria: heterogeneous cytokine responses to blood-stage Plasmodium falciparum correlate with parasitological and clinical outcomes. *J. Immunol.* **177**, 5736–45 (2006).
115. Amanna, I. J., Carlson, N. E. & Slifka, M. K. Duration of Humoral Immunity to Common Viral and Vaccine Antigens. *N. Engl. J. Med.* **357**, 1903–1915 (2007).
116. Kinyanjui, S. M., Conway, D. J., Lanar, D. E. & Marsh, K. IgG antibody responses to Plasmodium falciparum merozoite antigens in Kenyan children have a short half-life. *Malar. J.* **6**, 82 (2007).

117. Illingworth, J. *et al.* Chronic exposure to Plasmodium falciparum is associated with phenotypic evidence of B and T cell exhaustion. *J. Immunol.* **190**, 1038–47 (2013).
118. Obeng-Adjei, N. *et al.* Circulating Th1-Cell-type Tfh Cells that Exhibit Impaired B Cell Help Are Preferentially Activated during Acute Malaria in Children. *Cell Rep.* **13**, 425–39 (2015).
119. Weiss, G. E. *et al.* Atypical Memory B Cells Are Greatly Expanded in Individuals Living in a Malaria-Endemic Area. *J. Immunol.* **183**, (2009).
120. Clyde, D. F., Most, H., McCarthy, V. C. & Vanderberg, J. P. Immunization of man against sporozite-induced falciparum malaria. *Am. J. Med. Sci.* **266**, 169–77 (1973).
121. Hoffman, S. L. *et al.* Protection of Humans against Malaria by Immunization with Radiation-Attenuated *Plasmodium falciparum* Sporozoites. *J. Infect. Dis.* **185**, 1155–1164 (2002).
122. Hoffman, S. L., Vekemans, J., Richie, T. L. & Duffy, P. E. The march toward malaria vaccines. *Vaccine* **33**, D13–D23 (2015).
123. Sissoko, M. S. *et al.* Safety and efficacy of PfSPZ Vaccine against Plasmodium falciparum via direct venous inoculation in healthy malaria-exposed adults in Mali: a randomised, double-blind phase 1 trial. *Lancet. Infect. Dis.* **17**, 498–509 (2017).
124. Jongo, S. A. *et al.* Safety, Immunogenicity, and Protective Efficacy against Controlled Human Malaria Infection of Plasmodium falciparum Sporozoite Vaccine in Tanzanian Adults. *Am. J. Trop. Med. Hyg* **99**, 338–349 (2018).
125. Mordmüller, B. *et al.* Sterile protection against human malaria by chemoattenuated PfSPZ vaccine. *Nature* **542**, 445–449 (2017).
126. World Health Organisation. First malaria vaccine in Africa: A potential new tool for child health and improved malaria control. (2019). Available at: https://apps.who.int/iris/bitstream/handle/10665/272456/WHO-CDS-GMP-2018.05-eng.pdf?ua=1. (Accessed: 4th July 2019)
127. Kaslow, D. C. & Biernaux, S. RTS,S: Toward a first landmark on the Malaria Vaccine Technology Roadmap. *Vaccine* **33**, 7425–7432 (2015).
128. Mishra, S., Nussenzweig, R. S. & Nussenzweig, V. Antibodies to Plasmodium circumsporozoite protein (CSP) inhibit sporozoite's cell traversal activity. *J. Immunol. Methods* **377**, 47–52 (2012).

129. Foquet, L. *et al.* Vaccine-induced monoclonal antibodies targeting circumsporozoite protein prevent Plasmodium falciparum infection. *J. Clin. Invest.* **124**, 140–4 (2014).
130. RTS,S Clinical Trials Partnership. Efficacy and safety of RTS,S/AS01 malaria vaccine with or without a booster dose in infants and children in Africa: final results of a phase 3, individually randomised, controlled trial. *Lancet (London, England)* **386**, 31–45 (2015).
131. Collins, K. A., Snaith, R., Cottingham, M. G., Gilbert, S. C. & Hill, A. V. S. Enhancing protective immunity to malaria with a highly immunogenic virus-like particle vaccine. *Sci. Rep.* **7**, 46621 (2017).
132. Ewer, K. J. *et al.* Progress with viral vectored malaria vaccines: A multi-stage approach involving “unnatural immunity”. *Vaccine* **33**, 7444–7451 (2015).
133. Ewer, K. J. *et al.* Protective CD8+ T-cell immunity to human malaria induced by chimpanzee adenovirus-MVA immunisation. *Nat Commun* **4**, 2836 (2013).
134. Sullivan, N. J. *et al.* Immune Protection of Nonhuman Primates against Ebola Virus with Single Low-Dose Adenovirus Vectors Encoding Modified GPs. *PLoS Med.* **3**, e177 (2006).
135. Swadling, L. *et al.* A human vaccine strategy based on chimpanzee adenoviral and MVA vectors that primes, boosts, and sustains functional HCV-specific T cell memory. *Sci. Transl. Med.* **6**, 261ra153-261ra153 (2014).
136. Cappuccini, F., Stribbling, S., Pollock, E., Hill, A. V. S. & Redchenko, I. Immunogenicity and efficacy of the novel cancer vaccine based on simian adenovirus and MVA vectors alone and in combination with PD-1 mAb in a mouse model of prostate cancer. *Cancer Immunol. Immunother.* **65**, 701–713 (2016).
137. O’Hara, G. A. *et al.* Clinical assessment of a recombinant simian adenovirus ChAd63: a potent new vaccine vector. *J Infect Dis* **205**, 772–781 (2012).
138. Reyes-Sandoval, A. *et al.* Mixed Vector Immunization With Recombinant Adenovirus and MVA Can Improve Vaccine Efficacy While Decreasing Antivector Immunity. *Mol. Ther.* **20**, 1633–1647 (2012).
139. Sultan, A. A. *et al.* TRAP is necessary for gliding motility and infectivity of plasmodium sporozoites. *Cell* **90**, 511–22 (1997).
140. Gilbert, S. C. *et al.* A protein particle vaccine containing multiple malaria epitopes. *Nat. Biotechnol.* **15**, 1280–1284 (1997).

141. Afolabi, M. O. *et al.* Safety and Immunogenicity of ChAd63 and MVA ME-TRAP in West African Children and Infants. *Mol Ther* **24**, 1470–1477 (2016).
142. Ogwang, C. *et al.* Prime-boost vaccination with chimpanzee adenovirus and modified vaccinia Ankara encoding TRAP provides partial protection against Plasmodium falciparum infection in Kenyan adults. *Sci. Transl. Med.* **7**, 286re5 (2015).
143. Tiono, A. B. *et al.* First field efficacy trial of the ChAd63 MVA ME-TRAP vectored malaria vaccine candidate in 5-17 months old infants and children. *PLoS One* **13**, e0208328 (2018).
144. Hodgson, S. H. *et al.* Evaluation of the efficacy of ChAd63-MVA vectored vaccines expressing circumsporozoite protein and ME-TRAP against controlled human malaria infection in malaria-naive individuals. *J. Infect. Dis.* **211**, 1076–86 (2015).
145. Longley, R. J. *et al.* Comparative assessment of vaccine vectors encoding ten malaria antigens identifies two protective liver-stage candidates. *Sci. Rep.* **5**, 11820 (2015).
146. Douglas, A. D. *et al.* The blood-stage malaria antigen PfRH5 is susceptible to vaccine-inducible cross-strain neutralizing antibody. *Nat. Commun.* **2**, 601 (2011).
147. Payne, R. O. *et al.* Human vaccination against RH5 induces neutralizing antimalarial antibodies that inhibit RH5 invasion complex interactions. *JCI Insight* **2**, (2017).
148. Sheehy, S. H. *et al.* ChAd63-MVA-vectored blood-stage malaria vaccines targeting MSP1 and AMA1: assessment of efficacy against mosquito bite challenge in humans. *Mol Ther* **20**, 2355–2368 (2012).
149. Draper, S. J. *et al.* Malaria Vaccines: Recent Advances and New Horizons. *Cell Host Microbe* **24**, 43–56 (2018).
150. Weiss, G. E., Crabb, B. S. & Gilson, P. R. Overlaying Molecular and Temporal Aspects of Malaria Parasite Invasion. *Trends Parasitol.* **32**, 284–295 (2016).
151. Talaat, K. R. *et al.* Safety and Immunogenicity of Pfs25-EPA/Alhydrogel®, a Transmission Blocking Vaccine against Plasmodium falciparum: An Open Label Study in Malaria Naïve Adults. *PLoS One* **11**, e0163144 (2016).
152. MacDonald, N. J. *et al.* Structural and Immunological Characterization of Recombinant 6-Cysteine Domains of the *Plasmodium falciparum* Sexual Stage

Protein Pfs230. *J. Biol. Chem.* **291**, 19913–19922 (2016).

153. Molina-Cruz, A. *et al. Plasmodium* evasion of mosquito immunity and global malaria transmission: The lock-and-key theory. *Proc. Natl. Acad. Sci.* **112**, 15178–15183 (2015).
154. Carter, R. & Chen, D. H. Malaria transmission blocked by immunisation with gametes of the malaria parasite. *Nature* **263**, 57–60 (1976).
155. Jiang, V., Jiang, B., Tate, J., Parashar, U. D. & Patel, M. M. Performance of rotavirus vaccines in developed and developing countries. *Hum Vaccin* **6**, 532–542 (2010).
156. Mangtani, P. *et al.* Protection by BCG vaccine against tuberculosis: a systematic review of randomized controlled trials. *Clin Infect Dis* **58**, 470–480 (2014).
157. Colditz, G. A. *et al.* Efficacy of BCG vaccine in the prevention of tuberculosis. Meta-analysis of the published literature. *JAMA* **271**, 698–702 (1994).
158. Roy, A. *et al.* Effect of BCG vaccination against Mycobacterium tuberculosis infection in children: systematic review and meta-analysis. *BMJ* **349**, g4643 (2014).
159. Adu, F. D., Akinwolere, O. A., Tomori, O. & Uche, L. N. Low seroconversion rates to measles vaccine among children in Nigeria. *Bull World Heal. Organ* **70**, 457–460 (1992).
160. Kambarami, R. A., Nathoo, K. J., Nkrumah, F. K. & Pirie, D. J. Measles epidemic in Harare, Zimbabwe, despite high measles immunization coverage rates. *Bull World Heal. Organ* **69**, 213–219 (1991).
161. Cunnington, A. J. & Riley, E. M. Suppression of vaccine responses by malaria: insignificant or overlooked? *Expert Rev Vaccines* **9**, 409–429 (2010).
162. Malhotra, I. *et al.* Effect of antenatal parasitic infections on anti-vaccine IgG levels in children: a prospective birth cohort study in Kenya. *PLoS Negl Trop Dis* **9**, e0003466 (2015).
163. Rampling, T. *et al.* Safety and High Level Efficacy of the Combination Malaria Vaccine Regimen of RTS,S/AS01B With Chimpanzee Adenovirus 63 and Modified Vaccinia Ankara Vectored Vaccines Expressing ME-TRAP. *J Infect Dis* **214**, 772–781 (2016).
164. Polhemus, M. E. *et al.* Evaluation of RTS,S/AS02A and RTS,S/AS01B in adults in a high malaria transmission area. *PLoS One* **4**, e6465 (2009).

165. Kimani, D. *et al.* Translating the immunogenicity of prime-boost immunization with ChAd63 and MVA ME-TRAP from malaria naive to malaria-endemic populations. *Mol Ther* **22**, 1992–2003 (2014).
166. Rytter, M. J. H., Kolte, L., Briend, A., Friis, H. & Christensen, V. B. The immune system in children with malnutrition--a systematic review. *PLoS One* **9**, e105017 (2014).
167. Redeker, A. *et al.* The Contribution of Cytomegalovirus Infection to Immune Senescence Is Set by the Infectious Dose. *Front. Immunol.* **8**, (2018).
168. Frimpong, A. *et al.* Phenotypic Evidence of T Cell Exhaustion and Senescence During Symptomatic Plasmodium falciparum Malaria. *Front. Immunol.* **10**, 1345 (2019).
169. Ohkura, N., Kitagawa, Y. & Sakaguchi, S. Development and maintenance of regulatory T cells. *Immunity* **38**, 414–23 (2013).
170. Vignali, D. A. A., Collison, L. W. & Workman, C. J. How regulatory T cells work. *Nat. Rev. Immunol.* **8**, 523–532 (2008).
171. Sakaguchi, S., Sakaguchi, N., Asano, M., Itoh, M. & Toda, M. Immunologic self-tolerance maintained by activated T cells expressing IL-2 receptor alpha-chains (CD25). Breakdown of a single mechanism of self-tolerance causes various autoimmune diseases. *J. Immunol.* **155**, 1151–64 (1995).
172. Hori, S., Nomura, T. & Sakaguchi, S. Control of Regulatory T Cell Development by the Transcription Factor Foxp3. *Science (80-.).* **299**, 1057–1061 (2003).
173. Fontenot, J. D., Gavin, M. A. & Rudensky, A. Y. Foxp3 programs the development and function of CD4+CD25+ regulatory T cells. *Nat. Immunol.* **4**, 330–336 (2003).
174. Lee, W. & Lee, G. R. Transcriptional regulation and development of regulatory T cells. *Exp. Mol. Med.* **50**, e456–e456 (2018).
175. Roth, D. B. V(D)J Recombination: Mechanism, Errors, and Fidelity. *Microbiol. Spectr.* **2**, (2014).
176. Lio, C.-W. J. & Hsieh, C.-S. A Two-Step Process for Thymic Regulatory T Cell Development. *Immunity* **28**, 100–111 (2008).
177. Burchill, M. A. *et al.* Linked T Cell Receptor and Cytokine Signaling Govern the Development of the Regulatory T Cell Repertoire. *Immunity* **28**, 112–121 (2008).

178. Oh, J. & Shin, J.-S. The Role of Dendritic Cells in Central Tolerance. *Immune Netw.* **15**, 111 (2015).
179. Chen, W. *et al.* Conversion of Peripheral CD4+ CD25− Naive T Cells to CD4+ CD25+ Regulatory T Cells by TGF-β Induction of Transcription Factor Foxp3. *J. Exp. Med.* **198**, 1875–1886 (2003).
180. Apostolou, I. & von Boehmer, H. In Vivo Instruction of Suppressor Commitment in Naive T Cells. *J. Exp. Med.* **199**, 1401–1408 (2004).
181. Josefowicz, S. Z. *et al.* Extrathymically generated regulatory T cells control mucosal TH2 inflammation. *Nature* **482**, 395–399 (2012).
182. Horbelt, D., Denkis, A. & Knaus, P. A portrait of Transforming Growth Factor beta superfamily signalling: Background matters. *Int J Biochem Cell Biol* **44**, 469–474 (2012).
183. Verma, R. *et al.* A network map of Interleukin-10 signaling pathway. *J Cell Commun Signal* **10**, 61–67 (2016).
184. Gu, Y. *et al.* Interleukin 10 suppresses Th17 cytokines secreted by macrophages and T cells. *Eur. J. Immunol.* **38**, 1807–1813 (2008).
185. Buelens, C. *et al.* Interleukin-10 prevents the generation of dendritic cells from human peripheral blood mononuclear cells cultured with interleukin-4 and granulocyte/macrophage-colony-stimulating factor. *Eur J Immunol* **27**, 756–762 (1997).
186. Chadban, S. J. *et al.* Interleukin-10 differentially modulates MHC class II expression by mesangial cells and macrophages in vitro and in vivo. *Immunology* **94**, 72–78 (1998).
187. Schneider, H. *et al.* Reversal of the TCR stop signal by CTLA-4. *Science (80-.).* **313**, 1972–1975 (2006).
188. Qureshi, O. S. *et al.* Trans-endocytosis of CD80 and CD86: a molecular basis for the cell-extrinsic function of CTLA-4. *Science (80-.).* **332**, 600–603 (2011).
189. Boyman, O. & Sprent, J. The role of interleukin-2 during homeostasis and activation of the immune system. *Nat Rev Immunol* **12**, 180–190 (2012).
190. Couper, K. N. *et al.* IL-10 from CD4+CD25−Foxp3−CD127− Adaptive Regulatory T Cells Modulates Parasite Clearance and Pathology during Malaria Infection. *PLoS Pathog.* **4**, e1000004 (2008).
191. Amante, F. H. *et al.* A role for natural regulatory T cells in the pathogenesis of experimental cerebral malaria. *Am. J. Pathol.* **171**, 548–59 (2007).

192. Blanc, A.-L. *et al.* Suppression of CD4+ Effector Responses by Naturally Occurring CD4+ CD25+ Foxp3+ Regulatory T Cells Contributes to Experimental Cerebral Malaria. *Infect. Immun.* **84**, 329–38 (2016).
193. Jangpatarapongsa, K. *et al.* Plasmodium vivax parasites alter the balance of myeloid and plasmacytoid dendritic cells and the induction of regulatory T cells. *Eur. J. Immunol.* **38**, 2697–705 (2008).
194. Cambos, M., Belanger, B., Jacques, A., Roulet, A. & Scorza, T. Natural regulatory (CD4+CD25+FOXP+) T cells control the production of pro-inflammatory cytokines during Plasmodium chabaudi adami infection and do not contribute to immune evasion. *Int. J. Parasitol.* **38**, 229–238 (2008).
195. Nie, C. Q., Bernard, N. J., Schofield, L. & Hansen, D. S. CD4+ CD25+ Regulatory T Cells Suppress CD4+ T-Cell Function and Inhibit the Development of Plasmodium berghei-Specific TH1 Responses Involved in Cerebral Malaria Pathogenesis. *Infect. Immun.* **75**, 2275–2282 (2007).
196. Hisaeda, H. *et al.* Escape of malaria parasites from host immunity requires CD4+CD25+ regulatory T cells. *Nat. Med.* **10**, 29–30 (2004).
197. Vigário, A. M. *et al.* Regulatory CD4+CD25+ Foxp3+ T cells expand during experimental Plasmodium infection but do not prevent cerebral malaria. *Int. J. Parasitol.* **37**, 963–973 (2007).
198. Long, T. T. A., Nakazawa, S., Onizuka, S., Huaman, M. C. & Kanbara, H. Influence of CD4+CD25+ T cells on Plasmodium berghei NK65 infection in BALB/c mice. *Int. J. Parasitol.* **33**, 175–83 (2003).
199. Modiano, D. *et al.* The lower susceptibility to Plasmodium falciparum malaria of Fulani of Burkina Faso (west Africa) is associated with low frequencies of classic malaria-resistance genes. *Trans. R. Soc. Trop. Med. Hyg.* **95**, 149–52 (2001).
200. Torcia, M. G. *et al.* Functional deficit of T regulatory cells in Fulani, an ethnic group with low susceptibility to Plasmodium falciparum malaria. *Proc. Natl. Acad. Sci. U. S. A.* **105**, 646–51 (2008).
201. Minigo, G. *et al.* Parasite-Dependent Expansion of TNF Receptor II–Positive Regulatory T Cells with Enhanced Suppressive Activity in Adults with Severe Malaria. *PLoS Pathog.* **5**, e1000402 (2009).
202. Walther, M. *et al.* Distinct Roles for FOXP3+ and FOXP3− CD4+ T Cells in Regulating Cellular Immunity to Uncomplicated and Severe Plasmodium

falciparum Malaria. *PLoS Pathog.* **5**, e1000364 (2009).
203. Torres, K. J. *et al.* Relationship of regulatory T cells to Plasmodium falciparum malaria symptomatology in a hypoendemic region. *Malar. J.* **13**, 108 (2014).
204. Finney, O. C., Riley, E. M. & Walther, M. Phenotypic analysis of human peripheral blood regulatory T cells (CD4+FOXP3+CD127lo/-) ex vivo and after in vitro restimulation with malaria antigens. *Eur. J. Immunol.* **40**, 47–60 (2009).
205. Todryk, S. M. *et al.* Multiple functions of human T cells generated by experimental malaria challenge. *Eur J Immunol* **39**, 3042–3051 (2009).
206. Kurup, S. P. *et al.* Regulatory T cells impede acute and long-term immunity to blood-stage malaria through CTLA-4. *Nat. Med.* **23**, 1220–1225 (2017).
207. Boyle, M. J. *et al.* Decline of FoxP3+ Regulatory CD4 T Cells in Peripheral Blood of Children Heavily Exposed to Malaria. *PLoS Pathog* **11**, e1005041 (2015).
208. Wammes, L. J. *et al.* Asymptomatic Plasmodial Infection Is Associated With Increased Tumor Necrosis Factor Receptor II–Expressing Regulatory T Cells and Suppressed Type 2 Immune Responses. *J. Infect. Dis.* **207**, 1590–1599 (2013).
209. de Jong, S. E. *et al.* Longitudinal study of changes in γδ T cells and CD4+ T cells upon asymptomatic malaria infection in Indonesian children. *Sci. Rep.* **7**, 8844 (2017).
210. Hisaeda, H. *et al.* Resistance of regulatory T cells to glucocorticoid-viduced TNFR family-related protein (GITR) duringPlasmodium yoelii infection. *Eur. J. Immunol.* **35**, 3516–3524 (2005).
211. Hisaeda, H. *et al.* Malaria Parasites Require TLR9 Signaling for Immune Evasion by Activating Regulatory T Cells. *J. Immunol.* **180**, 2496–2503 (2008).
212. Maizels, R. M. & Smith, K. A. Regulatory T cells in infection. *Adv Immunol* **112**, 73–136 (2011).
213. Berod, L., Puttur, F., Huehn, J. & Sparwasser, T. Tregs in infection and vaccinology: heroes or traitors? *Microb Biotechnol* **5**, 260–269 (2012).
214. Abdeltawabi, M. S., El Seddik, N. & Salem, H. K. World Wide Epidemiology of Helminths Infection. in *Human Helminthiasis* (InTech, 2017). doi:10.5772/67273
215. Degarege, A. & Erko, B. Epidemiology of *Plasmodium* and Helminth Coinfection and Possible Reasons for Heterogeneity. *Biomed Res. Int.* **2016**,

1–6 (2016).
216. Watanabe, K. *et al.* T regulatory cell levels decrease in people infected with Schistosoma mansoni on effective treatment. *Am J Trop Med Hyg* **77**, 676–682 (2007).
217. Wammes, L. J. *et al.* Regulatory T cells in human lymphatic filariasis: stronger functional activity in microfilaremics. *PLoS Negl Trop Dis* **6**, e1655 (2012).
218. Turner, J. D. *et al.* Intensity of intestinal infection with multiple worm species is related to regulatory cytokine output and immune hyporesponsiveness. *J Infect Dis* **197**, 1204–1212 (2008).
219. Grainger, J. R. *et al.* Helminth secretions induce de novo T cell Foxp3 expression and regulatory function through the TGF-beta pathway. *J Exp Med* **207**, 2331–2341 (2010).
220. Maizels, R. M. & McSorley, H. J. Regulation of the host immune system by helminth parasites. *J Allergy Clin Immunol* **138**, 666–675 (2016).
221. Portugal, S. *et al.* Malaria-associated atypical memory B cells exhibit markedly reduced B cell receptor signaling and effector function. *Elife* **4**, (2015).
222. Urban, B. C. *et al.* Plasmodium falciparum-infected erythrocytes modulate the maturation of dendritic cells. *Nature* **400**, 73–77 (1999).
223. Urban, B. C., Willcox, N. & Roberts, D. J. A role for CD36 in the regulation of dendritic cell function. *Proc. Natl. Acad. Sci.* **98**, 8750–8755 (2001).
224. Yu, Y. *et al.* Recent advances in CD8+ regulatory t cell research (Review). *Oncology Letters* **15**, 8187–8194 (2018).
225. Akane, K., Kojima, S., Mak, T. W., Shikud, H. & Suzuki, H. CD8+CD122+CD49dlow regulatory T cells maintain T-cell homeostasis by killing activated T cells via Fas/FasL-mediated cytotoxicity. *Proc. Natl. Acad. Sci. U. S. A.* **113**, 2460–2465 (2016).
226. Jarvis, L. B., Goodall, J. C. & Gaston, J. S. H. Human leukocyte antigen class I-restricted immunosuppression by human CD8+ regulatory T cells requires CTLA-4-mediated interaction with dendritic cells. *Hum. Immunol.* **69**, 687–95 (2008).
227. Dai, Z. *et al.* Natural CD8+CD122+ T cells are more potent in suppression of allograft rejection than CD4+CD25+ regulatory T cells. *Am. J. Transplant.* **14**, 39–48 (2014).
228. Endharti, A. T. *et al.* Cutting Edge: CD8 + CD122 + Regulatory T Cells

Produce IL-10 to Suppress IFN-γ Production and Proliferation of CD8 + T Cells . *J. Immunol.* **175**, 7093–7097 (2005).

229. Rosser, E. C. & Mauri, C. Regulatory B Cells: Origin, Phenotype, and Function. *Immunity* **42**, 607–612 (2015).
230. Mizoguchi, A., Mizoguchi, E., Takedatsu, H., Blumberg, R. S. & Bhan, A. K. Chronic intestinal inflammatory condition generates IL-10-producing regulatory B cell subset characterized by CD1d upregulation. *Immunity* **16**, 219–230 (2002).
231. Tian, J. *et al.* Lipopolysaccharide-activated B cells down-regulate Th1 immunity and prevent autoimmune diabetes in nonobese diabetic mice. *J. Immunol.* **167**, 1081–9 (2001).
232. Evans, J. G. *et al.* Novel Suppressive Function of Transitional 2 B Cells in Experimental Arthritis. *J. Immunol.* **178**, 7868–7878 (2007).
233. Eberl, G., Colonna, M., Di Santo, J. P. & McKenzie, A. N. J. Innate lymphoid cells: A new paradigm in immunology. *Science (80-.).* **348**, aaa6566–aaa6566 (2015).
234. Wang, S. *et al.* Regulatory Innate Lymphoid Cells Control Innate Intestinal Inflammation. *Cell* **171**, 201-216.e18 (2017).
235. Atri, C., Guerfali, F. Z. & Laouini, D. Role of human macrophage polarization in inflammation during infectious diseases. *International Journal of Molecular Sciences* **19**, (2018).
236. Vogel, D. Y. S. *et al.* Human macrophage polarization in vitro: Maturation and activation methods compared. *Immunobiology* **219**, 695–703 (2014).
237. Martinez, F. O., Helming, L. & Gordon, S. Alternative Activation of Macrophages: An Immunologic Functional Perspective. *Annu. Rev. Immunol.* **27**, 451–483 (2009).
238. Arnold, L. *et al.* Inflammatory monocytes recruited after skeletal muscle injury switch into antiinflammatory macrophages to support myogenesis. *J. Exp. Med.* **204**, 1057–1069 (2007).
239. H. Munn, D. Indoleamine 2,3-dioxygenase, Tregs and Cancer. *Curr. Med. Chem.* **18**, 2240–2246 (2011).
240. Baumgartner, R., Forteza, M. J. & Ketelhuth, D. F. J. The interplay between cytokines and the Kynurenine pathway in inflammation and atherosclerosis. *Cytokine* **122**, (2019).

241. Pallotta, M. T. *et al.* Indoleamine 2,3-dioxygenase is a signaling protein in long-term tolerance by dendritic cells. *Nat. Immunol.* **12**, 870–878 (2011).
242. Forteza, M. J. *et al.* Activation of the regulatory T-cell/indoleamine 2,3-dioxygenase axis reduces vascular inflammation and atherosclerosis in hyperlipidemic mice. *Front. Immunol.* **9**, (2018).
243. Bejon, P. *et al.* Analysis of Immunity to Febrile Malaria in Children That Distinguishes Immunity from Lack of Exposure. *Infect. Immun.* **77**, 1917–1923 (2009).
244. Manske, M. *et al.* Analysis of Plasmodium falciparum diversity in natural infections by deep sequencing. *Nature* **487**, 375–379 (2012).
245. Stanisic, D. I., McCarthy, J. S. & Good, M. F. Controlled Human Malaria Infection: Applications, Advances, and Challenges. *Infect. Immun.* **86**, e00479-17 (2018).
246. Snounou, G. & Pérignon, J.-L. Malariotherapy – Insanity at the Service of Malariology. in *Advances in parasitology* **81**, 223–255 (2013).
247. Coatney, H. R. & Cooper, W. C. Studies in human malaria; trials of quinacrine, colchicine (SN 12,080) and quinine against Chesson strain vivax malaria. *Am. J. Hyg.* **50**, 194–9 (1949).
248. Beadle, C. *et al.* Diagnosis of malaria by detection of Plasmodium falciparum HRP-2 antigen with a rapid dipstick antigen-capture assay. *Lancet* **343**, 564–568 (1994).
249. Hodgson, S. H. *et al.* Evaluating controlled human malaria infection in Kenyan adults with varying degrees of prior exposure to Plasmodium falciparum using sporozoites administered by intramuscular injection. *Front Microbiol* **5**, 686 (2014).
250. Hodgson, S. H. *et al.* Lessons learnt from the first controlled human malaria infection study conducted in Nairobi, Kenya. *Malar. J.* **14**, 182 (2015).
251. Njue, M. *et al.* Ethical considerations in Controlled Human Malaria Infection studies in low resource settings: Experiences and perceptions of study participants in a malaria Challenge study in Kenya. *Wellcome Open Res.* **3**, 39 (2018).
252. Roestenberg, M. *et al.* Controlled Human Malaria Infections by Intradermal Injection of Cryopreserved Plasmodium falciparum Sporozoites. *Am. J. Trop. Med. Hyg* **88**, 5–13 (2013).

253. Sheehy, S. H. *et al.* Optimising Controlled Human Malaria Infection Studies Using Cryopreserved P. falciparum Parasites Administered by Needle and Syringe. *PLoS One* **8**, e65960 (2013).
254. Elias, D. *et al.* Effect of deworming on human T cell responses to mycobacterial antigens in helminth-exposed individuals before and after bacille Calmette-Guerin (BCG) vaccination. *Clin Exp Immunol* **123**, 219–225 (2001).
255. Malhotra, I. *et al.* Helminth- and Bacillus Calmette-Guerin-induced immunity in children sensitized in utero to filariasis and schistosomiasis. *J Immunol* **162**, 6843–6848 (1999).
256. Riner, D. K. *et al.* Schistosoma mansoni Infection Can Jeopardize the Duration of Protective Levels of Antibody Responses to Immunizations against Hepatitis B and Tetanus Toxoid. *PLoS Negl Trop Dis* **10**, e0005180 (2016).
257. Nookala, S., Srinivasan, S., Kaliraj, P., Narayanan, R. B. & Nutman, T. B. Impairment of tetanus-specific cellular and humoral responses following tetanus vaccination in human lymphatic filariasis. *Infect Immun* **72**, 2598–2604 (2004).
258. Cooper, P. J., Espinel, I., Paredes, W., Guderian, R. H. & Nutman, T. B. Impaired tetanus-specific cellular and humoral responses following tetanus vaccination in human onchocerciasis: a possible role for interleukin-10. *J Infect Dis* **178**, 1133–1138 (1998).
259. Esen, M. *et al.* Reduced antibody responses against Plasmodium falciparum vaccine candidate antigens in the presence of Trichuris trichiura. *Vaccine* **30**, 7621–7624 (2012).
260. Klein Klouwenberg, P. & Bont, L. Neonatal and Infantile Immune Responses to Encapsulated Bacteria and Conjugate Vaccines. *J. Immunol. Res.* **2008**, (2008).
261. McSorley, H. J. & Maizels, R. M. Helminth infections and host immune regulation. *Clin Microbiol Rev* **25**, 585–608 (2012).
262. Coleman, M. M., Keane, J. & Mills, K. H. Editorial: Tregs and BCG--dangerous liaisons in TB. *J Leukoc Biol* **88**, 1067–1069 (2010).
263. Zuany-Amorim, C. *et al.* Suppression of airway eosinophilia by killed Mycobacterium vaccae-induced allergen-specific regulatory T-cells. *Nat Med* **8**, 625–629 (2002).
264. Akkoc, T. *et al.* Neonatal BCG vaccination induces IL-10 production by CD4+

CD25+ T cells. *Pediatr Allergy Immunol* **21**, 1059–1063 (2010).

265. Hougardy, J. M. *et al.* Regulatory T cells depress immune responses to protective antigens in active tuberculosis. *Am J Respir Crit Care Med* **176**, 409–416 (2007).
266. Ho, P., Wei, X. & Seah, G. T. Regulatory T cells induced by Mycobacterium chelonae sensitization influence murine responses to bacille Calmette-Guerin. *J Leukoc Biol* **88**, 1073–1080 (2010).
267. Burl, S. *et al.* Delaying bacillus Calmette-Guerin vaccination from birth to 4 1/2 months of age reduces postvaccination Th1 and IL-17 responses but leads to comparable mycobacterial responses at 9 months of age. *J Immunol* **185**, 2620–2628 (2010).
268. Borkow, G. & Bentwich, Z. Chronic parasite infections cause immune changes that could affect successful vaccination. *Trends Parasitol* **24**, 243–245 (2008).
269. Elias, D., Britton, S., Aseffa, A., Engers, H. & Akuffo, H. Poor immunogenicity of BCG in helminth infected population is associated with increased in vitro TGF-beta production. *Vaccine* **26**, 3897–3902 (2008).
270. Wammes, L. J. *et al.* Community deworming alleviates geohelminth-induced immune hyporesponsiveness. *Proc Natl Acad Sci U S A* **113**, 12526–12531 (2016).
271. Wammes, L. J. *et al.* Regulatory T cells in human geohelminth infection suppress immune responses to BCG and Plasmodium falciparum. *Eur J Immunol* **40**, 437–442 (2010).
272. Weatherhead, J. E. & Hotez, P. J. Worm Infections in Children. *Pediatr Rev* **36**, 341–344 (2015).
273. Kapulu, M. C., Njuguna, P., Hamaluba, M. & Team, C.-S. S. Controlled Human Malaria Infection in Semi-Immune Kenyan Adults (CHMI-SIKA): a study protocol to investigate in vivo Plasmodium falciparum malaria parasite growth in the context of pre-existing immunity. *Wellcome Open Res.* **3**, 155 (2018).
274. Bliss, C. M. *et al.* Assessment of novel vaccination regimens using viral vectored liver stage malaria vaccines encoding ME-TRAP. *Sci. Rep.* **8**, 3390 (2018).
275. Mensah, V. A. *et al.* Safety, Immunogenicity and Efficacy of Prime-Boost Vaccination with ChAd63 and MVA Encoding ME-TRAP against Plasmodium falciparum Infection in Adults in Senegal. *PLoS One* **11**, e0167951 (2016).

276. Venkatraman, N. *et al.* Safety and immunogenicity of heterologous prime-boost immunization with viral-vectored malaria vaccines adjuvanted with Matrix-M™. *Vaccine* **35**, 6208–6217 (2017).
277. Venkatraman, N. *et al.* Safety and Immunogenicity of a Heterologous Prime-Boost Ebola Virus Vaccine Regimen in Healthy Adults in the United Kingdom and Senegal. *J. Infect. Dis.* (2018). doi:10.1093/infdis/jiy639
278. Ndungu, F. M. *et al.* Memory B cells are a more reliable archive for historical antimalarial responses than plasma antibodies in no-longer exposed children. *Proc. Natl. Acad. Sci. U. S. A.* **109**, 8247–52 (2012).
279. Ewer, K. *et al.* A Monovalent Chimpanzee Adenovirus Ebola Vaccine Boosted with MVA. *N Engl J Med* **374**, 1635–1646 (2016).
280. Ting, A. & Morris, P. J. A Technique for Lymphocyte Preparation from Stored Heparinized Blood. *Vox Sang.* **20**, 561–563 (1971).
281. Kutscher, S. *et al.* Overnight Resting of PBMC Changes Functional Signatures of Antigen Specific T- Cell Responses: Impact for Immune Monitoring within Clinical Trials. *PLoS One* **8**, e76215 (2013).
282. Moll, K., Kaneko, A., Scherf, A. & Wahlgren, M. *Methods in Malaria Research Sixth Edition*. (BEI Resources, 2013).
283. Schmittgen, T. D. & Livak, K. J. Analyzing real-time PCR data by the comparative CT method. *Nat. Protoc.* **3**, 1101–1108 (2008).
284. Ritchie, M. E. *et al.* limma powers differential expression analyses for RNA-sequencing and microarray studies. *Nucleic Acids Res.* **43**, e47–e47 (2015).
285. Langhorne, J., Ndungu, F. M., Sponaas, A.-M. & Marsh, K. Immunity to malaria: more questions than answers. *Nat. Immunol.* **9**, 725–732 (2008).
286. Spring, M., Polhemus, M. & Ockenhouse, C. Controlled human malaria infection. *J Infect Dis* **209 Suppl**, S40-5 (2014).
287. Sauerwein, R. W., Roestenberg, M. & Moorthy, V. S. Experimental human challenge infections can accelerate clinical malaria vaccine development. *Nat. Rev. Immunol.* **11**, 57–64 (2011).
288. Mordmüller, B. *et al.* Direct venous inoculation of Plasmodium falciparum sporozoites for controlled human malaria infection: a dose-finding trial in two centres. *Malar. J.* **14**, 117 (2015).
289. Sheehy, S. H. *et al.* Phase Ia Clinical Evaluation of the Plasmodium falciparum Blood-stage Antigen MSP1 in ChAd63 and MVA Vaccine Vectors. *Mol. Ther.*

19, 2269–2276 (2011).

290. Shekalaghe, S. *et al.* Controlled Human Malaria Infection of Tanzanians by Intradermal Injection of Aseptic, Purified, Cryopreserved Plasmodium falciparum Sporozoites. *Am. J. Trop. Med. Hyg.* **91**, 471–480 (2014).
291. National Malaria Control Programme, M. of H. & Noor, A. M. *The epidemiology and control profile of malaria in Kenya: reviewing the evidence to guide the future vector control*. (2016).
292. Ministry of Health of Tanzania. *Tanzania Demographic and Health Survey and Malaria Indicator Survey*. (2015).
293. Mogeni, P. *et al.* Age, Spatial, and Temporal Variations in Hospital Admissions with Malaria in Kilifi County, Kenya: A 25-Year Longitudinal Observational Study. *PLoS Med* **13**, e1002047 (2016).
294. Bousema, T., Okell, L., Felger, I. & Drakeley, C. Asymptomatic malaria infections: detectability, transmissibility and public health relevance. *Nat. Rev. Microbiol.* **12**, 833–840 (2014).
295. Couper, K. N. *et al.* IL-10: the master regulator of immunity to infection. *J. Immunol.* **180**, 5771–7 (2008).
296. Santegoets, S. J. A. M. *et al.* Monitoring regulatory T cells in clinical samples: consensus on an essential marker set and gating strategy for regulatory T cell analysis by flow cytometry. *Cancer Immunol Immunother* **64**, 1271–1286 (2015).
297. Mangold, K. A. *et al.* Real-Time PCR for Detection and Identification of Plasmodium spp. *J. Clin. Microbiol.* **43**, 2435 (2005).
298. Millington, O. R., Di Lorenzo, C., Phillips, R. S., Garside, P. & Brewer, J. M. Suppression of adaptive immunity to heterologous antigens during Plasmodium infection through hemozoin-induced failure of dendritic cell function. *J. Biol.* **5**, 5 (2006).
299. Chemtai, A. K. & Okelo, G. B. Suppression of T-cell proliferative response in Plasmodium falciparum malaria patients--preliminary results. *East Afr. Med. J.* **66**, 787–91 (1989).
300. Hou, P. F., Zhu, L. J., Chen, X. Y. & Qiu, Z. Q. Age-related changes in CD4+CD25+FOXP3+ regulatory T cells and their relationship with lung cancer. *PLoS One* **12**, e0173048 (2017).
301. Zhu, L. J. *et al.* Changes in CD4+CD25+Foxp3+ Regulatory T Cells in Relation

to Aging and Lung Tumor Incidence. *Int. J. Gerontol.* **6**, 187–191 (2012).
302. Afshan, G., Afzal, N. & Qureshi, S. CD4+CD25(hi) regulatory T cells in healthy males and females mediate gender difference in the prevalence of autoimmune diseases. *Clin. Lab.* **58**, 567–71 (2012).
303. Riley, E. M. & Stewart, V. A. Immune mechanisms in malaria: new insights in vaccine development. *Nat Med* **19**, 168–178 (2013).
304. Bryl, E. & Witkowski, J. M. Decreased proliferative capability of CD4+ cells of elderly people is associated with faster loss of activation-related antigens and accumulation of regulatory T cells. *Exp. Gerontol.* **39**, 587–595 (2004).
305. Sambhara, S. & McElhaney, J. E. Immunosenescence and Influenza Vaccine Efficacy. in 413–429 (Springer, Berlin, Heidelberg, 2009). doi:10.1007/978-3-540-92165-3_20
306. Nichol, K. L., Nordin, J. D., Nelson, D. B., Mullooly, J. P. & Hak, E. Effectiveness of Influenza Vaccine in the Community-Dwelling Elderly. *N. Engl. J. Med.* **357**, 1373–1381 (2007).
307. Gross, P. A. Review: inactivated vaccines provide the greatest protection against influenza in healthy persons. *ACP J. Club* **136**, 103
308. Fulop, T. *et al.* Immunosenescence and Inflamm-Aging As Two Sides of the Same Coin: Friends or Foes? *Front. Immunol.* **8**, 1960 (2017).
309. Xu, W. & Larbi, A. Markers of T Cell Senescence in Humans. *Int. J. Mol. Sci.* **18**, (2017).
310. Liu, W. *et al.* CD127 expression inversely correlates with FoxP3 and suppressive function of human CD4+ T reg cells. *J. Exp. Med.* **203**, 1701–11 (2006).
311. Livak, K. J. & Schmittgen, T. D. Analysis of relative gene expression data using real-time quantitative PCR and the 2-ΔΔCT method. *Methods* **25**, 402–408 (2001).
312. Shatrova, A. N. *et al.* Time-dependent regulation of IL-2R α-chain (CD25) expression by TCR signal strength and IL-2-induced STAT5 signaling in activated human blood T lymphocytes. *PLoS One* **11**, (2016).
313. Hawkins, S. F. C. & Guest, P. C. Multiplex Analyses Using Real-Time Quantitative PCR. in *Methods in molecular biology (Clifton, N.J.)* **1546**, 125–133 (2017).
314. Lowe, R., Shirley, N., Bleackley, M., Dolan, S. & Shafee, T. Transcriptomics

technologies. *PLOS Comput. Biol.* **13**, e1005457 (2017).
315. Wang, Z., Gerstein, M. & Snyder, M. RNA-Seq: a revolutionary tool for transcriptomics. *Nat. Rev. Genet.* **10**, 57–63 (2009).
316. Su, Z. *et al.* An investigation of biomarkers derived from legacy microarray data for their utility in the RNA-seq era. *Genome Biol.* **15**, 523 (2014).
317. Nelson, N. J. Microarrays have arrived: gene expression tool matures. *J. Natl. Cancer Inst.* **93**, 492–4 (2001).
318. Johnson, S. *et al.* Cooperativity of HIV-Specific Cytolytic CD4 T Cells and CD8 T Cells in Control of HIV Viremia. *J. Virol.* **89**, 7494–7505 (2015).
319. Gasper, M. A. *et al.* BCG vaccination induces HIV target cell activation in HIV-exposed infants in a randomized trial. *JCI Insight* **2**, e91963 (2017).
320. Li, G. *et al.* An introduction to multiplicity issues in clinical trials: the what, why, when and how. *Int. J. Epidemiol.* **46**, dyw320 (2016).
321. Pawitan, Y., Michiels, S., Koscielny, S., Gusnanto, A. & Ploner, A. False discovery rate, sensitivity and sample size for microarray studies. *Bioinformatics* **21**, 3017–3024 (2005).
322. Durham, G. A., Williams, J. J. L., Nasim, M. T. & Palmer, T. M. Targeting SOCS Proteins to Control JAK-STAT Signalling in Disease. *Trends Pharmacol. Sci.* **40**, 298–308 (2019).
323. Goldstein, J. D. *et al.* Inhibition of the JAK/STAT Signaling Pathway in Regulatory T Cells Reveals a Very Dynamic Regulation of Foxp3 Expression. *PLoS One* **11**, e0153682 (2016).
324. Abdulghani, J. & El-Deiry, W. S. TRAIL receptor signaling and therapeutics. *Expert Opin. Ther. Targets* **14**, 1091–1108 (2010).
325. Hellwig, C. T. & Rehm, M. TRAIL Signaling and Synergy Mechanisms Used in TRAIL-Based Combination Therapies. *Mol. Cancer Ther.* **11**, 3–13 (2012).
326. Hughes, C. E. & Nibbs, R. J. B. A guide to chemokines and their receptors. *FEBS J.* **285**, 2944–2971 (2018).
327. Ioannidis, L. J., Nie, C. Q. & Hansen, D. S. The role of chemokines in severe malaria: more than meets the eye. *Parasitology* **141**, 602–13 (2014).
328. Rothen, J. *et al.* Whole blood transcriptome changes following controlled human malaria infection in malaria pre-exposed volunteers correlate with parasite prepatent period. *PLoS One* **13**, e0199392 (2018).
329. Kamath, A. T., Sheasby, C. E. & Tough, D. F. Dendritic cells and NK cells

stimulate bystander T cell activation in response to TLR agonists through secretion of IFN-alpha beta and IFN-gamma. *J. Immunol.* **174**, 767–76 (2005).

330. Heide, J., Vaughan, K. C., Sette, A., Jacobs, T. & Schulze zur Wiesch, J. Comprehensive Review of Human Plasmodium falciparum-Specific CD8+ T Cell Epitopes. *Front. Immunol.* **10**, 397 (2019).
331. Schwenk, R. *et al.* Ex vivo tetramer staining and cell surface phenotyping for early activation markers CD38 and HLA-DR to enumerate and characterize malaria antigen-specific CD8+ T-cells induced in human volunteers immunized with a Plasmodium falciparum adenovirus-vectored malaria vaccine expressing AMA1. *Malar. J.* **12**, 376 (2013).
332. Kulkarni, A., Anderson, A. G., Merullo, D. P. & Konopka, G. Beyond bulk: a review of single cell transcriptomics methodologies and applications. *Curr. Opin. Biotechnol.* **58**, 129–136 (2019).
333. Hwang, B., Lee, J. H. & Bang, D. Single-cell RNA sequencing technologies and bioinformatics pipelines. *Exp. Mol. Med.* **50**, 96 (2018).
334. Lu, Y.-C. *et al.* An Efficient Single-Cell RNA-Seq Approach to Identify Neoantigen-Specific T Cell Receptors. *Mol. Ther.* **26**, 379–389 (2018).
335. Eltahla, A. A. *et al.* Linking the T cell receptor to the single cell transcriptome in antigen-specific human T cells. *Immunol. Cell Biol.* **94**, 604–611 (2016).
336. Nguyen, Q. H., Pervolarakis, N., Nee, K. & Kessenbrock, K. Experimental Considerations for Single-Cell RNA Sequencing Approaches. *Front. Cell Dev. Biol.* **6**, 108 (2018).
337. Chen, G., Ning, B. & Shi, T. Single-Cell RNA-Seq Technologies and Related Computational Data Analysis. *Front. Genet.* **10**, 317 (2019).
338. Gao, S. Data Analysis in Single-Cell Transcriptome Sequencing. in *Methods in molecular biology (Clifton, N.J.)* **1754**, 311–326 (2018).
339. Tran, D. Q. & Shevach, E. M. Response: Anti human FOXP3 mAb PCH101 stains activated human naive T cells nonspecifically. *Blood* **111**, 464–466 (2008).
340. Law, J. P. *et al.* The importance of Foxp3 antibody and fixation/permeabilization buffer combinations in identifying CD4+CD25+Foxp3+ regulatory T cells. *Cytometry. A* **75**, 1040–50 (2009).
341. Schmidt, A., Oberle, N. & Krammer, P. H. Molecular mechanisms of treg-mediated T cell suppression. *Front. Immunol.* **3**, 51 (2012).

342. Rothstein, D. M. & Camirand, G. New insights into the mechanisms of Treg function. *Curr. Opin. Organ Transplant.* **20**, 376–84 (2015).
343. Seiler, M. P., Cerullo, V. & Lee, B. Immune response to helper dependent adenoviral mediated liver gene therapy: challenges and prospects. *Curr. Gene Ther.* **7**, 297–305 (2007).
344. Nayak, S. & Herzog, R. W. Progress and prospects: immune responses to viral vectors. *Gene Ther.* **17**, 295–304 (2010).
345. Dooley, A., Quintana, M., Cheung, M., Sun, L. L. & Gupta, N. The B cell IL-10 receptor suppresses antibody production. *J. Immunol.* **200**, 164.9 LP-164.9 (2018).
346. Gros, M. J., Naquet, P. & Guinamard, R. R. Cell Intrinsic TGF-β1 Regulation of B Cells. *J. Immunol.* **180**, 8153 LP – 8158 (2008).
347. Sage, P. T., Paterson, A. M., Lovitch, S. B. & Sharpe, A. H. The coinhibitory receptor CTLA-4 controls B cell responses by modulating T follicular helper, T follicular regulatory, and T regulatory cells. *Immunity* **41**, 1026–39 (2014).
348. Wing, J. B., Tekgüç, M. & Sakaguchi, S. Control of Germinal Center Responses by T-Follicular Regulatory Cells. *Front. Immunol.* **9**, 1910 (2018).
349. Ndure, J. & Flanagan, K. L. Targeting regulatory T cells to improve vaccine immunogenicity in early life. *Front Microbiol* **5**, 477 (2014).
350. Ndure, J. *et al.* Negative Correlation between Circulating CD4+FOXP3+CD127− Regulatory T Cells and Subsequent Antibody Responses to Infant Measles Vaccine but Not Diphtheria–Tetanus–Pertussis Vaccine Implies a Regulatory Role. *Front. Immunol.* **8**, 921 (2017).
351. Gething, P. The Malaria Atlas Project. Available at: https://map.ox.ac.uk/. (Accessed: 17th June 2019)
352. Rech, A. J. *et al.* CD25 blockade depletes and selectively reprograms regulatory T cells in concert with immunotherapy in cancer patients. *Sci Transl Med* **4**, 134ra62 (2012).
353. Rech, A. J. & Vonderheide, R. H. Clinical Use of Anti-CD25 Antibody Daclizumab to Enhance Immune Responses to Tumor Antigen Vaccination by Targeting Regulatory T cells. *Ann. N. Y. Acad. Sci.* **1174**, 99–106 (2009).
354. Noordam, L. *et al.* Low-dose cyclophosphamide depletes circulating naïve and activated regulatory T cells in malignant pleural mesothelioma patients synergistically treated with dendritic cell-based immunotherapy.

Oncoimmunology **7**, e1474318 (2018).

355. Macatangay, B. J. C., Szajnik, M. E., Whiteside, T. L., Riddler, S. A. & Rinaldo, C. R. Regulatory T Cell Suppression of Gag-Specific CD8+ T Cell Polyfunctional Response After Therapeutic Vaccination of HIV-1-Infected Patients on ART. *PLoS One* **5**, e9852 (2010).
356. Moore, A. C. *et al.* Anti-CD25 antibody enhancement of vaccine-induced immunogenicity: increased durable cellular immunity with reduced immunodominance. *J Immunol* **175**, 7264–7273 (2005).
357. Olotu, A. *et al.* Estimating Individual Exposure to Malaria Using Local Prevalence of Malaria Infection in the Field. *PLoS One* **7**, e32929 (2012).
358. Bejon, P. *et al.* Stable and Unstable Malaria Hotspots in Longitudinal Cohort Studies in Kenya. *PLoS Med.* **7**, e1000304 (2010).
359. Drakeley, C. J. *et al.* Estimating medium- and long-term trends in malaria transmission by using serological markers of malaria exposure. *Proc Natl Acad Sci U S A* **102**, 5108–5113 (2005).
360. Bagayan, M. *et al.* Prévalence de la schistosomose et des géohelminthiases chez des élèves de l'école primaire au Burkina Faso. *Med. Sante Trop.* **26**, 267–272 (2016).
361. World Health Organisation. Prevention and control of schistosomiasis and soil-transmitted helminthiasis: report of a WHO expert committee. (2002). Available at: https://apps.who.int/iris/bitstream/handle/10665/42588/WHO_TRS_912.pdf?sequence=1&isAllowed=y. (Accessed: 29th July 2019)
362. World Health Organisation. WHO | Neglected tropical diseases − Summary. (2016). Available at: https://www.who.int/neglected_diseases/diseases/summary/en/. (Accessed: 23rd August 2019)
363. Caraballo, L. & Coronado, S. Parasite allergens. *Mol. Immunol.* **100**, 113–119 (2018).
364. Kilama, M. *et al.* Estimating the annual entomological inoculation rate for Plasmodium falciparum transmitted by Anopheles gambiae s.l. using three sampling methods in three sites in Uganda. *Malar. J.* **13**, 111 (2014).
365. Corran, P., Coleman, P., Riley, E. & Drakeley, C. Serology: a robust indicator of malaria transmission intensity? *Trends Parasitol.* **23**, 575–582 (2007).

366. Martinez, D. R., Permar, S. R. & Fouda, G. G. Contrasting Adult and Infant Immune Responses to HIV Infection and Vaccination. *Clin. Vaccine Immunol.* **23**, 84–94 (2016).
367. Simon, A. K., Hollander, G. A. & McMichael, A. Evolution of the immune system in humans from infancy to old age. *Proceedings. Biol. Sci.* **282**, 20143085 (2015).
368. Bejon, P. *et al.* The Induction and Persistence of T Cell IFN-γ Responses after Vaccination or Natural Exposure Is Suppressed by *Plasmodium falciparum*. *J. Immunol.* **179**, 4193–4201 (2007).
369. Williamson, W. A. & Greenwood, B. M. Impairment of the immune response to vaccination after acute malaria. *Lancet (London, England)* **1**, 1328–9 (1978).
370. Greenwood, B. M. *et al.* The immune response to a meningococcal polysaccharide vaccine in an African village. *Trans. R. Soc. Trop. Med. Hyg.* **74**, 340–6 (1980).
371. Maizels, R. M., Pearce, E. J., Artis, D., Yazdanbakhsh, M. & Wynn, T. A. Regulation of pathogenesis and immunity in helminth infections. *J. Exp. Med.* **206**, 2059–66 (2009).
372. Delemarre, B. J. & van der Kaay, H. J. Tropical malaria contracted the natural way in the Netherlands. *Ned. Tijdschr. Geneeskd.* **123**, 1981–2 (1979).
373. Preston, M. D. *et al.* A barcode of organellar genome polymorphisms identifies the geographic origin of Plasmodium falciparum strains. *Nat. Commun.* **5**, 4052 (2014).
374. Le, D. T. & Jaffee, E. M. Regulatory T-cell modulation using cyclophosphamide in vaccine approaches: a current perspective. *Cancer Res* **72**, 3439–3444 (2012).